ЖУРНАЛ
ЭКСПЕРИМЕНТАЛЬНОЙ И ТЕОРЕТИЧЕСКОЙ
ФИЗИКИ
АКАДЕМИЯ НАУК СССР

SOVIET PHYSICS

JETP

VOLUME 2 NUMBER 2

A Translation

of the

Journal of Experimental and Theoretical Physics

of the

Academy of Sciences of the USSR

MARCH, 1956

Published by the

AMERICAN INSTITUTE OF PHYSICS
INCORPORATED

SOVIET PHYSICS
JETP

A translation of the Journal of Experimental and Theoretical Physics of the USSR.

A publication of the
AMERICAN INSTITUTE OF PHYSICS

SOVIET PHYSICS is a bi-monthly journal published by the American Institute of Physics for the purpose of making available in English reports of current Soviet research in physics as contained in the Journal of Experimental and Theoretical Physics of the Academy of Sciences of USSR. The page size of SOVIET PHYSICS will be 7⅞" x 10½", the same as other Institute journals.

Transliteration of the names of Russian authors follows the system employed by the Library of Congress.

This translating and publishing project was undertaken by the Institute in the conviction that dissemination of the results of researchs everywhere in the world is invaluable to the advancement of science. The National Science Foundation of the United States encouraged the project initially and is supporting it in large part by a grant.

The American Institute of Physics and its translators propose to translate faithfully all the material in the Journal of EXPERIMENTAL & THEORETICAL PHYSICS OF THE USSR appearing after January 1, 1955. The views expressed in the translated material, therefore, are intended to be those expressed by the original authors, and not those of the translators nor of the American Institute of Physics.

One volume is published annually. Volume 1 (1955) contains three issues. Subsequent volumes, beginning with January 1956, will contain six issues.

Subscription Prices:

Per year (6 issues)
United States and Canada $30.00
Elsewhere 32.00

1st Volume (3 issues)
United States and Canada $15.00
Elsewhere 16.00

Back Numbers
Single copies ..... $ 6.00

Subscriptions should be addressed to the American Institute of Physics, 57 East 55 Street, New York 22, New York.

SOVIET PHYSICS

JETP

SOVIET PHYSICS JETP VOLUME 2, NUMBER 2 MARCH, 1956

Academician Nikolai Nikolaevich Andreev

(*On his 75th Birthday*)

J. Exper. Theoret. Phys. USSR 28, 137-139 (August, 1955)

A PROMINENT place among the Soviet scientists working in the field of acoustics belongs to Academician Nikolai Nikolaevich Andreev, whose fruitful activity is distinguished both for great scientific accomplishments and for active participation in the national-economic life of our country. Nikolai Nikolaevich's name is continuously associated with solutions to many vital problems in technical and architectural acoustics and with the application of these solutions to industrial and civilian construction.

Nikolai Nikolaevich Andreev was born on July 28, 1880, in Moscow. After completing the Moscow higher technical school (1900) he entered the Moscow University as a non-matriculated student, and from 1904 through 1909 he continued his education in universities abroad, first in Goettingen and then in Basel.

From 1909 through 1917 Andreev taught in the Moscow middle schools and in 1912 he became, in addition, a laboratory assistant in the Moscow University. In 1914 Andreev was appointed lecturer. During these years Andreev carried out scientific work in optics, molecular physics, and electrical oscillations. One of the works by Andreev, "Grating, Prism, Resonator", was published in 1915 (J. Russian Phys. Chem Sci. 47, No. 5) and has not lost its value for many years, exerting an influence on further spectrum analysis investigations made in the Soviet Union. Andreev's work of that period was by way of transition to subsequent work in the field of acoustics.

Andreev's 1917 Master's thesis was devoted to "Electrical Oscillations and their Spectra". In 1918-1920 he was professor of physics at the Omsk Polytechnic and Omsk Agricultural Institutes.

Andreev's work in the field of acoustics began in 1920, when he returned to Moscow and organized the Acoustic Laboratory in the All-union Electrotechnical Institute (VEI). In 1926 Andreev moved to Leningrad, where he directed the acoustic laboratory of the Leningrad Electrophysical Institute (LEFI).

Notable among the projects handled by Andreev in the Leningrad Laboratory is the development of acoustic measurement methods and the design of new measuring apparatus. Andreev suggested many original and yet simple methods for precise acoustic measurement, among them an elegant method for the absolute measurement of amplitudes of mechanical vibrations, namely, the fine-sand method, an extension of which (the small-hammer method) is particularly valuable for the study of surface distribution of vibration amplitudes by determining the equal-amplitude lines; he suggested methods of measuring acoustic impedances and of investigating acoustic filters. He also proposed several new instruments for acoustic measurements: a precise wide-range technical amplitude meter; and a widely-used automatic frequency analyzer for electric currents and for sounds. The production of Russian noise and reverberation meters is due to Andreev's initiative.

All these investigations at Andreev's laboratory provided a solid foundation for further development of Soviet acoustics. It must be noted that all the measurement methods and instruments developed by him incorporated the most modern accomplishments of electro-acoustics and electronics of our time.

The new instruments were used with success for a vigorous development of many very important problems in acoustics, such as the study of the vibrations of telephone membranes and of sound

recorders, study of the carbon microphone, investigations of the radiation and directivity of loud speakers, the development of loud-speaker horns, mesaurement of acoustic impedances, the study of engine noise, measurement of noise absorption and noise insulation and investigation of sound production by musical instruments and by air propellers. Important work was performed in non-linear acoustics and in acoustical and electroacoustical properties of solids (quartz, Rochelle salt and wood for musical instruments).

This list alone shows the wide scope and extent of Andreev's interests in modern acoustic problems. These investigations by Andreev and his students have been important steps, the value of many of which was not recognized by foreign science until the most recent years.

Andreev's theoretical accomplishments were also considerable. Nikolai Nikolaevich and his students formulated and successfully solved many difficult problems in the theory of non-linear acoustic vibrations and the associated effects of sound pressure (radiation pressures) and sound wind, as well as problems in hydrodynamic sound formation. The principal premises of the acoustics of a moving medium were formulated and published in Andreev's monograph " Acoustics of a Moving Medium" (1934). He made the first formulation of the principal premises of the reciprocity theorem not only for mechanical but also for electromechanical sytsems. In the field of atmospheric acoustics Andreev developed the theory of sound propagation near the earth's surface and has subsequently (1932-1933) participated directly in the planning and performance of experiments with pilot balloons in the stratosphere at polar latitudes.

Another branch of Andreev's theoretical investigations was closely related to pressing practical problems of industry and construction. As early as 1933 he developed together with his collaborators, the theory of the sound from an air propeller.

Andreev's Leningrad activities include the founding in 1931 of the Scientific Research Institute of the Musical Industry (NIIMP). In this Institute N. N. Andreev was the principal scientific leader and inspirer of many interesting and original projects in the development of the physical theory, research and quality control of musical instruments. Belonging to this period are his investigations of the properties of resonant wood, of the construction and tempering of many various instruments, and of sound production in string and wind instruments.

In 1940 N. N. Andreev turned his efforts to the USSR Academy of Sciences. He assumed the leadership of the acoustic laboratory of the P. N. Lebedev Physics Institute of the USSR Academy of Sciences (FIAN). The Moscow period of Andreev's scientific activity was just as successful and fruitful as the Leningrad period. N. N. Andreev surrounded himself with a strong group of talented students and followers, carrying out investigations in a variety of fields. Important works were devoted to the propagation of sound in inhomogeneous media, to correlation-statistical methods in acoustics, to non-linear acoustics, to ultrasonics, to architectural acoustics and to many other branches. Andreev headed up a group of investigations on the theory of sound absorption in porous and perforated materials. In connection with the construction of the Palace of the Soviets, with Andreev in close collaboration , a special laboratory on architectural acoustics was formed in Moscow before the war. Under Andreev's leadership the FIAN laboratory has assumed and important place in Soviet science and was reorganized in 1954 into the Acoustic Institute of the Academy of Sciences.

At the present time Andreev carries on important scientific work. During the past five years he published works on non-linear acoustics, on electrostriction and on physiological acoustics.
N. N. Andreev is widely known as an author of many scientific-popular works on acoustics, relativity, wave mechanics, thermodynamics, and electrodynamics. He thoroughly revised Michelson's widely known physics textbook and wrote many sections of the physics textbook edited and compiled by Academician N. D. Papaleksi.

Andreev is just as well known as an editor or as a member of the editorial staff of physics journals (Journal of Technical Physics, Journal of Experimental and Theoretical Physics, Proceedings of the Commission on Acoustics of the USSR Academy of Sciences); recently added to this list is the Acoustic Journal, in the foundation of which Andreev participated most actively.

Andreev devoted considerable attention to pedagogical activity. He was professor of the M. I. Kalinin Leningrad Polytechnical Institute, S. M. Budenny Leningrad Military Electrotechnical Academy and Moscow Correspondence Electrotechnical Institute.

Academician Andreev's students and followers were always stimulated and inspired by the breadth of his scientific interests, by this thorough knowledge of mathematics and by the high theoretical level of his approach to the solution of problems and by his tendency of invariably relating the scientific accomplishments to practical problems of Russia's national economy. Andreev succeeded also in imparting these principal approaches to the representatives of the scientific school he founded.

Andreev has always been a central figure in the acoustic fraternity of the Soviet Union; he unified about him all the activities in the organization, planning, and coordination of the scientific and scientific-technical work performed. He has been in charge of periodic conferences on acoustics since 1931, and of extended conventions of the Commission on Acoustics of the USSR Academy of Science, since 1936.

The Soviet Government has highly valued Andreev's services and has awarded him three Orders of Lenin, the Order of the Labor Red Banner, and several medals. In 1933 N. N. Andreev was selected an associated member of the USSR Academy of Science, and became a full member in 1953.

All Soviet men of science wish this great jubilarian, Nikolai Nikolaevich Andreev, many years of activity just as fruitful as he has so far been carrying on.

Translated by J. G. Adashko
165

SOVIET PHYSICS JETP VOLUME 2, NUMBER 2 MARCH, 1956

The Thermodynamic Theory of Magnetic Relaxation

G. R. KUTSISHVILI
Institute of Physics, Academy of Sciences, Georgian SSR
(Submitted to JETP editor May 22, 1954)
J. Exper. Theoret. Phys. USSR 29, 329-333 (September, 1955)

A thermodynamic consideration of magnetic relaxation is presented. With the aid of a symmetry principle of the kinetic coefficients, the time dependence of the magnetization and the internal temperature of the spin system has been found. Consideration is given to the conditions under which the internal spin-equilibrium is achieved far more rapidly than the equilibrium of the spin system with the lattice.

WE consider a condensed system (crystal, amorphous solid, liquid), which contains nuclei possessing spins. If initially the system of nuclear spins is not in thermal equilibrium with the other degrees of freedom of the body (with the "lattice"), then equilibrium is established within a certain length of time.

During the past few years, relaxation times of nuclear spins have been determined in various substances with the help of a study of nuclear magnetic resonance. We note that, in accord with experiment, the time path of approach to equilibrium has an exponential character (the law of the approach of nuclear magnetization to its equilibrium value has been determined in several experiments): The characteristic relaxation time is known as the relaxation time of the nuclear spins with the lattice.

In the case of paramagnetic relaxation the picture is much more complex: according to experiment, two relaxations occur, known as the spin-lattice and internal spin relaxations; the latter are observed only at high frequencies. Evidently two relaxations take place in the nuclear case also, but in the experiments which have been carried out at the present time, one of them (the internal spin) is not observed*.

Thermodynamic consideration of magnetic relaxation was first treated by Casimir and DuPre[1] under the assumption that internal equilibrium always exists in the spin system. A more general thermodynamic consideration was given in the researches of Shaposhnikov[2,3]. However, in these researches it was tacitly assumed that the internal relaxation time was much less than the time of spin-lattice relaxation. Although this is usually the case, it is nevertheless of interest to give a more general thermodynamic consideration of magnetic relaxation, making use of a basic principle of physical kinetics---the principle of the symmetry of the kinetic coefficients of Onsager. We also note that it is assumed in references 2,3 that the heat transferred from the lattice to the spin-system is proportional to the temperature difference which generally speaking, does not even occur (see below).

The consideration which we give is correct both for paramagnetic and for nuclear magnetic relaxation; in the latter case we shall assume that there is no strong electronic paramagnetism (i.e., our consideration will not be applicable to nuclear magnetic relaxations in paramagnetic salts and even less, to ferromagnetics).

We consider the case of a body which possesses magnetic isotropy; we shall consider the external magnetic field applied to the body to be homogeneous (the direction of the field we take to be the z direction) and constant in time. As a consequence of the fact that the direction of the external field is an axis of axial symmetry (thanks to the magnetic isotropy of the body), it is evident that the relaxation of the components of magnetization perpendicular to the field (in the case of nuclear magnetic relaxation, by magnetization we understand nuclear magnetization) M_x and M_y are independent of the relaxation of the longitudinal component M_z (which, for brevity, will be denoted by M) and the internal temperature of the spin system T.

In the present work we give the solution of the

* To avoid misunderstanding we note that by internal spin relaxation time we mean the time of establishing the internal equilibrium in the spin system; in contradistinction, in some researches in nuclear magnetism there is introduced the spin-spin relaxation, which is the inverse of the absorption line width.

[1] H. B. G. Casimir and F. K. DuPre, Physica 5, 507 (1938)

[2] I. G. Shaposhnikov, J. Exper. Theoret. Phys. USSR 18, 533 (1948)

[3] I. G. Shaposhnikov, J. Exper. Theoret. Phys. USSR 19, 225 (1949)

following problem: the initial state of the system is given with the aid of the initial values T_0 (the temperature of the lattice), T and M; it is required to find the time path of approach of these quantities to their equilibrium values. In this work we are not interested in the relaxations of the magnetization components perpendicular to the field.

We use a thermodynamic method; for its application it is necessary that the time required for the establishment of a state with definite T_0, T and M would be sufficiently small in comparison with the time of establishment of complete equilibrium (i.e., we assume that three time intervals are small: the time for the lattice to reach its equilibrium state, the time for the spins to reach equilibrium relative to the internal degrees of freedom, and the time for the spins to reach equilibrium relative to the Zeeman levels in the external field). We introduce the quantities m and τ

$$m = M - M_0, \quad \tau = \frac{1}{T} - \frac{1}{T_0}, \tag{1}$$

where M_0 is the equilibrium magnetization at temperature T_0. We decompose $\dot{m}$ and $\dot{\tau}$ (the dot denotes the time derivative) into powers of m and τ, and limit ourselves to linear terms:

$$\dot{m} = -\alpha m - \beta\tau, \quad \dot{\tau} = -\gamma m - \varepsilon\tau, \tag{2}$$

where the coefficients α, β, γ, and ϵ depend on the intensity of the external field and on the equilibrium temperature. With the substitutions $H \to -H$, $m \to -m$, $\tau \to \tau$ Eqs. (2) can be transformed into themselves; hence, we conclude that

$$\alpha(-H) = \alpha(H), \qquad \varepsilon(-H) = \varepsilon(H), \tag{3}$$
$$\beta(-H) = -\beta(H), \qquad \gamma(-H) = -\gamma(H).$$

We solve Eqs. (2) by taking m and τ proportional to $\exp(-\lambda t)$; for λ we obtain two values:

$$\lambda_{\pm} = {}^1/_2(\alpha + \varepsilon) \pm {}^1/_2\sqrt{(\alpha - \varepsilon)^2 + 4\beta\gamma}. \tag{4}$$

The real parts of λ_+ and λ_- must be positive; therefore,

$$\alpha + \varepsilon > 0, \quad \alpha\varepsilon - \beta\gamma > 0. \tag{5}$$

For m and τ we obtain solutions with two relaxations

$$m = C_+ \exp(-\lambda_+ t) + C_- \exp(-\lambda_- t), \tag{6}$$

$$\tau = \frac{1}{\beta}\{(\lambda_+ - \alpha) C_+ \exp(-\lambda_+ t) + (\lambda_- - \alpha) C_- \exp(-\lambda_- t)\}.$$

Among the quantities α, β, γ and ϵ there must be established one relation which makes use of the principle of the symmetry of kinetic coefficients[4,5]; for this purpose we introduce the equations (S = entropy of the entire system):

$$X_m = -\partial S / \partial m, \quad X_\tau = -\partial S / \partial \tau.$$

It is easy to obtain

$$\dot{X}_m = (\alpha S_{mm} + \gamma S_{m\tau})\, m + (\beta S_{mm} + \varepsilon S_{m\tau})\, \tau, \tag{7}$$
$$\dot{X}_\tau = (\alpha S_{\tau m} + \gamma S_{\tau\tau})\, m + (\beta S_{\tau m} + \varepsilon S_{\tau\tau})\, \tau.$$

The second derivatives of the entropy S_{mm}, $S_{m\tau}$, etc., in Eq. (7) are taken at full equilibrium.

Further, applying the principle of the symmetry of the kinetic coefficients, (assuming that m changes sign upon reversal of direction of the time, but τ does not change), we obtain

$$\beta S_{mm} - \gamma S_{\tau\tau} = (\alpha - \varepsilon) S_{\tau m}. \tag{8}$$

We shall assume that we are dealing with an ideal paramagnetic, so that we have for the heat capacity of the spin system (at constant magnetization) and for M_0

$$C = A / T^2, \tag{9}$$
$$M_0 = aH / T_0, \tag{10}$$

where A and a are constants (a = Curie's constant) Since we consider the case in which there is no spin system equilibrium between the internal and external (Zeeman) degrees of freedom, then, generally speaking,

$$M \neq aH / T.$$

In the work of Shaposhnikov[2] expression is found for the non-equilibrium thermodynamic potential of the spin system, in particular for an ideal paramagnetic substance,

$$\Phi = -\frac{A}{2T} - HM + \frac{TM^2}{2a}.$$

It is then easy to obtain the differential entropy of the spin system:

$$dS' = \frac{C}{T}\, dT - \frac{M}{a}\, dM.$$

Thus, for the entire system (lattice plus spin system), we obtain the second law of thermodynamics in the form (C_0 = heat capacity of the lattice):

$$dS = \frac{C_0}{T_0} dT_0 + \frac{C}{T} dT - \frac{M}{a} dM, \tag{11}$$

---

[4] L. D. Landau and E. M. Lifshitz, *Statistical Physics*, GITTL, Moscow, 1951

[5] S. R. deGroot, *Thermodynamics of Irreversible Processes*, North Holland Publishing Company, Amsterdam, 1952

according to the first law we have

$$C_0 dT_0 + C\,dT - H\,dM = 0 \qquad (12)$$

For the m and τ derivatives of S we get

$$S_m = -\frac{1}{a}\frac{\partial M}{\partial m}\,m + C\frac{\partial T}{\partial m}\,\tau,$$

$$S_\tau = -\frac{1}{a}\frac{\partial M}{\partial \tau}\,m + C\frac{\partial T}{\partial \tau}\,\tau$$

(the coefficients of m and τ are evaluated at equilibrium). We therefore get for the second derivatives of the entropy, taken at complete equilibrium,

$$S_{mm} = -\frac{1}{a}\frac{\partial M}{\partial m}, \quad S_{\tau\tau} = C\frac{\partial T}{\partial \tau}, \qquad (13)$$

$$S_{\tau m} = -\frac{1}{a}\frac{\partial M}{\partial \tau} = C\frac{\partial T}{\partial m}.$$

Making use of Eqs. (1) and (12), it is easy to obtain, after several transformations,

$$\frac{\partial M}{\partial m} = \frac{(C_0+C)\,T^2}{G}, \quad \frac{\partial T}{\partial \tau} = -\frac{(C_0T^2+aH^2)\,T^2}{G}, \qquad (14)$$

$$\frac{\partial M}{\partial \tau} = -aC\frac{\partial T}{\partial m} = -\frac{aCHT^2}{G},$$

where

$$G = (C_0+C)\,T^2 + aH^2. \qquad (15)$$

Thus, for an ideal paramagnetic substance, Eq. (8) takes the form

$$aC(C_0T^2+aH^2)\gamma - (C_0+C)\beta = aCH(\alpha-\varepsilon). \qquad (16)$$

Equations (4), (6) and (16) give the solution of the problem under discussion for an ideal paramagnetic which has magnetic isotropy.

In particular, we consider the case in which the interaction of the lattice with the internal degrees of freedom of the spin-system is much stronger than its interaction with the external degrees of freedom of the spin system; in such a case we can assume that the amount of heat dQ transferred from the lattice to the spin system in the time dt is

$$dQ = \varkappa(T_0 - T)\,dt, \qquad (17)$$

where $\varkappa$ is the coefficient of thermal conduction between the lattice and the spin system [in the general case Eq. (17) would also contain terms proportional to $(M_0 - M)\,dt$]. According to Shaposhnikov[2] (who considered the case in which the departure from equilibrium is small), we then have

$$C\dot{T} - H\dot{M} = \varkappa T^2\tau.$$

Making use of Eqs. (2) and (14), and taking into account the fact that the latter equation must hold for the m and τ derivatives, it is easy to obtain

$$\gamma = -(H/CT^2)\alpha, \qquad (18)$$

$$H\beta + CT^2\varepsilon = (G/C_0)\varkappa. \qquad (19)$$

From (16), (18) and (19) we can easily obtain the relations

$$\beta = -aH\left(\alpha - \frac{\varkappa}{C_0}\right), \qquad (20)$$

$$\varepsilon = \frac{aH^2}{CT^2}\alpha + \frac{C_0+C}{C_0C}\varkappa, \qquad (21)$$

$$\alpha\varepsilon - \beta\gamma = \frac{G}{C_0T^2C}\varkappa\alpha. \qquad (22)$$

It follows from Eqs. (5), (21) and (22) that the following inequalities must hold:

$$\alpha > 0, \quad \varepsilon > \frac{aH^2}{CT^2}\alpha, \quad \varepsilon > \frac{C_0+C}{C_0C}\varkappa. \qquad (23)$$

Thus, to satisfy the condition (17) we have three independent relations among the coefficients α, β, γ, and ϵ [e.g., Eqs. (18), (19) and (21)]. Let

$$C_0 \gg C, \quad C_0 \gg aH^2/T^2. \qquad (24)$$

In the nuclear case, the conditions (24) prevail for all fields and temperatures currently attainable; in the paramagnetic case, (24) holds for temperatures above 1° K. In such a case, Eqs. (20), (21) and (22) take on the form

$$\beta = -aH\alpha, \qquad (25)$$

$$\varepsilon = (aH^2/CT^2)\alpha + (\varkappa/C), \qquad (26)$$

$$\alpha\varepsilon - \beta\gamma = (\varkappa/C)\alpha. \qquad (27)$$

Now suppose that the following condition is satisfied, in addition to (17) and (24):

$$\alpha + \varepsilon \gg \varkappa/C \qquad (28)$$

or, what amounts to the same thing,

$$\alpha \gg (\varkappa T^2/A)(1-F), \qquad (29)$$

where

$$F = aH^2/(A + aH^2). \qquad (30)$$

In this case, Eq. (4) takes the form

$$\lambda_+ = \alpha + \varepsilon; \tag{31}$$

$$\lambda_- = (\varkappa / C)\alpha / (\alpha + \varepsilon) \ll \lambda_+. \tag{32}$$

We thus obtain one fast relaxation time ($1/\lambda_+$) and one slow one ($1/\lambda_-$). According to Eq. (6), after a lapse of time much greater than $1/\lambda_+$,

$$m = C_- \exp(-\lambda_- t), \quad \tau = C_- \frac{\lambda_- - \alpha}{\beta} \exp(-\lambda_- t),$$

and we obtain [keeping in mind that, by (29) and (32), $\lambda_- \ll \alpha$]

$$m/\tau = -\beta/\alpha = aH. \tag{33}$$

On the other hand it is easy to see that the ratio m/τ must be just the same if $M = aH/T$ (i.e., if there is equilibrium between the internal and external degrees of freedom of the spin system).

We thus see that if the conditions (17), (24) and (28) are satisfied, then the picture of magnetic relaxation must be the following: first, after a short time [relaxation time $\rho_s = (1 - F)/\alpha$] internal equilibrium is achieved in the spin-system; the equilibrium of the spin-system with the lattice is achieved more slowly [relaxation time $\rho_l = A/(1 - F)\varkappa T^2 = C/\varkappa(1 - F)$]*. Since, by experiment, the picture of magnetic relaxation is in most cases exactly the same, we must conclude that the conditions (17) and (28) are ordinarily satisfied.

In conclusion, I wish to express my gratitude to Academician L. D. Landau for his constant interest in the present research.

* If the weaker condition $(\varkappa/C)\alpha \ll (\alpha + \epsilon)^2$ is satisfied rather than (28), then Eqs. (31) and (32) remain valid, but if $H > \sqrt{A/a}$, Eq. (33) is not obtained, since the inequality $\lambda_- \ll \alpha$ is not satisfied. In this case, we obtain one fast and one slow relaxation as before, but the internal spin equilibrium is achieved only along with the establishment of equilibrium of the spin system with the lattice.

Translated by R. T. Beyer
199

The Effect of the Method of Demagnetization of the Specimen on the Temperature Dependence of the Magnetization of Nickel in Weak Fields

A. I. DROKIN AND V. L. IL'IUSHENKO
Krasnoyarsk State Teachers' Institute
(Submitted to JETP editor June 10, 1954)
J. Exper. Theoret. Phys. USSR 29, 339-344 (September, 1955)

By two different methods, a study was made of the effect of the method of demagnetization of the specimen on the temperature variation of the intensity of magnetization of nickel in weak magnetic fields.

1. INTRODUCTION

THE temperature dependence of the magnetization of nickel in weak fields depends materially on the method of demagnetization of the specimen before the start of the measurements. Analysis of the works of various investigators[1,4] on the study of magnetic temperature-hysteresis of ferromagnetics, in which the ascending branch of a cycle portrays the temperature variation of the magnetization in weak fields, shows that the demagnetization of the specimen before the measurements was usually carried out with alternating current, gradually decreased to zero.

However, a study of the magnitude of the observed magnetostriction, carried out by Vlasov[5], and the change of shape of the magnetization curve for different methods of demagnetization, studied by Kondorskii[6], suggest that the results of measurements of the temperature dependence of the magnetization of nickel in weak fields may depend on the method of demagnetization of the specimen before the start of the measurements.

In the present work, a study was made of the effect of two methods of demagnetization of the specimen on the temperature variation of magnetization in nickel. One method consisted in heating above the Curie point and then cooling in the absence of a magnetic field. The other was the method of alternating current of diminishing amplitude. at the initial test temperature.

2. SPECIMENS STUDIED AND METHOD OF MEASUREMENT

The experiments were done on a cylindrical specimen of pure nickel (99.98%), of diameter 1.05 mm and length 100 mm. To relieve the internal stresses, the specimen was annealed in a vacuum for eight hours at 1000° C and then cooled slowly in a magnetic shield. During the measurements, steps were taken to prevent work-hardening or strain of the specimen. The investigations were carried out by two methods: the method of automatic photographic recording on a vertical astatic magnetometer, and the method of counting the discontinuous changes of magnetization on a special amplifier.

The diagram of the vertical astatic magnetometer is shown in Fig. 1. A beam of light, reflected by the mirror of the astatic suspension, fell on the slit of the camera Ф. On this same slit there fell a beam from the mirror of the pyrometer galvanometer G_2, connected in the circuit of a thermocouple; one junction of the thermocouple was in direct contact with the specimen, the other was in a constant-temperature bath of melting ice. The construction of the vertical astatic magnetometer has been described in detail in the literature[1-4]

A novel experimental feature of the present investigation is the simultaneous automatic photographic recording of the intensity of magnetization and of the temperature, in the form of a magnetothermogram. The camera is a cylindrical drum of diameter 6 cm and length 30 cm, inserted in a cylindrical jacket, along a generator of which there runs a narrow slit. To the camera drum is fastened the photographic film, clamped with a special holder. At the time of the measurements the camera drum is rotated about a horizontal axis by

[1] Ia. S. Shur and V. I. Drozhzhina, J. Exper. Theoret. Phys. USSR 17, 607 (1947)

[2] V. I. Drozhzhina and Ia. S. Shur, Izv. Akad. Nauk SSSR, Ser. Fiz. 11, 539 (1947)

[3] Ia. S. Shur, N. A. Baranova and V. A. Zaikova, Dokl. Akad. Nauk SSSR 81, 557 (1951)

[4] Ia. S. Shur and N. A. Baranova, J. Exper. Theoret. Phys. USSR 20, 183 (1950)

[5] A. Ia. Vlasov, Izv. Akad. Nauk SSSR, Ser. Fiz. 16, 680 (1952)

[6] E. I. Kondorskii, J. Exper. Theoret. Phys. USSR 10, 420 (1940)

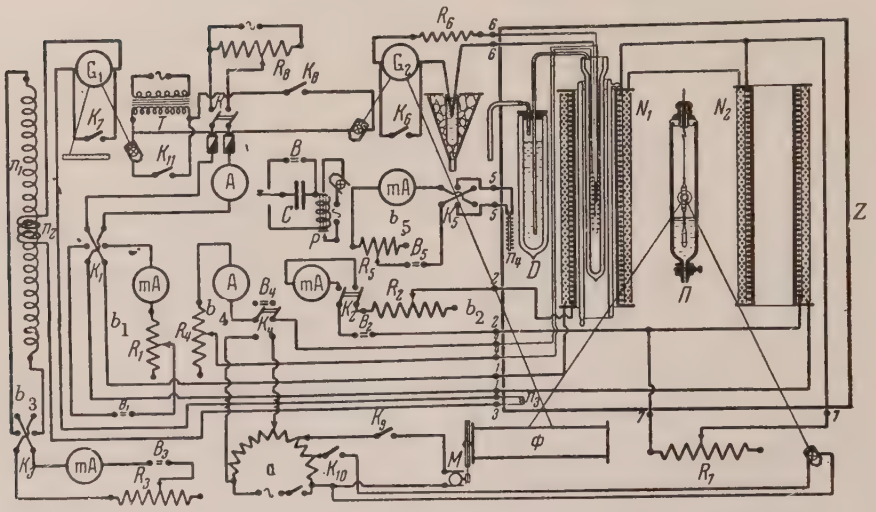

FIG. 1. Diagram of the astatic photographically recording magnetometer. N_1 and N_2, magnetometer coils; П, astatic suspension; D, liquid oxygen system; b_1, magnetizing circuit; consisting of battery B_1, rheostat R_1, milliammeter mA, reversing switch K_1, and magnetizing windings of the magnetometer coils. b_2, compensating circuit, consisting of battery B_2, switch K_2, milliammeter mA, rheostat R_2 and compensating windings on the magnetometer coils. b_3, calibrating circuit consisting of standard solenoid with windings n_1 and n_2, ballistic galvanometer G_1, damping switch K_7, reversing switch K_3, milliammeter mA, battery B_3, rheostat R_3 and calibrating solenoid n_3. b_4, heating circuit, consisting of bifilar furnace winding, supplied with alternating current from autotransformer a or with direct current from battery B_4, selecting switch K_4, ammeter A and rheostat R_4. b_5, means of calibrating camera with respect to magnetization of specimen, consisting of calibrated coil n_4, reversing switch K_5, milliammeter mA, rheostat R_5 and battery B_5. The demagnetizing circuit is connected to potentiometer R_8; it functions when switch K is closed and reversing switch K_1 is open. B, battery for the automatic device for horizontal light marks. C and P, condenser and relay of the automatic marker. G_2, galvanometer; K_6, damping switch; R_6, thermocouple resistance; T, lamp transformer; K_{10} and K_{11}, lamp switches; K_9, switch for motor M; Φ, camera; R_7, shunt; Z, magnetic shield.

the Warren motor M. The speed of rotation of the drum is 1 revolution per hour.

By means of an automatic marking device, there are produced on the magnetothermogram marks of equal width, which simultaneously determine a magnetization and a temperature of the specimen. The calibration of the camera scale for intensity of magnetization is accomplished by means of the calibrating solenoid n_3*, inserted in place of the specimen, on the basis of the current through its winding[7].

Translator's note: From the context, this appears to be an error for "calibrated coil n_4".

[7] I. V. Antik, E. I. Kondorskii et al, Magnetic Measurements (State Institute of Technology, 1939), p. 29

Before the start of the measurements, the specimen was heated to 400° C and cooled in a magnetic shield to – 183° C. During this step, the vertical component of the earth's magnetic field and of other extraneous parasitic fields was compensated with the single-layer compensating winding of the magnetometer. During the cooling, the magnetometer mirror remained steadily at the zero position.

A magnetizing field of strictly constant magnitude was applied, and the specimen was heated to 400° C. During the heating of the specimen, the camera operated, and the variation of the temperature and magnetization of the specimen was recorded on the film. After this the camera was

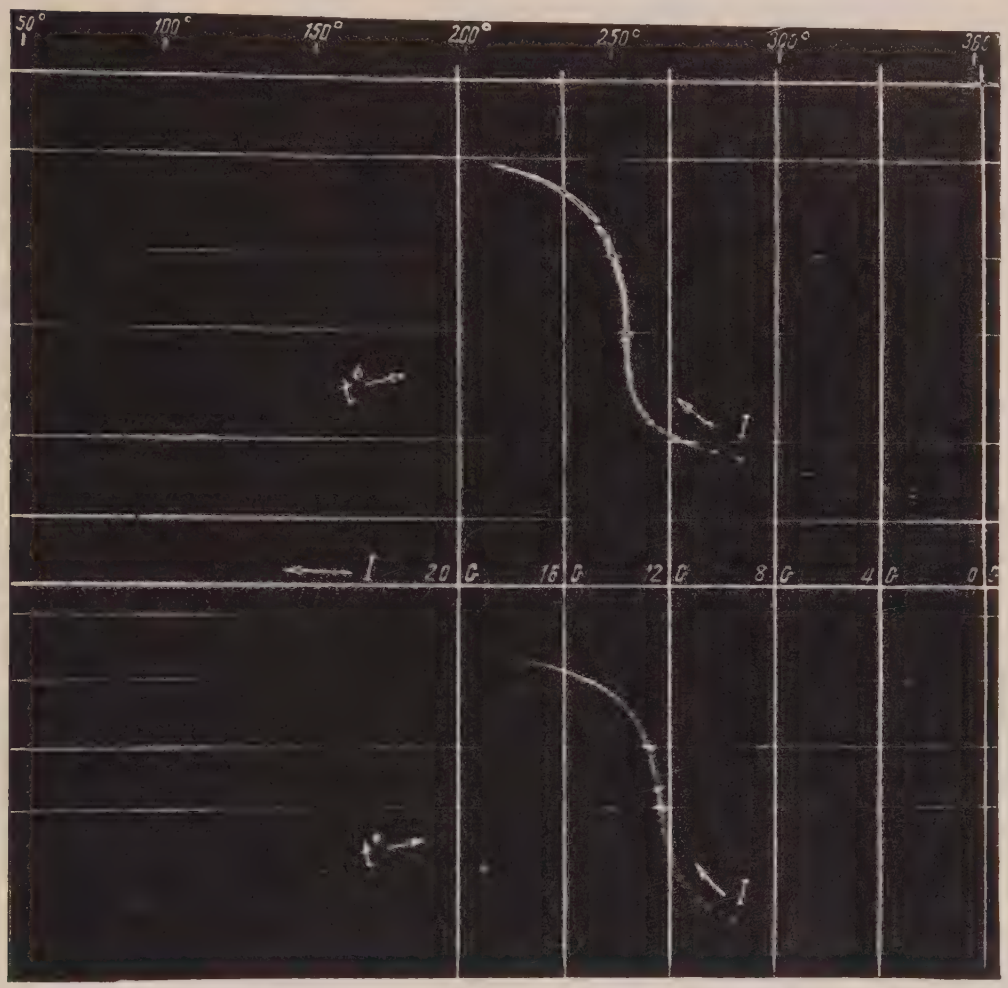

FIG. 2. Magnetothermograms. t^0 → variation of the temperature of the specimen, I → resulting variation of the intensity of magnetization of the specimen. *a*, specimen demagnetized in the initial state with alternating current, gradually diminished to zero; *b*, specimen demagnetized by heating to 400° C and cooling in a magnetic shield to the initial state (-183° C). The variation of the temperature from -183 to 50° is suppressed.

closed and stopped. The magnetizing field was removed, and the specimen was cooled to - 183° C. The specimen was demagnetized with alternating current, whose amplitude was gradually diminished to zero by means of the potentiometer R_8.

Then the same magnetizing field was applied, the camera slit was opened, the camera motor was connected and the specimen was heated to 400° C.

The experiment was carried out in various fields; and consistent differences were observed, in the temperature behavior of the curves of intensity of magnetization, between the two methods of demagnetizing the specimen. The differences were more noticeable, however, in weak fields than in fields of order 2 to 3 oersteds and higher. For illustration, Fig. 2 shows a magnetothermogram taken in a field of 0.39 oersted.

In the investigation by the method of counting discontinuous changes of magnetization, apparatus was used whose measurement principle has been described in detail in the literature[8,9]. A somewhat modified, improved scheme is depicted in Fig. 3.

The same specimen was used in this investigation as in the first case. The specimen with a thermocouple was placed inside a bifilarly wound furnace,

---

[8] B. F. Tsomakion and V. F. Ivlev, Dokl. Akad. Nauk SSSR 76, 205 (1951)

[9] V. F. Ivlev, Izv. Akad. Nauk SSSR, Ser. Fiz. 16, 664 (1952)

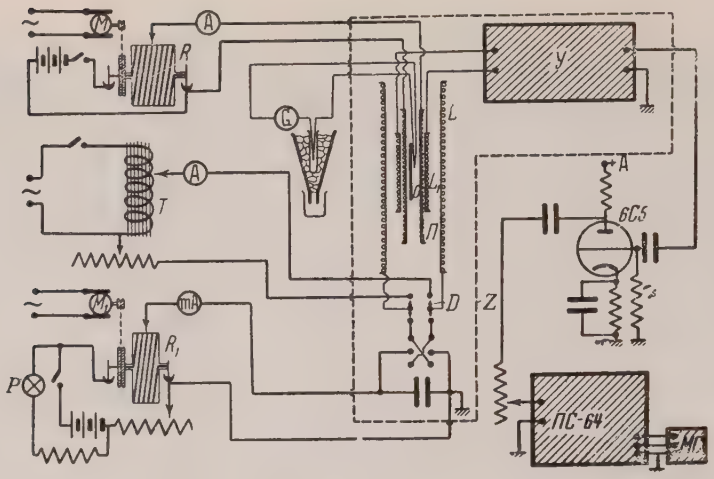

FIG. 3. Schematic diagram of the apparatus. R and R_1, rotating rheostats; M and M_1, Warren motors; T, autotransformer; y, amplifier; L, magnetizing coil; L_1, test coil; П, furnace; 0, specimen; ПС-64 (PS-64), counter circuit; MC, mechanical counters; D, reversing switch; Z, magnetic shield; P, pilot lamp; G, pyrometer; A, ammeter; mA, milliammeter.

which was inside a test coil L_1. The test coil was connected to the input terminals of a three-stage amplifier. A gradual change of temperature was produced by variation of the furnace current by means of a rotating rheostat R. Upon change of the temperature of the specimen---which was in a constant magnetic field, produced by the magnetizing coil L---, there occurred at the terminals of the test coil short-time voltage impulses, caused by Barkhausen jumps. These impulses indicated changes of magnetization; they were picked up by the amplifier and entered the input terminals of a counter circuit, type PS-64. The number of discontinuous changes of magnetization was registered on mechanical counters, type SB-1 M/100.

Before the start of the measurements, the specimen was demagnetized with alternating current of diminishing amplitude at temperature -183° C. The magnitude of the alternating current in the coil 1 (Fig. 3) was gradually decreased to zero by means of the rheostat and autotransformer T. The magnetizing field was applied with reversing switch D, and the specimen was slowly heated to 400° C. The discontinuous changes of magnetization upon heating of the specimen were registered on the mechanical counters. The number of jumps was recorded in each of the temperature intervals - 183 to 0, 0 to 150, 150 to 300 and 300 to 360° C.

Separate counters registered discontinuities of different volumes.. Then the specimen was demagnetized by heating to 400° C and cooling in a magnetic shield to - 183° C. The magnetizing field and the measuring apparatus were again connected, and the specimen was heated to 400° C.

The mechanical counters registered the discontinuous changes of magnetization during the heating.

3. RESULTS OF THE MEASUREMENTS

The data from the magnetothermogram of Fig. 2 are plotted in Fig. 4. It is evident that when the specimen was demagnetized by heating to 400° C and then cooling in a magnetic shield, heating in a field of 0.39 oersted produced an increase in the intensity of magnetization (Curve 1). At 180° C the rate of increase slowed down, and at 250° C there was a point of inflection; this corresponded to intensity of magnetization 12.3 gauss. Further heating of the specimen again speeds up the increase of the intensity of magnetization; near the Curie point (360° C) the intensity of magnetization reaches a maximum value of 19.2 gauss (Hopkinson's maximum)[10] and then drops to zero.

Demagnetization of the specimen in the initial thermal state, with alternating current of diminishing amplitude, and subsequent heating in a field of 0.39 oersted, give qualitatively the same

[10] J. Hopkinson, Trans. Roy. Soc. (London) 153, 443 (1885)

picture; but the curve of intensity of magnetization, in every section of the temperature range studied, is higher (Curve 2), and the point of inflection occurs at temperature 200° C, which corresponds to intensity of magnetization 13.3 gauss. The magnitude of Hopkinson's maximum remains the same.

The investigations by counting discontinuous changes of magnetization showed that the number of these jumps also depends on the method of demagnetizing the specimen. Demagnetization of the specimen in the initial state, with alternating current of diminishing amplitude, produces consistently more discontinuous changes of magnetization than does demagnetization of the specimen by heating and then cooling in a magnetic shield.

In Tables I and II are presented the data taken with the counters on heating the specimen in the same field of 0.39 oersted. In fields of other magnitudes, the same relation was observed.

These Tables show the dependence of the number of discontinuities of different magnitudes (volumes)[8] on temperature.

The apparatus permitted detection of discontinuous changes of magnetization of regions whose dimensions exceeded 2×10^{-9} cm^3. In the temperature interval 300-360° C (near the Curie point), the jumps were not detected by the apparatus because of the small volumes of the reversing

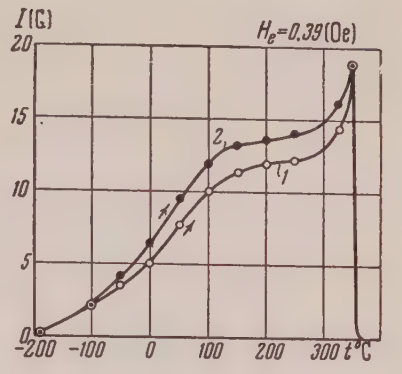

FIG. 4. Effect of the method of demagnetization of the specimen on the temperature variation of the intensity of magnetization of nickel in a field of 0. 39 oersted. *1*, specimen demagnetized by heating to 400° C and cooling in a magnetic shield to -183° C; *2*, specimen demagnetized in the initial state with alternating current, gradually decreased to zero.

TABLE I

Specimen demagnetized by heating to 400° C

t °C	$V \times 10^9$ cm^3						Combined number of jumps
	2,5	3,5	4,5	5,5	6,5	7,5	
	Number of jumps, registered by separate counters						
—183—0	5	3	0	0	1	1	10
0—150	6	2	0	1	0	1	10
150—300	3	0	0	0	0	0	3
300—360	0	0	0	0	0	0	0

TABLE II

Specimen demagnetized by alternating current with amplitude diminishing to zero

t °C	$V \times 10^9$ cm^3						Combined number of jumps
	2,5	3,5	4,5	5,5	6,5	7,5	
	Number of jumps, registered by separate counters						
—183—0	18	4	3	3	1	2	31
0—150	13	8	4	4	1	2	32
150—300	4	0	0	1	0	0	5
300—360	0	0	0	0	0	0	0

regions. From the data of Tables I and II, Table III has been constructed; here is shown the dependence of the combined volume of all the reversing regions on the temperature.

TABLE III

t° C	Method of demagnetization	
	demagnetization by heating	demagnetization by alternating current
	Volume × 10^9 cm^3	
—183—0	37	110.5
0—150	35	122
150—300	7.5	15.5
300—360	0	0

4. ANALYSIS OF RESULTS AND CONCLUSIONS

Upon demagnetization of the specimen with alternating current, gradually diminished to zero, there is created a definite texture of antiparallel orientations of spin moments, which we must suppose also causes differences in the temperature variation of the intensity of magnetization of nickel. Such a texture insures principally longitudinal inversions, which occur in weaker fields than do transverse inversions.

Heating of the specimen in a constant field, after its demagnetization with diminishing alternating current, causes a more abrupt rise of the intensity of magnetization than in the case of demagnetization of the specimen by heating to the Curie point and then cooling in a magnetic shield to -183° C. The formation of such a texture is also indicated by the investigations conducted on discontinuous changes of magnetization. The number of jumps after demagnetization of the specimen by alternating current is greater than the number after demagnetization by heating above the Curie point and then cooling in a magnetic shield; this can be explained by the fact that in demagnetization of the specimen by alternating current, an antiparallel texture is created, and heating of the specimen in a field causes reorientation of domains of magnetic reversal along new directions of easy magnetization, and then along the field. In the case of demagnetization by heating above the Curie point, there is a random distribution of domains of magnetization, and heating in the field causes only reorientation along the field.

Since the temperature variation of the intensity of magnetization of the specimen forms the ascending branch of the magnetic temperature-hysteresis curve, it follows that in studies of magnetic temperature hysteresis, the specimen must be demagnetized by heating; for demagnetization with alternating current leads to production of a magnetic texture.

In conclusion, we remark that in order to obtain not merely qualitative but also quantitative demonstrations of the inferences from the present investigation, it is desirable to conduct, in parallel, measurements of the temperature variation of the intensity of magnetization and of the magnetostriction or electrical resistivity of the specimen in the field under study.

The conduct of such an investigation involves well-known technical and experimental difficulties. Nevertheless, the authors are setting themselves the task of accomplishing such an investigation in the future.

Translated by W. F. Brown, Jr.
201

The Scalar Field of a Stationary Nucleon in a Non-linear Theory

N. V. MITSKEVICH
Moscow State University

(Submitted to JETP editor May 12, 1954)
J. Exper. Theoret. Phys. USSR 29, 354-361 (September, 1955)

The properties of a spherically symmetrical non-linear scalar potential are investigated in detail, using the method of Chaplygin. An approximate numerical solution is derived, and the relation between self-energy and charge of a nucleon is obtained.

1. INTRODUCTION

NON-LINEAR generalizations of various fields (in particular the Maxwell field and the meson field) follows inescapably both from experimental facts and from the ideas of modern relativistic quantum field theory[1,2]. The polarization of the vacuum, and the transmutability of elementary particles, necessarily lead to non-linear effects. It is possible that a non-linear approach may explain to some extent the detailed structure of elementary particles. For example, one may imagine that the specific repulsive force between nucleons at very short distances[3] may be deduced theoretically from the non-linear equations of the meson field. Moreover, some versions of non-linear field theory[1,4] lead in the classical approximation to finite self-energies and thus solve the problem of particle stability. These theories predict from classical considerations effects which formerly were deduced from quantum-mechanical arguments, for example, the refraction of light by a constant field, and the scattering of light by light or by the field of a point charge[5-7]. In this connection it is clearly of great interest to transfer non-linear methods from electrodynamics into mesodynamics[2], a domain where all phenomena are microscopic and where it seems that non-linear effects should be more prominent.

The non-linear generalization of a classical theory can be made in various ways. For example, one may use the Lagrangian

$$L_N = \frac{b^2}{4\pi}\left(1 - \sqrt{1 - \frac{L}{b^2}}\right) \tag{1}$$

(see the work of Born and Infeld[4,8], and also reference 2). Here b is a constant, the maximum possible field-strength, and L and L_N are the Lagrangians of the linear and non-linear theory respectively. This Lagrangian can be used either for vector or scalar theory.

A second method is to look for a non-linear Lagrangian which has the form of a series in powers of the field-invariants[1,2]. To start with, one may be content to keep only the first non-linear term in the series, assuming that the remaining terms will give only small corrections. We shall apply this method to scalar meson theory (the results will apply equally to a free pseudo-scalar field). We shall investigate the meson field equation

$$\Box\varphi - (k_0^2 + \lambda\varphi^2)\varphi = 0, \tag{2}$$

which is obtained from the Lagrangian

$$L_{NS} = -\frac{1}{8\pi}\left\{\frac{\partial\varphi}{\partial x^\nu}\frac{\partial\varphi}{\partial x^\nu} + k_0^2\varphi^2 + \frac{\lambda}{2}\varphi^4\right\}.$$

This equation has been studied by several authors; it leads to the appearance of stauration in nuclear forces[9,10]. We consider the constant λ to be arbitrary. The theory of the nucleon-antinucleon vacuum and various other arguments indicate that $\lambda > 0$ if the non-linearity is of field-theoretic origin[11,12]. However, several authors[10,13] have found this type of theory to be unsatisfactory, both in its internal structure and in its relation to experiment.

---

[1] D. Ivanenko and A. Sokolov, *Classical Field Theory*, 2nd Ed. (GTTI, 1951)

[2] A. Sokolov and D. Ivanenko, *Quantum Field Theory*, (GTTI, 1952)

[3] R. Jastrow, Phys. Rev. **81**, 165, 636 (1951)

[4] M. Born and L. Infeld, Proc. Roy. Soc. **A144**, 425 (1934)

[5] C. Shubin and A. Smirnov, Dokl. Akad. Nauk SSSR **10**, 69 (1936)

[6] E. Schrödinger, Proc. Roy. Irish Acad. **47**, 77(1942); **49**, 59(1943)

[7] F. Rohrlich and R. L. Gluckstern, Phys. Rev. **86**, 1 (1952); H. A. Bethe and F. Rohrlich, Phys. Rev. **86**, 10 (1952)

[8] Ia. I. Frenkel', *Electrodynamics*, 1 (GTTI, 1934)

[9] L. I. Schiff, Phys. Rev. **84**, 1 (1951)

[10] W. Thirring, Z. f. Naturforsch **7a**, 63 (1952)

[11] B. J. Malenka, Phys. Rev. **85**, 686(1952)

[12] D. Ivanenko, D. Kurdgelaidze and S. Larin, Dokl. Akad. Nauk SSSR **88**, 245 (1953)

[13] H. Byfield, J. Kessler and L. M. Lederman, Phys. Rev. **86**. 17 (1952)

Other investigators[14-16] have considered the case $\lambda < 0$, which is also possible a priori, treating the non-linearity as a free invention which may lead to interesting consequences. Such a free non-linearity, not connected with quantum effects, and belonging to a purely classical field, may give effects which go outside the framework of ordinary classical and quantum-mechanical models.

Our discussion here will be purely classical. In the static spherically symmetrical case Eq. (2) takes the form

$$\varphi'' + \frac{2}{r}\varphi' - (k_0^2 + \lambda\varphi^2)\varphi = 0; \qquad (3)$$

For brevity we write $w(r, \varphi, \varphi', \varphi'')$ for the left side of Eq. (3).

2. GENERAL PROPERTIES OF THE SOLUTION AND CONDITIONS WHICH IT MUST SATISFY

We first formulate the general conditions which the potential must satisfy. We start from the fact that the total energy of the static field must be bounded. The total energy is given by

$$U = \iiint T_{44}\, d\tau \doteq \frac{1}{2}\int_0^\infty \left(\varphi'^2 + k_0^2\varphi^2 + \frac{\lambda}{2}\varphi^4\right) r^2\, dr. \qquad (4)$$

As $r \to \infty$ the solution must tend to a Yukawa potential (this first condition follows from the correspondence principle), and so the integral converges at infinity. From the requirement that the integral converge at zero, we deduce that as $r \to 0$ the leading term in φ must have the form $\varphi \sim cr^\alpha$ with $\alpha > -1/2$. This is the second condition on the solution.

From the form of Eq. (3) one can establish the general behavior of the potential φ at the origin. Observe first that our equation is exactly satisfied by the constant potentials[12,14]

$$\varphi_\pm = \pm k_0/\sqrt{-\lambda};\ \varphi = 0, \qquad (5)$$

and so we may have $\varphi' = 0$ at $r = 0$. We suppose that φ is bounded. Then we deduce

$$\lim_{r\to 0}(r\varphi'' + 2\varphi') = 0.$$

Suppose that in the neighborhood of $r = 0$ there exists a series[17] $\varphi' = \sum_{k=0}^{\infty} C_k r^k$; . Then

$$\lim_{r\to 0}\sum_{k=0}^{\infty} 2C_k r^k = -\lim_{r\to 0}\sum_{k=1}^{\infty} kC_k r^k;$$

from which follows $C_0 = 0$, so that if φ is bounded at zero then $\varphi'(0) = 0$. We shall consider the solutions which are not bounded at zero separately for each sign of λ.

Since Eq. (3) is unchanged when the sign of φ is changed, it is sufficient to treat the case where $\varphi \geq 0$ on some interval of values of r.

3. SOLUTIONS OF EQ. (3) WITH $\lambda > 0$

a) *Monotonicity of the Potential φ and Its First Two Derivatives*

Suppose that φ possesses an extremum. Then Eq. (3) at the extremum becomes

$$\varphi'' = (k_0^2 + \lambda\varphi^2)\varphi > 0,$$

showing that the extremum is a minimum. Since the equation has no singular points except $r = 0$, it follows from the first condition (the correspondence principle) that such a solution is to be rejected. Thus, any solution which tends to zero at infinity is monotonic.

Consider the condition for an inflection. At a point of inflection Eq. (3) becomes

$$\mathcal{L}\varphi' = r(k_0^2 + \lambda\varphi^2)\varphi > 0,$$

which contradicts the monotone property of φ ($\varphi' < 0$ for $r < \infty$). Therefore φ' is also monotonic.

Differentiating Eq. (3) once and substituting for $(k_0^2 + \lambda\varphi^2)$ from Eq. (3), we find

$$r\varphi''' + 2\varphi'' = r\left(k_0^2 + 3\lambda\varphi^2 + \frac{2}{r^2}\right)\varphi' < 0.$$

At an extremum of the second derivative we should have $\varphi'' < 0$, which contradicts the absence of inflections, because $\varphi' < 0$ implies that $\varphi'' > 0$ for sufficiently large r and hence $\varphi'' > 0$ everywhere.

In this way we have proved that a solution φ of Eq. (3) for $\lambda > 0$ which vanishes at infinity is monotonic together with its first two derivatives. From this it follows, by the earlier argument about the behavior at zero, that $\varphi(0) = \infty$.

---

[14] R. Finkelstein, R. Le Levier and M. Ruderman, Phys. Rev. 83, 326 (1951)

[15] N. Rosen and H. B. Rosenstock, Phys. Rev. 85, 257 (1952)

[16] H. B. Rosenstock, Phys. Rev. 93, 331 (1954)

[17] R. Emden. Gaskugeln, (Teubner, Leipzig and Berlin, 1907)

b) *Behavior of φ in the Neighborhood of Zero*

We here apply a method due to Chaplygin[18] for the approximate integration of differential equations, only we proceed rather differently from Chaplygin. The method gives, in a very simple and exact way, qualitative information about the solutions of various non-linear equations. In spite of the obvious deficiencies of the method, which were emphasized by Chaplygin, we believe that it has not yet received the attention it deserves. According to the theorem which Chaplygin proved, if y is a solution of the equation

$$y'' - f(x, y, y') = 0,$$

and z is a comparison function satisfying the inequality

$$z'' - f(x, z, z') > 0.$$

in the neighborhood of a given point x_0, with $z_0 = y_0$, $z_0' = y_0'$ at $x = x_0$, then $z > y$ in the neighborhood of x_0. A lower bound for y is obtained in the same way. Chaplygin's method is presumably related in some way to variational methods.

The theorem is valid provided that the equation has no singular points in the region under consideration. In our case we have to investigate $\varphi(r)$ as r tends to zero. Taking for a comparison function the hyperbola

$$y = \frac{C_1}{r} + C_2, \quad y' = -\frac{C_1}{r^2},$$

which touches the graph of the potential φ at $r = r_0$, we find according to Chaplygin's method

$$w(r, y, y', y'') = -(k_0^2 + \lambda y^2)\, y < 0,$$

and therefore $\varphi > y$ in the neighborhood of the point r_0 where the two curves touch. As we move the point r_0 closer to zero, we obtain a sequence of hyperbolas which descend more and more steeply (by the monotonicity property) with increasing r. Consider two consecutive hyperbolas; they intersect in a single point which lies between their points of contact. Therefore, the region in which y_{n-1} and φ do not intersect can be extended to the left to include the region in which $\varphi > y_n$. In this process the successive positions of r_0 cannot have a condensation-point other than zero, since otherwise we could apply Chaplygin's theorem at the condensation-point.

Thus it is proved that for $\lambda > 0$ the potential φ increases at the origin not slower than hyperbolically, and hence the requirement of a finite total field-energy is violated.

We make now a further estimate of the behavior of φ at the origin. Writing $x = k_0 r$ and $u = \sqrt{\lambda}\, r\varphi$, Eq. (3) takes the simpler form[15]

$$u'' = u + (u^3 / x^2). \tag{3a}$$

If now we suppose u bounded at zero (from the discussion by Chaplygin's method we know that $u_{x=0} \neq 0$), then for small x we have approximately $u'' = -C/x^2$ and hence $u = -C \ln x + C_1 x + C_2$, which contradicts our hypothesis. If we take for comparison a function $y = C_1 r^{\alpha} + C_2$ with $\alpha < -1$, then the graph of the solution of Eq. (3) lies below the graph of y in the neighborhood of the point where the two curves touch. Therefore, the departure of the potential φ from the Yukawa form in the neighborhood of the origin is expressed by a factor which diverges not more rapidly than logarithmically.

4. DISCUSSION OF EQ. (3) WITH $\lambda < 0$

a) *Existence of Non-monotone Solutions, and Behavior of the Potential at the Origin*

For convenience we write $\mu = -\lambda$. Then Eq. (3) becomes

$$\varphi'' + \frac{2}{r}\varphi' - (k_0^2 - \mu\varphi^2)\,\varphi = 0. \tag{6}$$

When $\varphi' < 0$, $\varphi''' > 0$, the inequality

$$\varphi > k_0 / \sqrt{\mu}. \tag{7}$$

is a necessary condition for either a maximum or an inflection.

To define the behavior of the potential at the origin, we consider first the acceptability of a potential which increases to infinity at the origin, in agreement with the second condition of Section 2. Taking a comparison function of the form $y = C_1 r^{\alpha} + C_2$ with $\alpha = -1/2$, it is easy to prove by Chaplygin's method that the potential increases faster than the comparison function at the origin. This is proved most conveniently by using an equation analogous to Eq. (3a) and making r tend to zero. Therefore, it is sufficient to confine our attention to the case $\varphi'(0) = 0$, which implies that the potential is finite in the whole space.

---

[18] S. A. Chaplygin, *A New Method for the Approximate Integration of Differential Equations*, (GTTI, 1950)

b) *Condition for an Inflection when* $\varphi' > 0$, $\varphi''' < 0$

We apply Chaplygin's theorem, taking as comparison function the straight line which touches the curve φ at a point of inflection ρ, namely

$$y = C_1 r + C_2;\ y' = C_1 > 0.$$

Then

$$w(r, y, y', y'') = (2C_1/r) - (k_0^2 - \mu y^2)\, y = z.$$

Assuming that $\varphi' > 0$, $\varphi''' < 0$, the condition for an inflection is

$$z > 0 \quad \text{for} \quad r_+ > \rho;\ z < 0 \quad \text{for} \quad r_- < \rho. \tag{8}$$

From this it follows at once that $k_0^2 > \mu y^2$. We now find a lower bound for φ. Eq. (8) implies

$$\begin{aligned}(k_0^2 - \mu y_-^2)\, y_- &> (k_0^2 - \mu y_0^2)\, y_0 \\ &> (k_0^2 - \mu y_+^2)\, y_+.\end{aligned} \tag{9}$$

Here y_0 is the potential at the point of inflection. We substitute in Eq. (9) $y_+ = C_1(\rho + \delta) + C_2 = y_0 + C_1\delta$, $y_0 = C_1\rho + C_2$, and then take the limit $\delta \to 0$, which gives

$$-3\mu y_0^2 + k_0^2 < 0;$$

We obtain the same result from the other half of Eq. (9) by taking $y_- = y_0 - C_1\delta$. Therefore, a necessary condition for such a point of inflection is

$$\frac{k_0}{\sqrt{\mu}} > y_0 > \frac{k_0}{\sqrt{3\mu}}. \tag{10}$$

a) *Investigation of the Solutions of Eq. (6) in a Phase Plane*

When the solutions of Eq. (6) are considered in a phase plane[14], the potential φ becomes the x-coordinate of the moving point, and the distance r from the origin becomes the "time" t. With these notations the equation becomes

$$\ddot{x} = -\frac{2}{t}\dot{x} + (k_0^2 + \lambda x^2)\, x = -\frac{2}{t}\dot{x} - \frac{dv}{dx}.$$

On the right stands a "force", which can be formally separated into the gradient of a potential plus a term which depends on the velocity and on the time. If the term $(2/t)\dot{x}$ were absent, the motion of the point would be conservative and its total energy K would be given by

$$K = \frac{\dot{x}^2}{2} + v(x) = \frac{\dot{x}^2}{2} - \frac{1}{2}\left(k_0^2 + \frac{\lambda}{2}x^2\right)x^2;\ \lambda < 0.$$

so that

$$dK/dt = [\ddot{x} - (k_0^2 + \lambda x^2)\, x]\,\dot{x} = 0.$$

Evidently the system will tend toward this state as $t \to \infty$.

The total energy of the point in its non-conservative motion will satisfy

$$\frac{dK'}{dt} = -\frac{3\dot{x}^2}{t} < 0,$$

as can be seen by considering a generalized potential which depends on x, $\dot{x}$ and t. In Fig. 1 the continuous lines are lines of constant energy for the conservative system. In non-conservative motions the energy will steadily decrease, and the orbits will cut continuous lines, as shown by the dotted lines in Fig. 1. Three families of solutions are obtained. Two of them represent functions which oscillate in space and tend to the special constant solutions (stationary points); these do not tend to zero at infinity. The third family is completely different. It is in the first place discrete since the point $\varphi = 0$, $\varphi' = 0$ is a saddlepoint in the phase plane and does not have stability against small changes of the potential at the origin. Secondly, the solutions of this family tend to zero at infinity. These solutions may be spoken of[15] as "particles"; a particular one which is without nodes has been derived in reference 14.

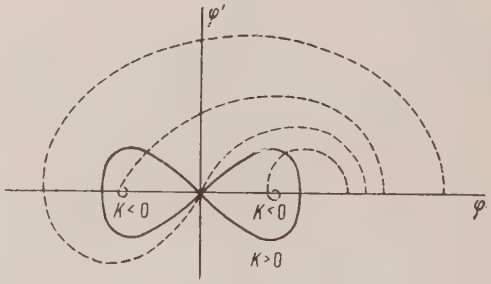

FIG. 1

Summarizing our qualitative investigation, we may say that Chaplygin's method enables us to obtain detailed information about the behavior of a non-linear potential, which is especially important for constructing solutions which change sign as r increases. Solutions with this property are of interest, because they correspond to particles with a repulsive interaction. We have also analyzed the reasons why divergent potentials cannot be used in

a theory which requires a finite total field-energy (the divergence is never weak enough). It has been proposed[9] that the divergences in the theory with $\lambda > 0$ and point charges will be weakened because the extended potential has a screening effect on the charges. This proposal is incorrect, although the potential in that case is repulsive.

5. APPLICATION OF THE RITZ METHOD TO FIND AN APPROXIMATE SOLUTION IN EQ. (6)

Eq. (6) is obtained by varying the functional

$$I = \int_0^\infty \left(\varphi'^2 + k_0^2\varphi^2 - \frac{\mu}{2}\varphi^4\right) r^2 dr. \qquad (11)$$

We substitute an approximate solution defined by joining together the functions

$$\begin{aligned} \varphi_1 &= a - br^2, \qquad r < \rho; \\ \varphi_2 &= g\left(\frac{e^{-k_0 r}}{r}\right), \qquad r > \rho. \end{aligned} \qquad (12)$$

The function and its first derivative must be continuous at the join ρ, which is taken as the parameter to be varied. Thus the important condition $\varphi'(0) = 0$ is maintained. From the variation of ρ we obtain a relation between ρ and μg^2. With the notation $\epsilon = k_0\rho$, the relation is

$$\mu g^2 = \frac{63 + 126\varepsilon + 111\varepsilon^2 + 54\varepsilon^3 + 13\varepsilon^4 + 2\varepsilon^5}{45{,}7 + 77{,}7\varepsilon + 55{,}6\varepsilon^2 + 19{,}6\varepsilon^3 + 3{,}45\varepsilon^4 + 0{,}2\varepsilon^5}. \qquad (13)$$

Since we cannot a priori attach any definite meaning to the quantity μ or even to the charge g, we proceed to a general discussion of Eq. (13). It is curious that an unbounded solution ($\epsilon = 0$) is obtained already when $g^2 = 1.378$, and not when g^2 tends to zero. Also, if we keep the value of φ at zero bounded for each μ, then g increases without limit as $\mu \to 0$. A similar picture (g decreasing) is obtained when we make $\mu \to \infty$. We find

$$10^{16}\,\mathrm{CGSU} < \mu < 10^{18}\,\mathrm{CGSU},$$

if g is confined within the physically interesting range $5e \leq g \leq 20e$. For other values of μ (for example greater values) one would have to look for a solution with one or more nodes.

The condition (7) for the possible occurrence of a maximum is easily shown to be satisfied for all physically interesting ϵ ($\epsilon < 1$). This fact is important, because the non-linearity must become significant somewhere "inside" the particle.

6. SELF-ENERGY OF A NUCLEON AT REST

To find the self-energy of a nucleon at rest, we substitute the approximate solution into Eq. (4). Expressing the coefficients a and b in terms of the other parameters by means of the continuity conditions, and carrying out the integrations, we find

$$u = u_1 + u_2, \qquad (14)$$

where

$$\begin{aligned} u_1 &= (g^2 k_0/210)(21\varepsilon^{-1} + 42 + 72\varepsilon + 18\varepsilon^2)\, e^{-2\varepsilon} \\ &\quad - (k_0\mu g^4/11080)(20523\varepsilon^{-1} + 16096 \\ &\quad + 5664\varepsilon + 960\varepsilon^2 + 64\varepsilon^3)\, e^{-4\varepsilon}, \end{aligned} \qquad (15)$$

$$u_2 = (g^2 k_0/2)(1 + \varepsilon^{-1})\, e^{-2\varepsilon} - k_0\mu g^4 \left\{0{,}25\varepsilon^{-1} e^{-4\varepsilon} + \int_{4\varepsilon}^{\infty} \frac{e^{-x}}{x}\, dx\right\}.$$

We substitute into Eq. (14) various values of ϵ, with the values of μg^2 which correspond to them according to Eq. 13), and thus obtain the results given in Table 1.

The ratio g/e is obtained here by comparing the expression for the self-energy of a nucleon of mass $1836.5m_e$ and unit quasi-electric charge with the approximate values which we have calculated.

ε	0.0	0.01	0.1	0.3	0.5	0.7	1,0	2,0
μg^2	1,378	1.41	1.735	2.46	4.35	6.83	13.56	126.9
$u/k_0 g^2$		4,0	1.48	0.74	0.368	0,226	0.126	
g/e		15.3	25.1	36.5	50.3	64.2	85.8	
$10^3\mu e^2$		6.02	2.76	1.95	1.72	1 66	1.84	

It is supposed that the whole of the nucleon mass is of pi-mesonic origin. If only a part of the mass is due to the meson field, the quantity g/e will be smaller.

We see that the results come close to the generally accepted values. It is interesting to observe that as ϵ varies μ remains roughly constant and has the order of magnitude 10^{16} CGSU The other quantities also vary over relatively narrow ranges, so that the agreements which are obtained do not seem to be due to chance.

In conclusion I express my deep gratitude to Professor D. D. Ivanenko, who set the theme of this work and gave much valuable advice, and also to Professors A. N. Tikhonov and V. V. Lebedev who took part in discussions.

Note added in proof.- Early in 1955 there appeared a paper by Fornaguera [19], in which non-linear equations are discussed for $\lambda > 0$ without imposing the condition that the total energy of a particle be finite. This paper includes some interesting observations about the many-particle interactions arising from non-linear equations. The results are also valid for the original case $(\lambda > 0)$ of our equation, although the interactions are then degenerate. Fornaguera's methods are elegant, and his work supplements the present paper so far as equations of the Schiff type are concerned.

[19] R. O. Fornaguera, Nuovo Cimento 1, 132 (1955)

Translated by F. J. Dyson
203

The Theory of the Acceleration of Charged Particles by Isotropic Gas Magnetic Turbulent Fields

S. A. KAPLAN
L'vov University

(Submitted to JETP editor May 31, 1954)
J. Exper. Theoret. Phys. USSR 29, 406-416 (October, 1955)

A theory of the acceleration of charged particles of an isotropic gas magnetic turbulence is developed. A kinetic equation is derived to determine the spectrum of rapid particles, and a method is given for solving this equation for various cases (stationary and non-stationary spectrum, account of magnetic-braking losses, etc.). The investigation makes wide use of the method of the theory of shower processes in cosmic rays.

THE considerable recent progress in the determination of the origin of cosmic rays is due to the rapid development of radio-astronomy[1,2]. It has become clear thereby that the most likely mechanism of cosmic-ray formation is the statistical acceleration of charged particles in a turbulent gas magnetic medium [2,3]. A certain role may also be played by the mechanism of induction acceleration in an increasing magnetic field[4,5]. An interesting variant of the statistical mechanism was proposed by Fermi[6], namely, the acceleration of particles in a "trap" between two approaching magnetic bursts such as may form in gas magnetic shock waves.

The present theories of statistical or induction acceleration[3,5] are not entirely satisfactory in view of their sketchiness, and in view of the incomplete account of the braking and absorption of particles. The question of the source of the primary acceleration of the particles, the so-called injection, still remains unsolved.

This article develops a theory of gas magnetic acceleration of charged particles, taking into account both the statistical and the induction mechanisms, and permitting us, at least in principle, to account for all possible conditions of injection, braking, and absorption of particles[7]. In the development of the theory we shall employ the mathematical methods of the theory of cosmic showers.

1. ACCELERATION OF CHARGED PARTICLES BY GAS MAGNETIC FIELDS

1. Statistical Acceleration by Gas Magnetic Turbulence. This mechanism is discussed in many investigations[2,3,7,8]. We shall therefore cite here only the final equations. When particles "collide" with a magnetic field fluctuation that moves with a velocity u, the energy E of the particle (including the rest energy) changes by an amount

$$|\Delta E| \approx \frac{uv(E)}{c^2} E, \tag{1}$$

here $v(E)$ is the velocity of the particle, and c is the velocity of light. The quantity ΔE is positive if u and v are in opposite directions, and negative otherwise. Thanks to the unequal probability of the positive and negative variations of the mean energy increment, we have

$$\overline{\Delta E} \approx \frac{u^2}{c^2} E. \tag{2}$$

The particles are thus systematically accelerated in this case. The magnitude of this acceleration computed per unit length, is given by the following equation

$$\left(\frac{dE}{dx}\right)_{\text{turb}} = \left(\frac{\overline{u^2}}{c^2 l}\right) E = \alpha_1(t) E, \tag{3}$$

where the averaging is performed over all vortex dimensions l that satisfy the conditions $l > r$ (inasmuch as Eqs. (1) and (2) are correct only in that case, in which the characteristic dimension of the fluctuation is greater than the radius of curvature r of the particle trajectory[7,8]). As the measure of the intensity of the energy fluctuations $D(E,t)$, namely the coefficient of diffusion along the "energy axis", we have

$$D(E, t) = (\overline{\Delta E})^2 / 2l = \frac{1}{2c^2} \alpha_1(t) [Ev(E)]^2. \tag{4}$$

[1] I. S. Shklovskii, Astr. Zhurnal 30, 577 (1953)

[2] V. L. Ginzburg, Usp. Fiz. Nauk 5, 343 (1953)

[3] E. Fermi, Phys. Rev. 75, 1169 (1949)

[4] Ia. P. Terletskii, Usp. Fiz. Nauk 44, 46 (1951)

[5] A. A. Logunov and Ia. P. Terletskii, Izv. Akad. Nauk SSSR, Ser. Fiz. 17, 119 (1953)

[6] E. Fermi, Astrophys. J. 119, 1 (1954)

[7] S. A. Kaplan, Circ. of L'vov Astronom. Obs. No. 27, 1953

[8] A. A. Logunov and Ia. P. Terletskii, J. Exper. Theoret. Phys. USSR 26, 129 (1954)

2. **Induction Acceleration by Gas Magnetic Fields.** It is well known that if the magnetic field intensity H increases systematically, the energy of the particles contained in that field also increases. To calculate the change in energy in this case it is most convenient to employ the adiabatic invariant[4]:

$$I = 3\pi c p_t^2 / eH. \tag{5}$$

Here p_t is the tangential component of the momentum and e is the charge of the particle. Assuming the velocities of the particles to be isotropic and using the well known relationship between the momentum and energy of the particles, we have

$$\frac{d \ln p_t^2}{dt} = \frac{d}{dt} \ln\left(\frac{E^2}{c^2} - m^2c^2\right) = \frac{d \ln H}{dt}.$$

Hence

$$\left(\frac{dE}{dx}\right)_{\text{ind}} = \frac{1}{v(E)} \left(\frac{dE}{dt}\right)_{\text{ind}} \tag{6}$$

$$= \frac{v(E)\,E}{2c^2} \frac{d \ln H}{dt} = \alpha_2(t) \frac{v(E)}{c} E.$$

3. **Acceleration in Gas Magnetic Bursts.** If a shock wave is formed in a gas located in a magnetic field, a sharp change in the field intensity and direction of the magnetic field takes place in the wave in addition to the discontinuity in density and pressure. If a particle is subjected to multiple "reflections" from a system of such bursts, the energy of the charged particle may increase by a noticeable fraction of its inertial value (reference 6 estimates this increase to be approximately 10-20%). It must be noted that the formation of a whole system of gas magnetic shock waves is quite frequently encountered in cosmic conditions. For example, the Crab Nebula, which is one of the most powerful sources of radio waves, is undoubtedly such a system, and is consequently also a source of cosmic radiation (according to references 1 and 2). However, this mechanism of acceleration[6] which, generally speaking, is a variant of the statistical mechanism, has not yet been studied in detail, and it is therefore still difficult to estimate its validity. If its role is really important, a very rough approximation can be obtained by using equations similar to (3) and (4), with additional factors, depending on multiplicity of the reflections in the "trap" – using Fermi's terminology[6]– i.e., in the region between two approaching bursts. For a more accurate analysis it is necessary to calculate the mean energy charge in the "trap" and then take into account the probability of the particle falling into this trap. For this, however, it is necessary to know the detailed structure of the system of gas-magnetic shock waves.

Although the acceleration by gas-magnetic shock waves is probably less important than the statistical or induction acceleration, this mechanism is apparently of primary importance for the injection, i.e., for the initial acceleration of the particles to a threshold that exceeds the level of energy losses by ionization. Let us first remark here that we detected intense sources of radio waves (testifying to the presence of rapid electrons) in the exact places where systems of gas magnetic shock waves exist (Crab Nebula, colliding galaxies, and similar objects[9]). Shklovskii[9] notes that when the shock waves have velocities of the same order as observed in the Crab Nebula, the thermal velocities of the electrons behind the wave front already approach the injection threshold. True, this does not explain the primary accelerations of the protons and of the heavy nuclei which, generally speaking, should be more probable than the acceleration of the electrons[2]. It seems to us that a thorough examination of the processes occurring in a gas-magnetic shock wave (including the process of the acceleration-in-a- "trap" type) will confirm the hypothesis concerning the injection of charged particles in gas magnetic shock waves. We shall not concern ourselves here with this question, partly because of its difficulty, and partly because the only thing we need to know for future considerations is the quantity $\nu(t)$, the total number of particles injected per unit volume per second. It is evident that

$$\nu(t) = \int_0^\infty \nu(E, t)\, dE, \tag{7}$$

where $\nu(E,t)$ is the number of injected particles with energies ranging from E to $E + dE$. The quantities $\nu(E,t)$ are obtainable by analysis of the acceleration process in gas magnetic shock waves. As far as $\nu(t)$ is concerned, we generally surmise that $\nu(t)$ is proportional to the energy dissipated in the gas magnetic shock waves. In the future this assumption will provide us with at least a qualitative estimate of the injection.

4. **Expression for the Acceleration Parameters in Terms of Spectral Functions of Gas Magnetic Turbulence.** If the gas magnetic medium in which the particles are accelerated is in a state of isotropic turbulence, the quantities u, l and H in Eqs. (3), (4) and (6) can be expressed in terms of

[9] I. S. Shklovskii, Dokl. Akad. Nauk SSSR 98, 353 (1954)

$F(k, t)$ and $M(k, t)$, namely, the spectral functions of the kinetic energy[10], respectively:

$$\alpha_1(t) = \frac{1}{\pi c^2}\int_0^\infty F(k, t)\, k\, dk, \tag{8}$$

$$\alpha_2(t) = \frac{1}{4c}\frac{d}{dt}\ln\int_0^\infty M(k, t)\, dk. \tag{9}$$

Taking into account the assumption that $\nu(t)$ is proportional to the energy dissipation in the gas magnetic shock waves, we can also write

$$\nu(t) \sim \int_0^\infty [F(k, t)\, k^3]^{1/2}\,[\zeta_f(k)\, F(k, t) - \zeta_m(k)\, M(k, t)]\, dk. \tag{10}$$

here the wave number $k = 2\pi/l$ and $\zeta_f(k)$ and $\zeta_m(k)$ are positive, slowly varying functions on the order of 1/10. The quantities $F(k,t)$ and $M(k,t)$ determine the kinetic and magnetic energy per unit mass, respectively, contained in vortices having wave numbers ranging from k to $k + dk$. For more details concerning the spectra of gas magnetic turbulence see reference 10.

2. BRAKING AND ABSORPTION OF PARTICLES

Along with the acceleration considered above, the moving particle will also experience braking because of the following processes:

(a) Ionization losses, as determined by the following equation[2]:

$$-\left(\frac{dE}{dx}\right)_{\text{ion}} = \frac{4\pi n_e e^4}{m_e v^2(E)}\, p(E, n_e) = \frac{\gamma c^2}{v^2(E)}, \tag{11}$$

where p is a function that exhibits a weak dependence on its arguments, and ranging approximately from 20 to 200 under cosmic conditions[2].

(b) Braking of rapid electrons by radiation in the magnetic field.

$$-\left(\frac{dE}{dx}\right)_{\text{mag}} = \frac{2}{3}\left(\frac{e}{m_e c^2}\right)^4 H_\perp^2 E^2 = \beta(t)\, E^2, \tag{12}$$

$$\beta(t) = \frac{16\pi\rho}{9}\int_0^\infty M(k, t)\, dk,$$

where ρ is the gas density. Here it is assumed $H_\perp^2 = 2H^2/3$.

(c) Braking of electrons by photon radiation and braking of protons by meson radiation. We shall denote by $(1/x_0)\,\varphi_0(y)\,dy$, where x_0 is the radiation unit length, the differential probability that a particle with energy E will have an energy in the interval from $(1 - y)E$ to $(1 - y - dy)E$ after radiating a photon or a meson over a one centimeter path. For the braking of electrons in un-ionized hydrogen we have:

$$\frac{1}{x_0} = \frac{4n}{137}\ln(137)\left(\frac{e^2}{mc^2}\right)^2. \tag{13}$$

If the hydrogen is ionized, x_0 is several times greater. The value of x_0 for the braking of protons by meson radiation is on the order of 13 (this is a coincidence). In the case of total shielding, the function $\varphi_0(y)\,dy$ has the following form[11]:

$$\varphi_0(y)\, dy = \left[1 + y^2 - \frac{2}{3}\, y\right] dy/y. \tag{13'}$$

Usually the acceleration particles occur in regions where the gas is ionized and where the shielding consequently takes place only in the case of very large energies. In the absence of shielding it is necessary to multiply (13′) by a factor that is logarithmically dependent on the energy. But this factor, which complicates the theory excessively, does not appear to be of importance in the problems discussed by us. So far, we know of no equations analogous to (13′) for the braking of protons by meson radiation.

(d) Energy pulses by electron due to the inverse Campton effect[12]:

$$-\left(\frac{dE}{dx}\right)_{\text{Comp}} = \frac{8\pi}{3}\left(\frac{e^2}{m_e c^2}\right)^2 \bar{n}_{\text{ph}}\bar{\varepsilon}_{\text{ph}}\left(\frac{E}{m_e c^2}\right)^2 \tag{14}$$

Here $\bar{n}_{\text{ph}}$ and $\bar{\varepsilon}_{\text{ph}}$ are the average number and average energy of the scattering photons. This mechanism is thus analogous in its energy dependence to the braking of electrons in a magnetic field, differing from it only in that in this case the energy losses occur, so to speak, in large doses.

(e) Finally, in some cases it is also necessary to take into account the "annihilation" of fast particles, for example, in the case of nuclear reactions. We shall denote the length of the mean free path for this process by Λ. Evidently

$$1/\Lambda = \sum_A n_A \sigma_A, \tag{15}$$

[10] S. A. Kaplan, Dokl. Akad. Nauk SSSR **94**, 33 (1954); J. Exper. Theoret. Phys. USSR **27**, 699 (1954)

[11] S. Z. Belen'kii, *Shower Processes in Cosmic Rays*, GITTL, Moscow, 1948

[12] L. D. Landau and Iu. B. Rumer, Proc. Roy. Soc. (London) A166, 213 (1938)

where n_A is the number of nuclei capable of entering into reaction per unit volume and σ_A is the corresponding effective cross section.

The first two energy-loss mechanisms are continuous. We shall take account of them by writing the algebraic sum for the value of the systematic change in energy.

$$\left(\frac{dE}{dx}\right)_{\text{tot}} = \left(\frac{dE}{dx}\right)_{\text{turb}} + \left(\frac{dE}{dx}\right)_{\text{ind}} + \left(\frac{dE}{dx}\right)_{\text{mag}} + \left(\frac{dE}{dx}\right)_{\text{ion}} \tag{16}$$

The remaining loss mechanisms should be accounted for by the corresponding terms in the kinetic equation. The most difficult to account for is the inverse Compton effect, because of its nonlinear dependence on the energy. In those (relatively rare) cases, when this effect must be taken into account, we shall therefore simply add Eq. (14) to Eq. (16).

In concluding this section, let us note that along with the acceleration, absorption, and braking of particles, it is also necessary in certain cases to take into account the direct formation of fast particles, for example, in the decomposition of mesons into electrons, in pair formations, in nuclear reactions, etc. These processes can be accounted for either by adding corresponding terms in the expressions for the injection, or else by setting up a system of kinetic equations with terms that account for the production of particles of a given kind by particles of another kind.

3. KINETIC EQUATION FOR THE SPECTRUM OF RAPID PARTICLES

In many cases of practical interest we can assume that the particle accelerates in the region of isotropic and homogeneous gas magnetic turbulence, where the primary sources, the injectors, are also uniformly distributed. This condition is satisfied, for example, if the injectors are gas-magnetic shock waves, which are bound to occur in a region occupied by a supersonic gas magnetic turbulence. In these cases we can disregard the spatial diffusion of particles, greatly simplifying the subsequent computations. Let us remark, however, that accounting for the spatial diffusion does not lead to any difficulties, in principle, in the mathematics[5] (see below).

In formulating the kinetic equation for the distribution function $N(E,t)$ of rapid electrons we must take into account both the systematic and stochastic accelerations of the particles (section 1), as well as the energy losses and absorption of the particles (section 2), and finally the injection. The systematic and stochastic acceleration, as well as the "continuous" losses, are taken into account using a method that is customary in this theory, that is, by writing down the expression[5]:

$$-\frac{\partial}{\partial E}\left[\left(\frac{dE}{dx}\right)_{\text{tot}} N(E,\ t)\right] + \frac{\partial^2}{\partial E^2}\left[D\,(E,\ t)\,N(E,\ t)\right]. \tag{17}$$

The braking by the radiation is taken into account in accordance with the theory of cosmic showers, using the following expression[11]:

$$\frac{1}{x_0}\int_0^1 \left[\frac{1}{1-y} N\left(\frac{E}{1-y},\ t\right) - N(E,\ t)\right]\varphi_0(y)\,dy. \tag{18}$$

The absorption of particles is accounted for by a term $\frac{1}{\Lambda} N(E,t)$. We thus have for the total change in the number of particles per unit volume per second

$$\frac{1}{v(E)}\frac{\partial N(E,t)}{\partial t} = -\frac{\partial}{\partial E}\left[\left(\frac{dE}{dx}\right)_{\text{tot}} N(E,\ t)\right] + \frac{\partial^2}{\partial E^2}\left[D\,(E,\ t)\,N\,(E,\ t)\right] + \frac{1}{x_0}\int_0^1 \left[\frac{1}{1-y} N\left(\frac{E}{1-y},\ t\right) - N(E,\ t)\right]\varphi_0(y)\,dy - \frac{1}{\Lambda} N(E,\ t) + \frac{\nu\,(E,\ t)}{v\,(E)} \tag{19}$$

This equation, together with Eqs. (3), (4), (6), (8) to (13), (15), and (16), determines the spectrum of the rapid particles. When solving this equation it is necessary to assume that the coefficients of this equation, together with the expression for the injection and the initial distribution function of the particles, areknown.

Equation (19) is valid for both relativistic and nonrelativistic regions of the particle spectrum. From now on, we shall restrict ourselves to the simpler and at the same time more interesting relativistic particles. In fact, if we exclude the corpuscular streams from the sun, where the acceleration is probably of more complicated character than the acceleration of the isotropic gas magnetic turbulence considered here, we need consider in all the remaining cases only the relativistic

region of the spectrum, both with respect to cosmic rays directly, as well as with respect to the magnetic-braking radiation. Besides, all the simplifications are reduced in the relativistic case to the assumption $v(E) = c$. The results obtained below will, therefore, be valid, in rough approximation, for nonrelativistic particles that are not too slow.

Thus, assuming $v(E) = c$, and taking into account the expressions given above for the coefficients of Eq. (19), we obtain

$$\frac{\partial N(E,t)}{dt} = -c\frac{\partial}{\partial E}\left[\left(\alpha(t)E - \beta(t)E^2 - \gamma\right)N(E,t)\right] + \frac{1}{2}c\alpha_1(t)\frac{\partial^2}{\partial E^2}[E^2N(E,t)] + \frac{c}{x_0}\int_0^1\left[\frac{1}{1-y}N\left(\frac{E}{1-y},t\right) - N(E,t)\right]\varphi_0(y)\,dy - \frac{c}{\Lambda}N(E,t) + \nu(E,t). \tag{20}$$

Here $\alpha(t) = \alpha_1(t) + \alpha_2(t)$, where we shall also include the acceleration in the "traps". The solution of Eq. (20) will be discussed below

Let us remark again that Eq. (20), like Eq. (19), does not take into account the spatial diffusion of the charged particles, occurring when the injector distribution is non-uniform. If it is necessary to take this into account, a term $lc\Delta_r N(E,t,r)/3$ is added to the first part of Eq. (20), where Δ_r is the Laplacian and the spectrum $N(E,t,r)$ depends also on the coordinate r.

Equations of the type (20), taking into account the spatial diffusion, are discussed in reference 5, where it is assumed, however, that the acceleration of the particles was due to an induction mechanism that becomes operative when the magnetic field intensity increases. In addition, reference 5 does not account for the braking with sufficient accuracy (the third term of the right half of (20) is lacking). Instead of taking into account the last term of (20), reference 5 seeks a source-type of solution, i.e., all particles are assumed to "escape" into the accelerating medium with the same energy. Thus Eq. (20) (see also reference 7) is more general than the analogous equation in reference 5 (in the sense that the braking and the acceleration of the particles are accounted for), and as we shall see below, it permits finding a more general solution, one that approximates more closely the actual cosmic conditions.

In conclusion let us remark, that if we are not interested in the dependence of the particle spectrum on the coordinates it is easy to calculate the particle diffusion from the region of the gas-magnetic medium consideration, by adding to the right half of (20) a term $(2cl/L^2)N(E,t)$, where L represents the linear dimensions of the system. In other words, instead of Λ it is now necessary to substitute in Eq. (20) the quantity

$$\frac{1}{\Lambda} = \sum n_A z_A + \frac{2\overline{l}}{L^2}. \tag{15'}$$

Equation (20), together with (15'), accounts for the diffusion of particles from the acceleration region with sufficient accuracy for the assumptions of the theory. Generally speaking, as follows from the observed fact that the proton spectra are similar to those of heavy particles, the first term of (15') is smaller than the second term[6].

4. SOLUTION OF KINETIC EQUATION

Equation (20), the same as the kinetic equations of the theory of cosmic showers, is best investigated with the aid of the Mellin transform[1,2]. Multiplying (20) by $E^s\,dE$, integrating from 0 to ∞, and assuming that the distribution function vanishes both at $E = 0$ as well as at $E \to \infty$, we obtain

$$\partial\mathfrak{N}(s,t)/\partial t = {}^1/_2 c\,[s(s+1)\alpha_1(t) + 2s\alpha_2(t)]\,\mathfrak{N}(s,t) - cs\beta(t)\,\mathfrak{N}(s+1,t) - c\gamma\mathfrak{N}(s-1,t) - \frac{c}{x_0}A(s)\,\mathfrak{N}(s,t) - \frac{c}{\Lambda}\mathfrak{N}(s,t) + \int_0^\infty E^s\nu(E,t)\,dE. \tag{21}$$

The following designations are used here:

$$\mathfrak{N}(s,t) = \int_0^\infty E^s N(E,t)\,dE \tag{22}$$

and

$$A(s) = \int_0^1 [1-(1-y)^s]\,\varphi_0(y)\,dy. \tag{23}$$

The function $A(s)$ is tabulated in reference 11 for electron braking by photon radiation. The quantity s, which becomes the variable in Eq. (21) instead of the variable E in Eq. (20), can be complex. After finding the function $\mathfrak{N}(s,t)$ from (21), the particle spectrum is determined with the inverse Mellin transform:

$$N(E, t) = \frac{1}{2\pi i} \int_{\delta-i\infty}^{\delta+i\infty} E^{-s-1} \Re(s, t)\, ds, \qquad (24)$$

where the path of integration is a straight line parallel to the imaginary axis in the positive half of the complex plane[11].

Equation (21) is a differential equation in t and a finite difference equation in s. The general solution of (21) will be discussed below, and we shall restrict ourselves at the present time to the case when the terms with $\beta(t)$ and γ can be neglected. Then (21) can be integrated with respect to time directly

$$\Re(s, t) = \int_0^t \nu(s, t') \exp\{I(s, t, t')\} dt'. \qquad (25)$$

where the following designations are introduced:

$$\nu(s, t) = \int_0^\infty \nu(E, t) E^s dE, \qquad (26)$$

$$\Phi(s, t) = \frac{1}{2} c\,[s(s+1)\alpha_1(t) + 2s\alpha_2(t)] - c\left[\frac{A(s)}{x_0} + \frac{1}{\Lambda}\right], \qquad (27)$$

$$I(s, t, t') = \int_{t'}^{t} \Phi(s, t'')\, dt''.$$

In addition, we subject (25) to an initial condition $\Re(s, 0) = 0$, which does not limit the physical generality of the solution. The particle spectrum is obtained, as was already noted, but inserting (25) into (24)

$$N(E, t) = \frac{1}{2\pi i E} \int_{\delta-i\infty}^{\delta+i\infty} \frac{ds}{E^s} \int_0^t dt' \nu(s, t') \exp[I(s, t, t')]. \qquad (28)$$

Expression (28) is calculated by the method of steepest descents, as is usually done in the theory of cosmic showers. This equation can be rewritten in the following form

$$N(E, t) = \frac{1}{2\pi i E} \int_0^t dt' \int_{\delta-i\infty}^{\delta+i\infty} \frac{\nu(s, t')}{(mc^2)^s} \times \exp\left\{-s \ln \frac{E'}{mc^2} + I(s, t, t')\right\} ds. \qquad (29)$$

The factor before the exponential in (29) is slowly-varying in s. As s varies along the real axis, the exponential index reaches a minimum at the point $s = s_m(I_{t'})$ under the following condition

$$\ln \frac{E}{mc^2} = \int_{t'}^{t} \left(\frac{\partial \Phi(s, t'')}{\partial s}\right)_{s=s_m} dt'', \qquad (30)$$

and consequently the integrand has a maximum at these points as s varies along the imaginary axis. Continuing with the usual procedure of the method of steepest descents[11], we obtain

$$N(E, t) = \frac{1}{E} \int_0^t \frac{\nu(s_m, t')}{(mc^2)^{s_m}} \left[\exp\left\{-s_m \ln \frac{E}{mc^2} + I(s_m, t, t')\right\}\right] \Big/ \sqrt{2\pi \left|\int_{t'}^{t} \left(\frac{\partial^2 \Phi}{\partial s^2}\right)_{s=s_m} dt''\right|} \qquad (31)$$

Further integration with respect to time depends naturally on the actual form of the dependence of ν and α on t. In this integration it is necessary to bear in mind that the value of s_m also depends on time as in Eq. (30).

Let us note that if nonrelativistic particles are injected (for example in the case of gas magnetic shock waves), we have

$$\nu(s, t) \approx (mc^2)^s \int_0^\infty \nu(E, t)\, dE = (mc^2)^s \nu(t) \qquad (32)$$

in accordance with (7).

Furthermore, it follows from (22) that $\Re(0,t)$ is the total number of high speed particles per unit volume, and $\Re(1,t)$ is the total energy of the rapid particles. Consequently, Eq. (25) at $s = 0$ and at $s = 1$ determines the time dependence of the total number of particles per unit volume and of their total energy per unit volume, respectively. Let us apply the solution of (25) and (31) to the case of a stationary turbulence, that is, let us assume that α and ν are independent of time. Then

$$\Re(s, t) = \nu (mc^2)^s (e^{\Phi(s)t} - 1)/\Phi(s), \qquad (33)$$

$$N(E,t) = \frac{\nu}{E}\int_0^t \left[\exp\left\{-s_m \ln\frac{E}{mc^2} + \Phi(s_m)(t-t')\right\}\right] \Big/ \sqrt{2\pi\left|\frac{d^2\Phi}{ds^2}\Big|_{s=s_m}(t-t')}\,dt', \quad (34)$$

where s_m is determined from the condition:

$$\ln = \left(\frac{d\Phi}{ds}\right)_{s=s_m}(t-t'). \quad (35)$$

and

$$\Phi(s) = \frac{1}{2}c\left[s(s+1)\alpha_1 + 2s\alpha_2\right] - c\left[\frac{A(s)}{x_0} + \frac{1}{\Lambda}\right]. \quad (36)$$

For large values of t, integral (34) can also be evaluated by the method of steepest descents. If we ignore the dependence of the factor in front the exponent in (34) on t', the exponent reaches a maximum at

$$\frac{ds_m}{dt'}\left\{-\ln\frac{E}{mc^2} + \left(\frac{d\Phi}{ds}\right)_{s=s_m}(t-t')\right\} - \Phi(s_m) = 0, \quad (37)$$

hence, according to (35), $\Phi(s_m) = 0$. After simple calculation we obtain finally

$$N(E)\,dE = \frac{\nu}{\left|\frac{d\Phi}{ds}\right|}\left(\frac{mc^2}{E}\right)^{s_0+1}\frac{dE}{mc^2}, \quad (38)$$

where s_0 is the root of equation $\Phi(s) = 0$. If this equation has two positive nonvanishing roots, it is necessary to take the smaller of the two, for in view of the statistical character of the acceleration mechanism, the system comprising the gas magnetic medium and rapid particles will tend toward equipartition of the energy, that is, to a more sloping spectrum of rapid particles.

It also follows from (35) that the time $\tau(E)$ required to establish an equilibrium spectrum is on the order of

$$(E) \approx \frac{1}{\left|\frac{d\Phi}{ds}\right|_{s_0}}\ln\frac{E}{mc^2}. \quad (39)$$

The spectrum (38) occurs also in the nonstationary turbulence state, provided the characteristic time of its variation exceeds $\tau(E)$ from (39).

By way of illustration let us give the following example. By reference 2, the values of $c\alpha$ and c/Λ in interstellar space can be assumed to be

$$c\alpha_1 = 5\times10^{-17}\ \text{sec}^{-1},$$

$$c\alpha_2 = 0,\ c/\Lambda = cn\sigma = 3\times10^{10}\times0.1\times2.5\times10^{-26}.$$

Substituting these values into (36) and assuming $\Phi(s_0) = 0$, we obtain $s_0 = 1.3$. Substituting into (38) we get:

$$N(E)\,dE = \nu\cdot10^{16}\left(\frac{10^9}{E}\right)^{2.3}\frac{dE}{10^9},$$
$$N(E>E_0) = \nu\,\frac{10^{16}}{1.3}\left(\frac{10^9}{E}\right)^{1.3}. \quad (40)$$

Here the energy is given in electron volts. According to references 1 and 2, the sources of cosmic radiation are supernova bursts. Considering them to be injectors, we have as an estimate for

$$\nu = \frac{\text{number of rapid particles formed in supernova}}{\text{frequency of supernova burst} \times \text{volume of galaxy}} \approx \frac{10^{51}}{30\times3\times10^7\times10^{68}} \approx 10^{-26}\,\text{sec}^{-1}\,\text{cm}^{-3}. \quad (41)$$

Substituting into (40) we get

$$N(E)\,dE \approx 10^{-10}\left(\frac{10^9}{E}\right)^{2.3}\frac{dE}{10^9},$$
$$N(E>1.5\cdot10^9) \approx 5\cdot10^{-11}\ \text{cm}^{-3}$$

which is in rather good agreement with observed data.

We gave this simple numerical calculation only as an example, without dwelling at all on the great importance of particular acceleration in interstellar space. It is also possible to consider in an analogous manner the acceleration of particles in the expanding ejected supernova shells. Inasmuch as we deal here with a nonstationary problem the starting equation is (31).

In conclusion let us dwell shortly on the calculation of the ionization and magnetic-braking losses. Inasmuch as the former occur at low particle energies, and the latter at large energies, there is no practical interest in joint evaluation of both effects. We shall restrict ourselves here only to a treatment of the method of computing the magnetic-braking losses. The ionization losses are evaluated in a similar manner. Let us note here that both losses will be evaluated by a method developed by Belen'kii[11] for the calculation of ionization losses in the theory of cosmic showers.

It is difficult to obtain a general solution for (21) when $\beta(t) \neq 0$. It is much easier to solve the problem in that case when the turbulence can be assumed stationary, that is, when α, β, and ν are independent of time. We shall restrict ourselves to this case.

Taking the Laplace transform of (21) at $\gamma = 0$, we obtain

$$[\Phi(s) - \lambda] R(s, \lambda) - c\beta s R(s+1, \lambda) + \nu (mc^2)^s/\lambda = 0, \tag{42}$$

where

$$R(s, \lambda) = \int_0^\infty e^{-\lambda t} \mathfrak{N}(s, t)\, dt. \tag{43}$$

Writing analogous equations for $R(S+1, \lambda)$, $R(s+2, \lambda)$, etc. and using successive elimination, we obtain

$$R(s, \lambda) = -\frac{\nu}{\lambda [\Phi(s) - \lambda]} \sum_{k=0}^{\infty} \frac{(-\beta mc^3)^k (s+1)(s+2)\ldots(s+k+1)}{[\Phi(s+1) - \lambda][\Phi(s+2) - \lambda]\ldots[\Phi(s+k+1) - \lambda]}. \tag{44}$$

Equation (44) is the solution to the problem. The transformation from $R(s, \lambda)$ to $N(E, t)$ is performed with the aid of the inverse Mellin and Laplace transform[11]:

$$N(E, t) = -\frac{1}{4\pi} \int_{\delta - i\infty}^{\delta + ic,} ds \int_{d-i\infty}^{d+i\infty} d\lambda R(s, \lambda) E^{-s-1} e^{\lambda t}. \tag{45}$$

The series (44) is essentially an expression of $R(s, \lambda)$ in powers of $\beta mc^2/\alpha$, i.e., this series should converge quite rapidly. It is therefore necessary to retain only one or two terms when substituting (44) into (45). In analogy with reference 11, it is possible to simplify the calculation by using the following approximation: $\Phi(s) - \lambda = f(\lambda)[s - s_1(\lambda)][s - s_2(\lambda)]$. This approximation is accurate when $x_0 \to \infty$. Here s_1 and s_2 are the roots of the equation $\Phi(s) - \lambda = 0$.

Finally, taking only the inverse Laplace transform of (44) and assuming $s = 0$ or $s = 1$, it is possible to obtain the total number of particles and their total energy per unit volume respectively. We shall not go through all these computations here.

It follows therefore from all that has been said above that in many cases of practical interest we can calculate the principal characteristics of the particle spectrum of particles accelerated by a gas magnetic turbulence to a sufficient degree of accuracy using relatively simple mathematical methods. The methods of these computations account for the various types of possible injectors and lead to sufficiently general assumptions concerning the gas magnetic turbulence that accelerates the particle.

Translated by J. G. Adashko
220

Fluctuations during Collision of High Energy Particles

M. I. PODGORETSKII, I. L. ROZENTAL' AND D. S. CHERNAVSKII
P. N. Lebedev Institute of Physics, Academy of Sciences, USSR
(Submitted to JETP editor May 26, 1954)
J. Exper. Theoret. Phys. USSR 29, 296-303 (September, 1955)

On the basis of the Fermi-Landau theory, we calculate the fluctuations in energy and number of particles during collisions of high energy nuclear-active particles.

1. FERMI[1] proposed a statistical theory of the collision of very high energy nucleons. Later the theory was developed and changed fundamentally by Landau[2]. The purpose of the present work is to give a preliminary discussion of the role of fluctuations in such processes.

We should anticipate that fluctuations will be considerable, since the number of particles produced and, especially, the number of particles which carry off a large fraction of the energy will be relatively small. Thus, the calculation of the fluctuation in the number of particles and, even more so, in the energy distribution, is a very real problem. This problem is, however, complicated by the fact that all sorts of undetermined parameters appear in the theory. For example, the final temperature when the breakup of the system begins is not completely determined. At present, therefore, one cannot give a rigorous and consistent treatment of the fluctuations, and we shall limit ourselves to an approximate qualitative discussion.

We shall start from the same assumptions as Landau, i.e., we shall consider the whole system to be some sort of continuous medium, subject to the equation of state of an ideal ultra-relativistic fluid. This system can, however, be divided into elements within each of which there is statistical equilibrium. We shall assume that the entropy of each element is constant, and that the number of particles in it is sufficiently large (unless specifically stated). From these assumptions it follows that the energy distribution of the particles in each element satisfies the law of black-body radiation.

In addition, we shall use classical methods for calculating fluctuations in systems in thermodynamic equilibrium; the influence of dynamical factors associated with the time development of the system will be treated indirectly.

2. In accordance with Landau's theory, we shall consider the motion of an ideal ultra-relativistic fluid, each of whose elements is characterized by a definite four-velocity and temperature. If we assume that exchange of thermal energy between the elements can occur*, then we can calculate the fluctuations in the number of particles, n, and the thermal energy E.

We assume first that there are only Bose particles inside the element. The average number of particles is

$$\bar{n} = \frac{a\Omega}{2\pi^2(\hbar c)^3}\int_0^\infty \frac{\varepsilon^2 e^{-\varepsilon/kT}}{1-e^{-\varepsilon/kT}}\,d\varepsilon = 2.41\,b, \qquad (1)$$

$$b = \frac{a\Omega}{2\pi^2}\left(\frac{kT}{\hbar c}\right)^3,$$

where Ω is the volume of the element and a is the number of internal degrees of freedom of the particle (e.g., $a = 3$ for π-mesons).

The average energy $\bar{E}$ concentrated in the volume Ω is

$$\bar{E} = \frac{a\Omega}{2\pi^2(\hbar c)^3}\int_0^\infty \frac{\varepsilon^3 e^{-\varepsilon/kT}}{1-e^{-\varepsilon/kT}}\,d\varepsilon = 6.49\,bkT. \qquad (2)$$

The dispersion of the number of particles is

$$D(n) = \frac{a\Omega}{2\pi^2(\hbar c)^3}\int_0^\infty \frac{\varepsilon^2 e^{-\varepsilon/kT}}{(1-e^{-\varepsilon/kT})^2}\,d\varepsilon = 3.29\,b. \qquad (3)$$

The dispersion of the energy is

$$D(E) = \frac{a\Omega}{2\pi^2(\hbar c)^3}\int_0^\infty \frac{\varepsilon^4 e^{-\varepsilon/kT}}{(1-e^{-\varepsilon/kT})^2}\,d\varepsilon \qquad (4)$$

$$= 25.97\,b\,(kT)^2$$

[1] E. Fermi, Progr. Theor. Phys. 5, 570 (1950)

[2] L. D. Landau, Izv. Akad. Nauk SSSR, Ser. Fiz. 17, 51 (1953)

* We shall refer to this case as isothermal. The case of adiabatic isolation of the elements will be considered separately.

and

$$\overline{(n-\bar{n})(E-\bar{E})} \tag{5}$$

$$= \frac{a\Omega}{2\pi^2(\hbar c)^3}\int_0^\infty \frac{\varepsilon^3 e^{-\varepsilon/kT}(1+e^{-\varepsilon/kT})}{(1-e^{-\varepsilon/kT})^2}\,d\varepsilon = 7.65\,bkT.$$

Similarly, for Fermi particles:

$$\bar{n} = \frac{a\Omega}{2\pi^2(\hbar c)^3}\int_0^\infty \frac{\varepsilon^2 e^{-\varepsilon/kT}}{1+e^{-\varepsilon/kT}}\,d\varepsilon = 1.81\ b \tag{6}$$

(for nucleons, $a = 8$),

$$\bar{E} = \frac{a\Omega}{2\pi^2(\hbar c)^3}\int_0^\infty \frac{\varepsilon^3 e^{-\varepsilon/kT}}{1+e^{-\varepsilon/kT}}\,d\varepsilon = 5.68\,bkT; \tag{7}$$

$$D(n) = \frac{a\Omega}{2\pi^2(\hbar c)^3}\int_0^\infty \frac{\varepsilon^2 e^{-\varepsilon/kT}}{(1+e^{-\varepsilon/kT})^2}\,d\varepsilon = 1.64\,b; \tag{8}$$

$$D(E) = \frac{a\Omega}{2\pi^2(\hbar c)^3}\int_0^\infty \frac{\varepsilon^4 e^{-\varepsilon/kT}}{(1+e^{-\varepsilon/kT})^2}\,d\varepsilon \tag{9}$$

$$= 22.72\,b\,(kT)^2;$$

$$\overline{(n-\bar{n})(E-\bar{E})} \tag{10}$$

$$= \frac{a\Omega}{2\pi^2(\hbar c)^3}\int_0^\infty \frac{\varepsilon^3 e^{-\varepsilon/kT}}{1+e^{-\varepsilon/kT}} = \bar{E}.$$

The joint distribution of particle number and energy is given by the two-dimensional Gauss law:

$$f(n,E) \tag{11}$$

$$= \frac{\sqrt{\Delta}}{2\pi}\exp\{-{}^1/_2[c_{11}(n-\bar{n})^2$$

$$+2c_{12}(n-\bar{n})(E-\bar{E})$$

$$+c_{22}(E-\bar{E})^2]\},$$

where

$$c_{11} = \Delta D(E);\ c_{22} = \Delta D(n);$$

$$c_{12} = -\Delta\,\overline{(n-\bar{n})(E-\bar{E})};\ \Delta = c_{11}c_{22} - c_{12}^2.$$

3. According to Landau's theory, there is no heat exchange between different elements (adiabatic motion). Then, if we fix the value of E in Eq. (11), we find for the dispersion of the particle number

$$D'(n) = D(n) - \frac{\overline{[(n-\bar{n})(E-\bar{E})]^2}}{D(E)}, \tag{12}$$

where the quantities $D(n)$, $\overline{(n-\bar{n})(E-\bar{E})}$, $D(E)$ are calculated from formulas (8) - (10), i.e., are calculated for varying energy.

From Eq. (12) we get, for Bose particles,

$$D'(n) = 1.03\,b \tag{13}$$

and for Fermi particles,

$$D'(n) = 0.22\,b. \tag{14}$$

The assumption that the energy is fixed is equivalent to requiring energy conservation. The inclusion of other conservation laws (momentum, angular momentum, charge) does not affect the fluctuations in the number of particles, since the corresponding correlation terms of the type $\overline{(e-\bar{e})(n-\bar{n})}$ are equal to zero (or are close to zero).

4. From Eqs. (1), (3), (6) and (8) it follows that

$$D(n) = \alpha\bar{n}, \tag{15}$$

where $\alpha = 1.37$ for Bose particles and $\alpha = 0.91$ for Fermi particles in the isothermal case, while in the adiabatic case $\alpha = 0.43$ and 0.12, respectively. The relatively small value of the fluctuation for Fermi particles is related to the Pauli principle*. The essential point is that in all cases the value of α does not depend on either the volume of the element or its temperature. Therefore, no matter what the temperature distribution is, we may suppose that the relation (15) also holds for the total number of particles (with the same values of α).

Thus, the fact that the system, according to Landau, is not in thermodynamic equilibrium, does not effect the fluctuations of the number of

* If $kT \sim mc^2$, the difference between the values of α decreases. Improvement of the results for this case requires consideration of the interaction between the particles.

particles in first approximation* .

5. The relation (15) does not depend on either the details of the mechanism of collision or on the energy E_0 of the initial particle. This permits us to express Eq. (15) in another form which is more suitable for comparison with experiment. Let us assume, say, that for energies of the order of $10^{12} - 10^{13}$ ev, the energy spectrum of the initial particles follows the power law $\frac{\gamma-1}{W_0^{\gamma}} E_0^{\gamma-1}$, where W_0 is some threshold energy determined by the conditions of the experiment. Noting that in the Fermi-Landau theory the average number of particles generated in each elementary act is proportional to $E_0^{1/4}$, and using Eq (15), we easily obtain the relation**

$$\overline{\sigma^2} = \frac{(\gamma - 5/4)^2}{(\gamma - 3/2)(\gamma - 1)} (\bar{\sigma})^2 - \alpha\bar{\sigma}, \qquad (16)$$

where $\bar{\sigma} = \Sigma n_i / N$; $\overline{\sigma^2} = \Sigma n_i^2 / N$, n_i is the number of particles in the ith process, and N is the number of processes observed. An essential point is that the value of the threshold energy W_0, which we do not know, does not appear in Eq. (16).

In analyzing experiments in emulsions, we must take into account the fact that only charged particles are seen in the emulsion. An elementary computation shows that this merely results in changing the quantity α to

$$\alpha' = 1 + (\alpha - 1) p, \qquad (17)$$

where p is the probability that a particle of a given type is charged ($p = \frac{1}{2}$ for nucleons, for π-mesons, $p = \frac{2}{3}$). Fluctuations can also be studied by comparing the numbers n_1 and n_2 of prongs inside narrow and wide cones in stars accompanied by small numbers of black and gray tracks (nucleon-nucleon collision). If we assume that the total thermal energy in both cones is the same, then $\bar{n}_1 = \bar{n}_2$, and because of the statistical independence,

$$D(n_1 - n_2) = D(n_1 + n_2) = \alpha(\bar{n}_1 + \bar{n}_2). \qquad (18)$$

Since $\alpha \sim 1$, for not too high energy, both n_1 and n_2 and, in particular, their difference $n_1 - n_2$ can fluctuate quite strongly*. This has to be considered, for example, in those comparisons of the number of particles formed in each act with the total energy liberated, which are made to test the theory. We note that the energy of the initial particle, which is usually determined from the well-known relation**

$$E_0 \sim \cot \vartheta_f \cot \vartheta_{1-f}/2,$$

also can only be evaluated very roughly, since the number of particles which emerge within a small solid angle fluctuates relatively more strongly than the total number of particles.

6. Now let us consider the energy fluctuation. In our opinion, the most interesting question in interpreting experimental facts is: what is the probability that some one of the secondary particles carries off a considerable fraction of the total energy?

Suppose that some element of the nuclear matter, at temperature T, moves relative to the laboratory coordinate system with velocity $\beta = v/c$. We shall characterize the state of motion by the quantity $\gamma = 1/\sqrt{1 - \beta^2}$. We transform to a reference frame fixed in the volume under consideration, and fix our attention on some particle. Its angular distribution is obviously isotropic, while its energy distribution $p(\epsilon)$ is determined by the relation between kT and mc^2. The energy distribution will follow the Planck law if $kT/mc^2 \gg 1$, or will be Maxwellian if $kT/mc^2 \ll 1$. So, after making some simple kinematical transformations (cf, for example, reference 3,) we can calculate the energy distribution of the particle in

---

* The last conclusion is valid so long as we can neglect surface effects and specifically, quantum fluctuations, i.e., so long as the wavelength $\lambda \sim \hbar c/kT$ is small compared to the dimensions of the system $R \sim \hbar/\mu c$, which reduces to the condition $\mu c^2/kT < 1$.

** In deriving Eq. (16) it was assumed that the number of secondary particles does not depend on the impact parameter. Including this dependence would have given rise to additional fluctuations. Lack of a sufficiently complete theory of the elementary process, which would also include peripheral collisions, prevents us from making this correction in Eq. (16).

* The first stage of Landau's process (passage of the shock wave) also is statistical. It is therefore not excluded that $\bar{n}_1 \neq \bar{n}_2$ in the individual processes. If the number of particles produced is small, the symmetry of the cones is also disturbed because the colliding particles can be of different types (e.g., collision of proton and neutron). Both of these causes may increase the fluctuation of the difference $n_1 - n_2$.

** θ_f, θ_{1-f} are angles containing the fractions f and $1 - f$ of the total number of shower particles.

[3] I. L. Rozental', Usp. Fiz. Nauk **54**, 405 (1954)

the laboratory coordinate system. It is then clear than in the region $kT < mc^2$ the energy fluctuation must drop sharply with decreasing temperature, since for $kT/mc^2 \to 0$, the particle energy will always be the same value $m\gamma$. Now going over to a quantitative discussion, we first treat the auxiliary problem for particles whose rest mass can be neglected (photons). In addition, we shall impose the condition $\gamma \gg 1$, which is always fulfilled for the narrow cone.

The required energy distribution in the laboratory system has the form[3]

$$p_{\text{lab}}(E)\,dE = \frac{dE}{2\gamma}\int\limits_{E/2\gamma}^{\infty} \frac{\rho(\varepsilon)}{\varepsilon}\,d\varepsilon. \tag{19}$$

If we measure the energy in units of $2\gamma kT$, i.e., if we introduce the variable $\xi = E/2\gamma kT$, we get the relations

$$u_{\text{B}}(\xi)\,d\xi = \frac{d\xi}{2{,}4}\int\limits_{\xi}^{\infty} \frac{x\,dx}{e^x - 1} \tag{20}$$

for Bose particles

$$u_{\text{F}}(\xi)\,d\xi = \frac{d\xi}{1{,}8}\int\limits_{\xi}^{\infty} \frac{x\,dx}{e^x + 1} \tag{21}$$

for Fermi particles; these do not contain the quantities γ or kT. The corresponding curves are shown in Fig. 1, from which we see that the difference between them is small.

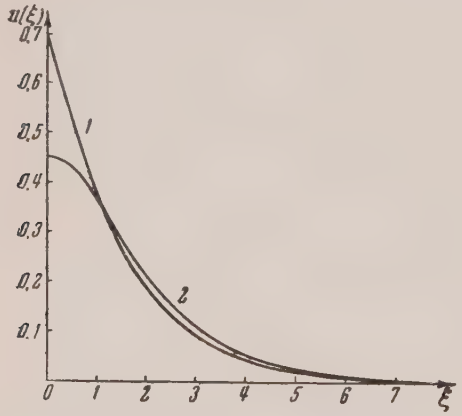

FIG. 1. 1. $u_{\text{B}}(\xi)$, 2. $u_{\text{F}}(\xi)$.

From Eqs. (20) and (21) it also follows that the relative fluctuation of the energy, $\delta = \sqrt{D(E)}/E$, also does not depend on kT and γ. It is very large --- $\delta = 1.1$ for bosons and $\delta = 0.75$ for fermions; thus, in both cases the fluctuations are of the same order of magnitude as the average energy.

7. We now take account of the finite mass of the particles. We shall assume that the average velocity of the thermal motion is smaller than the translational velocity, i.e., $\overline{\gamma}_{\text{T}} < \gamma$. This is the case which usually occurs in experiment. Then

$$p_{\text{lab}}(E) = \frac{1}{2\gamma}\int\limits_{E/2\gamma}^{\infty} \frac{p(\varepsilon)}{\sqrt{\varepsilon^2 - m^2c^4}}\,d\varepsilon, \tag{22}$$

$$p(\varepsilon) = \left[\int\limits_{mc^2}^{\infty} \frac{x\sqrt{x^2 - m^2c^4}}{\exp(x/kT) \mp 1}\,dx\right]^{-1} \cdot \frac{\varepsilon\sqrt{\varepsilon^2 - m^2c^4}}{\exp(\varepsilon/kT) \mp 1} \tag{23}$$

(the minus sign refers to bosons, the plus sign to fermions).

From Eq. (22) it follows that in the case of finite mass, except for an unimportant normalization factor, the distribution functions $v_{\text{B}}(\xi)$ and $v_{\text{F}}(\xi)$ are related to the functions $u_{\text{B}}(\xi)$ and $u_{\text{F}}(\xi)$ by

$$v_{\text{B}}(\xi) = u_{\text{B}}\left[\xi + \left(\frac{mc^2}{2kT}\right)^2 \frac{1}{\xi}\right], \qquad v_{\text{F}}(\xi) = u_{\text{F}}\left[\xi + \left(\frac{mc^2}{2kT}\right)^2 \frac{1}{\xi}\right]. \tag{24}$$

It is easy to show that all these distributions have their maxima at $\xi = \gamma mc^2/2kT$, i.e., at $E = \gamma mc^2$, and that the upper end ($E > \gamma mc^2$) is spread out more for larger values of kT/mc^2. If $kT/mc^2 \ll 1$, the distribution becomes symmetric, and all the possible values of the energy are concentrated in a narrow range around $E = \gamma mc^2$. Figure 2 shows the distributions for a particle of mass μ for the cases $kT = mc^2$ and $kT = \mu c^2$ ($\mu = 1/6\ m$).

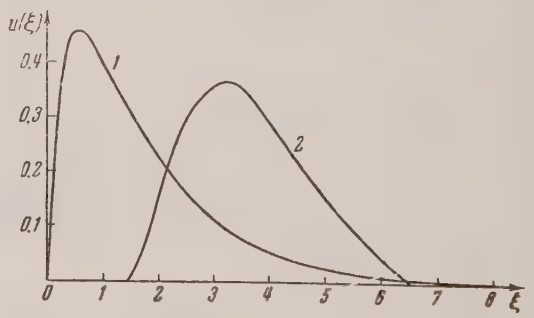

FIG. 2. 1. $kT = mc^2$, 2. $kT \sim mc^2/6$.

The relations obtained apply to any volume element filled with nuclear matter, and describe the

energy fluctuations of the particles which constitute that element. We must remember the following: all the calculations were made on the assumption that just before the start of the stage of free breakup the quantity γ has a completely definite value for each element (i.e., it does not fluctuate). Strictly speaking, this is not so, because of the occurrence of fluctuations in the dynamical characteristics of the process (pressure fluctuations). However, in first approximation we need not consider pressure fluctuations, since they average out over the course of the whole stage of hydrodynamic expansion.

8. In order to obtain final numerical estimates of the probability that some one particle carries off a definite fraction of the energy of the initial particle, we must average Eq. (24) over the various parts of the volume containing the nuclear matter, using the distribution of energy and number of particles given by Landau's theory. However, such a procedure actually has little meaning, since it is clear beforehand that the region close to the front surface of the volume plays a fundamental role.

Actually, according to Landau's theory, the entropy and the quantity γ are distributed nonuniformly over the volume. Most of the particles have relatively low velocity ($\gamma \sim 1$); at the same time the front region, which contains only a small fraction of the particles, carries the main part of the energy and has a high velocity ($\gamma \gg 1$). Therefore, for an approximate evaluation of the energy fluctuation it is sufficient to consider only the region near the front surface. Unfortunately, the solution obtained by Landau is not sufficiently accurate in just this region, since in getting the solution it was assumed that the quantity γ varies sufficiently slowly, and this condition is not fulfilled in this region. We have, therefore, not used the velocity and energy distribution over this region but have regarded the whole front surface as a single entity. Its entropy and energy were calculated from the difference between the total entropy (or energy) and the entropy of the whole region back of the front surface (where it is permissible to use Landau's solution).

Separating out the region of the front surface in this way,* we determined the number of particles in it and the total energy. For the temperature at breakup we chose the values $kT \sim mc^2$ or $kT \sim \mu c^2$ *. Using the fact that in the system of reference in which the front surface is at rest, the energy distribution of the particles is that of black body radiation, we can calculate the probability $p(\delta)$ that one particle will carry off more than the fraction δ of the total energy (in the lab system). The results are given in the Table.

$p(\delta)$	0.25	0.33	0.40
δ	0.5	0.25	0.10

From the Table we see that these probabilities are very large. We should also remark that they vary slowly with energy of the initial particle in the interval from 10^{14} to 10^{16} ev.

The Table applies to the fluctuations in energy of protons when the temperature at breakup is determined by the proton mass ($kT \sim mc^2$); it also describes the energy fluctuations of mesons if the breakup temperature is $kT \sim \mu c^2$**.

We should emphasize that the number of particles near the front surface is relatively small (this number hardly depends on the energy of the initial particle in the interval from 10^{14} to 10^{16} ev, and is approximately five). Therefore, the application of thermodynamic formulas (black body radiation law) to the energy distribution of the particles in the front surface is not entirely justified. More correct would be the application of statistical laws, for example, in the spirit of Fermi's first paper[1], where a system is considered which consists of a small number of particles. We have, however, not carried out such computations because of the complexity of the resulting expressions, since we expect that the order of magnitude of the fluctuation will not be changed.

So the energy fluctuation is large and it may be essential to consider it for various processes. For example, inclusion of fluctuations may affect the altitude variation of wide atmospheric showers.

* Although most quantities (temperature, γ, etc.) change markedly when we go from the main mass to the front surface, this separation of the front surface is still not entirely unique. Therefore, the question arises to what extent the result depends on the choice of the boundary which separates the system into a front surface and a residual part. Computations showed that the dependence is slight, so that the element of uncertainty in this choice is small.

* The temperature at breakup, i.e., the temperature at which the particles (mainly π-mesons) cease interacting strongly, was taken to be $\sim \mu c^2/k$ in Landau's work. There is, however, some basis for assuming (for example, if we suppose that the mesons interact with one another via virtual nucleon pairs) that the interaction of two π-mesons is large only when their relative energy is $\sim mc^2$. On this basis, the temperature at breakup will be $\sim mc^2/k$.

** It is also assumed that there are particles of only a single kind in the region of the front surface. If this is not the case, then in calculating the fluctuations of energy we must assign the ratio of the numbers of particles of various types.

Thus, it was shown that the absorption coefficient of wide showers, calculated according to Landau's theory, is somewhat greater than the experimental value[4]. The altitude variation of showers is determined to a large extent by high energy particles, so that the absorption coefficient is decreased if one of the secondary particles takes a large part of the energy of the initial particle.

According to our estimates, inclusion of fluctuations lowers the value of the absorption coefficient of wide showers at high altitude by approximately 10%, which greatly improves the agreement between experiment and theory*.

CONCLUSIONS

1. The fluctuations in number of particles are proportional to the square root of the number of particles and are very large in absolute value. The coefficient of proportionality is essentially different for fermions (nucleons and antinucleons) and bosons (π-mesons).

2. It was shown that the fluctuations in the energy carried off by a single particle are very large. This applies especially to the narrow cone of particles, in which most of the energy is contained in the laboratory system. Marked fluctuations should also be observed in the angular distribution of the energy in an elementary process.

3. The energy fluctuations are important for the interpretation of the altitude variation of wide atmospheric showers. The theoretical absorption coefficient is decreased when we include fluctuations, which improves the agreement of theory with experiment.

The authors thank S. Z. Belen'kii for valuable comments.

* We should remark that the absence of fundamental data concerning nuclear interactions at moderate energies $\sim 10^{10} - 10^{12}$ ev prevents us from making a sufficiently accurate calculation of the altitude variation of wide showers.

[4] G. T. Zatsepin and L .I. Sarycheva, Dokl. Akad. Nauk SSSR 99, 951 (1954)

Translated by M. Hamermesh
196

Fluctuations in Oscillating Systems of the Thomson Type. I

S. M. RYTOV
P. N. Lebedev Institute of Physics, Academy of Sciences, USSR
(Submitted to JETP editor December 2, 1954)
J. Exper. Theoret. Phys. USSR 29, 304-314 (September, 1955)

Fluctuations of phase and amplitude in weakly non-linear oscillating systems amenable, in the periodic mode, to calculation through an expansion in terms of a small parameter are considered. In contrast with previous studies[1-5], the Einstein-Fokker equations are not used; instead, symbolic differential equations containing random functions which describe the fluctuations are used in conjunction with methods of correlation theory.

The first part of the paper is devoted to a consideration of a system with one degree of freedom; to illustrate the method, the general theory is applied to the case of an isolated system, which has been studied earlier[2], and to the physical example of a weakly self-excited vacuum-tube oscillator.

1. INTRODUCTION

THE problem of the behavior of dynamic systems in the presence of random effects has been treated in very general form in reference 1, which is undoubtedly fundamental in this particular field. In this paper the statistical approach was that of the Einstein-Fokker transition-probability equation; i.e., it was assumed that the random process taking place in the system is a Markov process.

The general considerations developed in reference 1 were applied further in the study of the natural bandwidth of a vacuum-tube oscillator[2], in which connection the oscillator was assumed to be a system of the Thomson type; i.e., approximately a conservative harmonic oscillator. The theoretical results were shown to be in good qualitative agreement with experiment[3].

Because of the considerable improvement in the sensitivity of receiving and measuring apparatus, fluctuation effects have received a good deal of attention in recent years. In particular, fluctuations in oscillating systems, aside from their theoretical interest, have now acquired direct practical importance, for example in determining the limiting frequency stability which can be achieved in quartz-crystal frequency standards[6].

In further study of the problems in this field it would seem desirable both to attack new problems other than those considered in reference 2 and reference 3, and to apply other statistical methods. In connection with the first of these approaches mention should be made of reference 4 in which the Einstein-Fokker equations were used to study the behavior of a vacuum-tube oscillator in which the fluctuations were not assumed to be small and correlation time of which was large compared with the oscillation period, and of reference 5, in which the methods of references 2,3 were used in considering fluctuation in an oscillator with nonlinear inertial properties.

The present paper treats fluctuation in oscillating systems of the Thomson type having one or two degrees of freedom. The statistical approach is one first introduced by Langevin[7] in the theory of Brownian motion and in general is quite different from those used in the work cited above. In particular, in place of the Einstein-Fokker equations, we consider symbolic differential equations which contain explicitly the random forces acting in the system and determine the random functions themselves rather than the distribution functions. Without attempting a comprehensive comparison between these two methods, we may note here certain features of both.

Using Einstein-Fokker equations, one may easily take into account auxiliary conditions such as the existence of reflecting on absorbing boundaries in considering the region of variation of the random functions; this is done by imposing appropriate boundary conditions. In working with symbolic differential equations, the consideration of such conditions is more complicated. On the other hand, these equations are more general in that they are not limited to Markov processes; the random force

[1] L. Pontriagin, A. Andronov and A. Vitt, J. Exper. Theoret. Phys. USSR 3, 165 (1933)

[2] I. L. Bershtein, Dokl. Akad. Nauk SSSR 20, 11 (1938); J. Exper. Theoret. Phys. USSR 11, 305 (1941)

[3] I. L. Bershtein, Dokl. Akad. Nauk, SSSR 68, 469 (1949); Izv. Akad. Nauk SSSR , Ser. Fiz. 14, 145 (1950)

[4] P. I. Kuznetsov, R. L. Stratonovich and V. I. Tikhonov, Dokl. Akad. Nauk SSSR 97, 639 (1954)

[5] M. E. Zhabotinskii, J. Exper. Theoret. Phys. USSR 26, 758 (1954)

[6] A. Blaquière, Ann. de Radioélectricité 8, No. 31, 36 and No. 32, 153 (1953)

[7] P. Langevin, Compt.rend. 146, 530 (1908)

$F(t)$ need not have δ-correlation. The situation in which $F(t)$ is "absolutely random", i.e.,

$$\overline{F(t)F(t')} = C\delta(t-t') \tag{1.1}$$

and correspondingly, in which the impulse over the time T

$$I(t) = \int_t^{t+T} F(t)\,dt \tag{1.2}$$

is a non-correlated function, represents an exceptional case. As is well known, it is precisely in this case that the system fluctuations caused by $F(t)$ constitute a Markov process, and the consideration of the problem by correlation-theory methods is equivalent to its solution using transition probabilities. In general, however, the application of symbolic differential equations in conjuction with correlation theory seems to be simpler and more instructive, so that we shall use it here although we shall limit ourselves to random forces having δ-correlation.

First as an illustration of the method, an isolated oscillating system is considered, i.e., the problem solved in reference 2.

In the following paper our method is applied in somewhat more complicated problems: fluctuations in a non-isolated oscillating system with one degree of freedom, namely a vacuum-tube oscillator synchronized by an external driving force and fluctuations in an oscillating system having two degrees of freedom, more specifically, a vacuum-tube oscillator stabilized by coupling to a high-Q circuit.

2. STATEMENT OF THE PROBLEM

Since it is assumed that the systems being investigated are approximately conservative oscillators, it is reasonable to use for the solution of the equation of motion a method involving expansion in a small parameter. This parameter, which we call μ, determines slow variations of both amplitudes and phases of the oscillations at the fundamental frequency and at its harmonics, i.e., it enters not only directly, but also through the "slow" time

$$\tau = \mu t.$$

In other words, the solution will be in the form

$$x = R\cos(t-\varphi) + \mu\sum_n \{P_n \cos n(t-\varphi) + Q_n \sin n(t-\varphi)\},$$

$$R = R(\tau,\ \mu), \qquad \varphi = \varphi(\tau,\ \mu),$$

$$P_n = P_n(\tau,\ \mu), \qquad Q_n = Q_n(\tau,\ \mu).$$

The first question which must be settled in applying this treatment of random effects is the choice of the order of magnitude of the random force. Two reasonable choices are possible: first order, i.e., a force $\mu F(t)$, and second order, i.e., a force $\mu^2 F(t)$. In the following it will become apparent that over and above its greater convenience with regard to the numerical values which appear in the dimensionless-parameter equations, the second choice leads to a more consistent perturbation method. Thus,for a system with one degree of freedom the equation of motion will have the following form:

$$\frac{d^2x}{dt^2} + x = \mu f\left(x,\ \frac{dx}{dt},\ t,\ \mu\right) + \mu^2 F(t). \tag{2.1}$$

The explicit dependence of f on t (which arises in the synchronization problem) is assumed to be periodic with period 2π. In the case of the isolated system the time enters explicitly only through the random force $\mu^2 F(t)$.

As is well known, the equations for the amplitudes and the phase φ are obtained from the requirement that in x there be no terms (in any order in μ) which increase indefinitely with t. This means that, in looking for a solution in the form of a series in μ ($x = x_0 + \mu x_1 + \mu^2 x_2 + \ldots\ldots$), the right-hand member of the successive approximation equations must not contain resonance harmonics. According to Eq. (2.1), the random force enters in the right-hand member of the equation for x_2[$\ddot{x}_2 + x_2 = F(t) + \ldots.$], i.e., speaking formally, it should act as a conservative oscillator – a system with an infinitely large driving force. From this it is clear that in the spectrum of $F(t)$ only the immediate region of the fundamental frequency is of importance and thus $F(t)$ can be written in the form

$$F(t) = F_\parallel(\tau)\cos(t-\varphi) - F_\perp(\tau)\sin(t-\varphi), \tag{2.2}$$

where $F_\parallel$ and $F_\perp$ are the components of the force tangent to and normal to the generating circle

(more accurately, to the circle corresponding to the fundamental frequency).

In order to examine the significance of this representation of the force, we write its spectral function

$$F(t) = \int_0^\infty \{U(\omega)\cos\omega t + V(\omega)\sin\omega t\}\, d\omega. \quad (2.3)$$

Using the Fourier-transform formulas and the correlation function (1.1), it follows that

$$\overline{U(\omega)\,U(\omega')} = \frac{C}{\pi}\{\delta(\omega-\omega') + \delta(\omega+\omega')\},$$

$$\overline{V(\omega)\,V(\omega')} = \frac{C}{\pi}\{\delta(\omega-\omega') - \delta(\omega+\omega')\},\quad \overline{U(\omega)\,V(\omega')} = 0.$$

In the integration over ω and ω' from zero to infinity, terms with $\delta(\omega+\omega')$ always vanish, so that only the first term need be considered:

$$\overline{U(\omega)\,U(\omega')} = \overline{V(\omega)\,V(\omega')} = \frac{C}{\pi}\delta(\omega-\omega'),\quad \overline{U(\omega)\,V(\omega')} = 0. \quad (2.4)$$

Comparing Eqs. (2.2) amd (2.3), it follows that

$$F_\parallel(\tau) = \int_0^\infty \{U(\omega)\cos(\alpha\tau+\varphi) + V(\omega)\sin(\alpha\tau+\varphi)\}\, d\omega,$$

$$F_\perp(\tau) = \int_0^\infty \{U(\omega)\sin(\alpha\tau+\varphi) - V(\omega)\cos(\alpha\tau+\varphi)\}\, d\omega,$$

where

$$\alpha = (\omega-1)/\mu. \quad (2.5)$$

These expressions are completely rigorous although, strictly speaking, on the left-hand side one cannot write the "slow" time τ as the argument for $F_\parallel$ and $F_\perp$. In view of the smallness of μ, however, and in view of the fact that we are interested not in $F_\parallel$ and $F_\perp$ themselves, but only in their correlation functions, this expression is justified. Thus, for the correlation function of $F_\parallel$, we have

$$\overline{F_\parallel(\tau)F_\parallel(\tau')} = \int_0^\infty\int_0^\infty \overline{\{U\cos(\alpha\tau+\varphi) + V\sin(\alpha\tau+\varphi)\}\{U'\cos(\alpha'\tau'+\varphi') + V'\sin(\alpha'\tau'+\varphi')\}}\times d\omega d\omega'.$$

In view of Eqs. (2.4) and (2.5), this gives

$$\overline{F_\parallel(\tau)F_\parallel(\tau')} = \frac{C}{\pi}\int_0^\infty \cos[\alpha(\tau-\tau') + \varphi - \varphi']\, d\omega$$

$$= \frac{\mu C}{\pi}\cos(\varphi-\varphi')\int_{-1/\mu}^\infty \cos\alpha(\tau-\tau')\, d\alpha - \frac{\mu C}{\pi}\sin(\varphi-\varphi')\int_{-1/\mu}^\infty \sin\alpha(\tau-\tau')\, d\alpha.$$

It is clear that for $\mu \to 0$ the integral over $\cos\alpha(\tau-\tau')$ becomes $2\pi\delta(\tau-\tau')$ and the integral over $\sin\alpha(\tau-\tau')$ becomes zero. Thus, within the accuracy of the rapidly oscillating terms, one may use these limiting values of both integrals, and it is in just this sense that we interpret the statement that $F_\parallel$ and $F_\perp$ depend on the time only through $\tau = \mu t$.

In the factor which multiplies the δ-function one may assume that $\tau' = \tau$ so that $\overline{F_\parallel(\tau)F_\parallel(\tau')} = 2\mu C\delta(\tau-\tau')$. Incorporating this with the results of similar calculations for the other correlation functions we have finally,

$$\overline{F_\parallel(\tau)F_\parallel(\tau')} = \overline{F_\perp(\tau)F_\perp(\tau')} = 2\mu C\delta(\tau-\tau'),\quad \overline{F_\parallel(\tau)F_\perp(\tau')} = 0. \quad (2.6)$$

We now turn our attention to the solution of Eq. (2.1).

3. SUCCESSIVE APPROXIMATION EQUATIONS

In differentiating any function which not only depends on t explicitly but also through $\tau = \mu t$, we have

$$\frac{d}{dt} = \frac{\partial}{\partial t} + \mu\frac{\partial}{\partial\tau} = (\cdot) + \mu(\,)'. \quad (3.1)$$

For brevity we indicate the respective partial derivatives here and in the following through the dot and the prime-symbol.

In order to simplify the calculations, we make the assumption that the system being studied has cubic non-linearity only. This allows us to neglect the even harmonics, i.e., to look for a solution in the form

$$x = R\cos(t-\varphi) + \mu\{P\cos 3(t-\varphi) + Q\sin 3(t-\varphi) + \ldots\}. \tag{3.2}$$

Calculating $\frac{dx}{dt}$ and $\frac{d^2x}{dt^2}$ in accordance with Eq. (3.1), after substitution in Eq. (2.1), we get

$$\begin{aligned}
&[-2\mu R' + \mu^2(R\varphi'' + 2R'\varphi')]\sin(t-\varphi) + [2\mu R\varphi' \\
&+ \mu^2(R'' - R\varphi'^2)]\cos(t-\varphi) + [-8\mu Q + \mu^2(18Q\varphi' - 6P')]\sin 3(t-\varphi) \\
&+ [-8\mu P + \mu^2(18P\varphi' + 6Q')]\cos 3(t-\varphi) + \ldots = \\
&= \mu f\left(x, \frac{dx}{dt}, t, \mu\right) + \mu^2[F_\parallel(\tau)\cos(t-\varphi) - F_\perp(\tau)\sin(t-\varphi)].
\end{aligned} \tag{3.3}$$

Now we expand f in a Fourier series with respect to $t-\varphi$(keeping in mind the fact that the explicit dependence of f on t is assumed to be periodic with period 2π):

$$f\left(x, \frac{dx}{dt}, t, \mu\right) = \sum_k \{\Phi_k \sin k(t-\varphi) + \Psi_k \cos k(t-\varphi)\},$$

where $(k > 0)$

$$\left.\begin{matrix}\Phi_k \\ \Psi_k\end{matrix}\right\} = \frac{1}{\pi}\int_{-\pi}^{\pi} f\{R\cos u + \mu(P\cos 3u + Q\sin 3u) + \ldots, -R\sin u + \mu(R\varphi'\sin u + R'\cos u - 3P\sin 3u + \ldots), u+\varphi, \mu\}\left\{\begin{matrix}\sin ku \\ \cos ku\end{matrix}\right. du. \tag{3.4}$$

Now equating the coefficients of $\sin(t-\varphi)$, $\sin 3(t-\varphi)$ and $\cos(t-\varphi)$, $\cos 3(t-\varphi)$ to zero, we find

$$\begin{aligned}
&2R' + \Phi_1 - \mu(R\varphi'' + 2R'\varphi' + F_\perp) = 0, \\
&2R\varphi' - \Psi_1 + \mu(R'' - R\varphi'^2 - F_\parallel) = 0, \\
&8Q + \Phi_3 - \mu(18Q\varphi' - 6P') = 0, \\
&8P + \Psi_3 + \mu(18P\varphi' + 6Q') = 0, \\
&\ldots\ldots\ldots\ldots\ldots\ldots
\end{aligned}$$

The successive approximation equations are obtained from the substitution of a power series in μ:

$$R = R_0 + \mu R_1 + \ldots, \tag{3.5}$$

$$P = P_0 + \mu P_1 + \ldots,$$

$$\varphi = \varphi_0 + \mu\varphi_1 + \ldots, \quad Q = Q_0 + \mu Q_1 + \ldots,$$

in which Φ_k and Ψ_k are also resolved in terms of μ

$$\Phi_k = \Phi_{k0} + \mu\Phi_{k1} + \ldots,$$

$$\Psi_k = \Psi_{k0} + \mu\Psi_{k1} + \ldots$$

In accordance with Eqs. (3.4) and (3.5)

$$\left.\begin{matrix}\Phi_{k0} \\ \Psi_{k0}\end{matrix}\right\} = \frac{1}{\pi}\int_{-\pi}^{\pi} f(R_0\cos u, -R_0\sin u, u+\varphi_0, 0)\left\{\begin{matrix}\sin ku \\ \cos ku\end{matrix}\right. du, \tag{3.6}$$

$$\Phi_{k1} = R_1\frac{\partial\Phi_{k0}}{\partial R_0} + \varphi_1\frac{\partial\Phi_{k0}}{\partial\varphi_0} + A_k,$$

$$\Psi_{k1} = R_1\frac{\partial\Psi_{k0}}{\partial R_0} + \varphi_1\frac{\partial\Psi_{k0}}{\partial\varphi_0} + B_k,$$

where

$$\left.\begin{matrix}A_k \\ B_k\end{matrix}\right\} = \frac{1}{\pi}\int_{-\pi}^{\pi}\{f'_{x0}(R_0\varphi'_0\sin u + R'_0\cos u) + (f'_{x0}P_0 + 3f'_{x0}Q_0)\cos 3u + (f'_{x0}Q_0 - 3f'_{x0}P_0)\sin 3u + f'_{\mu 0}\}\left\{\begin{matrix}\sin ku \\ \cos ku\end{matrix}\right. du. \tag{3.7}$$

Equating the coefficients of terms of the same order in μ to zero, we find the equation for the first approximation

$$2R_0' + \Phi_{10} = 0, \qquad 8Q_0 + \Phi_{30} = 0,$$
$$2R_0\varphi_0' - \Psi_{10} = 0, \qquad 8P_0 + \Psi_{30} = 0, \tag{3.8}$$

and the equation for the second approximation

$$2R_1' + \frac{\partial\Phi_{10}}{\partial R_0}R_1 + \frac{\partial\Phi_{10}}{\partial\varphi_0}\varphi_1 = R_0\varphi_0'' + 2R_0'\varphi_0' - A_1 + F_\perp,$$
$$2R_0\varphi_1' + \left(2\varphi_0' - \frac{\partial\Psi_{10}}{\partial R_0}\right)R_1 - \frac{\partial\Psi_{10}}{\partial\varphi_0}\varphi_1 = R_0\varphi_0'^2 - R_0'' + B_1 + F_\parallel; \tag{3.9}$$
$$8Q_1 + 6P_0' - 18Q_0\varphi_0' + \Phi_{31} = 0,$$
$$8P_1 - 6Q_0' - 18P_0\varphi_0' + \Psi_{31} = 0. \tag{3.10}$$

The first two equations of (3.8) are the so-called reduced equations. We note that for the regular method of successive approximations being used here the basis of this designation is lost. We do not require the "rejection of quickly oscillating terms" nor averaging over phase, i.e., the usual procedures which are employed in the derivation of the first two equations of (3.8).

Equations (3.9), which are linear in R_1 and φ_1 permit us to express R_1 and φ_1 in terms of the fluctuation forces $F_\parallel$ and $F_\perp$ whose correlation functions are known, i.e., they permit us to find the correlation functions for the amplitude fluctuations and for the phase fluctuations, and eventually to determine their mean-square values. Thus, the problem of finding the statistical properties of the random process which takes place in the system being investigated is completely solved.

If in Eq. (2.1) the fluctuation force had been introduced in first order in μ, then in place of Eq. (3.8) we would have obtained the following equation for the first-order approximation:

$$2R_0' + \Phi_{10} = F_\perp, \quad 2R_0\varphi_0' - \Psi_{10} = F_\parallel. \tag{3.11}$$

Bershtein[2] started from these equations but in forming the corresponding Einstein-Fokker equations he was still forced to resort to perturbation methods, i.e., to the linearization of Eqs. (3.11). Taking R_0 and φ_0 to be the solutions of Eqs. (3.11) for $F_\perp = F_\parallel = 0$, and taking R_1 and φ_1 to be the small deviations caused by the fluctuation forces; resolving Eqs. (3.11) in powers of R_1 and φ_1 and limiting ourselves to linear terms, we have

$$2R_1' + \frac{\partial\Phi_{10}}{\partial R_0}R_1 + \frac{\partial\Phi_{10}}{\partial\varphi_0}\varphi_1 = F_\perp,$$
$$2R_0\varphi_1' + \left(2\varphi_0' - \frac{\partial\Psi_{10}}{\partial R_0}\right)R_1 - \frac{\partial\Psi_{10}}{\partial\varphi_0}\varphi_1 = F_\parallel. \tag{3.12}$$

The linearization of Eqs. (3.11) indicates that the fluctuation force is influenced by the behavior of higher order terms as is shown by a comparison of (3.9) and (3.12). In using the successive-approximation method this effect is introduced naturally as was done above. Furthermore, we see that the linearization of Eqs. (3.11) yields a result which coincides with that of Eq. (3.9) only in those cases for which all additional terms in Eq. (3.9) are either absent or can be set to zero. If one or the other of these conditions is not fulfilled (and this is entirely possible) then Eq. (3.12) does not take into account regular corrections to the amplitude and phase. It is to be understood that the presence of regular additional terms in the right-hand member of Eq. (3.9) is not essential to the fluctuations.

We now consider the case of fluctuations in an isolated oscillating system.

4. ISOLATED OSCILLATING SYSTEM

Since the time t does not appear in f explicitly in this case, the quantities Φ_{k0}, Ψ_{k0}, A_k and B_k do not depend on φ_0 as is seen from Eqs. (3.6) and (3.7). Hence in an isolated system, Eqs. (3.8) and (3.9) assume the form

$$2R_0' + \Phi_{10}(R_0) = 0, \quad 8Q_0 + \Phi_{30}(R_0) = 0, \tag{4.1}$$
$$2R_0\varphi_0' - \Psi_{10}(R_0) = 0, \quad 8P_0 + \Psi_{30}(R_0) = 0;$$

$$2R_1' + \frac{\partial\Phi_{10}}{\partial R_0}R_1 = R_0\varphi_0'' + 2R_0'\varphi_0' - A_1(R_0) + F_\perp,$$
$$2R_0\varphi_1' + \left(2\varphi_0' - \frac{\partial\Psi_{10}}{\partial R_0}\right)R_1 = R_0\varphi_0'^2 - R_0'' + B_1(R_0) + F_\parallel. \tag{4.2}$$

We are interested only in steady-state oscillations, so that $R' = 0$. The first equation of (4.1),

$$\Phi_{10}(R_0) = 0$$

determines only the constant (independent of τ) values of the radii of the generating circles in the zeroth approximation.

If $\Psi_{10}(R_0) \neq 0$, then, from the second equation of (4.1), we have

$$\varphi_0 = \delta\tau + \alpha,$$

where α is an arbitrary constant and the quantity

$$\delta = \varphi_0' = \frac{1}{2R_0}\Psi_{10}(R_0)$$

gives the first-order correction to the frequency.

Taking into account the constant R_0 (also P_0, Q_0) and φ_0', we get from Eq. (4.2)

$$\begin{aligned} 2R_1' + \frac{\partial\Phi_{10}}{\partial R_0}R_1 &= -A_1(R_0) + F_\perp, \\ 2R_0\varphi_1' + \left(2\delta - \frac{\partial\Psi_{10}}{\partial R_0}\right)R_1 &= R_0\delta^2 - B_1(R_0) + F_\parallel. \end{aligned} \tag{4.3}$$

Separating the regular components r_1 and δ_1 in R_1 and φ_1, i.e., taking

$$R_1 = r_1 + \rho(\tau), \quad \varphi_1 = \delta_1\tau + \chi(\tau), \tag{4.4}$$

we get, upon substitution of Eq. (4.4) in (4.3), the following values of the corrections to the radius of the generating circle r_1 and the second-order correction to the frequency δ_1:

$$r_1 = -\frac{A_1(R_0)}{\partial\Phi_{10}/\partial R_0},$$

$$\delta_1 = \frac{1}{2R_0}\left[R_0\delta^2 - B_1(R_0) - \left(2\delta - \frac{\partial\Psi_{10}}{\partial R_0}\right)r_1\right],$$

while the equations for the amplitude fluctuation ρ and the phase fluctuation χ assume the form

$$\rho' + p_1\rho = F_\perp(\tau)/2, \quad \chi' + q_1\rho = F_\parallel(\tau)/2R_0, \tag{4.5}$$

where

$$p_1 = \frac{1}{2}\frac{\partial\Phi_{10}}{\partial R_0},$$

$$q_1 = \frac{1}{2R_0}\left(2\delta - \frac{\partial\Psi_{10}}{\partial R_0}\right) = -\frac{1}{2}\frac{\partial}{\partial R_0}\left(\frac{\Psi_{10}}{R_0}\right).$$

The quantity p_1, the increment of the system, characterizes the "stability" of the generating circle with respect to radial departures (for a stable circle $p_1 > 0$). For ρ we have an equation of the relaxation type with a characteristic relaxation time $1/p_1$ in terms of τ (i.e., $1/\mu p_1$ in terms of t). The tracing point, after being displaced from the generating circle by the fluctuation force, is returned to it as though it were attached by a spring and moving in a viscous medium. The existence of a quasi-elastic force $-p_1\rho$ implies the stationary properties of the amplitude fluctuations and the existence of a finite steady-state value of $\overline{\rho^2}$.

In calculating the steady-state correlation function, one may use the solution of the first equation of Eq. (4.5) under initial conditions corresponding to the vanishing of the quantities of interest at $\tau = -\infty$.

$$\rho(\tau) = \frac{e^{-p_1\tau}}{2}\int_{-\infty}^{\tau} e^{p_1\theta}F_\perp(\theta)\,d\theta.$$

Using Eq. (2.4), we find

$$\begin{aligned} \overline{\rho(\tau)\rho(\tau')} &= \frac{\exp\{-p_1(\tau+\tau')\}}{4}\int_{-\infty}^{\tau} e^{p_1\theta_1}d\theta_1\int_{-\infty}^{\tau'} e^{p_1\theta_2}\,\overline{F_\perp(\theta_1)F_\perp(\theta_2)}\,d\theta_2 \\ &= \frac{\mu C}{2}\exp\{-p_1(\tau+\tau')\}\int_{-\infty}^{\tau} e^{p_1\theta_1}d\theta_1\int_{-\infty}^{\tau'} e^{p_1\theta_2}\delta(\theta_2-\theta_1)\,d\theta_2 = \frac{\mu C}{4p_1}\exp\{-p_1|\tau'-\tau|\}. \end{aligned} \tag{4.6}$$

In particular, the mean-square of ρ is

$$\overline{\rho^2} = \mu C/4p_1. \tag{4.7}$$

Because the system being considered is an isolated one, there is no steady state as far as phase fluctuations are concerned. If we take the phase $\chi = 0$ at time $\tau = 0$, i.e., if an ensemble of systems with this initial value of χ is considered, then, in the course of time, the tracing points spread apart on the generating circle on both sides of the regular ("dynamic") tracing points and the mean-square value of χ will increase in accordance with a diffusion law (proportional to τ). In reference 1 this situation was aptly described (in terms of the phase plane x_0, $\dot{x}_0$) as the "motion of an intoxicated person moving in a channel in which there is a steady current". In the plane which describes the slowly varying amplitudes, one in which the regular rotation along the generating circle is not shown, the indicated spreading is similar to the usual one-dimensional motion of a Brownian particle in a motionless medium except that the

fluctuations in χ depend not only on the direct effect of the random force $F_{\parallel}$ but also on the amplitude fluctuations. The effect of the latter, which are expressed by the term $q_1\rho$ in the second equation of (4.5) arises when $q_1 \neq 0$, i.e., either in the presence of a first-order frequency correction ($\Psi_{10} \neq 0$) or in the absence of isochronism in the neighborhood of the generating circle ($\partial\Psi_{10}/\partial R_0 \neq 0$), or as a result of both (if they do not cancel; this occurs when $\Psi_{10} \sim R_0$).

Taking into account the absence of a steady-state for χ, we take the solution of the second equation of (4.5) which corresponds to the initial conditions $\chi = 0$ for $\tau = 0$.

$$\chi(\tau) = -q_1\int_0^\tau \rho(\theta)\,d\theta + \frac{1}{2R_0}\int_0^\tau F_{\parallel}(\theta)\,d\theta.$$

Since, in this section, we wish only to illustrate the application of symbolic equations and correlation theory in problems which have already been solved, we will limit ourselves to the calculation of the mean-square value of χ. Assuming that the fluctuations of amplitude have already been determined, we make use of the correlation function (4.6) for ρ.

Since $\rho(\tau)$ and $F_{\parallel}(\tau)$ are not cross-correlated, we have

$$\overline{\chi^2(\tau)} = q_1^2\int_0^\tau d\theta_1\int_0^\tau \overline{\rho(\theta_1)\rho(\theta_2)}\,d\theta_2 + \frac{1}{4k_0^2}\int_0^\tau d\theta_1\int_0^\tau \overline{F_{\parallel}(\theta_1)F_{\parallel}(\theta_2)}\,d\theta_2.$$

Substituting Eq. (4.6) in (2.6), we have

$$\overline{\chi^2(\tau)} = \frac{\mu C}{2}\left\{\frac{q_1^2}{p_1^2}(p_1\tau + e^{-p_1\tau} - 1) + \frac{\tau}{R_0^2}\right\}.$$

The first term depends on the amplitude fluctuation, the second on the direct effect of the pulses. On the same basis, the second term increases in accordance with a diffusion law; the first, however, is subject to such a law only when $p_1\tau \gg 1$ and then

$$\overline{\chi^2(\tau)} = \frac{\mu C}{2}\left(\frac{q_1^2}{p_1^2} + \frac{1}{R_0^2}\right)\tau. \qquad (4.8)$$

If $p_1\tau \ll 1$ (and also if τ is much larger than the time between pulses, as is required for the formulation of the problem in terms of symbolic equations) then* $\overline{\chi^2(\tau)} = \frac{\mu C}{2}\left(\frac{\varsigma_1^2\tau^2}{2p_1} + \frac{\tau}{R_0^2}\right)$.

5. VACUUM-TUBE OSCILLATOR

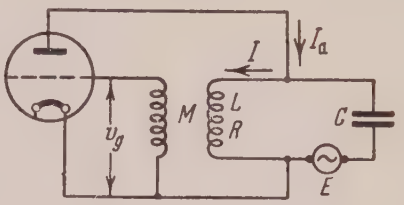

As an example, which will also be needed for what follows, we consider the vacuum-tube oscillator whose circuit is shown in the Figure. Using the symbols given in the Figure, we have the equation

$$L\frac{dI}{dt_1} + RI = \frac{1}{C}\int (I_a - I)\,dt_1 + \mathcal{E}_0 \sin\omega t_1,\ v_g = M\frac{dI}{dt_1} \qquad (5.1)$$

(The time is indicated by t_1 while the symbol t is is reserved for the dimensionless time). In the following paper, this same example will be considered in connection with synchronization; hence we introduce here a sinusoidal emf, which is included in the condenser branch to simplify the equations.

The plate current is given by the expression

$$I_a = Sv_g\left(1 - \frac{v_g^2}{3V^2}\right) + I_{\text{a-shot}}(t_1), \qquad (5.2)$$

where S and V are the usual parameters associated with the cubic characteristics of the tube and $I_{\text{a-shot}}$ is the random part of the plate arising from the shot effect**.

Introducing the dimensionless time $t = \omega t_1$ and the dimensionless current $x = I/I_0$, where

$$I_0^2 = V^2(MS - RC)/M^3S\omega, \qquad (5.3)$$

and using the notation

---

* *Note added in proof.*— In a recent paper by Gonorovskii [Dokl. Akad. Nauk SSSR 101, 657(1955)] it is found that for small τ the mean-square value of the random deviation of the phase, in general, does not contain terms to the first power in τ as though there were no direct effect of the pulses. We propose to examine the reasons for this disagreement elsewhere.

** For the present, in the interest of simplicity we omit the thermal emf in the R branch (cf. Sect. 6 of the following paper).

$$\omega_0^2 = \frac{1}{LC}, \quad \frac{\omega_0^2}{\omega^2} = 1 - \mu\Delta,$$
$$\frac{(MS - RC)\,\omega_0^2}{\omega} = \mu, \quad \frac{\omega_0^2 I_{a\tau}(t_1)}{\omega^2 I_0} = \mu^2 F(t), \qquad (5.4)$$
$$\frac{\mathcal{E}_0}{L\omega I_0} = 2\mu H,$$

from Eqs. (5.1) amd (5.2) we get equations in the form of Eq. (2.1) in which

$$f\left(x, \frac{dx}{dt}, t, \mu\right) = \frac{dx}{dt}\left[1 - \frac{1}{3}\left(\frac{dx}{dt}\right)^2\right] + \Delta x + 2H\cos t. \qquad (5.5)$$

In considering the case which is of interest to us at this time, the isolated system, it suffices to take $H = 0$ and $\Delta = 0$, i.e., to take $\omega = \omega_0$ everywhere in Eq. (5.4). Then

$$f\left(x, \frac{dx}{dt}, t, \mu\right) = \frac{dx}{dt}\left[1 - \frac{1}{3}\left(\frac{dx}{dt}\right)^2\right]. \qquad (5.6)$$

Assuming the shot-effect to be δ - correlated,

$$\overline{I_{\text{a-shot}}(t_1)\, I_{\text{a-shot}}(t_1')} = C_0\delta(t_1' - t_1) \qquad (5.7)$$

($C_0 = \overline{I}_a e$, e is the charge of the electron), and making use of the relations (5.4) between $F(t)$ and $I_{\text{a-shot}}(t_1)$,

$$\overline{I_{\text{a-shot}}(t')\, I_{\text{a-shot}}(t_1')} = \mu^4 I_0^2\, \overline{F(t)\,F(t')} = \mu^4 I_0^2\, C\frac{\delta(t_1' - t_1)}{\omega_0} \quad (\omega = \omega_0),$$

we get

$$\mu^4 C = C_0\omega_0/I_0^2. \qquad (5.8)$$

Omitting the intermediate steps, we can write directly Eq. (4.1) for the case (5.6)

$$2R_0' - R_0\left(1 - \frac{R_0^2}{4}\right) = 0, \quad Q_0 = \frac{R_0^3}{96},$$
$$2R_0\varphi_0' = 0, \quad P_0 = 0.$$

Thus $\Psi_{10} \equiv 0$, i.e., there is no first-order frequency correction, the system is completely isochronous and $R_0 = 2$. In Eqs. (4.3), $A_1 = 0$, since r_1 (the correction to the radius of the generating circle) does not appear and $B_1 = R_0^5/128 = 1/4$. Thus, taking into account second order corrections, the fundamental frequency is found to be $n = 1 - (\mu^2/16)$ and Eqs. (4.5) for ρ and χ are:

$$\rho' + \rho = F_\perp/2, \qquad \chi' = F_\parallel/4 \quad (p_1 = 1,\ q_1 = 0).$$

Expressions (4.7) and (4.8) for the mean-square values of ρ and χ assume the form

$$\overline{\rho^2} = \frac{\mu C}{4}, \quad \overline{\chi^2} = \frac{\mu C}{8}\tau \qquad (5.9)$$

We revert to the initial (physical) parameters. The amplitude fluctuations of the current in the circuit are $\Delta I = I_0\mu\rho$ and the phase fluctuations $\Delta\varphi = \mu\chi$. From Eqs. (5.3), (5.4), (5.8) and (5.9), we get, therefore,

$$\overline{\Delta I^2} = \frac{I_0^2\mu^3 C}{4} = \frac{C_0\omega_0}{4\mu} = \frac{C_0}{4(MS - RC)}, \qquad (5.10)$$

$$\overline{\Delta\varphi^2} = \frac{\mu^3 C\tau}{8} = \frac{C_0\omega_0^3 t_1}{8I_0^2} = \frac{C_0\omega_0^4 M^3 S}{8V^2(MS - RC)}\, t_1,$$

where $C_0 = \overline{I}_a e$ is the constant which appears in the correlation function of the shot-noise (5.7).

Close to the limit of self-excitation ($MS - RC \to 0$), i.e., close to the limit of stability of the oscillating mode, the "stability" of the generating circle tends toward zero. In this case there occurs an unlimited increase of the intensity of the amplitude fluctuations and of the diffusion coefficient of the phase fluctuations. Actually, the increase in the fluctuations is not unlimited; nevertheless it is large enough to invalidate the order-of-magnitude assumptions with regard to $\mu\rho$ and $\mu\chi$ upon which this analysis is based. The question of fluctuations close to the limit of self-excitation, in which the random effects in the generating circle become comparable to its radius, requires special attention.

Translated by H. Lashinsky
197

Fluctuations in Oscillating Systems of the Thomson Type. II

S. M. RYTOV
P. N. Lebedev Institute of Physics, Academy of Sciences, USSR
(Submitted to JETP editor December 2, 1954)
J. Exper. Theoret. Phys. USSR 29, 315-328 (September, 1955)

The theory developed in the preceeding paper is applied to a non-isolated system with one degree of freedom. A vacuum-tube oscillator synchronized by a harmonic driving force is considered as an example. The same method is applied in the study of a system with two degrees of freedom – a vacuum-tube oscillator coupled to a high-Q circuit – and in the elucidation of the influence of this method of frequency stabilization on fluctuations of amplitude and phase. The way in which thermal fluctuations are taken into account in this theory is considered.

1. INTRODUCTION

THE application of symbolic differential equations and correlation theory to the question of fluctuations in oscillating systems offers such a simplification of the statistical part of the problem that it becomes feasible to consider more complicated cases than that of the simple isolated system having one degree of freedom[1] (hereafter referred to as I). At the outset we may note certain results obtained below in connection with two such more complicated problems.

A *non-isolated* oscillating system having one degree of freedom is considered first, and the theory for this case is applied to a vacuum-tube oscillator synchronized by an external harmonic emf. The spectrum of the synchronized oscillator is shown to be discrete-continuous, since a strictly sinusoidal synchronizing emf implies the existence of a discrete line. Also, the forced synchronization leads to a situation in which the random excursions of the phase of the oscillations do not increase in accordance with a diffusion law but have, as do the amplitude fluctuations, a stationary spread about that value of the phase which the external emf imposes on the system in the absence of fluctuations. The dependence of the strength of the fluctuations on the amplitude of the synchronizing emf and on the difference between the frequency of this emf and the natural frequency of the oscillatory circuit is established. The ratio of the energies of the discrete line and the continuous part of the spectrum is also obtained.

The second of the problems considered in this paper is that of the fluctuations in a vacuum-tube oscillator stabilized by being coupled to a high-Q circuit (a system with two degrees of freedom). It is known that in order to apply a method involving an expansion in a small parameter this frequency-stabilization scheme can be treated in the first approximation as the synchronization of an oscillator by an external driving force[2]. It is clear that this treatment is applicable not only to the purely dynamic problem but also, to some extent, to the question of fluctuations in systems of this type; in particular, it is shown that stabilization by means of a high-Q oscillatory circuit reduces the phase diffusion coefficient in second order. Thus, in the first approximation, there occurs only a stationary spread about the value given by the initial conditions. The indicated attenuation of the phase diffusion means that the relative departure of the frequency for some fixed time is one order of magnitude smaller than that which obtains in the absence of stabilization. The analysis is based on deviations which can be attributed to fluctuations and not to the instability of the system parameters. The clear distinction between these effects and other pertinent considerations in regard to the natural and practical line-widths of the oscillator spectrum have been given by Gorelik[3].

2. SYNCHRONIZED OSCILLATING SYSTEM

Returning to Eqs. (3.8) of I in which, for the non-isolated system, Φ_{10} and Ψ_{10} now depend on R_0 and φ_0, the steady-state conditions require the vanishing of R_0 and φ_0. This requirement yields the equations

$$\Phi_{10}(R_0, \varphi_0) = 0, \quad \Psi_{10}(R_0, \varphi_0) = 0, \qquad (2.1)$$

[1] S. M. Rytov, J. Exper. Theoret. Phys. USSR, 29, 304 (1955); Soviet Phys. 2, 217 (1956). Hereafter referred to as I.

[2] S. M. Rytov, A. M. Prokhorov and M. E. Zhabotinskii, J. Exper. Theoret. Phys. USSR 15, 557, 613 (1945)

[3] G. S. Gorelik, J. Exper. Theoret. Phys. USSR 20, 351 (1950); Izv. Akad. Nauk SSSR, Ser. Fiz. 14, 187 (1950)

which determine the constants R_0 and φ_0 – the radius of the generating circle and the phase shift of the locked oscillations with respect to the synchronizing force. The generating point now fluctuates in a random fashion about the uniformly moving "dynamic" point, and is connected to it in terms of both radial and tangential fluctuations. In the steady state the "scatter region" performs uniform rotation around the generating circle without becoming deformed and, in particular, without spreading along the circle according to a diffusion law (Fig. 1).

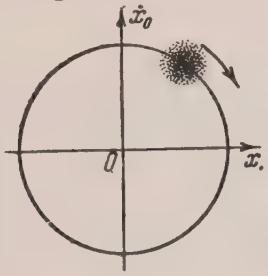

FIG. 1

Since the derivatives of R_0 and φ_0 are zero, Eqs. (3.9) of I assume the form

$$2R_1' + \frac{\partial\Phi_{10}}{\partial R_0} R_1 + \frac{\partial\Phi_{10}}{\partial\varphi_0}\varphi_1 = -A_1(R_0, \varphi_0) + F_\perp,$$
$$2R_0\varphi_1' - \frac{\partial\Psi_{10}}{\partial R_0} R_1 - \frac{\partial\Psi_{10}}{\partial\varphi_0}\varphi_1 = B_1(R_0, \varphi_0) + F_\parallel. \tag{2.2}$$

The constants A_1 and B_1, which arise from the non-linearity distortions, now represent regular correction terms to both R_1 and φ_1. Designating these regular correction terms by r_1 and ψ_1, i.e., taking

$$R_1 = r_1 + \rho(\tau), \quad \varphi_1 = \psi_1 + \chi(\tau), \tag{2.3}$$

From Eq. (2.2) we obtain expressions for r_1 and ψ_1:

$$r_1 = -\frac{q_2A_1 + p_2B_1}{p_1q_2 - p_2q_1}, \quad \psi_1 = \frac{q_1A + p_1B_1}{p_1q_2 - p_2q_1}, \tag{2.4}$$

and the following equations for the fluctuations of amplitude ρ and phase χ:

$$\rho' + p_1\rho + p_2\chi = F_\perp(\tau)/2,$$
$$\chi' + q_1\rho + q_2\chi = F_\parallel(\tau)/2R_0, \tag{2.5}$$

in which

$$p_1 = \frac{1}{2}\frac{\partial\Phi_{10}}{\partial R_0}, \quad p_2 = \frac{1}{2}\frac{\partial\Phi_{10}}{\partial\varphi_0},$$
$$q_1 = -\frac{1}{2R_0}\frac{\partial\Psi_{10}}{\partial R_0}, \quad q_2 = -\frac{1}{2R_0}\frac{\partial\Psi_{10}}{\partial\varphi_0}. \tag{2.6}$$

Being interested only in the steady state, we take solutions of Eqs. (2.5) for initial conditions, corresponding to the vanishing of the quantities of interest at $\tau = -\infty$:

$$\rho(\tau) = \frac{1}{2(\lambda_1 - \lambda_2)}\int_{-\infty}^{\tau}\Big\{[(p_1 + \lambda_1)e^{\lambda_2(\tau-\theta)} - (p_1 + \lambda_2)e^{\lambda_1(\tau-\theta)}]F_\perp(\theta) + \frac{p_2}{R_0}[e^{\lambda_2(\tau-\theta)} - e^{\lambda_1(\tau-\theta)}]F_\parallel(\theta)\Big\}d\theta,$$
$$\chi(\tau) = -\frac{1}{2(\lambda_1 - \lambda_2)}\int_{-\infty}^{\tau}\Big\{\frac{(p_1 + \lambda_1)(p_1 + \lambda_2)}{p_2}[e^{\lambda_2(\tau-\theta)} - e^{\lambda_1(\tau-\theta)}]F_\perp(\theta) + \frac{1}{R_0}[(p_1 + \lambda_2)e^{\lambda_2(\tau-\theta)} - (p_1 + \lambda_1)e^{\lambda_1(\tau-\theta)}]F_\parallel(\theta)\Big\}d\theta. \tag{2.7}$$

Here λ_1 and λ_2 are the roots of the characteristic equation

$$\lambda^2 + (p_1 + q_2)\lambda + p_1q_2 - p_2q_1 = 0, \tag{2.8}$$

having real negative values for the stable mode. Since λ_1 and λ_2 are complex conjugates, the expressions (2.7) are always real.

Omitting rather tedious but elementary calculations based on Eqs. (2.7), (2.8) and formulas (2.6) of I, we present the results of a calculation of the correlation functions for ρ and χ:

$$\overline{\rho(\tau)\rho(\tau')} = \frac{\mu C}{4(\lambda_1^2 - \lambda_2^2)} \times \Big\{\Big[(p_1 + \lambda_2)(\lambda_1 - q_2) + \frac{p_2^2}{R_0^2}\Big]\frac{1}{\lambda_1}e^{\lambda_1|\tau'-\tau|} - \Big[(p_1 + \lambda_1)(\lambda_2 - q_2) + \frac{p_2^2}{R_0^2}\Big]\frac{1}{\lambda_2}e^{\lambda_2|\tau'-\tau|}\Big\},$$
$$\overline{\chi(\tau)\chi(\tau')} = \frac{\mu C^*}{4(\lambda_1^2 - \lambda_2^2)}\Big\{\Big[q_1^2 + \frac{p_1^2 - \lambda_1^2}{R_0^2}\Big] \times \frac{1}{\lambda_1}e^{\lambda_1|\tau'-\tau|} - \Big[q_1^2 + \frac{p_1^2 - \lambda_2^2}{R_0^2}\Big]\frac{1}{\lambda_2}e^{\lambda_2|\tau'-\tau|}\Big\}. \tag{2.9}$$

Whence, if it is assumed that $\tau' = \tau$ and if use is again made of Eq. (2.8), the following expressions are obtained for the mean-square values of ρ and χ:

$$\overline{\rho^2} = \frac{\mu C}{4(p_1+q_2)}\left\{1 + \frac{q_2^2 + (p_2^2/R_0^2)}{p_1q_2 - p_2q_1}\right\}, \tag{2.10}$$

$$\overline{\chi^2} = \frac{\mu C}{4(p_1+q_2)}\left\{\frac{q_1^2 + (p_1^2/R_0^2)}{p_1q_2 - p_2q_1} + \frac{1}{R_0^2}\right\}.$$

According to Eq. (2.3) and formulas (3.2) and (3.5) of I the frequency of the fundamental oscillation is given by

$$x_{\text{fund}} = (R_0 + \mu r_1 + \mu\rho) \times \cos(t - \varphi_0 - \mu\psi_1 - \mu\chi).$$

We find the correlation function for χ_{fund} neglecting the amplitude correction μr_1 and the amplitude fluctuations $\mu\rho$. Then

$$\overline{x_{\text{fund}}(t)\, x_{\text{fund}}(t')} \tag{2.11}$$
$$= \frac{R_0^2}{2}\overline{\{\cos[t - t' - \mu(\chi - \chi')]}$$
$$\overline{+ \cos[t + t' - 2(\varphi_0 + \mu\psi_1) - \mu(\chi + \chi')]\}}.$$

In the case of an isolated system it is assumed that the random phase shift during the time $\tau' - \tau$, i.e., the quantity $u = \chi' - \chi$, has a normal distribution, and that, in the steady state, the sum $v = \chi' + \chi$ is distributed uniformly over the interval $(-\pi, \pi)$ and is not correlated with u. Under these assumptions, the second term in Eq. (2.11) vanishes and the first gives $\frac{R_0^2}{2} e^{-\mu^2\overline{u}^2/2} \times \cos(t - t')$, i.e., the result depends only on $t' - t$, as is to be expected for a stationary process.

In the present case, we do not make the same assumptions with regard to u and v. On the contrary, it is natural to assume on the basis of the central limit theorem, as before, that now the random tangential excursions of the "dynamic" point are also normally distributed as are the radial deviations. Thus, we assume that the two-dimensional distribution $\chi = \chi(t)$ and $\chi' = \chi(t')$ has the form

$$w(\chi, \chi')\, d\chi\, d\chi' = \frac{d\chi\, d\chi'}{2\pi\sigma^2\sqrt{1-r^2}} \exp\left\{-\frac{\chi^2 + \chi'^2 - 2r\chi\chi'}{2\sigma^2(1-r^2)}\right\},$$

where

$$\sigma^2 = \overline{\chi^2}, \qquad r = \frac{\overline{\chi(\tau)\,\chi(\tau')}}{\sigma^2}. \tag{2.12}$$

Then $u = \chi' - \chi$ and $v = \chi' + \chi$ are statistically independent, and are characterized by normal distributions and mean-square values $\overline{u}^2 = 2\sigma^2(1-r)$ and $\overline{v}^2 = 2\sigma^2(1+r)$. Taking averages in Eq. (2.11), we get

$$\overline{x_{\text{fund}}(t)\, x_{\text{fund}}(t')} = \frac{R_0^2}{2}\{\cos(t - t')\,\overline{\cos\mu u} + \cos[t + t' - 2(\varphi_0 + \mu\psi_1)]\,\overline{\cos\mu v}\} \tag{2.13}$$
$$= \frac{R_0^2}{2}\{\cos(t - t')\, e^{-\mu^2\sigma^2(1-r)} + \cos[t + t' - 2(\varphi_0 + \mu\psi_1)]\, e^{-\mu^2\sigma^2(1+r)}\},$$

i.e., as was to be expected, we get a correlation function corresponding to a non-stationary process.

As is well known, (see for example reference 4, Sec. 11) the average intensity at the output of a filter, into which is fed a non-stationary signal $\chi_{\text{fund}}(t)$, is determined from the time average of the correlation of $\chi_{\text{fund}}(t)$. In taking the time average of Eq. (2.13), designated by the wavy line, the second term vanishes so that

$$\overline{\overline{x_{\text{fund}}(t)\, x_{\text{fund}}(t')}} = \frac{R_0^2}{2} e^{-\mu^2\sigma^2(1-r)} \cos(t' - t), \tag{2.14}$$

in which $\sigma^2(1-r) = \overline{\chi^2} - \overline{\chi(\tau)\,\chi(\tau')}$ and the correlation function and the mean-square value of χ are given by formulas (2.9) and (2.10).

Using (2.14) one can, in the usual manner, determine the spectral density of the oscillations in which we are interested:

---

[4] V. I. Bunimovich, *Fluctuation Processes in Radio Receiving Apparatus*, published in "Soviet Radio", Moscow, 1951

$$g(\Omega) = \frac{2}{\pi}\int_0^\infty \overbrace{x_{\text{fund}}(t)\, x_{\text{fund}}(t+\theta)}\cos\Omega\theta\, d\theta$$

$$= \frac{R_0^2}{\pi}\int_0^\infty \exp\{\mu^2[\overline{\chi(\tau)\chi(\tau+\mu\theta)} - \overline{\chi^2}]\}\cos\theta\cos\Omega\theta\, d\theta.$$

Taking into account the fact that

$$\int_0^\infty \cos\theta\cos\Omega\theta\, d\theta = \frac{\pi}{2}\delta(\Omega-1),$$

we get for $g(\Omega)$ the expression

$$g(\Omega) = \frac{R_0^2}{2}\, e^{-\mu^2\overline{\chi^2}}\,\delta(\Omega-1)$$

$$+ \frac{R_0^2}{\pi}\, e^{-\mu^2\overline{\chi^2}}\int_0^\infty (\exp\{\mu^2\overline{\chi(\tau)\chi(\tau+\mu\theta)}\} - 1)$$

$$\times \cos\theta\cos\Omega\theta\, d\theta. \qquad (2.15)$$

The first term corresponds to a discrete line at the frequency of the synchronizing signal $\Omega = 1$, and the second gives the continuous part of the spectrum. We can now compare the total energy in the discrete line with the total energy of the continuous spectrum. In accordance with the separation of the correlation function in Eq. (2.15), in particular,

$$\overbrace{x_{\text{fund}}(t)\, x_{\text{fund}}(t+\theta)} = \frac{R_0^2}{2}\exp\{-\mu^2\overline{\chi^2}\}$$

$$\times[1 + (\exp\{\mu^2\overline{\chi(\tau)\chi(\tau+\mu\theta)}\} - 1)],$$

we have for $\theta = 0$

$$\overbrace{x_{\text{fund}}^2(t)} = W_d + W_c$$

$$= \frac{R_0^2}{2}\exp\{-\mu^2\overline{\chi^2}\} + \frac{R_0^2}{2}(1 - \exp\{-\mu^2\overline{\chi^2}\}).$$

Thus, the ratio of the noise energy to the energy in the discrete line is

$$W_c/W_d = \exp\{\mu^2\overline{\chi^2}\} - 1. \qquad (2.16)$$

If

$$\mu^2\overline{\chi^2} \ll 1, \qquad (2.17)$$

i.e., if the continuous spectrum is relatively weak, then its density can be found without difficulty. In this case, from the second term of formula (2.15), taking into account (2.9), we get

$$g_{\text{cont}}(\Omega) = \frac{\mu^2R_0^2}{\pi}\int_0^\infty \overline{\chi(\tau)\chi(\tau+\mu\theta)}\cos\theta\cos\Omega\theta\, d\theta$$

$$= \frac{\mu^2CR_0^2}{8\pi}\left(q_1^2 + \frac{p_1^2+\alpha^2}{R_0^2}\right)\frac{1}{(\alpha^2+\lambda_1^2)(\alpha^2+\lambda_2^2)}$$

where we have introduced the notation

$$\alpha = (\Omega - 1)/\mu.$$

Later we shall see (Section 3) that at the center of the synchronization band $p_2 = q_1 = 0$. In this case, according to Eq. (2.8), $\lambda_1 = -p_1$, $\lambda_2 = -q_2$ and the expression for the density of the continuous spectrum assumes the form

$$g_{\text{cont}}(\Omega) = \frac{\mu^2C}{8\pi}\frac{1}{\alpha^2+q_2^2}, \qquad (2.18)$$

i.e., the spectrum is in the form of a resonance curve with respect to the dimensionless parameter α and has a halfwidth q_2. In terms of the true frequency, this means a halfwidth $\delta\omega = \mu q_2\omega$. One should keep in mind that formula (2.18) is valid only under the conditions given in Eq. (2.17).

3. VACUUM-TUBE OSCILLATOR SYNCHRONIZED BY A HARMONIC EMF

We now apply the results of the preceding section to the oscillator whose circuit is shown in the Figure in I. In the presence of the synchronizing emf, the right-hand part of Eqs. (2.1) of I is given by Eq. (5.5). In this case Eqs. (2.1) of the preceding section become:

$$R_0(1-Z) + 2H\sin\varphi_0 = 0,$$
$$\Delta R_0 + 2H\cos\varphi_0 = 0 \qquad (Z = R_0^2/4). \qquad (3.1)$$

The constant correction terms (2.4) to the radius of the generating circle r_1, and to the phase shift ψ_1, are found to be

$$r_1 = -\frac{R_0Z^2\Delta}{8[(3Z-1)(Z-1)+\Delta^2]},$$

$$\psi_1 = \frac{Z^2(3Z-1)}{8[(3Z-1)(Z-1)+\Delta^2]},$$

and the coefficients in Eq. (2.5) have the form

$$p_1 = \frac{3Z-1}{2}, \quad p_2 = \frac{\Delta R_0}{2},$$
$$q_1 = -\frac{\Delta}{2R_0}, \quad q_2 = \frac{Z-1}{2}. \qquad (3.2)$$

Using Eq. (3.2) in formula (3.10) to calculate the mean-square values of the fluctuations of amplitude and phase, we get

$$\overline{\rho^2} = \frac{\mu C\,[(2Z-1)(Z-1)+\Delta^2]}{2(2Z-1)[(3Z-1)(Z-1)+\Delta^2]}, \quad (3.3)$$

$$\overline{\chi^2} = \frac{\mu C\,[(3Z-1)(2Z-1)+\Delta^2]}{8Z(2Z-1)[(3Z-1)(Z-1)+\Delta^2]}.$$

According to Eq. (3.1), the equation of the resonance curve in the synchronization case is

$$Z[(Z-1)^2+\Delta^2] = H^2, \quad (3.4)$$

so that the right-hand parts of (3.3) are determined (aside from the factor μC) only by the amplitude of the synchronizing force and the deviation Δ. In the theory of synchronization one distinguishes, as is known[5], between the cases of large and small amplitudes $H(H^2 \gtrless 8/27)$, which correspond to different types of loss of stability of the synchronized mode. If H is sufficiently small, then Z is close to unity and, according to Eq. (3.4), $Z \approx 1 + H$ at the center of the synchronization band. In this case it follows from Eq. (3.3) that

$$\overline{\rho^2} = \frac{\mu C}{4}, \quad \overline{\chi^2} = \frac{\mu C}{8H}$$

$$\left(\Delta = 0,\ H^2 \ll \frac{8}{27}\right). \quad (3.5)$$

Thus, at the center of the synchronization band the amplitude fluctuations in this case are the same as those of the isolated oscillator [see Eq. (5.9) of I] and the phase fluctuations which are now also stationary, increase indefinitely with the reduction of H. This increase is connected with the fact that the width of the synchronization band is proportional to H; at its boundaries the synchronized mode being studied loses stability and $\overline{\rho^2}$ and $\overline{\chi^2}$ become infinite [the second factor in the denominator of Eq. (3.3) approaches zero]. Within the band, the phase shifts associated with the frequency shifts are found to be more sensitive to the narrowing of the band limits than are the amplitude fluctuations.

In the case of small H, which is being considered, the halfwidth of the synchronization band (in terms of the dimensionless deviation Δ) is equal to H. The halfwidth of the continuous spectrum, according to Eq. (2.18) is $q_2 = (Z-1)/2 \approx H/2$. Thus, the continuous spectrum is one-half as wide as the synchronization band. This result is valid under the conditions given in Eq. (2.17), which, according to Eq. (3.5), can be put in the form

$$\mu^3 C/8H \ll 1$$

and consequently cannot be carried over to arbitrarily small values of H.

At the center of the synchronization band ($\Delta = 0$) and for large values of H we may take $Z \gg 1$; hence, from Eq. (3.4) we have $Z \approx H^{2/3}$. In this case Eq. (3.3) gives

$$\overline{\rho^2} = \frac{\mu C}{6H^{2/3}}, \quad \overline{\chi^2} = \frac{\mu C}{8H^{4/3}}, \quad (3.6)$$

i.e., with an increase in the value of H, the magnitude of the phase fluctuations falls off quicker than that of the amplitude fluctuations. For $H \gtrsim 8$, $\mu^2\overline{\rho^2}/R_0^2$ is reduced by a factor of 24 or more as compared with the isolated oscillator.

At the limits of the synchronization band [where the first factor in the denominator of the expressions in Eq. (3.3) becomes zero] we find that $\overline{\rho^2}$ and $\overline{\chi^2}$ can also increase without limit in the case of large H. As has already been noted, this means that in such cases the choices of the orders of magnitude ρ and χ made at the beginning of the analysis are no longer valid.

Equation (2.16) indicates that with the higher values of H, the ratio of the energy in the continuous spectrum to the energy in the discrete line approaches zero at the center of the synchronization band because

$$\frac{W_c}{W_d} = \mu^2\overline{\chi^2} = \frac{\mu^2 C}{8H^{4/3}} = \frac{C_0 M L\,\omega_0^3}{8}\sqrt[3]{\frac{2I\,\omega_0 S}{V^2\mathcal{E}_0^4}}. \quad (3.7)$$

However, close to the limits of the band, where $\overline{\chi^2} \to \infty$, the discrete line, whose existence in the oscillator spectrum is dependent on the sinusoidal synchronizing emf, "blends" in with the noise. If the spectrum of this emf is not monochromatic, there will be no discrete line, and the width of the continuous spectrum will be considerably increased. Strictly speaking, the oscillator synchronization force is not sinusoidal but the treatment of a randomly modulated synchronizing force requires special attention.

For large amplitudes of the synchronizing force the halfwidth of the synchronization band is $\sqrt{2}H$ while the halfwidth of the continuous spectrum is $q_2 = (Z-1)/2 \approx H^{2/3}/2$. Thus the relative halfwidth of the continuous spectrum is $1/(2\sqrt{2}H^{1/3})$. For

[5] A. A. Andronov and A. A. Vitt, Zh. Prikl. Fiz. 7, 3 (1930)

these results to be valid, the quantity given in Eq. (3.7) must be small compared with unity.

4. SYSTEMS WITH TWO DEGREES OF FREEDOM

In analyzing an oscillator which is frequency-stabilized through coupling to a high-Q system*, one finds typically an order-of-magnitude asymmetry in the right-hand side of the equations of motion[2]. Typical equations for the problem at hand, where we have introduced a fluctuation force of order μ^2, have the form

$$\frac{d^2x}{dt^2} + x = \mu f\left(x, \frac{dx}{dt}, y, \frac{dy}{dt}, \mu\right) + \mu^2 F(t);$$
$$\frac{d^2y}{dt^2} + y = \mu^2 g\left(x, \frac{dx}{dt}, y, \frac{dy}{dt}, \mu\right), \tag{4.1}$$

where x is the current in the oscillator circuit and y is the current in the stabilization element, which for convenience we will in all cases call the "crystal". Thus, to an accuracy of the order of μ, the crystal represents an independent conservative oscillator. It acts on the oscillator with a force of the first order and synchronizes the oscillator in the region of resonance (with deviations $\sim \mu$). The crystal losses and their influences on the oscillator are taken into account in second order. Furthermore – and is closely related to the question of fluctuations – the random force acting on the oscillator also enters in second order.

The accuracy of the solutions of equations (4.1) is the same as that for the case of a system having one degree of freedom. Since we are interested only in the effects of stabilization on fluctuations in vacuum-tube oscillators, we turn now from the general equations of (4.1) to a concrete frequency-stabilization circuit which has two degrees of freedom.

To facilitate comparison with the example considered earlier, we consider the coupling scheme (Fig. 2) which differs from the circuit of the Figure given in I in the presence of the stabilization loop L_1, C_1, R_1, which is inductively coupled to the oscillator circuit. The high-Q of the circuit L_1, C_1, R_1 is reflected in the following choices of the parameters: $L_1 \sim 1/\mu$, $C_1 \sim \mu$, $R_1 \sim \mu$. The mutual-inductance coefficient $N \sim \mu$. From these we have:

$$\frac{1}{L_1 C_1} = \omega^2, \quad \frac{R_1}{L_1 \omega} = \mu^2 h, \tag{4.2}$$
$$\frac{N}{L_1} = \mu^2 k_2, \quad \frac{N}{L} = \mu k_1.$$

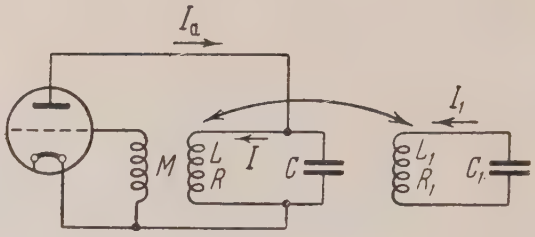

FIG. 2

Through these quantities and the parameters introduced earlier [cf. Eqs. (5.3) and (5.4)] the equations for the circuit of Fig. 2 can be written in the form:

$$\frac{d^2x}{dt^2} + x = \mu\left\{\frac{dx}{dt}\left[1 - \frac{1}{3}\left(\frac{dx}{dt}\right)^2\right] + \Delta x - k_1\frac{d^2y}{dt^2}\right\} + \mu^2 F(t),$$
$$\frac{d^2y}{dt^2} + y = -\mu^2\left(h\frac{dy}{dt} + k_2\frac{d^2x}{dt^2}\right). \tag{4.3}$$

Here as before, $t = \omega t_1$, $x = I/I_0$ and, in addition, $y = I_1/I_0$, where I_1 is the current in the "crystal".

We have a solution in the form

$$x = R\cos(t-\varphi) + \mu\{P\cos 3(t-\varphi) + Q\sin 3(t-\varphi) + \ldots\},$$
$$y = U\cos(t-\varphi) + V\sin(t-\varphi) + \mu\{\ldots\}. \tag{4.4}$$

There are no even harmonics in y because in the stabilized mode, in which we are interested, the "crystal" overtones appear only in order μ^3 [2].

Substituting Eq. (4.4) in Eq. (4.3), setting to zero the coefficients of $\sin(t-\varphi)$, $\sin 3(t-\varphi)$ and $\cos(t-\varphi)$, $\cos 3(t-\varphi)$ and expressing R, P, Q, U, V and φ in a power series in μ, we obtain the successive approximation equations. We will not, however, undertake the solution of these in their general form since we are interested only in the steady-state conditions ($R_0' = 0$), and the stabilized mode, in which $\varphi_0' = 0$, i.e., there are no first-order frequency corrections[2]. Under these conditions, the equations for the first approximation are as follows:

*In standard crystal oscillators there are also used simple circuits in which the crystal appears as the sole oscillatory element. When considering the properties of the equivalent circuit of the crystal in such oscillators one applies the theory of a system having one degree of freedom.

$$R_0\left(1-\frac{R_0^2}{4}\right)=k_1V_0, \qquad P_0=0,$$

$$-\Delta R_0=k_1U_0, \qquad Q_0=R_0^3/96, \tag{4.5}$$

and the equation for the second approximations have the form:

$$2R'-\left(1-\frac{3R_0^2}{4}\right)R_1+k_1V_1=F_\perp, \tag{4.6}$$

$$2R_0\varphi_1'-\Delta R_1-k_1U_1=\frac{R_0^5}{128}+F_\parallel;$$

$$P_1=-\frac{R_0^3}{256}\left(1-\frac{R_0^2}{2}\right), \tag{4.7}$$

$$Q_1-\frac{R_0^2}{32}R_1=-\frac{\Delta}{768}R_0^3;$$

$$2U_1'-2V_0\varphi_1'=-hU_0, \tag{4.8}$$

$$2V_1'+2U_0\varphi_1'=-hV_0+k_2R_0.$$

We now separate the constant terms r_1, u_1, v_1, δ_1 in R_1, U_1, V_1, φ_1:

$$R_1=r_1+\rho(\tau), \quad U_1=u_1+\xi(\tau), \tag{4.9}$$

$$V_1=v_1+\eta(\tau), \quad \varphi_1=\delta_1\tau+\chi(\tau).$$

Substituting these relations in Eqs. (4.6) and (4.8), we get equations for the constant terms

$$k_1v_1=\left(1-\frac{3R_0^2}{4}\right)r_1, \quad 2V_0\delta_1=hU_0, \tag{4.10}$$

$$k_1u_1=2R_0\delta_1-\Delta r_1-\frac{R_0^5}{128},$$

$$2U_0\delta_1=-hV_0+k_2R_0.$$

From the last two equations, it follows, first of all, that

$$h(U_0^2+V_0^2)=k_2R_0V_0 \quad ; \tag{4.11}$$

this equation, in conjunction with Eq. (4.5), determines R_0, U_0 and V_0. Secondly, using these same two equations we obtain the following expression for the second-order frequency correction δ_1:

$$\delta_1=hU_0\,2V_0. \tag{4.12}$$

For r_1, u_1 and v_1 there remain only the first two equations of Eq. (4.10). The missing third equation is obtained only in the next approximation* .

The variable terms satisfy the equations

$$2\rho'-\left(1-\frac{3R_0^2}{4}\right)\rho+k_1\eta=F_\perp, \tag{4.13}$$

$$\xi'-V_0\chi'=0,$$

$$2R_0\chi'-\Delta\rho-k_1\xi=F_\parallel, \quad \eta'+U_0\chi'=0.$$

In considering ξ and η one may take initial conditions corresponding to the vanishing of the quantities of interest at $\tau=-\infty$. Then, as follows from the last two equations of (4.13),

$$U_0\xi+V_0\eta=0.$$

We may note that $\mu(U_0U_1+V_0V_1)$ is the first-order correction to the amplitude in the "crystal". Thus, in first order, the "crystal" amplitude is not subject to fluctuations.

If we assume that the value of χ is zero at $\tau=0$, then

$$\xi=\xi(0)=V_0\chi, \quad \eta-\eta(0)=-U_0\chi, \tag{4.14}$$

in which $U_0\xi(0)+V_0\eta(0)=0$. Substituting $\eta=-(U_0/V_0)$ and $\chi'=(1/V_0)\xi'$ in the first two equations of (4.13), we obtain for ρ and ξ :

$$\rho'+p_1\rho+p_2\xi=F_\perp/2, \tag{4.15}$$

$$\xi'+q_1\rho+q_2\xi=(V_0/2R_0)F_\parallel,$$

where

$$p_1=\frac{1}{2}\left(\frac{3R_0^2}{4}-1\right), \quad p_2=-\frac{k_1U_0}{2V_0}, \tag{4.16}$$

$$q_1=-\frac{\Delta V_0}{2R_0}, \quad q_2=-\frac{k_1V_0}{2R_0}.$$

Before solving these equations, we present the the solutions of the first-approximation equations and the pertinent data on the stability limits of the stabilized mode[2]. For the stabilized branch we have, from Eqs. (4.5) and (4.11),

$$\frac{R_0^2}{4}=1-\sigma+\sqrt{\sigma^2-\Delta^2}, \quad U_0^2+V_0^2 \tag{4.17}$$

$$=\frac{8\sigma}{k_1^2}[(1-2\sigma)(\sigma-\sqrt{\sigma^2-\Delta^2})+\Delta^2], \quad \sigma_1=\frac{hU_0}{2V_0}$$

$$=-\frac{h}{2\Delta}(\sigma+\sqrt{\sigma^2-\Delta^2}),$$

where $\sigma=k_1k_2/2h$.

In Fig. 3 is shown the region of stability in terms of the variables Δ^2 and σ. Formally, the stabilization should extend up to $\Delta=0$, but in reality, at $\Delta\sim\mu^{1/4}$, the approximation on which our analysis is based is no longer valid (in particular, $\delta_1\to\infty$).

---

* It is derived, like Eq. (4.11), from the requirement that there be no regular increase in the second-order correction to the amplitude in the crystal and has the form:

$$2hU_0u_1+h\frac{V_0^2-U_0^2}{V_0}v_1-k_2V_0r_1=0.$$

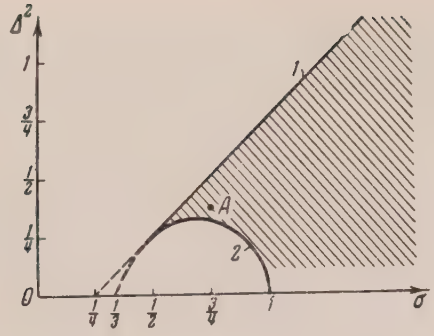

FIG. 3. $1 - \Delta^2 = \sigma - 1/4$; $2 - \Delta^2 = (1-\sigma)(3\sigma - 1)$

At this point there occurs a region of unstable solutions which carry over to the non-stabilized mode[2] and therefore the lower edge of the stability region is not extended to the abscissa axis in Fig. 3. The non-stabilized mode, for which the crystal is not excited in the zeroth approximation, will not be considered, since it is very much like the case of the simple oscillator (I, Sec. 5).

5. FLUCTUATION IN A COUPLED SYSTEM

Equations (4.15) coincide with Eqs. (2.5) if we replace $F_\parallel$ and χ of the latter by $V_0 F_\parallel$ and ξ. Using these substitutions we can apply formulas (2.7) – (2.10) to find ρ and ξ, thus we have

$$\overline{\rho^2} = \frac{\mu C}{4(p_1+q_2)}\left\{1+\frac{q_2^2+(V_0^2 p_2^2/R_0^2)}{p_1 q_2 - p_2 q_1}\right\}, \tag{5.1}$$

$$\overline{\xi(\tau)\,\xi(\tau')} = \frac{\mu C}{4(\lambda_1^2-\lambda_2^2)} \tag{5.2}$$

$$\times\left\{\left[q_1^2+\frac{V_0^2}{R_0^2}(p_1^2-\lambda_1^2)\right]\frac{1}{\lambda_1}e^{\lambda_1|\tau'-\tau|} - \left[q_1^2+\frac{V_0^2}{R_0^2}(p_1^2-\lambda_2^2)\right]\frac{1}{\lambda_2}e^{\lambda_2|\tau'-\tau|}\right\},$$

$$\overline{\xi^2} = \frac{\mu C}{4(p_1+q_2)}\left\{\frac{q_1^2+(V_0^2/R_0^2)p_1^2}{p_1 q_2 - p_2 q_1}+\frac{V_0^2}{R_0^2}\right\}$$

Using Eq. (4.14), we find the mean-square value of the phase fluctuations:

$$\overline{\chi^2(\tau)} = \frac{1}{V_0^2}\left[\overline{\xi^2(\tau)} - 2\overline{\xi(\tau)\,\xi(0)} + \overline{\xi^2(0)}\right] = \frac{2}{V_0^2}\left[\overline{\xi^2} - \overline{\xi(\tau)\,\xi(0)}\right] \tag{5.3}$$

and consequently formulas (5.2) can also be used to obtain $\overline{\chi^2}$. We now consider the amplitude fluctuations.

Substituting the values of the coefficients p_1, p_2, q_1, q_2 from Eq. (4.16) into Eq. (5.1), and using Eqs. (4.5), it is not difficult to reduce the expression for $\overline{\rho^2}$ to the form:

$$\overline{\rho^2} = \frac{\mu C\left[\left(\frac{R_0^2}{4}-1\right)\left(\frac{3R_0^2}{4}-1-2\sigma\right)+\Delta^2\right]}{4\left(\frac{R_0^2}{2}-1\right)\left[\left(\frac{R_0^2}{4}-1\right)\left(\frac{3R_0^2}{4}-1\right)+\Delta^2\right]}.$$

In turn, substituting the expression for $R_0^2/4$ given in Eq. (4.17), the above expression is transformed into the following:

$$\overline{\rho^2} = \frac{\mu C}{4(1-2\sigma)}\left\{\frac{1-4\sigma}{1-2\sigma+2\sqrt{\sigma^2-\Delta^2}} + \frac{\sigma}{1-2\sigma+\sqrt{\sigma^2-\Delta^2}}\right\}. \tag{5.4}$$

The denominator of the first term becomes zero for $\Delta^2 = \sigma - 1/4$, i.e., at the outer limit of the region of stability of the stabilized mode (Fig. 3). The denominator of the second term becomes zero for $\Delta^2 = (1-\sigma)(3\sigma-1)$, i.e., at the inner limit which obtains when $1/2 < \sigma < 1$. The appearance of stability limits at which the generating circle becomes completely "dissolved" means that the smallest value of $\overline{\rho^2}$ obtained outside the region of stability is higher than that of the simple oscillator.

If we assume a sufficiently strong coupling to the "crystal" ($\sigma > 1$, see Fig. 3), then the minimum $\overline{\rho^2}$ is obtained at a deviation Δ_{opt} determined by the equation

$$\sqrt{\sigma^2-\Delta_{opt}^2} = -\frac{4(1-2\sigma)+\sqrt{6(1-2\sigma)(2-3\sigma)}}{2}$$

This minimum is

$$\overline{\rho^2}_{min} = \frac{\mu C}{4(2\sigma-1)}\left\{\frac{4\sigma-1}{3(2\sigma-1)-\sqrt{6(1-2\sigma)(2-3\sigma)}} - \frac{2\sigma}{2(2\sigma-1)-\sqrt{6(1-2\sigma)(2-3\sigma)}}\right\}.$$

For $\sigma = 1$ we have $\Delta^2_{opt} = 0.4$ and $\overline{\rho^2}_{min} = 10\mu C_4$, i.e., it is 10 times larger than the level of amplitude fluctuations in the non-stabilized oscillator [see Eq. (5.9) in I]. With an increase of σ, $\overline{\rho^2}_{min}$ is reduced, but even for $\sigma \to \infty$ (in which case $\Delta^2_{opt} \to \sqrt{\sigma/2}$) we have $\overline{\rho^2}_{min} \to \mu C$, i.e., it is 4 times larger than in the simple oscillator. In the case of weak coupling to the "crystal", when the limits of the stability region become narrower, $\overline{\rho^2}$ becomes even larger inside the region. Thus, for example, at the point A in Fig. 3 ($\Delta^2 = 3/8$, $\sigma = 3/4$) we have $\overline{\rho^2} = 33.2\,\mu C/4$.

Hence, stabilization leads to the reduction of "stability" of the generating circle and to an increase of the strength of the amplitude fluctuation in the oscillator circuit. The relative amplitude fluctuation $\mu\sqrt{\overline{\rho^2}}/R_0$ is still larger since the radius of the generating circle R_0 in the stabilization case is always smaller than two; this is apparent from Eq. (4.17).

We now consider the phase fluctuations. From Eq. (5.2) the correlation function of ξ tends towards zero with an increase of $|\tau' - \tau|$. Consequently, for large τ the second term in Eq. (5.3) vanishes and χ^2 attains a *stationary* value:

$$\overline{\chi^2} = \frac{2\overline{\xi^2}}{V_0^2} = \frac{\mu C}{4(p_1 + q_2)} \left\{ \frac{(q_1^2/V_0^2) + (p_1^2/R_0^2)}{p_1 q_2 - p_2 q_1} + \frac{1}{R_0^2} \right\}.$$

Using Eqs. (4.5) and (4.16), this expression can be transformed to the same as Eq. (3.3), that of the synchronization case:

$$\overline{\chi^2} = \frac{\mu C [(3Z-1)(2Z-1) + \Delta^2]}{8Z(2Z-1)[(3Z-1)(Z-1) + \Delta^2]} \qquad (5.5)$$

$$\left(Z = \frac{R_0^2}{4} \right).$$

It is not necessary for us to analyze this expression. The important feature is that in the first-order correction to the phase there is no diffusion; a stationary process is set up very much like that which takes place in the synchronization of the oscillator by an external synchronizaforce. Hence, in the first approximation the effect of the "crystal" can be interpreted as that of a synchronizing force – not only as regards the dynamic behavior of the oscillator but also with regard to phase fluctuations. Using Eqs. (3.4) and (4.17), we find the amplitude of the equivalent synchronizing emf due to the "crystal"; we have

$$H^2 = Z[(Z-1)^2 + \Delta^2]$$
$$= 2(1 - \sigma + \sqrt{\sigma^2 - \Delta^2})(\Delta^2 + \sigma^2 - \sigma\sqrt{\sigma^2 - \Delta^2}).$$

There are, however, certain differences from the synchronization case. Firstly, in the synchronization case the phase φ_0 is determined by the external force, while here the random spread takes place about the value φ_0 which depends on the initial conditions. Secondly, and this is more important, in the isolated system, phase diffusion always takes place, while the result we have obtained here only indicates that, in the case of stabilization, the diffusion coefficient is of a smaller order of magnitude. If the phase fluctuation is written in the form $\Delta\varphi = \mu\chi + \mu^2\chi_1 + \mu^3\chi_2 \cdots$ then

$$\overline{\Delta\varphi^2} = \mu^2\overline{\chi^2} + 2\mu^3\overline{\chi\chi_1} + \mu^4(\overline{\chi_1^2} + 2\overline{\chi\chi_2}) + \ldots .$$

One is easily convinced that (for large τ) $\overline{\chi^2}$ does not contain terms proportional to τ. For calculation of the following terms we must turn to the equations for the higher approximations – the third for χ_1 and the fourth for χ_2. The calculation of χ_1 shows that the term $\overline{\chi\chi_1}$ also does not yield a diffusion dependence on τ, but undoubtedly it will appear in $\overline{\chi_1^2}$. Because it is excessively complicated the calculation of the diffusion coefficient cannot be carried out successfully and one can only draw the conclusion that stabilization reduces the phase diffusion coefficient by a factor $\sim \mu^2$, i.e., it multiplies the time required to establish a regular phase distribution along the generating circle by a factor $\sim 1/\mu^2$.

6. THERMAL NOISE

Up to this point only the shot-noise of the tube has been considered in the physical examples of the random force $F(t)$. However, our method based on the use of symbolic equation and correlation theory can also easily be applied to the calculation of thermal fluctuations. For this purpose, in forming the equations of motion one merely introduces a random thermal emf localized in the physical resistances of the circuit.

We will consider the coupled system which has already been treated (Fig. 2). If the branch containing R and R_1 now contains the emf sources $\mathcal{E}(t_1)$ and $\mathcal{E}_1(t_1)$, then in place of equations (4.3), we have

$$\frac{d^2x}{dt^2} + x = \mu\left\{\frac{dx}{dt}\left[1 - \frac{1}{3}\left(\frac{dx}{dt}\right)^2\right] + \Delta x - k_1\frac{d^2y}{dt^2}\right\} + \mu^2 F(t) + \frac{1}{L\omega^2 I_0}\frac{d\mathcal{E}}{dt_1}, \tag{6.1}$$

$$\frac{d^2y}{dt^2} + y = -\mu^2\left(h\frac{dy}{dt} + k_2\frac{d^2x}{dt^2}\right) + \frac{1}{L_1\omega^2 I_0}\frac{d\mathcal{E}_1}{dt_1}.$$

Here we have introduced the dimensionless parameters and the time $t = \omega t_1$ everywhere except in the last terms containing $\mathcal{E}$ and $\mathcal{E}_1$. In accordance with the Nyquist formula for the spectral intensity of a thermal emf, the correlation function of $\mathcal{E}_1(t)$ is

$$\overline{\mathcal{E}(t_1)\,\mathcal{E}(t_1')} = 2RkT\delta(t_1 - t_1'). \tag{6.2}$$

Inasmuch as R_1 and R_2 are taken to be quantities of the same order of magnitude (the first) with respect to μ, the emf $\mathcal{E}$ and the emf $\mathcal{E}_1$ are also of the same order. If the random force appears to second order in the first equation of (6.1), i.e.,

$$\frac{1}{L\omega^2 I_0}\frac{d\mathcal{E}}{dt_1} = \mu^2 G(t), \tag{6.3}$$

it will appear to order μ^3 in the second equation. Hence the thermal noise of the "crystal" need not be considered in calculations having an accuracy of the order μ^2.

In order to calculate the correlation function of $G(t)$ one must know the correlation function $\overline{\frac{d\mathcal{E}(t_1)}{dt_1}\frac{d\mathcal{E}(t_1')}{dt_1'}}$. The latter cannot be obtained from Eq. (6.2) in the usual manner because $\mathcal{E}(t_1)$ does not have a finite mean-square value. However, this difficulty can be circumvented if one notes that in the approximation which is of interest to $\frac{d\mathcal{E}}{dt_1} = \frac{\partial\mathcal{E}}{\partial t_1} = \dot{\mathcal{E}}$ so that the dependence of $\mathcal{E}$ on the fast time t_1 has the form

$$\mathcal{E}(t_1) = \mathcal{E}_{\parallel}(\tau_1)\cos\omega[t_1 - \varphi(\tau_1)] - \mathcal{E}_{\perp}(\tau_1)\sin\omega[t_1 - \varphi(\tau_1)],$$

where $\tau_1 = \mu t_1$. Consequently,

$$d\mathcal{E}(t_1)/dt_1 \approx -\omega\mathcal{E}_{\parallel}(\tau_1)\sin\omega[t_1 - \varphi(\tau_1)] - \omega\mathcal{E}_{\perp}(\tau_1)\cos\omega[t_1 - \varphi(\tau_1)].$$

Now, sice $\overline{\mathcal{E}_{\parallel}(\tau_1)\,\mathcal{E}_{\parallel}(\tau_1')} = \overline{\mathcal{E}_{\perp}(\tau_1)\,\mathcal{E}_{\perp}(\tau_1')}$ and $\mathcal{E}_{\parallel}$ and $\mathcal{E}_{\perp}$ are not cross-correlated, we have

$$\overline{\frac{d\mathcal{E}(t_1)}{dt_1}\frac{d\mathcal{E}(t_1')}{dt_1'}} = \omega^2\overline{\mathcal{E}_{\parallel}(\tau_1)\,\mathcal{E}_{\parallel}(\tau_1')} = \omega^2\overline{\mathcal{E}(t_1)\,\mathcal{E}(t_1')} = 2\omega^2 RkT\delta(t_1 - t_1'). \tag{6.4}$$

Thus, $G(t)$ has a correlation function of the form

$$\overline{G(t)\,G(t')} = D\delta(t - t'), \tag{6.5}$$

in which, according to Eqs. (6.3) and (6.4),

$$\mu^4\overline{G(t)\,G(t')} = \frac{\mu^4 D}{\omega}\delta(t_1 - t_1') = \frac{1}{L^2\omega^4 I_0^2}\overline{\frac{d\mathcal{E}(t_1)}{dt_1}\frac{d\mathcal{E}(t_1')}{dt_1'}} = \frac{2RkT}{L^2\omega^2 I_0^2}\delta(t_1 - t_1'),$$

i.e.,

$$\mu^4 D = 2RkT/L^2\omega I_0^2. \tag{6.6}$$

In our approximation the thermal emf calculation amounts to adding a random force $G(t)$ to $F(t)$ in the first equation of Eq. (6.1); this force is also characterized by δ - correlation and is independent of $F(t)$. Thus, in the problem of the simple oscillator (see Figure in I), taking $k_1 = 0$ and $\Delta = 0$ (i.e., $\omega = \omega_0$) in the first equation of (6.1), we have

$$\frac{d^2x}{dt^2} + x = \mu\frac{dx}{dt}\left[1 - \frac{1}{3}\left(\frac{dx}{dt}\right)^2\right] + \mu^2 F(t) + \mu^2 G(t).$$

It is apparent that all the bilinear quantities characterizing the correlation and intensity of the fluctuations will, in the approximation being considered, be formed additively from terms calculated before which depend on $F(t)$, and these same terms as determined by $G(t)$. Thus, for example, in place of formulas (5.9) of I for the fluctuations of amplitude and phase in the simple oscillator, we now have

$$\overline{\rho^2} = \frac{\mu}{4}(C + D), \quad \overline{\chi^2} = \frac{\mu}{8}(C + D)\tau.$$

The ratio of shot-noise to thermal noise is given by C/D, i.e., from Eqs. (5.7), (5.8) of I and Eq. (6.6) it is

$$\frac{\text{shot}}{\text{thermal}} = \frac{\mu^4 C}{\mu^4 D} = \frac{e}{2kT} \frac{L^2\omega_0^2 \bar{I}_a}{R}.$$

This expression can be written in a simple and descriptive form due to Gorelik. The second factor, since $\frac{L\omega_0}{R} \bar{I}_a = I_{amp}$, is equal to the voltage which appears across the condenser in the circuit:

$$\frac{L^2\omega_0^2 \bar{I}_a}{R} = L\omega_0 I_{amp} = \frac{I_{amp}}{\omega_0 C} = U_C.$$

Consequently,

$$\frac{\text{shot}}{\text{thermal}} = \frac{eU_C}{2kT}$$

The ratio of shot-noise to thermal noise is equal to the ratio of the work done in carrying an electron across the condenser (at maximum voltage) to twice the energy of the thermal noise in the circuit. For $T = 300°$ K, we have

$$\frac{\text{shot}}{\text{thermal}} = 17\, U_C,$$

Where U_C is given in volts.

Translated by H. Lashinsky
198

Relaxation Fluctuations in Condensed Systems

P. S. ZYRIANOV
Ural Polytechnic Institute
(Submitted to JETP editor May 21, 1954)
J. Exper. Theoret. Phys. USSR 29, 334-338 (September, 1955)

The question of the division of fluctuations into "fine-grained" (relaxational) and "coarse-grained" (vibrational) is considered. An estimate of the role of relaxation fluctuations in the electrical conductivity of metals is given.

1. INTRODUCTION

IT is impossible to describe the thermal motion in condensed systems completely by means of sound waves or photons, inasmuch as the discrete structure of the condensate is treated extremely crudely in such a description, through the introduction of the minimum wavelength λ_{min} of the acoustical vibrations; in this procedure a physical meaning is given only to those waves of length $\lambda > \lambda_{min}$. But by means of sound waves with $\lambda > \lambda_{min}$ it is impossible to describe fluctuations in the density of the number of particles taking place in regions of spatial dimensions $L < \lambda_{min}$. An analogous situation is found in wave optics: it is impossible to obtain an image of details of an object by means of light waves of lengths exceeding the linear dimensions of those details. In this way we conclude that it is possible to describe by means of acoustical waves only density fluctuations of spatial dimensions $L > \lambda_{min}$. We shall call these fluctuations "coarse-grained". It is impossible to describe fluctuations with $L < \lambda_{min}$, or "fine-grained" fluctuations, by means of sound waves.

Such a division of the fluctuations is introduced on the basis of general ideas, and it apparently has a meaning for condensed systems at sufficiently high temperatures such that it is already impossible to neglect processes of mixing of the particles of the condensate, or self-diffusion. From experiment it is known that such processes (self-diffusion) play a considerable role in liquids, as well as in solid bodies at high temperatures.

Having divided the fluctuations into "coarse-grained" and "fine-grained", one can draw several general conclusions about both the character of the behavior of these fluctuations and the role of their interactions. A "coarse-grained" fluctuation may be represented as a superposition (packet) of sound waves, and therefore it possesses a vibrational character. It is impossible to represent a "fine-grained" fluctuation in the form of a superposition of sound waves, and it possesses a relaxational character; i.e., it is dispersed by means of diffusion, like the density fluctuations of particles in an ideal gas. The interaction of these fluctuations leads to the damping of sound waves, the energy of the sound waves being dissipated in the "fine-grained" fluctuations. The situation here strongly resembles the mechanism of dissipation of the kinetic energy of a liquid in turbulent flow[1].

Ordinarily the "fine-grained" fluctuations are neglected. However, it is certainly not obvious that they always play a negligibly small role. On the contrary, as will be shown below, in several phenomena (e.g. electrical conductivity in metals at high temperatures) the "fine-grained" fluctuations play a role equal to that of the "coarse-grained" ones.

2. "FINE-GRAINED" FLUCTUATIONS

The division of fluctuations into "coarse-" and "fine-grained" undoubtedly possesses an approximate character, but this approximation allows one to carry out a synthesis of the discrete (corpuscular) and the continuous physical properties of condensed systems.

In what follows we shall consider only the "fine-grained" fluctuations. As far as the "coarse-grained" fluctuations are concerned, they are described in the ordinary way by means of acoustical vibrations. For the special case of the electron plasma of a metal, the "coarse-grained" fluctuations are described by means of the collective density oscillations[2].

As already stated above, the relaxation fluctuations are related to the mixing processes of the particles of the condensate (self-diffusion); therefore it is convenient to use the ideas of Frenkel' concerning the "hole" mechanism of self-diffusion. According to Frenkel'[3], the number N of

[1] L. D. Landau and E. M. Lifshitz, *Mechanics of Continuous Media*, GITL (1953)

[2] P. S. Zyrianov, J. Exper. Theoret. Phys. USSR 29, 193 (1955)

[3] Ia. I. Frenkel', *Introduction to the Theory of Metals*, GITTL (1948)

holes in a unit volume may be expressed by the formula

$$N = \frac{v - v_0}{v} N_0 = \frac{\Delta V}{V} N_0,$$

where v_0 is the volume occupied by one particle in the absence of holes at pressure p_0 and temperature T_0, v is the same at temperature T and pressure p, and N_0 is the average number of particles per unit volume.

At constant $p = p_0$ this formula can be written in another way, introducing the coefficient of thermal expansion $\alpha(T)$:

$$N/N_0 = (\Delta V / V)_{p=p_0} = 3 \int_{T_0}^{T} \alpha(T)\, dT. \qquad (1)$$

For our purposes it is preferable to treat the number of "holes" N as the number of particles of the condensate taking part in the relaxation fluctuations. Inasmuch as N/N_0 is not large, in calculating the fluctuations of the density of the number of particles N it is possible to neglect their interaction and use the apparatus of the theory of fluctuations in an ideal gas. Then

$$\overline{(\Delta N)^2} = \overline{(\bar{N} - N)^2} = \frac{\Delta V}{V} N_0. \qquad (2)$$

If one neglects thermal expansion, $\overline{(\Delta N)^2} = 0$.

3. INFLUENCE OF THE "FINE-GRAINED" FLUCTUATIONS ON THE ELECTRICAL RESISTIVITY OF METALS AT HIGH TEMPERATURES

The electrical resistivity of metals , which depends on the temperature, is caused by the interaction of the conduction electrons with the internal electric field of the fluctuations, which is created, in the final analysis, by the thermal motion of the ions.

In the theory of the electrical conductivity of metals one has heretofore considered only the interaction of the conduction electrons with the electric field of the sound waves(scattering of electrons by phonons) or, in other words, the interaction of the electrons with the electric field of the "coarse-grained" fluctuations. As regards the interactions of the electrons with the "fine-grained" fluctuations, these have been neglected without any justification whatever. It is possible to try to take account of the scattering of the conduction electrons on the electric field of the "fine-grained" fluctuations in the framework of the isotropic-plasma model of a metal[2].

To solve this problem we first of all compute the potential of the electric field of the "fine-grained" fluctuations. According to the result of reference 2, within the domain of the plasma model of a metal the potential of the electric field of an ion, screened by the collectively coherent electrons, has the form

$$\varphi(r) = (e_2 / r) \exp\{- q_D r\}, \qquad (3)$$

where e_2 is the charge of the ion, and q_D is the Debye wave number, equal[2] to ω_{02}/u_0 (ω_{02} = the Langmuir frequency of oscillation of the ions, u_0 = velocity of sound in the metal). This form of the potential also follows from simple physical ideas. In the electron plasma a charge moving with a velocity considerably smaller than the mean velocity of the chaotic electron motion, is screened by electrons over a distance of the Debye radius of polarization. In metals, the velocity of motion of the ions is considerably smaller than the mean velocity of the chaotic motion of the electrons, which are distributed according to Fermi statistics. Therefore,the Debye cloud of polarization of the ion will be practically indistinguishable from a sphere. Formula (3) also reflects this fact. The same form for the potential of the ion is used in the work of Nordheim[4], but the quantity analogous to q_D was considered as an unknown constant.

The potential Φ created by the density fluctuations of the electric charge $e_2(\delta\rho)$ is equal to

$$\Phi = e_2 \int \frac{\delta\rho(\mathbf{r}')}{|\mathbf{r} - \mathbf{r}'|} \exp\{- q_D |\mathbf{r} - \mathbf{r}'|\}\, d\mathbf{r}'. \qquad (4)$$

This formula can be rewritten in another form by introducing the Fourier components of the quantity $\delta\rho$ and of the potential $\varphi(r)$:

$$\Phi = \sum_q \frac{4\pi e_2}{q_D^2 + q^2} (\delta\rho)_q e^{i\mathbf{q}\mathbf{r}}. \qquad (5)$$

It is obvious that $\overline{(\delta\rho)_q^2} = \overline{(\Delta N)^2} = (\Delta V/V) N_0$, inasmuch as

$$\overline{|\int (\delta\rho)_q e^{i\mathbf{q}\mathbf{r}} d\mathbf{q}|^2} = (\Delta V / V) N_0 = \overline{(\delta\rho)^2}.$$

The scattering of the conduction electrons by the electric field of the "fine-grained" fluctuations can be evaluated by introducing the mean free path l_M. According to Seitz[5], l_M can be expressed in

---

[4] L. Nordheim, Ann. Phys. 9, 607 (1931)

[5] F. Seitz, *The Modern Theory of Solids*, McGraw-Hill, New York (1940), p. 526

terms of $B(\mathbf{k}, \mathbf{k}')$, the square of the matrix element of the interaction energy of the electron with the field Φ, by the formula

$$l_M^{-1} = 16\pi^3 \left(\frac{dk}{dE}\right)^2_{E=E_0} \quad (6)$$
$$Vk_0^2 \int B(\mathbf{k}, \mathbf{k}')(1 - \cos\vartheta)\sin\vartheta\, d\vartheta,$$

where V is the volume of the metal, $E_0 = \hbar^2 k_0^2 / 2m$ is the upper limit of the Fermi distribution. The quantity $B(\mathbf{k}, \mathbf{k}')$ depends on $|\mathbf{k}|$ and on the angle θ between $\mathbf{k}$ and $\mathbf{k}'$, the wave vectors of the electron in the initial and final states (elastic scattering), and it is equal to

$$B(\mathbf{k}, \mathbf{k}') = |\int \Psi_k^*(r)\, e\Phi(r)\, \Psi_{k'}(r)\, d\mathbf{r}|^2.$$

Substituting into this the wave functions of the free electron $\Psi_k(r)$, normalized with respect to the volume V, we find

$$B(\mathbf{k}, \mathbf{k}') = (4\pi e_2 e)^2 N V^{-1} [q_D^2 + (\mathbf{k} - \mathbf{k}')^2]^{-2}. \quad (7)$$

Substituting this expression into Eq. (6) we obtain

$$l_M^{-1} = [4\pi m^2 e_2^2 e^2 / (\hbar^4 k_0^4)]\, \Gamma(q_D, k_0)\, N. \quad (8)$$

Here

$$\Gamma(q_D, k_0) = q_D^2 (q_D^2 + 4k_0^2)^{-1} + \ln[1 + (4k_0^2/q_D^2)] - 1.$$

The electrical resistivity ρ_M caused by the scattering of the conduction electrons by the "fine-grained" fluctuations, is calculated by the well-known formula

$$\rho_M^{-1} = \frac{e^2 n_0}{m v(k_0)} l_M, \quad (9)$$

in which n_0 is the density of conduction electrons and $v(k_0)$ is the electron velocity at the Fermi surface. Substitution of (8) into (9) gives a formula for ρ_M:

$$\rho_M = \frac{\pi\sqrt{2m}\, e_2^2}{E_0^{3/2} n_0} \Gamma(q_D, k_0)\, N. \quad (10)$$

Noting (1) and the equality $N_0 = n_0/z$ (z is the number of conduction electrons per ion), we transform (10) into the form

$$\rho_M = \frac{\pi\sqrt{2m}\, e_2^2}{E_0^{3/2}} z \left(\frac{\Delta V}{V}\right) \Gamma(q_D, k_0). \quad (11)$$

The ordinary electrical resistivity ρ is composed of ρ_M and ρ_K, due to the scattering of the conduction electrons by the "fine-grained" and by the "coarse-grained" fluctuations respectively. The electrical resistivity ρ_K was computed in reference 2. Evaluation of ρ_M and ρ_K carried out for $T \gg \Theta_D$ (in the region in which our calculations are justified) shows that ρ_M and ρ_K are quantities of the same order of magnitude.

Let us consider the qualitative conclusions which can be drawn from equation (11).

(a) The temperature dependence of ρ_M is determined by the integral

$$\left(\frac{\Delta V}{V}\right)_{p=p_0} = 3 \int_{T_0}^{T} \alpha(T)\, dT.$$

According to the Grüneisen rule[6], the ratio of the specific heat c_v to the coefficient of thermal expansion $\alpha(T)$ does not depend on the temperature. For $T \gg \Theta_D$ (Θ_D is the Debye temperature) the specific heat c_v does not depend on T; consequently α also does not depend on T, so that $\rho_M \sim T$.

(b) ρ_M is proportional to the relative change of volume and does not depend on the causes of that change — external pressure or thermal expansion. This conclusion is apparently supported by the experimental data in the case of mercury[7].

(c) Equation (11) reflects the experimental fact of the discontinuous change of electrical resistivity of metals upon melting and the proportionality of the size of the discontinuity to the volume change at the melting point. For the metals Bi, Ga, and Sb, $\Delta V/V$ is negative at the melting point; consequently the electrical resistivity at the melting point must decrease. The thermodynamical theory of Mott[8] leads to an increase of the electrical resistivity of these metals, which is found to contradict experiment.

The order of magnitude of the discontinuity in the electrical resistivity also agrees with experiment. According to the experimental data the jump in the electrical resistivity is of the order of magnitude of the electrical resistivity in the solid phase. From reference 2 it follows that ρ_K does not change significantly in melting (by

[6] E. Grüneisen, Ann. Phys. **26**, 211, 393 (1908).

[7] S. Shubin, J. Exper. Theoret. Phys. USSR **3**, 461 (1933)

[8] N. F. Mott, Proc. Roy. Soc. **146**, 465 (1934)

only a few percent) in comparison with ρ_M. Consequently the discontinuity is essentially caused by the change in ρ_M in melting. It is known[3] that the volume change in melting is, for instance, equal to the increase in volume upon heating the metal from absolute zero to the melting point. Thus the change in ρ_M on melting is of the order of $\Delta\rho_M \sim \rho_M \sim \rho$.

I take this opportunity to thank Prof. V. L. Ginzburg for valuable advice.

Translated by C. W. Helstrom
200

Tensors Which are Characterized by Two Real Spinors

G. A. ZAITSEV

(Submitted to JETP editor April 3, 1954)
J. Exper. Theoret. Phys. USSR 29, 166-175 (August, 1955)

Formulas are obtained which enable one simply to determine a real spinor in terms of the primary tensor characterizing it. With the aid of these formulas we establish the relation between two spinors, corresponding to two given triples E, H, j. Tensors whose components are expressed in terms of two real spinors are investigated. Two types of spinor transformations are introduced, corresponding to different possible interpretations of the gauge transformation. The significance of the spinor transformations is established; it is shown that if we regard the group of tensors as initially defined, then we can with their aid find two real spinors to within a spinor transformation of one of the types studied. The components of the initial tensors can be expressed in terms of the spinors, in which case they will not change when the corresponding spinor transformation is carried out.

IN references 1 and 2 we studied some of the properties of real spinors --- systems of parameters defined by a four-dimensional antisymmetric tensor for which both invariants are equal to zero. In references 1, 3 and 4, the question of the use of real spinors in certain physical problems was considered. For further development of the ideas introduced in these papers it is necessary to investigate the more general case of tensors characterized by a pair of real spinors. The solution of this problem is the purpose of the present work. The notation used in the paper corresponds to that of the articles mentioned; we shall also make continual use of the properties of matrix-tensors considered in reference 4.

1. FUNDAMENTAL FORMULAS

A single real spinor ψ determines the matrix-tensors

$$F = \frac{1}{2} R_\alpha R_\beta F^{\alpha\beta} = R\underline{\mathbf{H}} + R_4\underline{\mathbf{E}}, \qquad (1)$$

$$P = R_\alpha \vec{j^\alpha} = \underline{\mathbf{j}} + \rho R_4;$$

where (cf references 2, 3 and 5):

$$\mathbf{E} = E_i R^i, \quad \mathbf{H} = H_i R^i, \qquad (2)$$

$$\rho^2 = \mathbf{E}^2 = \mathbf{H}^2, \quad \mathbf{j} = -(1/\rho) R\mathbf{E}\,\mathbf{H};$$

$$E_i = -\psi' J R^i \psi, \quad H_i = \psi' R^i \psi, \qquad (3)$$

$$j^i = \psi' R_4 R^i \psi, \quad \rho = \psi'\psi.$$

Since E and H are primary quantities, while ψ is a derived quantity, it is necessary to find a sufficiently simple method enabling one to find the components of the associated real spinor ψ if the E and H are given.

Suppose that for some matrix, such that $\mathbf{d} = d_i R^i$, $\mathbf{d}^2 = \rho^2$, the relation

$$\mathbf{d}\psi = \rho\psi. \qquad (4)$$

is satisfied.

Multiplying Eq. (4) on the left by ψ', $-\psi' J$, $\psi' R_4$, and using Eq. (3), we get

$$(\underline{\mathbf{H}}\,\underline{\mathbf{d}}) = \rho^2, (\underline{\mathbf{E}}\,\underline{\mathbf{d}}) = (\underline{\mathbf{j}}\,\underline{\mathbf{d}}) = 0, \qquad (5)$$

so that, since E, H and j are mutually orthogonal and have equal length, we have $\mathbf{d} = \mathbf{H}$. We thus find:

$$\mathbf{H}\psi = \rho\psi. \qquad (6)$$

It is not difficult to see that if the components H_i are related to ψ by formulas of the type of Eq. (3), then formula (6) will be valid.

In precisely the same way we get

$$-J\mathbf{E}\psi = \rho\psi. \qquad (7)$$

Using the fact that $\mathbf{EH} = \rho R\,\mathbf{j}$ and multiplying both sides of (6) from the left by $-J\mathbf{E}$, we have as a consequence

[1] G. A. Zaitsev, J. Exper. Theoret. Phys. USSR 25, 653 (1953)

[2] G. A. Zaitsev, J. Exper. Theoret. Phys. USSR 25, 667 (1953)

[3] G. A. Zaitsev, J. Exper. Theoret. Phys. USSR 25, 675 (1953)

[4] G. A. Zaitsev, J. Exper. Theoret. Phys. USSR 28, 524 (1955); Soviet Phys. 1, 411 (1955)

[5] G. A. Zaitsev, J. Exper. Theoret. Phys. USSR 28, 530 (1955); Soviet Phys. 1, 491 (1955)

$$-R^4\mathbf{j}\,\psi = R_4\mathbf{j}\,\psi = \rho\psi. \tag{8}$$

If E and H are given, the corresponding real spinor ψ can be found from Eqs. (6) and (7). (It is understood that the three-dimensional "vectors" E and H must have equal length and be orthogonal. Otherwise, these equations will be incompatible.)

Formulas (6), (7) and (8), which we shall call the fundamental formulas for a single real spinor, will be very important for what follows.

We observe that it follows from Eq. (8) that

$$P\psi = 0, \tag{9}$$

and from Eqs. (6) and (7) that $F\psi = 0$, where the last relation is obtained from Eq. (9) if we multiply both sides from the left by the matrix $-(1/\rho)\mathbf{E}$. Also, if the relation $D\psi = 0$ holds for any matrix four-vector D, then the matrix D is proportional to P.

On the basis of formulas (6)-(8), we consider the question of the relation of two real spinors defined by two different antisymmetric tensors of the second rank having invariants equal to zero. In doing this we shall assume that the position of one triple, E, H, j, relative to the other triple characterizing the second tensor, is known; i.e., we assume, for example, that we know the Euler angles characterizing the rotation of the one triple relative to the other, and also the ratio $\rho_{(2)}/\rho_{(1)}$ of the lengths of the vectors. When we deal with several real spinors, we shall distinguish them by an additional index in parentheses, e.g., $\psi_{(1)}$, $\psi_{(2)}$, etc. We shall also give the index in parentheses for the corresponding vectors E, H, j. In our case we can use the designations 1 and 2.

The real spinor $\psi_{(2)}$ can be obtained from $\psi_{(1)}$ by rotation or reflection of the four-dimensional space and subsequent multiplication by some real number. We shall make use of the fact that the matrix of an arbitrary rotation or reflection can be written in the form of a product of matrices which are linear combinations of the R^α (cf reference 2). Since each of the three spatial basis vectors can be represented as a linear combination of the three linearly independent spatial vectors E, H, j, (strictly speaking, E and H do not behave like the spatial parts of vectors under a general Lorentz transformation, but this does not matter for the present case), the matrices R^i can be expressed as linear combinations of the matrices E, H, j, corresponding to an arbitrary real spinor ψ. Using formulas (6)-(8) we find that under a four-dimensional symmetry transformation, and consequently, also under an arbitrary rotation and reflection, a real spinor ψ will be multiplied by matrices of the type

$$K = k_4 + k_1R_4 + k_2R + k_3J. \tag{10}$$

In this way we can establish that $\psi_{(2)}$ is related to $\psi_{(1)}$ by the formula

$$\psi_{(2)} = K\psi_{(1)}, \tag{11}$$

where the matrix K can be written in the form of Eq. (10).

Let us study in more detail the question of the form of the parameters k_α. First of all, we note that matrices of the type of Eq. (10) are isomorphic to quaternions; to the matrices R_4, R, J, there correspond the quaternion units i, j, k. In particular,

$$K'K = k_1^2 + k_2^2 + k_3^2 + k_4^2 = \tau^2 \tag{12}$$

can be regarded as the norm of the quaternion, so that it follows from Eq. (11) that

$$\rho_{(2)} = \tau^2\rho_{(1)}. \tag{13}$$

Using formulas (3), (10) and (11), we express $\mathbf{E}_{(2)}$, $\mathbf{H}_{(2)}$ and $\mathbf{j}_{(2)}$ in terms of $\mathbf{E}_{(1)}$, $\mathbf{H}_{(1)}$, $\mathbf{j}_{(1)}$, and the parameters k_α. After simple calculations we obtain

$$\begin{aligned}\mathbf{E}_{(2)} = {} & (k_4^2 + k_1^2 - k_2^2 - k_3^2)\,\mathbf{E}_{(1)} \\ & + (-2k_4k_3 + 2k_1k_2)\,\mathbf{H}_{(1)} \\ & + (2k_4k_2 + 2k_1k_3)\,\mathbf{j}_{(1)},\end{aligned} \tag{14}$$

$$\begin{aligned}\mathbf{H}_{(2)} = {} & (2k_4k_3 + 2k_1k_2)\,\mathbf{E}_{(1)} \\ & + (k_4^2 - k_1^2 + k_2^2 - k_3^2)\,\mathbf{H}_{(1)} \\ & + (-2k_4k_1 + 2k_2k_3)\,\mathbf{j}_{(1)},\end{aligned} \tag{15}$$

$$\begin{aligned}\mathbf{j}_{(2)} = {} & (-2k_4k_2 + 2k_1k_3)\,\mathbf{E}_{(1)} \\ & + (2k_4k_1 + 2k_2k_3)\,\mathbf{H}_{(1)} \\ & + (k_4^2 - k_1^2 - k_2^2 + k_3^2)\,\mathbf{j}_{(1)}.\end{aligned} \tag{16}$$

From Eqs. (14)-(16) it is evident that the k_α coincide with the well-known Rodrigues parameters, relating one triple of mutually orthogonal vectors of equal length with a second triple (cf, for example, reference 6, pp. 183-184, where k_4, k_1, k_2

---

[6] W. D. MacMillan, *Dynamics of Rigid Bodies*, McGraw-Hill, 1936

and k_3 are denoted by the symbols ρ, λ, μ and ν)*. From them we obtain the connection of the parameters k_α to the Euler angles characterizing the rotation of the triple $\mathbf{E}_{(2)}$, $\mathbf{H}_{(2)}$, $\mathbf{j}_{(2)}$ relative to $\mathbf{E}_{(1)}$, $\mathbf{H}_{(1)}$, $\mathbf{j}_{(1)}$

$$k_4 = -\tau \cos\tfrac{1}{2}\vartheta \cos\tfrac{1}{2}(\psi+\varphi), \tag{17}$$

$$k_1 = \tau \sin\tfrac{1}{2}\vartheta \cos\tfrac{1}{2}(\psi-\varphi),$$

$$k_2 = \tau \sin\tfrac{1}{2}\vartheta \sin\tfrac{1}{2}(\psi-\varphi),$$

$$k_3 = \tau \cos\tfrac{1}{2}\vartheta \sin\tfrac{1}{2}(\psi+\varphi).$$

The Euler angles are chosen so that the angle between the vectors $\mathbf{j}_{(2)}$, $\mathbf{j}_{(1)}$ corresponds to the angle between the z axes of the coordinate systems considered in the kinematics of rigid bodies, the angle between $\mathbf{E}_{(2)}$ and $\mathbf{E}_{(1)}$ corresponds to the angle between the x axes, and the angle between $\mathbf{H}_{(2)}$ and $\mathbf{H}_{(1)}$ to the angle between the y axes.

Formulas (17) enable us to understand the meaning of the parameters k_α. Here we should note that, for given $P_{(1)}$, $F_{(1)}$, and $P_{(2)}$, $F_{(2)}$, the matrix K is determined only to within a sign, as follows from the properties of real spinors (which are determined only to within a common sign). However, another approach to this problem is possible, if we start from other primary tensors, to which we shall return later.

2. TENSORS EXPRESSED IN TERMS OF TWO REAL SPINORS

Let us turn to the important question of the various tensors whose components are expressible in terms of the components of two real spinors. Here we shall use the representation of a tensor in matrix form.

First of all, we can form various matrix four-vectors and matrix antisymmetric tensors of the second rank by taking linear combinations of the matrices $P_{(1)}$, $P_{(2)}$ and $F_{(1)}$, $F_{(2)}$. In particular, we set

$$P_{(+)} = P_{(1)} + P_{(2)}, \tag{18}$$

$$F_{(+)} = F_{(1)} + F_{(2)}. \tag{19}$$

In addition, we can obtain, from two real spinors, tensors formed in another way. From the law of transformation of real spinors, considered in reference 2, it follows that

$$\Omega_1 = \psi'_{(2)} R \psi_{(1)} \tag{20}$$

is invariant, not changing its form under any rotations or reflections of four-dimensional space. (For example, under the symmetry transformation A_1, $A_1^2 = \pm 1$, Ω_1 goes over into $\pm \psi'_{(2)} A_1' R A_1 \psi = \Omega_1$, etc.) We observe that the ambiguity of sign of the matrix K can be eliminated by requiring, say, that the invariant Ω_1 have a definite sign.

We also introduce the matrix-pseudoscalar

$$S = \Omega_2 J, \qquad \Omega_2 = \psi'_{(2)} R_4 \psi_{(1)}, \tag{21}$$

whereupon it is easy to see that Ω_2 is a pseudo-invariant, changing sign under reflections of the four-dimensional space and remaining unchanged under four-dimensional rotations. Using formulas (10), (17) and (13), we can write the following expressions for Ω_1 and Ω_2:

$$\Omega_1 = k_2 \rho_{(1)} = \tau \rho_{(1)} \sin\tfrac{1}{2}\vartheta \sin\tfrac{1}{2}(\psi-\varphi) \tag{22}$$

$$= \sqrt{\rho_{(1)}\rho_{(2)}} \sin\tfrac{1}{2}\vartheta \sin\tfrac{1}{2}(\psi-\varphi),$$

$$\Omega_2 = k_1 \rho_{(1)} = \tau \rho_{(1)} \sin\tfrac{1}{2}\vartheta \cos\tfrac{1}{2}(\psi-\varphi) \tag{23}$$

$$= \sqrt{\rho_{(1)}\rho_{(2)}} \sin\tfrac{1}{2}\vartheta \cos\tfrac{1}{2}(\psi-\varphi).$$

From the law of transformation of real spinors, it further follows that we can also introduce a four-dimensional vector, a pseudovector and an antisymmetric tensor, defined according to the formulas:

$$q^\alpha = \psi'_{(2)} R_4 R^\alpha \psi_{(1)}, \qquad Q = q^\alpha R_\alpha = \mathbf{q} + q^4 R_4, \tag{24}$$

$$n^\alpha = \psi'_{(2)} R R^\alpha \psi_{(1)}, \qquad N = J n^\alpha R_\alpha = J\mathbf{n} + n^4 R, \tag{25}$$

$$\Phi^{\alpha\beta} = -\psi'_{(2)} R^\alpha R^\beta \psi_{(1)},$$

$$\Phi = R\,\mathbf{B} + R_4 \mathbf{D}, \quad B_i = \psi'_{(2)} R^i \psi_{(1)},$$

$$D_i = -\psi'_{(2)} J R^i \psi_{(1)}. \tag{26}$$

Using (10), we can express all these quantities in terms of k_α, $\rho_{(1)}$ and the components of $\mathbf{E}_{(1)}$, $\mathbf{H}_{(1)}$ and $\mathbf{j}_{(1)}$. Thus, for example,

$$\mathbf{q} = -k_2 \mathbf{E}_{(1)} + k_1 \mathbf{H}_{(1)} + k_4 \mathbf{j}_{(1)}, \quad q^4 = k_4 \rho_{(1)}, \tag{27}$$

$$\mathbf{n} = k_1 \mathbf{E}_{(1)} + k_2 \mathbf{H}_{(1)} + k_3 \mathbf{j}_{(1)}, \quad n^4 = k_3 \rho_{(1)}, \tag{28}$$

$$\mathbf{B} = k_3 \mathbf{E}_{(1)} + k_4 \mathbf{H}_{(1)} - k_1 \mathbf{j}_{(1)}, \tag{29}$$

* In reference 6 there is a typographical error in the equation for $\tau^2 \beta_3$; there should be a plus sign on the right instead of a minus sign.

$$\mathbf{D} = k_4 \mathbf{E}_{(1)} - k_3 \mathbf{H}_{(1)} + k_2 \mathbf{j}_{(1)}.$$

This in turn enables us easily to find the relations between different tensors, to which we shall return later.

If we make use of the operation of differentiation, then we can obtain, from two real spinors, another whole set of four-dimensional tensors. For example, the quantities $\frac{\partial \psi'_{(1)}}{\partial x^\alpha} R \psi_{(1)}$ are components of a four-dimensional vector, etc.

We see that we can, from two real spinors $\psi_{(1)}$ and $\psi_{(2)}$, obtain a large number of different tensors. In establishing relations between them and in studying their properties, it is expedient to look at groups of tensors which are related through some common property. As such properties we consider two types of transformations of real spinors, and shall distinguish the set of tensors whose components remain invariant with respect to one of these transformations.

A spinor transformation of the first type is one for which simultaneously $\psi_{(1)}$ changes to $[\exp(Jf)]\psi_{(1)}$ and $\psi_{(2)}$ to $[\exp(-Jf)]\psi_{(2)}$, where f is an arbitrary pseudo-invariant function. It corresponds to a gauge transformation in the form introduced in reference 5 in considering systems of relativistically invariant differential equations of first order for two real spinors. It is not difficult to see that under such a transformation, Ω_1, Ω_2 and the components of $P_{(1)}$, $P_{(2)}$ and Φ remain unchanged. There are no other tensors which are expressed linearly in terms of two real spinors (and do not contain their derivatives with respect to x^α).

We say that a spinor transformation is of the second type if it changes $\psi_{(1)}$ to $\cos f \psi_{(1)} + \sin f \psi_{(2)}$ and $\psi_{(2)}$ to $\cos f \psi_{(2)} - \sin f \psi_{(1)}$, where f is an arbitrary invariant function. Under transformations of the second type, Ω_1, Ω_2 and the components of the matrix-vector $P_{(+)}$, the matrix-pseudovector N and the matrix-tensor of second rank $F_{(+)}$ do not change. The transformation we are considering will be shown in a later paper to correspond to the gauge transformation of the wave function which appears in the Dirac equation for the electron. In studying quantities which are invariant with respect to this transformation, it is convenient to use the notation:

$$\psi_{(+)} = \psi_{(1)} + i\psi_{(2)}, \quad \psi^*_{(+)} = \psi'_{(1)} - i\psi'_{(2)}. \tag{30}$$

Then

$$\Omega_1 = \tfrac{1}{2} i\psi^*_{(+)} R \psi_{(+)}, \quad \Omega_2 = \tfrac{1}{2} i\psi^*_{(+)} R_4 \psi_{(+)}, \tag{31}$$

$$F^{\alpha\beta}_{(+)} = -\psi^*_{(+)} R R^\alpha R^\beta \psi_{(+)}, \tag{32}$$

$$P^\alpha_{(+)} = j^\alpha_{(1)} + j^\alpha_{(2)} = \psi^*_{(+)} R_4 R^\alpha \psi_{(+)}, \tag{33}$$

$$n^\alpha = \tfrac{1}{2} i\psi^*_{(+)} R R^\alpha \psi_{(+)}. \tag{34}$$

Of course, the imaginary unit i is introduced only for convenience of notation, and need not be used.

3. PROPERTIES OF TENSORS WHICH ARE INVARIANT WITH RESPECT TO SPINOR TRANSFORMATIONS OF THE FIRST TYPE

We first consider the question of the properties of the quantities Ω_1, $S = \Omega_2 J$, $P_{(1)}$, $P_{(2)}$, Φ, which do not change under spinor transformations of the first type.

From Eq. (29) we have

$$\mathbf{B}^2 - \mathbf{D}^2 = \Omega_2^2 - \Omega_1^2, \quad (\mathbf{BD}) = -\Omega_1\Omega_2, \tag{35}$$

i.e.,

$$\Phi^2 = \Omega_1^2 - \Omega_2^2 - 2\Omega_1\Omega_2 J \tag{36}$$

$$= (\Omega_1 - \Omega_2 J)^2 = (\Omega_1 - S)^2.$$

As for the matrices $P_{(1)}$ and $P_{(2)}$, their squares are obviously equal to zero,

$$P^2_{(1)} = P^2_{(2)} = 0. \tag{37}$$

We calculate the products of these matrix-vectors. According to reference 4,

$$P_{(1)}P_{(2)} = (\mathbf{j}_{(1)}\mathbf{j}_{(2)}) - \rho_{(1)}\rho_{(2)} \tag{38}$$

$$+ R[\mathbf{j}_{(1)}\mathbf{j}_{(2)}] + R_4(\rho_{(1)}\mathbf{j}_{(2)} - \rho_{(2)}\mathbf{j}_{(1)}).$$

Furthermore, in accordance with Eqs. (13), (16) and (29),

$$(\mathbf{j}_{(1)}\mathbf{j}_{(2)}) - \rho_{(1)}\rho_{(2)} = -2(\Omega_1^2 + \Omega_2^2), \tag{39}$$

$$[\mathbf{j}_{(1)}\mathbf{j}_{(2)}] = -2\Omega_1\mathbf{B} - 2\Omega_2\mathbf{D}, \tag{40}$$

$$\rho_{(1)}\mathbf{j}_{(2)} - \rho_{(2)}\mathbf{j}_{(1)} = -2\Omega_1\mathbf{D} + 2\Omega_2\mathbf{B}, \tag{41}$$

so that

$$P_{(1)}P_{(2)} = -2(\Omega_1^2 + \Omega_2^2) - 2(\Omega_1 + \Omega_2 J)\Phi, \tag{42}$$

$$P_{(2)}P_{(1)} = -2(\Omega_1^2 + \Omega_2^2) + 2(\Omega_1 + \Omega_2 J)\Phi. \tag{43}$$

In addition, we get from Eqs. (26) and (16)

$$[\mathbf{BD}] = -\frac{1}{2}(\rho_{(1)}\mathbf{j}_{(2)} + \rho_{(2)}\mathbf{j}_{(1)}), \tag{44}$$

so that

$$\rho_{(1)}\mathbf{j}_{(2)} = -\Omega_1\mathbf{D} + \Omega_2\mathbf{B} - [\mathbf{BD}], \tag{45}$$

$$\rho_{(2)}\mathbf{j}_{(1)} = \Omega_1\mathbf{D} - \Omega_2\mathbf{B} - [\mathbf{BD}].$$

Thus, assignment of Φ, Ω_1 and Ω_2 determines the directions of the vectors $\mathbf{j}_{(1)}$ and $\mathbf{j}_{(2)}$, but not their lengths $\rho_{(1)}$ and $\rho_{(2)}$ (since the components of Φ do not change under simultaneous multiplication of $\psi_{(1)}$ by some number and division of $\psi_{(2)}$ by that same number, etc.). On the other hand, according to Eqs. (42) and (43), the matrix-tensor Φ is uniquely determined by giving $P_{(1)}$, $P_{(2)}$, Ω_1 and Ω_2, so long as Ω_1 and Ω_2 are not simultaneously equal to zero.

Multiplying both sides of Eqs. (42) and (43) on the left and on the right by the matrices $P_{(1)}$ and $P_{(2)}$, we obtain

$$\Phi P_{(1)} = (\Omega_1 - \Omega_2 J)P_{(1)}, \tag{46}$$

$$\Phi P_{(2)} = -(\Omega_1 - \Omega_2 J)P_{(2)},$$

$$P_{(1)}\Phi = -P_{(1)}(\Omega_1 - \Omega_2 J),$$

$$P_{(2)}\Phi = P_{(2)}(\Omega_1 - \Omega_2 J).$$

Now let us settle the question of the effect on $\psi_{(1)}$ and $\psi_{(2)}$ of various matrix-tensors which are invariant with respect to spinor transformations of the first type. From Eqs. (26) and (29) it follows that

$$\Phi\psi_{(1)} = (R\mathbf{B} + R_4\mathbf{D})\psi_{(1)} = (\Omega_1 - \Omega_2 J)\psi_{(1)}. \tag{47}$$

Similarly, we get

$$\Phi\psi_{(2)} = -(\Omega_1 - \Omega_2 J)\psi_{(2)}, \tag{48}$$

whose validity can be established by interchanging $\psi_{(1)\alpha}$ and $\psi_{(2)\alpha}$ in Eq. (47).

Furthermore, we find from Eqs. (10) and (16)

$$P_{(2)}\psi_{(1)} = 2(\Omega_2 - \Omega_1 J)\psi_{(2)} \tag{49}$$

$$= -2J(\Omega_1 + \Omega_2 J)\psi_{(2)}.$$

Finally, interchanging $\psi_{(1)\alpha}$ and $\psi_{(2)\alpha}$ in Eq. (49), we will have

$$P_{(1)}\psi_{(2)} = -2(\Omega_2 - \Omega_1 J)\psi_{(1)} \tag{50}$$

$$= 2J(\Omega_1 + \Omega_2 J)\psi_{(1)}.$$

It is easy to see that the relations (47)-(50) are not changed by a spinor transformation of the first type.

Up to now we have started from the two spinors $\psi_{(1)}$ and $\psi_{(2)}$ and have found, with their aid, tensors which are invariant under spinor transformations of the first type. A completely different approach is possible here. We could consider that the primary quantities are $P_{(1)}$, $P_{(2)}$, Ω_1 and Φ, connected by the relations given above [cf Eqs. (35)-(46)]*. We define the real spinors $\psi_{(1)}$ and $\psi_{(2)}$ as columns of four numbers which are found from Eqs. (49) and (50). Then, after multiplying both sides of Eqs. (49) and (50) on the left by $P_{(1)}$ and $P_{(2)}$, we get Eqs. (47) and (48).

We show that if we determine $\psi_{(1)}$ and $\psi_{(2)}$ in accordance with Eqs. (49) and (50), then by a suitable choice of the common factor in $\psi_{(1)}$ and $\psi_{(2)}$, we shall have

$$j^{\alpha}_{(1)} = P^{\alpha}_{(1)} = \psi'_{(1)}R_4R^{\alpha}\psi_{(1)}, \tag{51}$$

$$j^{\alpha}_{(2)} = \psi'_{(2)}R_4R^{\alpha}\psi_{(2)}, \quad \Omega_1 = \psi'_{(2)}R\psi_{(1)},$$

$$\Omega_2 = \psi'_{(2)}R_4\psi_{(1)}, \quad \Phi^{\alpha\beta} = -\psi'_{(2)}RR^{\alpha}R^{\beta}\psi_{(1)}.$$

For the proof of this important theorem, we find any solution of Eqs. (49) and (50). From these $\psi_{(1)}$ and $\psi_{(2)}$, we can, by using formulas like (51), find associated quantities which are unchanged by transformations of the first type, and which we designate as $\tilde{j}^{\alpha}_{(1)}$, $\tilde{\Omega}_1$, etc. [Formulas (35)-(46) also enable us to write similar relations for $\tilde{P}_{(1)}$, $\tilde{P}_{(2)}$, $\tilde{\Omega}_1$, $\tilde{\Omega}_2$ and $\tilde{\Phi}$] Multiplying Eq. (50) on the left by $\psi'_{(2)}R$ we get $\Omega_1/\tilde{\Omega}_1 = \Omega_2/\tilde{\Omega}_2 = C$. We shall choose the common factor in $\psi_{(1)}$ and $\psi_{(2)}$, so that $C = 1$. Then from Eqs. (49) and (50) and the corresponding equations obtained by replacing $P_{(1)}$ and $P_{(2)}$ by $\tilde{P}_{(1)}$ and $\tilde{P}_{(2)}$, we have

$$(P_{(2)} - \tilde{P}_{(2)})\psi_{(1)} = 0, \quad (P_{(1)} - \tilde{P}_{(1)})\psi_{(2)} = 0.$$

From the first equation it follows that $P_{(2)} - \tilde{P}_{(2)} = C'\tilde{P}_{(1)}$. Since $\tilde{P}^2_{(1)} = 0$, $\tilde{P}^2_{(2)} = 0$, $C' = 0$, and $P_{(2)} = \tilde{P}_{(2)}$. Similarly, we verify that $P_{(1)} = \tilde{P}_{(1)}$, from which we finally get $\Phi = \tilde{\Phi}$, since Φ is expressed in terms of $P_{(1)}$, $P_{(2)}$, Ω_1 and Ω_2. Thus our assertion is completely demonstrated.

* In this case, as pointed out above, Φ is determined by the assignment of other quantities.

As for the law of transformation of $\psi_{(1)}$ and $\psi_{(2)}$, which are defined according to Eqs. (49) and (50), or equivalently from Eq. (51), in order to preserve the tensor character of the initial quantities, it is necessary to suppose that $\psi_{(1)}$ and $\psi_{(2)}$ transform like real spinors, defined according to reference 2, but only to within a transformation of the first type (which is unimportant, since it does not change the fundamental initial quantities). We arrive at the conclusion that if in any problem we have to deal with a pair of real spinors, and if all the fundamental formulas and physically meaningful quantities are unchanged by spinor transformations of the first type, then we may regard the quantities $P_{(1)}$, $P_{(2)}$, Ω_1, Ω_2, Φ as the initial quantities in the problem, and the real spinors will be parameters determined by assigning the initial quantities.

In reference 5 we saw that under a spinor transformation of the first type, the components of the vector potential are changed to $A_\alpha - (\hbar c/e) \times \partial f/\partial x^\alpha$. If we make use of the components A_α, which change under a spinor transformation of the first type in this fashion, then we can construct another sequence of tensors containing products of x^α and A_α, whose components are not changed by such transformations. It is easy to verify that the following quantities are unchanged by such a transformation:

$$e_\alpha = \psi'_{(1)} R \frac{\partial \psi_{(2)}}{\partial x^\alpha} + \frac{e}{\hbar c} \Omega_2 A_\alpha, \tag{52}$$

$$m_\alpha = \psi'_{(1)} R_4 \frac{\partial \psi_{(2)}}{\partial x^\alpha} - \frac{e}{\hbar c} \Omega_1 A_\alpha, \tag{53}$$

$$T^{(1)}_{\alpha\beta} = \psi'_{(1)} R R_\alpha \frac{\partial \psi_{(1)}}{\partial x^\beta} + \frac{e}{\hbar c} \psi'_{(1)} R^4 R_\alpha \psi_{(1)} A_\beta, \tag{54}$$

$$T^{(2)}_{\alpha\beta} = \psi'_{(2)} R R_\alpha \frac{\partial \psi_{(2)}}{\partial x^\alpha} - \frac{e}{\hbar c} \psi'_{(2)} R^4 R_\alpha \psi_{(2)} A_\beta. \tag{55}$$

Here e_α and m_α are the components of a vector and a pseudovector, $T^{(1)}_{\alpha\beta}$ and $T^{(2)}_{\alpha\beta}$ are the components of pseudotensors of the second rank. They are connected to the other quantities considered in this section and to one another by certain relations. Thus, from Eqs. (52) and (53) we get

$$\Omega_1 e_\alpha + \Omega_2 m_\alpha = \Omega_1 \psi'_{(1)} R \frac{\partial \psi_{(2)}}{\partial x^\alpha} \tag{56}$$

$$+ \Omega_2 \psi'_{(1)} R_4 \frac{\partial \psi_{(2)}}{\partial x^\alpha} = -\frac{1}{2} \frac{\partial (\Omega_1^2 + \Omega_2^2)}{\partial x^\alpha}$$

$$- \Omega_1 \frac{\partial \psi'_{(1)}}{\partial x^\alpha} R \psi_{(2)} - \Omega_2 \frac{\partial \psi'_{(1)}}{\partial x^\alpha} R_4 \psi_{(2)}$$

$$= -\frac{1}{4} \frac{\partial (\Omega_1^2 + \Omega_2^2)}{\partial x^\alpha} + \frac{1}{4} \frac{\partial \psi'_{(2)}}{\partial x^\alpha} R J P_{(1)} \psi_{(2)}$$

$$- \frac{1}{4} \frac{\partial \psi'_{(1)}}{\partial x^\alpha} R J P_{(2)} \psi_{(1)} = -\frac{1}{4} \frac{\partial (\Omega_1^2 + \Omega_2^2)}{\partial x^\alpha}.$$

Furthermore, we have from Eqs. (54) and (55)

$$j^\alpha_{(1)} T^{(1)}_{\alpha\beta} = 0, \quad j^\alpha_{(2)} T^{(2)}_{\alpha\beta} = 0, \tag{57}$$

from which, taking account of Eqs. (49) and (50) we find

$$(j^\alpha_{(1)} + j^\alpha_{(2)})(T^{(1)}_{\alpha\beta} + T^{(2)}_{\alpha\beta}) = 2\Omega_2 \frac{\partial \Omega_1}{\partial x^\beta} - 2\Omega_1 \frac{\partial \Omega_2}{\partial x^\beta}. \tag{58}$$

4. PROPERTIES OF TENSORS WHICH ARE INVARIANT WITH RESPECT TO SPINOR TRANSFORMATIONS OF THE SECOND TYPE

Just as in the previous section, we can also consider the properties of quantities which are invariant with respect to spinor transformations of the second type. From Eqs. (14) and (15) we obtain

$$(F_{(1)} + F_{(2)})^2 = F^2_{(+)} \tag{59}$$

$$= 4(\Omega_2 + \Omega_1 J)^2 = -4(\Omega_1 - \Omega_2 J)^2.$$

In addition, we obtain from Eq. (28) and Eqs. (14)-(16) by simple calculations,

$$-4N^2 = P^2_{(+)} = -4(\Omega_1^2 + \Omega_2^2), \tag{60}$$

$$\mathfrak{n}(\mathbf{j}_{(1)} + \mathbf{j}_{(2)}) - n^4 \rho_{(+)} = 0, \tag{61}$$

$$[\mathfrak{n}, \mathbf{j}_{(1)} + \mathbf{j}_{(2)}] = [\mathfrak{n}, \mathbf{j}_{(+)}] = \Omega_1 \mathbf{E}_{(+)} - \Omega_2 \mathbf{H}_{(+)}, \tag{62}$$

$$n^4 \mathbf{j}_{(+)} - \rho_{(+)} \mathfrak{n} = -\Omega_2 \mathbf{E}_{(+)} - \Omega_1 \mathbf{H}_{(+)}, \tag{63}$$

$$[\mathbf{E}_{(+)}, \mathbf{H}_{(+)}] = \rho_{(+)} \mathbf{j}_{(+)} - 4n^4 \mathfrak{n}. \tag{64}$$

Then, since

$$-JNP_{(+)} = (\mathfrak{n}\mathbf{j}_{(+)}) - n^4 \rho_{(+)} + R[\mathfrak{n}\mathbf{j}_{(+)}] + R_4 (n^4 \mathbf{j}_{(+)} - \rho_{(+)} \mathfrak{n}),$$

we shall have

$$NP_{(+)} = P_{(+)} N = -(\Omega_1 + \Omega_2 J) F_{(+)}. \tag{65}$$

Using Eq. (60) we get, from Eq. (65),

$$P_{(+)} F_{(+)} = 4(\Omega_1 + \Omega_2 J) N, \tag{66}$$

$$N F_{(+)} = -(\Omega_1 + \Omega_2 J) P_{(+)}.$$

From Eq. (65) it follows that if we know Ω_1, Ω_2,

$P_{(+)}$ and N, we can find the matrix-tensor $F_{(+)}$. On the other hand, the matrices $P_{(+)}$ and N are not uniquely determined by the assignment of $F_{(+)}$, Ω_1 and Ω_2. This follows from the fact that the relations (60), (61) and (65) remain the same if we replace $P_{(+)}$ and $2N$ by

$$P_1 = (\cos\alpha/\sqrt{\cos 2\alpha})\,P_{(+)} - (\sin\alpha/\sqrt{\cos 2\alpha})\,2JN,$$

$$2N_1 = (\cos\alpha/\sqrt{\cos 2\alpha})\,2N + (\sin\alpha/\sqrt{\cos 2\alpha})\,JP_{(+)}.$$

Now we can proceed to the question of the effect of applying these matrix-tensors, which are invariant with respect to spinor transformations of the second type, to real spinors. Starting from Eqs. (10), (14), (15), (22) and (23), we get

$$F_{(+)}\psi_{(1)} = 2(\Omega_1 - \Omega_2 J)\,\psi_{(2)}. \tag{67}$$

Similarly,

$$F_{(+)}\psi_{(2)} = -2(\Omega_1 - \Omega_2 J)\,\psi_{(1)}, \tag{68}$$

Operating from the left on both sides of Eq. (67) with the matrix $P_{(+)}$ and using Eq. (66), we get

$$P_{(+)}\psi_{(2)} = 2N\psi_{(1)}. \tag{69}$$

and, similarly, applying the matrix N on the left and using Eq. (66) we find

$$P_{(+)}\psi_{(1)} = -2N\psi_{(2)}. \tag{70}$$

These same formulas could also have been obtained from Eq. (68). Formulas (67)-(70) are invariant with respect to spinor transformations of the second type.

Just as in the previous section, we may consider that the restriction to quantities invariant with respect to spinor transformations of the second type can be related to the fact that the quantities Ω_1, Ω_2, $P_{(+)}$and N, and the matrix tensor $F_{(+)}$ found from them, are regarded as primary. If they are given, then the corresponding real spinors $\psi_{(1)}$ and $\psi_{(2)}$ will be determined to within a spinor transformation of the second type, by Eqs. (69) and (70).

In conclusion, we note that if together with $\psi_{(1)}$ and $\psi_{(2)}$ we consider the components of a vector A_α, which transform under a spinor transformation of the second type into $A_\alpha + (1/\epsilon)[\partial f/\partial x^\alpha]$, then the quantities

$$\psi^*_{(+)}R\frac{\partial\psi_{(+)}}{\partial x^\alpha} + 2\varepsilon\Omega_1 A_\alpha,$$

$$\psi^*_{(+)}R_4\frac{\partial\psi_{(+)}}{\partial x^\alpha} + 2\varepsilon\Omega_2 A_\alpha,$$

$$\psi^*_{(+)}R_4R_\alpha\frac{\partial\psi_{(+)}}{\partial x^\beta} + i\varepsilon P_{(+)\alpha}A_\beta$$

and $$\psi^*_{(+)}RR_\alpha\frac{\partial\psi_{(+)}}{\partial x^\beta} + 2\varepsilon n_\alpha A_\beta,$$

which are the components of a vector, pseudovector, second rank tensor, and second rank pseudotensor, respectively, will not change under such a transformation. Just as in the previous section, we could establish relations connecting them with one another and with other quantities, but we shall not take this up here.

Translated by M. Hamermesh
170

SOVIET PHYSICS JETP VOLUME 2, NUMBER 2 MARCH, 1956

On a Theory of the Electrical Conductivity of Metals

P. S. ZYRIANOV
Ural Polytechnical Institute, Sverdlovsk
(Submitted to JETP editor May 21, 1954)
J. Exper. Theoret. Phys. USSR 29, 193-200 (August, 1955)

The fluctuations of potential of the internal electric field in the electron-ion plasma of a metal are calculated, also, the electrical resistivity dependent on the scattering of electrons by these fluctuations.

1. INTRODUCTION

AT present, mathematical methods have been developed for calculating the collective Coulomb interactions in a system of many particles (a plasma)[1-4]. Up to now, however, these methods have not found wide use in the theory of metals. This is apparently no accident and is explained by the circumstance that in the approximation of a metal by an isotropic plasma, the periodic distribution of the ions of the metal (crystalline lattice) and the presence of "non-collectivized" electrons in the atomic cores (ions) are not taken into consideration.

The consideration of periodicity in a three-dimensional distribution of ions[5] is linked with mathematical difficulties. Non-collectivized electrons of the atomic cores generally were not allowed for in the foundations of plasma theory. Disregarding these difficulties, it makes sense to attempt to apply the theory of an isotropic plasma to the study of certain physical properties of the alkali metals with the aim of clarifying the results which come out of the plasma model of a metal. In the alkali metals, the periodicity in distribution of ions and the non-collectivized electrons of the atomic cores apparently play a lesser role than in non-alkali metals, and in the former, the "valence" electrons can be considered completely collectivized.

In the theory of a plasma, essentially the dynamics of the electrons were studied and only in a few works[1,6] was the motion of the ions also taken into account. In the investigation of the physical properties of a metallic plasma which depend on temperature (for example, the electrical and thermal conductivity, scattering of light, specific heat, surface tension and others), along with the dynamics of the electrons it is also necessary to take into account the motion of the ions. Precisely in these cases the motion of the ions plays a basic role; it determines the temperature of the metal and thus also the character of the behavior of the "free" electrons. The thermal motion of the ions leads to fluctuations of physical quantities such as the density of the number of particles, the energy, the internal electric field and others. Fluctuations of physical quantities play a significant role in applications. Thus, for example, the scattering of light is computed through fluctuations of the density of the number of particles. Through fluctuations of the density of electric charge the internal electric field is calculated which determines the temperature dependent electrical resistance of metals.

The aims of the present paper were (1) the computation of the fluctuations associated with thermal motion, taking into account the collective Coulomb interactions between the electrons and the ions, and (2), the computation of the electrical resistivity of a metal plasma which depends on the scattering of conduction electrons by fluctuations of the internal electric field.

II. THE FLUCTUATIONS OF PHYSICAL QUANTITIES IN THE ELECTRON-ION PLASMA

In the study of fluctuations in a plasma, it is convenient to express all physical quantities through the fluctuation of density of the number of particles. Fluctuations of large absolute value have slight probability and do not play a substantial role. The study of small fluctuations, however, is equivalent to the study of small oscillations of the plasma about a fundamental state characterized by an absence of fluctuations.

We take the state of the plasma at the absolute zero of temperature as its fundamental state.

[1] A. A. Vlasov, *Theory of Many Particles* GITTL, 1950

[2] Iu. L. Klimontovich and V. P. Silin, J. Exper. Theoret. Phys. USSR **23**, 151 (1952)

[3] D. N. Zubarev, J. Exper. Theoret. Phys. USSR **25**, 548 (1953)

[4] D. Bohm and D. Pines, Phys. Rev. **82**, 625 (1951); **85**, 338 (1952)

[5] P. S. Zyrianov, J. Exper. Theoret. Phys. USSR **25**, 441 (1953)

[6] V. P. Silin, J. Exper. Theoret. Phys. USSR **23**, 649 (1952)

Moreover, the distribution of electrons in energy or wave number conforms to a Fermi function f_{01}, and of ions to a δ-like function f_{02} (for example, a Bose function), but the spatial distribution of each is of the same kind. At temperatures of the metal plasma different from absolute zero, thermal motion begins, and leads to fluctuations.

The character of the behavior of fluctuations of density in ensembles of "ideal" and "non-ideal" particles is essentially different. In ensembles of "ideal" particles, fluctuations of density are resolved by diffusion in the course of time, whereas in ensembles of "non-ideal" particles the behavior of the fluctuations with time suggests the propagation of a disturbance in an elastic string. On consideration of the details of the fluctuations of density in "non-ideal" ensembles it is necessary to take into account collective interactions. For the calculation of these interactions, one can employ a kinetic equation with a self-consistent field[1] or the methods of references 3 and 4, having generalized them to two kinds of particles (electrons and ions).

The equations which allow for collective interactions have the form[1]

$$\frac{\partial f_i}{\partial t} + (\mathbf{v}\nabla_{\mathbf{r}}) f_i + \frac{e_i}{m_i}(\mathbf{E}\nabla_{\mathbf{v}}) f_i = 0, \qquad (1)$$

$$\mathbf{E} = -\nabla\Phi,$$

$$\Delta\Phi = -4\pi \sum_{i=1}^{2} e_i \int f_i \, d\mathbf{v} \qquad (i = 1, 2),$$

where the f_i are the distribution functions of the electrons and of the ions. The symbol $i = 1$ refers to the electrons and $i = 2$ to the ions. In equations (1) only the Coulomb interactions are treated.

For the study of fluctuations (small variations) the non-linear system of equations (1) can be linearized, assuming in Eq. (1)

$$f_i = f_{0i} + \varphi_i(\mathbf{r}, \mathbf{v}, t) \qquad \varphi_i \ll f_{0i} \qquad (2)$$

and retaining terms linear in φ_i. A solution of the linearized equations can be sought in the form of a superposition of plane waves

$$\varphi_i = \sum_{q} g_i(\mathbf{q}, \mathbf{v}) e^{i\omega t - i\mathbf{qr}}. \qquad (3)$$

Substituting Eq (3) in the linearized equations, we find

$$\varphi_i = \sum_{q} \alpha_i^{-1} F_i(\mathbf{q}, \mathbf{v}) \frac{1}{2}(R_i e^{-i\mathbf{qr}} + R_i^* e^{i\mathbf{qr}}), \qquad (4)$$

where

$$R_i(\mathbf{q}, t) = e^{i\omega t} \int g_i(\mathbf{q}, \mathbf{v}) \, d\mathbf{v}, \quad R_i(\mathbf{q}) = R_i^*(-\mathbf{q}),$$

$$F_i(\mathbf{q}, \mathbf{v}) = (\mathbf{q}\nabla_{\mathbf{v}}) f_{0i} [m_i(\omega - \mathbf{qv})]^{-1};$$

f_{01} and f_{02} are degenerate functions, Fermi and Bose, respectively:

$$\alpha_i = \int F_i(\mathbf{v}, \mathbf{q}) \, d\mathbf{v}.$$

The condition for existence of non-zero solutions gives the dispersion equation

$$1 - V^{(11)}(q)\alpha_1 - V^{(22)}(q)\alpha_2 = 0, \qquad (5)$$

where $V^{(ii)}(q) = 4\pi e_i^2 / q^2$ is the Fourier component of the Coulomb potential.

In reference 6 it was shown that the dispersion equation (5) gives two branches of oscillations: acoustical and electronic. Thermal motion excites only the acoustical branch of vibrations. For excitation of electronic oscillations an energy $\hbar\omega_{01}$ (ω_{01} is the Langmuir frequency of electronic oscillations) of the order of 10^{-11} erg is needed. This corresponds to temperatures of the order of 10^4 °K, at which metals no longer exist. For the acoustical vibrations, $\omega^2/q^2 \ll p_0^2/m_1$ (p_0 is the limiting Fermi momentum), and the damping is negligibly small[6].

For these conditions, we get from Eq (5)

$$\omega^2 = \frac{\omega_{02}^2 u_0^2}{\omega_{02}^2 + u_0^2 q^2} q^2, \qquad (6)$$

where

$$\omega_{02}^2 = 4\pi\rho_{02}\frac{e_2^2}{m_2}, \qquad u_0^2 = \frac{z}{3}\frac{p_0^2}{m_1 m_2}, \qquad z = \left|\frac{e_2}{e_1}\right|,$$

ρ_{02} is the mean density of the number of ions.

In case $q^2 \ll \omega_{02}^2/u_0^2 = q_D^2$ the dispersion vanishes and Eq. (6) goes over to $\omega = u_0 q$; u_0 plays the role of the velocity of sound in the metal plasma, q_D ---the role of Debye wave number.

By means of Poisson's equation and Eqs. (4) and (5), we find

$$\Phi = 4\pi e_2 \sum_{q} \left[\frac{\omega^2_{02}}{\omega^2} q^2 V^{(22)}(q)\right]^{-1} \frac{1}{2}(R_2 e^{-i\mathbf{qr}} - R_2^* e^{i\mathbf{qr}}) \qquad (7)$$

The distribution functions of electrons and ions (4) describe in the linear approximation the possible states of the system of electrons and ions, wherein one state differs from another only in the set of superposition coefficients $R_i(q)$ (the Fourier component of density). Therefore, it is very convenient to accept the quantities $R_i(q)$ as

dynamical variables which describe the state of the system. The advantages of such a choice of variables are evident if one goes over to the Hamiltonian method of description of small oscillations. The density of the Hamiltonian function of the system of electrons and ions, considering only the Coulomb forces, has the form

$$H = \frac{1}{2}\int m_1 v^2 f_1\, d\mathbf{v} + \frac{1}{2}\int m_2 v^2 f_2\, d\mathbf{v} \qquad (8)$$
$$+ \frac{1}{8\pi}(\nabla\Phi)^2 + \Phi\sum_{i=1}^{2} e_i \int f_i\, d\mathbf{v}.$$

The first two terms represent the density of the kinetic energy of the electrons and of the ions, the third, the energy of the electric field, and the fourth, the energy of interaction of the electrons and ions with this field.

Differentiating Eq (8) with respect to time and substituting for $\partial f/\partial t$ From Eq. (1), we obtain from

$$\frac{\partial H}{\partial t} = -\sum_{i=1}^{2} \operatorname{div} \mathbf{T}_i - {}^1/_2 e_i \mathbf{E}\int v^2 (\nabla_{\mathbf{v}} f_i)\, d\mathbf{v} \qquad (9)$$
$$+ \frac{1}{8\pi}\frac{\partial}{\partial t}(\nabla\Phi)^2 + \frac{\partial}{\partial t}\Big[\Phi\sum_{i=1}^{2} e_i \int f_i d\mathbf{v}\Big],$$

where

$$\mathbf{T}_i = {}^1/_2 \int m_i v^2 (\mathbf{v} f_i)\, d\mathbf{v}$$

is the vector of current density of the kinetic energy.

Transforming the second term in Eq. (9) by integration by parts, assuming minuteness of the deviation of the distribution functions f_i from their equilibrium values f_{0i} and using the solutions (4), we get, in place of Eq. (9),

$$\frac{\partial H}{\partial t} = \sum_{i=1}^{2}\Big\{-\operatorname{div}\mathbf{T}_i + e_i \mathbf{E}\int \mathbf{v}\Big[f_{0i} + \sum_q \frac{F_i}{2\alpha_i}(R_i e^{-i\mathbf{qr}} + R_i^* e^{-i\mathbf{qr}})\Big] d\mathbf{v}\Big\} \qquad (10)$$
$$+ \frac{1}{8\pi}\frac{\partial}{\partial t}\Big[\sum_q \frac{2\pi e_2 \omega^2}{\omega_{02}^2 q^2} i\mathbf{q}(R_2 e^{-i\mathbf{qr}} + R_2^* e^{i\mathbf{qr}})\Big]^2$$
$$+ \frac{\partial}{\partial t}\Big\{\sum_{i=1}^{2}\frac{2\pi e_2\omega^2}{\omega_{02}^2 q^2}(R_i e^{-i\mathbf{qr}} - R_i^* e^{i\mathbf{qr}})\, e_i \int\Big[f_{0i} + \sum_q \frac{F_i}{2\alpha_i}(R_i e^{-i\mathbf{qr}} + R_i^* e^{i\mathbf{qr}})\Big] d\mathbf{v}\Big\}.$$

In the case of acoustical vibrations, it is possible to disregard the kinetic energy of the well-regulated movement of the electrons. Thereupon, integrating Eq. (10) first over the volume of the system, with the hypothesis that the current T_i through the boundary of the system reduces to zero, and then over time, we get for the complete Hamiltonian function $\mathcal{H}$ the expression

$$\mathcal{H} = \sum_q \frac{m_2\omega^2}{4\rho_{02}q^2}\Big(1 + \frac{\omega^2}{\omega_{02}^2}\Big)(R_2 R_2^* + R_2^* R_2) \qquad (11)$$
$$+ \text{const.}$$

We introduce new variables with the aid of the equation

$$R_2(q) = i\sqrt{2}\,\frac{\rho_{02} q}{(1 + \omega^2/\omega_{02}^2)^{1/4}} X_q. \qquad (12)$$

Considering that $X_q \sim R_2(q) = \rho_2(q) e^{i\omega t}$, and assuming $im_2\omega\rho_{02} X_q = i\mu\omega X_q = P_q$, we transform $\mathcal{H}$ to the form

$$\mathcal{H} = \sum_q \Big\{\frac{P_q P_{-q}}{2\mu} + \frac{\mu\omega^2 X_q X_{-q}}{2}\Big\} + \text{const}, \qquad (13)$$

where

$$\text{const} = \int\sum_{i=1}^{2}\frac{m v_i^2}{2} f_{0i}\, d\mathbf{v}\, d\mathbf{r} + \int\Big(\sum_{i=1}^{2} e_i f_{0i}\, d\mathbf{v}\,\Phi\Big) d\mathbf{r}.$$

The Fourier components of the potential of the internal electric field are expressed in terms of X_q by the formula

$$\Phi_q = \frac{i}{\sqrt{2}}\frac{m_2}{e_2}\Big[1 + \frac{\omega^2}{\omega_{02}^2}\Big]^{-1}\frac{\omega^2}{q} X q. \qquad (14)$$

The transition to the quantum description of small oscillations (fluctuations) is achieved by the replacement of P_q by the operator $-i\hbar\,\partial/\partial X_q$. For the characteristic values of the energy of the vibrations, we get the formula

$$\mathcal{E} = \text{const} + \sum_q (N_q + {}^1/_2)\,\hbar\omega(q). \qquad (15)$$

In the case of thermodynamic equilibrium, N_q is a Bose-Planck function, and the mean-square values can be found by means of the probability distribution of the coordinate of an oscillator[7] Thus, using the kinetic equations (1) and quantization of small oscillations (fluctuations), we have found formulas for the fluctuations of the density of the number of particles, the Fourier component

[7] L. D. Landau and E. M. Lifshitz, *Statistical Physics*, Clarendon, 1938

of the potential of the internal electric field and the energy density.

In the following we shall take up a case which is not without interest. If we carry out calculations, analogous to those done above, for a system consisting of one sort of particle with mass m_2 and charge e_2, but with the interaction potential

$$V(r) = \left(\frac{e}{r}\right)\exp(-q_D r), \qquad (16)$$

which satisfies the equation

$$\Delta V - q_D^2 V = 0, \qquad (17)$$

where $q_D = \omega_{02}/u_0$, then we get formulas in exact agreement with Eq. (6) and Eqs. (12)-(14).

From this observation it follows that in the calculation of fluctuations of physical quantities in an electron-ion plasma (accounting for collective Coulomb interactions) the role of the electrons boils down to a Debye screening of the electric charge of the ion-points. For this reason and, of course, since the mean speed of the chaotic motions of the ions is significantly less than the mean speed of the electrons, the Debye cloud of polarization is nearly indistinguishable from a sphere.

III. ON THE ELECTRICAL CONDUCTIVITY OF METALS

The motion of conduction electrons through an ideal periodic metal lattice takes place entirely without hindrance, i.e., the electrical resistivity is zero. In order to explain the incidence of the finite electrical resistivity of a metal, it is necessary to consider the thermal motion of the atomic residues (lattice vibrations). Owing to this motion, the periodicity of the potential of the lattice is disturbed and electrons are no longer able to travel unimpeded through the metal. This circumstance, in the final analysis, also leads to the emergence of electrical resistivity.

In other words, the thermal motion of the ions sets up fluctuations in the potential of the internal electric field in the metal, and the scattering of electrons by these fluctuations is the cause of the finite value of the electrical resitivity. Thus, for computing the electrical resistivity of a metal, it is necessary to know the fluctuations of potential in the internal electric field. The phenomenological introduction of these fluctuations (of the perturbing potential) in Bloch's theory[8] was combined with additional hypotheses. Thus, for instance, in references 8-10 the hypothesis of "deformed" ions was proposed, but in reference 11 a hypothesis of "rigid" ions. For such an introduction of fluctuations of potential, the "constant" of the interaction between electrons and thermal vibrations of the lattice remains unknown and this makes a comparison of theory with experiment difficult.

The thermal motion of ions of a metal in the solid phase bears the character of oscillations about equilibrium positions which are considered stationary (held fast). If we disregard thermal expansion, then a change in temperature causes only a change in the amplitude of vibrations of the ions. Such a (oscillatory) motion of the ions of a metal can be described by an equivalent system of non-interacting oscillators. For this, quantities proportional to the Fourier components of the density of the number of ions serves as dynamical variables (the coordinates of the oscillators or the independent variables). These variables we shall call collective variables. They describe the collective oscillations of the density of ions. Experiment shows that in a solid metal the ions possess also, so to speak, individual degrees of freedom, which lead to the chaotic progressive transfer of ions or to self-diffusion (intermixing). This will be gone into in more detail in another place, in connection with the discussion of the question of the electrical resistivity of liquid metals.

For the calculation of the electrical resistivity of metals in the solid phase, one can apparently disregard the individual degrees of freedom of ions (inasmuch as the number of such ions is comparatively small) and compute the scattering of the conduction electrons by the fluctuations of potential of the internal electric field, determined only by the collective oscillations. The calculations are especially simple in the case of high temperatures $T > \Theta_D$, where Θ_D is the Debye characteristic temperature. In this case, as is known, it is possible to introduce the free-path length of a conduction electron l_x. This length is expressed by the square of a matrix element of the interaction energy of an electron with the internal electric field: $B(\mathbf{k}, \mathbf{k}')$. According to reference 12, this

[8] F. Bloch, Z. Phys. 59, 208 (1930)

[9] H. A. Bethe and A. Sommerfeld, *Electron Theory of Metals*, 1938

[10] L. Brillouin, *Les Statistiques Quantiques*, Paris, 1930

[11] L. Nordheim, Ann. Physik 9, 607 (1931)

[12] F. Seitz, *Modern Theory of Solids*, McGraw-Hill, New York, 1940, p. 526

relation has the form

$$\frac{1}{l_x} = 16\pi^3 \left(\frac{dk}{dE}\right)_0^2 \times V k_0^2 \int_0^\pi B(\mathbf{k}, \mathbf{k}')(1 - \cos\vartheta)\sin\vartheta\, d\vartheta, \quad (18)$$

where V is the volume of the metal (we assume in the following $V = 1$ cm^3), $\hbar k_0^2 / 2m_1 = E_0$ is the limiting energy of the Fermi distribution, the quantity $B(\mathbf{k}, \mathbf{k}')$ depends on $\mathbf{k}$ and on the angle ϑ between $\mathbf{k}$ and $\mathbf{k}'$,

$$|\mathbf{k}| = |\mathbf{k}'|; \quad (19)$$

in accordance with Eq. (14) and with the definition of the matrix element.

$$B|\mathbf{k}, \mathbf{k}'| = |(\psi_{\mathbf{k}}|e_1\Phi|\psi_{\mathbf{k}'})|^2. \quad (20)$$

Substituting normalized free-electron wave functions here in place of the $\psi_{\mathbf{k}}$, we find

$$B(\mathbf{k}, \mathbf{k}') = \left[\frac{m_2^2\omega_{02}^4 u_0^4 q^2 X_q^2}{2(\omega_{02}^2 + 2u_0^2q^2)(\omega_{02}^2 + u_0^2q^2)}\right]_{\mathbf{q}=\mathbf{k}'-\mathbf{k}} \quad (21)$$

For $T > \Theta$ the mean square value of the coordinate of an oscillator with mass μ and frequency ω is

$$\overline{X_q^2} = \frac{\varkappa T}{\mu\omega^2} = \frac{\varkappa T}{m_2\rho_{02}\omega^2} \quad (22)$$

($\varkappa$ is Boltzmann's constant).

Substituting the expressions (20) and (22) in Eq. (18) and carrying out the integration over ϑ, taking Eq. (19) into account, we find

$$l_x = \frac{16\pi z\rho_{02}E_0^2}{\varkappa T m_2 u_0^2 I(q_D)}, \quad (23)$$

where

$$I(q_D) = \int_0^{q_D} q^3[1 + 2u_0^2q^2/\omega_{02}^2]^{-1}\, dq \approx {}^1/_8\, q_D^4.$$

Substituting l_x in the well-known formula for the electrical conductivity σ

$$\sigma = \rho^{-1} = \frac{e_1^2\rho_{01}}{m_1 v(k_0)} l_x$$

[m_1 is the mass of an electron, e_1 its charge, ρ_{01} is the mean density of electrons, $v(k_0)$ is the limiting velocity of the Fermi distribution], we get after the simplifications

$$\sigma = \rho^{-1} = \frac{10\pi\hbar^3}{(m_1e_1z)^2}\frac{p}{\varkappa T}, \quad (24)$$

where p is the pressure of the degenerate electron gas, equal to

$${}^1/_5(3\pi^2)^{2/3}(\hbar^2/m)(\rho_{01})^{5/3}.$$

For the alkali metals one can assume the number of collectivized electrons per atom $z = 1$. For $T = 273°\,\mathrm{K} > \Theta_D$ formula (24) gives the following values (in units of 10^{16} cps):

$$\sigma_{Na} = 26, \quad \sigma_K = 10, \quad \sigma_{Rb} = 6, \quad \sigma_{Cs} = 4.$$

These values do no differ appreciably from those measured experimentally in the same units:

$$\sigma_{Na} = 21, \quad \sigma_K = 13, \quad \sigma_{Rb} = 7, \quad \sigma_{Cs} = 5.$$

It is not difficult to compute $\Theta = \hbar\omega_{max}/\varkappa$ as well. The maximum frequency of the acoustical vibrations ω_{max} which enters in here is determined by Eq. (6) if the q in it is set equal to q_D, the maximum wave number. Finally, we get

$$\Theta = \hbar\omega_{02}/\sqrt{2}\varkappa.$$

The values of Θ calculated by this formula:

$$\Theta_{Na} = 230°, \quad \Theta_K = 130°,$$

$$\Theta_{Rb} = 78°, \quad \Theta_{Cs} = 58°,$$

are close to the Debye characteristic temperatures, found from measurements of specific heats:

$$(\Theta_D)_{Na} = 150° - 202°\,\mathrm{K},$$

$$(\Theta_D)_K = 100° - 126°\mathrm{K},$$

$$(\Theta_D)_{Rb} = 62° - 85°\mathrm{K},$$

$$(\Theta_D)_{Cs} = 55° - 68°\mathrm{K}.$$

Other authors[6, 13] have compared the experimentally measured velocity of propagation of sound in the alkali metals with that calculated from the plasma model. The discrepancy between theory and experiment in this case did not exceed 15%.

The quantitative comparison of theory with experiment shows us to what extent the properties of alkali metals can be approximated by the properties of an electron-ion plasma.

---

[13] D. Bohm and T. Staver, Phys. Rev. 84, 836 (1951)

Translated by R. L. Eisner
173

The Formation of Negative Oxygen Ions in the Collisions of Positive Oxygen Ions with Gas Molecules

IA. M. FOGEL' AND L. I. KRUPNIK
Physico-technical Institute of Ukrainian Academy of Sciences
(Submitted to JETP editor April 3, 1954)
J. Exper. Theoret. Phys. USSR **29**, 209-220 (August, 1955)

Using a double mass-spectrometer a study was made of the capture of two electrons by positive atomic and molecular ions of oxygen in collisions with molecules of hydrogen, oxygen and nitrogen. The effective cross sections for these processes were measured for oxygen ions with energies between 14 and 41 kev.

INTRODUCTION

VARIOUS phenomena connected with the formation of negative ions comprise a branch of physics of elementary processes that has been only slightly investigated thus far. This fact is apparent in the monograph[1] in which the chapter devoted to a survey of various processes of formation of negative ions contains mostly a discussion of theoretical work. The most thoroughly studied processes have been the formation of negatively charged ions by means of surface ionization[2,3], by collisions of slow electrons with molecules[4,5] and by bombardment of metallic surfaces by positive ions[6,7].

The formation of negative ions can take place by collisions of fast particles with atoms or molecules accompanied by exchange of charges. Such collisions may result in exchange of one, two or a larger number of electrons, with occurence of processes of the following type:

$$A + B \rightarrow A^- + B^+; \quad (1)$$

$$A^+ + B \rightarrow A^- + B^{++}; \quad (2)$$

$$A^{++} + B \rightarrow A^- + B^{+++}. \quad (3)$$

The existence of process (2) was discovered by us during a study of collisions of protons with molecular hydrogen[8], but the processes (1) and (3) have not been studied at all. The goal of the present work is a more detailed study of process (2), i.e., the formation of negative ions by collisions of singly charged positive ions with molecular gas accompanied by capture of two electrons during each collision.

As a subject of our study we selected the collision processes of positive atomic and molecular ions of oxygen with molecules of hydrogen, oxygen and nitrogen. The above processes were selected because the electron affinity of the oxygen atom is known with sufficient accuracy and has a fairly large value (2.2 ev). In addition, it is possible to compare the previously determined effective cross sections of process (2) with the effective cross section of formation of negative ions of oxygen by collisions of slow electrons with the molecules of a series of gases.

DESCRIPTION OF THE APPARATUS AND THE METHOD OF MEASUREMENT

A schematic diagram of the apparatus used for the study of the processes of formation of negative ions of oxygen is shown in Fig. 1.

A beam of positive ions of oxygen was obtained from a high frequency ion source *1*. The ions emitted by the source were accelerated in tube *2*; they then entered a magnetic mass-monochromator *3*, where the beam was rotated by 60°. The monochromator was capable of separating from the beam the ions of O_1^+ with energy up to 50 kev. Measurement of the current of the undecomposed beam was carried out by means of a movable Faraday cylinder *6*. An electrostatic deflection system *4* was used to correct the trajectory of the beam.

The beam of positive oxygen ions selected by the mass-monochromator then entered the collision

[1] H. S. W. Massey, *Negative Ions*, 1950

[2] V. M. Dukel'skii and N. I. Ionov, J. Exper. Theoret. Phys. USSR **10**, 1248 (1940)

[3] N. I. Ionov, J. Exper. Theoret. Phys. USSR **18**, 174 (1948)

[4] M. M. Mann, A. Hustrulid and J. T. Tate, Phys. Rev. 58, 340 (1940)

[5] H. D. Hagstrum and J. T. Tate, Phys. Rev. **59**, 354 (1941)

[6] R. H. Sloane and H. M. Love, Nature **159**, 302 (1947)

[7] V. I. Veksler and G. N. Shuppe, Z. Tekhn. Fiz. **23**, 1573 (1953)

[8] Ia. M. Fogel', L. I. Krupnik and B. G. Safronov, J. Exper. Theoret. Phys. USSR **28**, 589 (1955); Soviet Phys. **1**, 415 (1955)

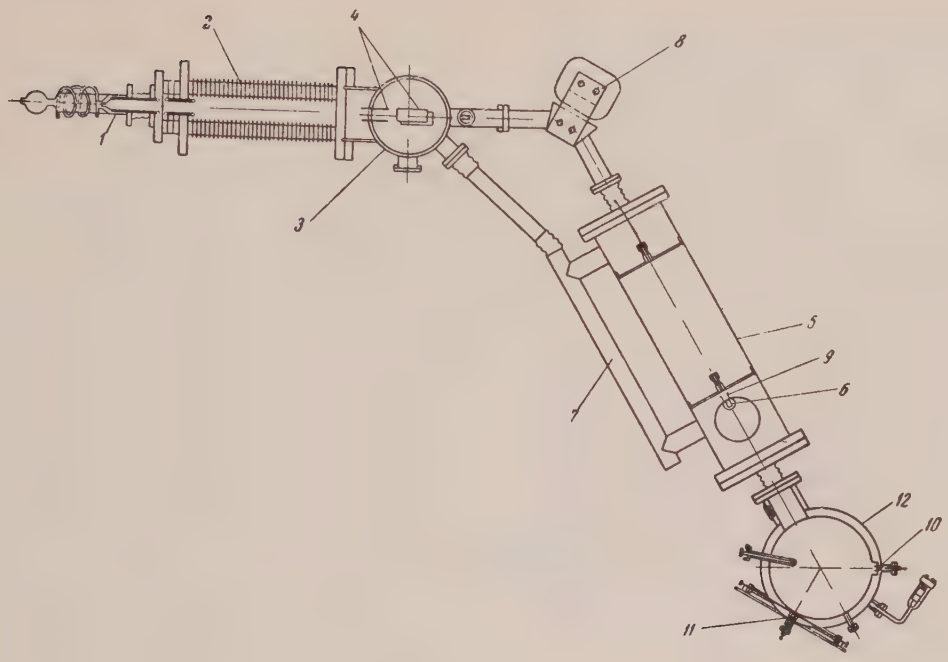

FIG. 1. Arrangement of the experimental apparatus.

chamber 5, whose cross section is drawn in larger scale in Fig. 2. At the entry to the collision chamber the beam was limited in size by a diaphragm a_1 of diameter 3 mm, and then passed through an entry tube b_1 of diameter 5 mm and length 50 mm. Having passed through the chamber, the beam again passed through a second diaphragm a_2, and then left the chamber by a second tube b_2 of the same dimensions as the entry tube. The presence of diaphragms at the entrance and exit of the collision chamber prevented the beam particles from falling on the walls of the tubes.

The evacuation of the gas admitted to the chamber and escaping through the entry and exit tubes was accomplished by means of a bypass pipe 7, flexibly connected with a branch pipe 3, which was connected to the pump MM-1000. With the above quoted dimensions of entry and exit tubes of the collision chamber a considerable pressure difference existed across these tubes, so that with a pressure of gas 10^{-3} mm inside the chamber, the pressure in the rest of the system was only 10^{-5} mm.

In the present experiments the collision chamber was filled with hydrogen, oxygen or nitrogen. Hydrogen was admitted to the chamber over a palladium filter. Oxygen, containing 1 % of impurities, was admitted through a bimetallic valve. Nitrogen, obtained by evaporation of liquid nitrogen and passed over hot copper shavings, was admitted from a glass flask through a capillary tube. The regulation of the flow of gas was done in that case by compression of rubber tubing connecting the flask with the capillary. All gases admitted into the chamber passed through a glass trap filled with liquid nitrogen. The trap was connected to a copper tube which was then soldered to an inlet valve of the chamber. In such a way all gases and vapors condensable at liquid nitrogen temperatures were eliminated from the admitted gases. The pressure of the gas in the collision chamber was measured by a McLeod gauge with a constant of 2.2×10^{-6}. The entry of mercury vapors from the gauge into the chamber was again prevented by a liquid nitrogen trap.

The current strength of the ion beam that had passed through the collision chamber was measured by a Faraday cylinder 6 with magnetic control that made possible removal and insertion of the cylinder into the beam. The secondary emission from the Faraday cylinder was suppressed by application of negative potential on the cylinder 9. The measurement of the current of the ion beam that had passed through the collision chamber was made with a mirror galvanometer of sensitivity 9×10^{-10} A/div. The current of the beam of

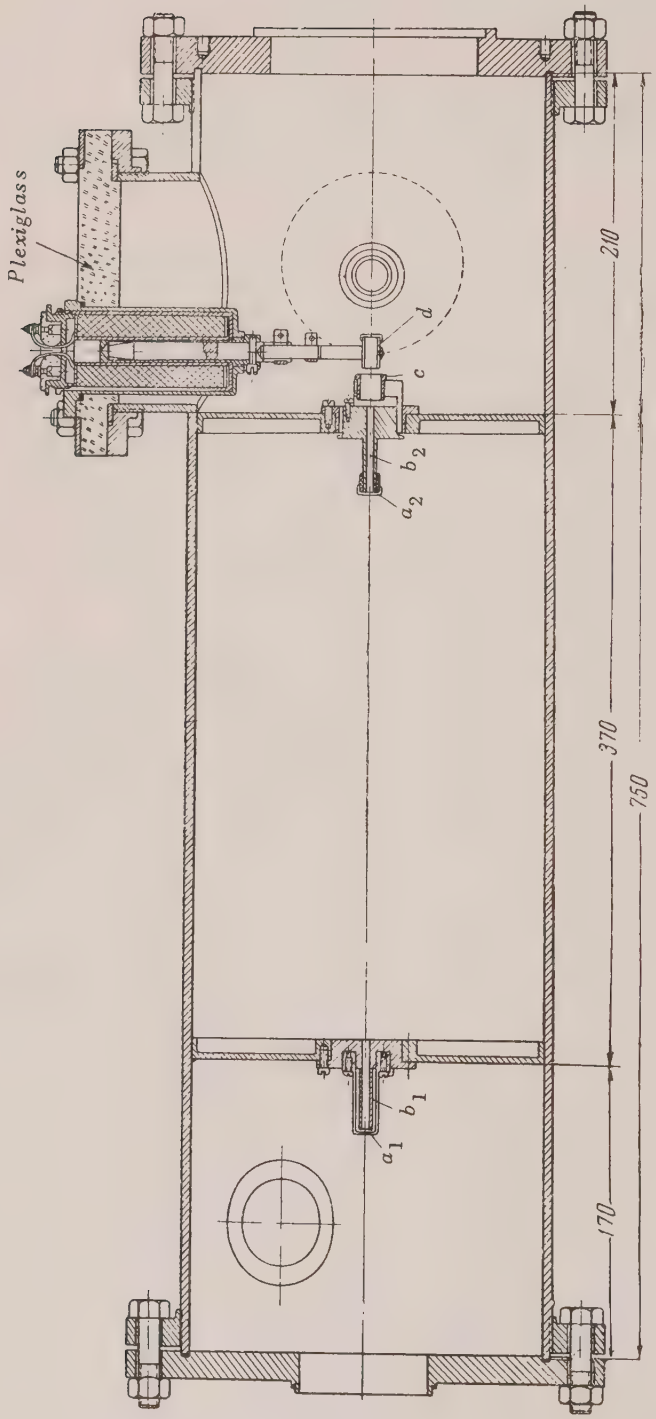

FIG. 2. Diagram of the collision chamber: a_1 and a_2 are entry and exit diaphragms, b_1 and b_2 entry and exit tubes, c is a cylinder for suppression of secondary electron emission from the Faraday cylinder, d is the Faraday cylinder with magnetic control.

ions that had passed through the chamber was usually 0.02 – 0.04 μA even though it was easily increased to 0.1 μA. The beam of particles resulting from the passage of positive oxygen ions through the collision chamber then entered a magnetic analyzer *12*, described by us previously[8].

The measurement of currents of positive and negative ions of oxygen was made by means of the Faraday cylinders *10* and *11*, connected with a string electrometer using a constant deflection scheme. Because of the non-linear characteristic of the electrometer we made use of the same resistance 3.9×10^9 ohms during measurements of the current of both positive and negative ions.

The emission and focusing potentials were measured by electrostatic voltmeters and the accelerating potential was measured by means of a system of calibrated resistances. The error of measurement of the ion energies was of the order of 3%.

The method of measurement of the effective cross section of formation of negative ions as a result of capture of two electrons by positive ions of oxygen was as follows. First, the dependence of the current of positive and negative ions of oxygen passing through the collision chamber was studied as a function of the magnetic field intensity in the analyzer chamber. Since the beam diameter, limited by the two diaphragms, was considerably smaller than the diameter of the Faraday cylinders ($\sim$ 15 mm), the curves $I = f(H)$ had a plateau of a width approximately 300 oersteds. The measurements of the current were made thereafter at the intensity of the magnetic field corresponding to the center of the plateau.

The measurements of the currents of positive and negative ions were not made simultaneously and as a result, the error in determination of the measured quantities could be considerably larger due to the fluctuations in the intensity of the ion beam that passed through the collision chamber. To minimize such effects the current strength I_0 of the beam leaving the collision chamber was measured with Faraday cylinder *6* every time the current strength of the positive ion beam I_+ or of the negative ion beam I_- was measured. The ratio of the currents I_-/I_+ was calculated in the form of a ratio of the quantities I_-/I_0 and I_+/I_0, and in that way the error of measurements connected with the fluctuations in the beam intensity was decreased considerably.

To determine the effective cross section for capture of two electrons it was necessary to obtain the dependence of the ratio of currents I_-/I_+ on pressure p of the gas in the collision chamber. These measurements had to be corrected for the fraction of the negative ions in the analyzed beam that was formed by collisions with the residual gas (other than the gas under study) in the chamber. On interruption of the flow of gas into the collision chamber, the pressure of residual gas was $2 - 3.5 \times 10^{-5}$ mm. The ratio I_-/I_+ for the beam that passed through the residual gas in the chamber was of the order of 2%, giving the background reading. It should be noted that a substantial fraction of the negative ions appearing in the beam that passed through the residual gas in the collision chamber is formed as a result of capture of electrons from molecules of condensable vapors whose pressure is not measured by the McLeod gauge. Indeed, if the pressure in the collision chamber is increased to twice the residual pressure, then the ratio I_-/I_+ increases only by 0.2 – 0.3%.

The following procedure was followed during the determination of the dependence of I_-/I_+ on the pressure of gas in the collision chamber. First, the residual pressure in the chamber p_ϕ and the ratio $(I_-/I_+)_\phi$ at that pressure were determined. Gas was admitted continuously to the chamber until pressure p was reached. Then the ratio I_-/I_+ for the pressure p was obtained. Then the flow of gas was again interrupted, and the residual pressure p_ϕ and the ratio $(I_-/I_+)_\phi$ for the residual gas were measured. By computing the average value of $(I_-/I_+)_\phi$ for the residual gas from the two measurements at the pressure p_ϕ, the influence of the formation of negative ions by collisions with residual gas on the ratio I_-/I_+ at the pressure p was eliminated from the data. The pressure of the admitted gas was obtained as the difference $p - p_\phi$. A graph of $I_-/I_+ - (I_-/I_+)_\phi$ versus $p - p_\phi$ was obtained from the data. The values of I_-/I_+ both at the residual pressures and at the pressure p were computed as averages of 5 – 6 measurements.

As an example, the graph of the functional dependence for ions O_1^+ with energies 41 kev is shown in Fig. 3 for a beam passing through the collision chamber filled with oxygen. The dependence is linear for the lowest pressures, which testifies to the process of capture of two electrons by the ion O_1^+ in a single collision with a molecule O_2. Beginning with pressures of the order of 2×10^{-4} mm, the increase of the ratio I_-/I_+ with pressure becomes non-linear

because of the formation of negative ions of oxygen in two consecutive collisions of the ion 0_1^+ with molecules of oxygen ($0_1^+ \rightarrow 0_1$, $0_1 \rightarrow 0_1^-$).

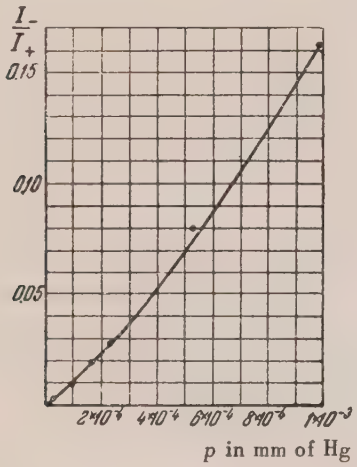

FIG. 3. Graph of dependence of $I_-/I_+ - (I_-/I_+)_\phi = f(p - p_\phi)$ for 0_1^+ ions with energy 41 kev in 0_2.

Evaluating the slope of the linear portion of the graph $I_-/I_+ - (I_-/I_+)_\phi = f(p - p_\phi)$, the effective cross section σ_{1-1} for capture of two electrons is computed according to the following formula [cf. Eq.(24) in our previous work[8]]:

$$\sigma_{1-1} = 1.08 \times 10^{19} \frac{T}{L} \left[\frac{d\,(I_-/I_+)}{dp}\right]_{p=0}, \qquad (4)$$

where T is the absolute temperature of the gas, L the effective length of the collision chamber, equal to 35 cm in our case, and $\left[\frac{d(I_-/I_+)}{dp}\right]_{p=0}$ is the slope of the linear section of the curve. The error of measurement of the effective cross section σ_{1-1} was of the order of 50%. A considerable part of this error was due to the small accuracy of the measurements of pressure in the linear part of the curve.

As is evident from the curve in Fig. 3, the ratio I_-/I_+ reaches 16% with an increase of pressure in the collision chamber. In individual measurements even larger values of I_-/I_+ were obtained. For example, for 14 kev 0_1^+ ions and the pressure of oxygen in the collision chamber 4.7×10^{-3} mm, the ratio I_-/I_+ was 33%. With pressure of nitrogen 2.7×10^{-3} mm the ratio was as high as 40%.

EXPERIMENTAL RESULTS

The measurements of the effective cross section for the capture of two electrons accompanied by the formation of fast negative ions were carried out both for atomic oxygen ions 0_1^+ and for the molecular ion 0_2^+, by passing the ion beam through hydrogen, oxygen and nitrogen. The process $0_1^+ \rightarrow 0_1^-$ was studied for ion beams of energy between 15 and 41 kev. The results of these measurements are shown in Table I.

Effective cross section of the process $0_2^+ \rightarrow 0_2^-$ was determined only for ions of energy 18 kev. The values obtained for the cross section are given in Table II.

Since the apparatus utilized in the present investigation of the capture of two electrons on collision of fast ions with gas molecules was considerably better than the apparatus used in our previous study[8], we have repeated the measurements of the effective cross section of the process $H_1^+ \rightarrow H_1^-$ in hydrogen with the proton energy equal to 21 kev. The effective cross section σ_{1-1} of that process turned out to be 1.5×10^{-17} cm^2, which is a much larger value than the one obtained in the previous work. Considering the improvement of the experimental conditions in the present measurements in comparison with the previous work (established effective length of the collision chamber, larger pressure drop from the collision chamber to the analyzing chamber) it is necessary to consider the data of this work to be closer to reality.

On analysis of the beam formed by the passage of the 0_1^+ ions through the collision chamber, doubly charged oxygen ions 0_1^{++} were found to be present. The appearance of these ions in the beam was due to the loss of an electron by the ion 0_1^+ by collision with a gas molecule. By an investigation of the dependence on the pressure of gas in the collision chamber of the ratio of the current strength of ions 0_1^{++} to the current strength of 0_1^+ ions, we were able to plot the curve $I_{0_1}^{++}/I_{0_1}^{+}$ versus p. From the slope of this curve the effective cross section σ_{12} for the loss of electron by the ions 0_1^+ was evaluated. Table III gives the effective cross sections σ_{12} for the ions 0_1^+ with energy 34 kev in three gases. The dependence of the effective cross section σ_{12} on the energy of the ions 0_1^+ for their passage through nitrogen is evident from the data in Table IV.

TABLE I

Process $0_1^+ \rightarrow 0_1^-$

Hydrogen		Oxygen		Nitrogen	
Energy in kev	$\sigma_{1\text{-}1} \times 10^{16}$ cm^2	Energy in kev	$\sigma_{1\text{-}1} \times 10^{16}$ cm^2	Energy in kev	$\sigma_{1\text{-}1} \times 10^{16}$ cm^2
15.0	0.9	13.7	0.7	14.0	0.5
22.6	0.7	—	—	—	—
32.6	0.8	—	—	29.0	0.7
41.4	1.3	41.0	0.9	39.4	1.1

TABLE II

Process $0_2^+ \rightarrow 0_2^-$

Gas	$\sigma_{1\text{-}1} \times 10^{18}$ cm^2
Hydrogen	4.1
Oxygen	5.1
Nitrogen	4.9

TABLE III

Process $0_1^+ \rightarrow 0_1^{++}$

Gas	$\sigma_{12} \times 10^{17}$ cm^2
Hydrogen	3.0
Oxygen	6.7
Nitrogen	5.7

TABLE IV

Process $0_1^+ \rightarrow 0_1^{++}$

Energy in kev	$\sigma_{12} \times 10^{17}$ cm^2
12.5	0.3
19.2	1.3
27.0	3.1
34.0	5.7
41.0	7.5

Oxygen ions with a degree of ionization higher than two have not been observed in the beam even with the greatest sensitivity of the electrometer detection system (electrometer resistance 4.3×10^{11} ohms). We can conclude, therefore, that the cross section for loss of two or more electrons by the 0_1^+ ion is less than 10^{-19} cm^2 for the energy interval investigated in the present work. In the beam of 0_2^+ ions that passed through the collision chamber we have discovered 0_1^+ ions with energy half of the energy of the 0_2^+ ions. The presence of these ions in the beam gives evidence of dissociation of molecular ions 0_2^+ by collisions with gas molecules in the collision chamber. Having found the dependence of the ratio $I_{0_1^+}/I_{0_2^+}$ on the gas pressure in the collision chamber, we have determined the effective cross section for dissociation of 0_2^+ ions in three gases. Table V gives the values of the effective cross section for dissociation of 0_2^+ ions with energy 23 kev.

TABLE V

Process $0_2^+ \rightarrow 0_1^+ + 0_1$

Gas	$\sigma_{diss} \times 10^{16}$ cm^2
Hydrogen	2.2
Oxygen	2.7
Nitrogen	3.2

It should be added that in the beam of 0_2^+ ions that passed through the collision chamber, we have found 0_1^- ions as well. The appearance of these ions may be ascribed to one of the following processes: 1. part of the 0_2^- ions formed by the process $0_2^+ \rightarrow 0_2^-$ end in excited states and dissociate into ion 0_1^- and atom 0_1; 2. ions 0_1^+ formed by dissociation of 0_2^+ ions capture during a second collision of two electrons and form an ion 0_1^-. It is possible to determine which of the two processes takes place by a study of the dependence of $I_{0_1^-}/I_{0_2^+}$ on the pressure of gas in the collision chamber. Such dependence should be linear at low pressures if the first process takes place, while a deviation from linearity should be evident for the second process. We intend to clarify this question in the future.

A study was also undertaken to learn more about formation of negatively charged ions of oxygen by passage through thin metallic foils placed close to the entry into the magnetic analyzer. Aluminum and

silver foils of thickness about 0.01 mgm/cm^2 were used for this purpose. The preparation of these foils was described in a previous work[9] connected with a study of the formation of negatively charged ions of hydrogen by proton bombardment of such foils.

Silver foils were very rapidly attacked on exposure to the beam of 47 kev O_1^+ ions of current strength $2 - 3 \times 10^{-8}$ A. Aluminum foils were found to be more stable and withstood the ion beam under the above conditions for two hours. In the beam that passed through the aluminum foil, more negative than positive ions were found. However, the beam particles were strongly scattered, which made quantitative measurements impossible. These same foils were found to be too thick for ions O_1^+ with energy of the order of 50 kev. Our efforts to prepare thinner foils with diameter 4 - 5 mm have been unsuccessful thus far. Apparently, a study of the process $O_1^+ \rightarrow O_1^-$ in metallic foils will be possible either for ions of higher energy, or for foils with a thickness much smaller than 0.02 mgm/cm^2.

DISCUSSION OF RESULTS

Consideration of the data in Table I allows us to make several conclusions about the formation of negatively charged ions of oxygen during collisions of O_1^+ ions with molecules of hydrogen, oxygen and nitrogen. First, the magnitude of the effective cross section for capture of two electrons by O_1^+ ions during collisions with the above-mentioned gases is as high as 10^{-16} cm^2. It is of the same order of magnitude as the cross section for the capture of a single electron. Second, there is no evidence of a substantial dependence of effective cross section for capture of two electrons on the energy of O_1^+ ions, in the energy interval between 14 and 41 kev, or on the kind of gas in the collision chamber.

The data of Table II show that the effective cross section for capture of two electrons is considerably smaller for O_2^+ ions than for O_1^+ ions and is the same for all three investigated gases. It is interesting to notice that the effective cross section for formation of negative ions by capture of two electrons by positive ions is considerably larger than the effective cross section for formation of negative ions during collisions of slow electrons with molecules. For comparison it can be pointed out that the effective cross section for the process $O_2 + e \rightarrow O_1 + O_1^-$ is equal to 8×10^{-19} cm^2 and is the largest for processes of that kind[1].

Quantum mechanical calculations of the effective cross section for atomic collisions with exchange of an electron between the interacting particles were presented by Kallmann and Rosen[10]. According to these calculations the effective cross section for exchange of one electron depends on the magnitude of the resonance defect ΔE, i.e., on the change of the internal energy of the particles during their interaction. It is evident that for collisions with an exchange of a single electron the magnitude of ΔE is equal to the difference between the energy freed by neutralizing one particle and the energy necessary to ionize a second particle. It is assumed that the interacting particles are in the ground state both before and after the interaction.

The calculation[10] shows that with $\Delta E = 0$, the effective cross section is maximum (resonance charge exchange), and with $\Delta E \neq 0$ the effective cross section decreases monotonically with increasing resonance defect. This decrease is symmetric about the maximum. Experimental studies[11] have shown that in the regions of negative and small positive values of ΔE^*, the change in the effective cross section for single charge exchange as a function of the quantity ΔE agrees with the theoretical calculations. For larger positive values of ΔE we observe a considerable deviation of the experimental data from the theory.

The process of the exchange of two electrons during atomic collisions is also accompanied by a change in the internal energy and therefore may clarify the relationship between resonance defect and effective cross sections of those processes. First, it is necessary to calculate the resonance defect of the processes investigated in the present work.

We shall consider the resonance defect in the collision processes of ions O_1^+, O_2^+ and H_1^+ with a hydrogen molecule. In the first case, i.e., in the process $O_1^+ + H_2 \rightarrow O_1^- + H_1^+ + H_1^+$ the energy yielded by formation of a fast O_1^- ion is equal to

---

[9] Ia. M. Fogel', B. G. Safronov and L. I. Krupnik, J. Exper. Theoret. Phys. USSR **28**, 711 (1955); Soviet Phys. **1**, 546 (1955)

* The sign of the quantity ΔE for the process $A^+ + B \rightarrow A + B^+$ is determined by the difference $V_{iA} - V_{iB}$, where V_{iA} and V_{iB} are the ionization potentials of the particles A and B.

[10] H. Kallmann and B. Rosen, Z. Phys. **61**, 61 (1930)

[11] F. Wolf, Ann. Physik **30**, 313 (1937)

$V_{i0} + S_0$, i.e., to the sum of the ionization potential and the electron affinity of the oxygen atom.

The energy lost in formation of the two slow protons, which resulted from the removal of two electrons from the hydrogen molecule, is composed of the dissociation energy of hydrogen molecule, double ionization potential of H atom and the potential energy of two protons.

In such a way the resonance defect for the above process is computed from the following equation:

$$\Delta E = V_{i0} + S_0 - (E_{diss} + 2V_{iH} + E_{pot}) \quad (5)$$

Substituting into Eq.(5) the values $V_{i0} = 13.57$ ev, $S_0 = 2.2$ ev, $E_{diss} = 4.48$ ev and $E_{pot} = 18$ ev, we obtain**

$$\Delta E = -33.8 \text{ ev}.$$

To compute the resonance defect of the processes $O_2^+ + H_2 \rightarrow O_2^- + H_1^+ + H_1^+$ and $H_1^+ + H_2 \rightarrow H_1^- + H_1^+ + H_1^+$, it is necessary to obtain first the sums $V_{iO_2} + S_{O_2}$ in the first case and $V_{iH} + S_H$ in the second case.

Substituting the values $V_{iO_2} = 12.5$ ev, $S_{O_2} = 0.7$ ev, $V_{iH} = 13.54$ ev and $S_H = 0.75$ ev into Eq. (5), we obtain***

$$(\Delta E)_{O_2^+ \rightarrow O_2^-} = -36.4 \text{ eV}$$

$$(\Delta E)_{H_1^+ \rightarrow H_1^-} = -35.3 \text{ eV}.$$

Table VI gives the resonance defects and the corresponding effective cross sections of the processes discussed above. As is evident from the Table, in the processes involving an exchange of two electrons, the resonance defect has a large negative value. The effective cross section of the process increases rapidly with the decrease in the absolute magnitude of the resonance defect (Fig. 4). No definite correlation between the magnitude of the electron affinity of a neutral particle and the magnitude of the effective cross section σ_{1-1} is observed. It may be anticipated that the same correlation will be true for the processes of the type $A \rightarrow A^-$, even though it has been shown by Dukel'skii and Zandberg[14] that it does not appear for the reverse processes $A^- \rightarrow A$.

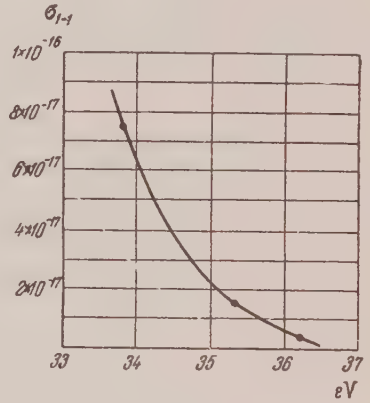

FIG. 4. The dependence of the cross section for the capture of two electrons on the absolute magnitude of the resonance defect $|\Delta E|$.

TABLE VI

Process	Gas	Energy of ions in kev	Electron affinity in ev	ΔE in ev	σ_{1-1} in cm^2
$O_1^+ \rightarrow O_1^-$	H_2	22.6	2.2	—33.8	7×10^{-17}
$H_1^+ \rightarrow H_1^-$	H_2	21.6	0.75	—35.3	1.5×10^{-17}
$O_2^+ \rightarrow O_2^-$	H_2	18.0	0.7	—36.4	0.4×10^{-17}

**The quantity $E_{pot} = e^2/R = 18$ ev, since the internuclear distance R is equal to 0.8 Å [12] for H_2 molecule in its ground state.

***The magnitude of the electron affinity of oxygen is calculated by Evans and Uri[13] from the Born-Haber cycle for the crystals KO_2, RbO_2 and CsO_2.

[12] Handb. d. Phys. **23**, part 1, p. 114 (1933)

[13] M. G. Evans and N. Uri, Trans. Farad. Soc. **45**, 224 (1949)

In the collision of fast ions with oxygen molecules, the process of exchange of two electrons may lead to the formation of various slow particles, namely: in the process $O_1^+ + O_2 \rightarrow O_1^- + O_2^{++}$ a slow, doubly charged, molecular ion of oxygen appears, while in the process $O_1^+ + O_2 \rightarrow O_1^- + O_1^+ + O_1^+$ two

[14] V. M. Dukel'skii and E. Ia. Zandberg, J. Exper. Theoret. Phys. USSR 21, 1270 (1951)

slow, singly charged oxygen ions O_1^+ are formed. Analogous possibilities are present in collisions of fast ions with the nitrogen molecules.

It is not possible to compute the resonance defect for the latter process since the potential energy of two ions O_1^+ or N_1^+ which are formed by removal of two electrons from the oxygen or nitrogen molecules is not known. If the process takes place by means of a formation of slow O_2^{++} or N_2^{++} ions, then the calculation of the resonance defect necessitates knowledge of the second ionization potential of the molecules O_2 or N_2.

Hagstrum and Tate[5] gave the ionization potentials of ions O_2^{++} and N_2^{++} as 50 ±0.5 ev and 49.5 ±0.5 ev, respectively. Using these numbers, it is possible to compute the resonance defect for the processes involving exchange of two electrons between the ions O_1^+ and O_2^+ on the one side and the molecules O_2 and N_2 on the other.

Tables VII and VIII give the values of the resonance defect and the effective cross sections for the processes $O_1^+ \rightarrow O_1^-$ and $O_2^+ \rightarrow O_2^-$ in three gases.

On the basis of the data given in Tables V, VI and VII the following conclusions can be made:

1. The resonance defect has a large positive value in all of the investigated processes involving exchange of two electrons.

2. For processes involving capture of two electrons by various ions from the molecules of the same gas the effective cross section increases with a decrease of the absolute value of the resonance defect.

3. For processes involving the capture of two electrons by the same ion from molecules of three different gases whose resonance defects were equal within the limits of experimental error, the effective cross sections were also equal.

How general these conclusions are is difficult to judge until measurements are carried out for a large number of ion-molecule pairs with various values of resonance defect. To enlarge the range of numerical values of the resonance defect in processes involving a two electron exchange, it will be necessary to investigate not only the processes of the type $A^+ \rightarrow A^-$, for which the resonance defect will always have a sufficiently large negative value, but also processes of the type $A^{++} \rightarrow A$ (neutralization of doubly charged ions), for which the resonance defect may have small positive and negative values, or even be equal to zero.

TABLE VII

Process	Gas	ΔE in ev	Energy of ions in kev	$\sigma_{1\text{-}1}$ in cm^2
$O_1^+ \rightarrow O_1^-$	H_2	—33.8	15.0	0.9×10^{-16}
	O_2	—34.2	13.7	0.7×10^{-16}
	N_2	—33.7	14.0	0.5×10^{-16}

TABLE VIII

Process	Gas	ΔE in ev	Energy of ions in kev	$\sigma_{1\text{-}1}$ in cm^2
$O_2^+ \rightarrow O_2^-$	H_2	—36.4	18	4.1×10^{-18}
	O_2	—36.8	18	5.1×10^{-18}
	N_2	—36.3	18	4.9×10^{-18}

The apparent lack of a strong dependence of the effective cross section of the process $O_1^+ \rightarrow O_1^-$ on ion energy (cf. Table I) is evidently connected with the fact that the energy interval investigated in the present work is not far from the energy for the maximum effective cross section.

As was shown previously by Hasted[15], position of the maximum on the curve giving the dependence of the effective cross section for single electron exchange on the ion energy agrees well with the

[15] J. B. Hasted, Proc. Roy. Soc. (London) A212, 235 (1952)

Massey criterion [16]

$$\frac{a|\Delta E|}{h\upsilon} = 1 \qquad (6)$$

where ΔE is the resonance defect, h is the Planck constant, υ is the velocity of the ion and a, equal to 7×10^{-8} cm, is the separation between the colliding particles at which the interaction forces become important (effective collision radius).

From Eq. (6) follows the relationship

$$V_{max} = 3.04 \cdot 10^{16}\ a^2 \cdot M_0 (\Delta E)^2, \qquad (7)$$

where V_{max} is the velocity of the ion corresponding to the maximum effective cross section, expressed in volts. Here M_0 is the mass number of the ion and ΔE is the resonance defect in electron volts.

If we assume that for the process $O_1^+ \rightarrow O_1^-$ the constant a has the same value 7×10^{-8} cm as in the processes of one electron exchange, then for ions O_1^+ with energy 15 kev the quantity $a\Delta E/h\upsilon \approx 14 \gg 1$ and $V_{max} = 2.75$ mev.

It is well-known that the equation $a\Delta E/h\upsilon \gg 1$ is a condition for adiabatic atomic collision and consequently, if it were satisfied for the process $O_1^+ \rightarrow O_1^-$ there would be a ground for considering the collision of O_1^+ ions with molecules H_2, O_2 and N_2 as adiabatic in the energy range studied. However, the effective cross section for such an adiabatic collision process should increase rapidly with the increase in the ion energy. There was no such increase in our work. Thus, the value $a = 7 \times 10^{-8}$ cm used for the process $O_1^+ \rightarrow O_1^-$ must be considered too large.

If we use $a = 10^{-8}$ cm, then $V_{max} = 56$ kev, according to Eq. (7). The energy interval investigated was in a region of a flat maximum, where a comparatively slow increase of effective cross section should be observed with increase in the energy of the ions. As is evident from Table I, the effective cross section $\sigma_{1,-1}$ has a small tendency to increase with increases in the energy of O_1^+ ions.

If $a = 10^{-8}$ cm, we obtain from Eq. (7) $V_{max} \approx 4$ kev for the process $H_1^+ \rightarrow H_1^-$ in hydrogen. With energies of the order of several tens of kev for H_1^+ one should then observe a decrease in the effective cross section for process $H_1^+ \rightarrow H_1^-$ with an increase in the ion energy. The experimental results, given in Table 2 of the previous work [8] show that the effective cross section of the process $H_1^+ \rightarrow H_1^-$ in hydrogen, in the energy interval 13 to 31 kev, indeed decreases with increase in the H_1^+ ion energy.

The above considerations, of course, cannot be considered a conclusive proof of appropriate application of the Massey criteria for determination of the maximum effective cross section of a process involving exchange of two electrons. For a fundamental judgment on this matter it will be necessary to carry out careful measurements of the dependence of the effective cross section for processes involving two electron exchange on the ion energy in a broad interval of energies and for a large number of ion-molecule pairs.

In conclusion, we would like to express our appreciation to Professor A. K. Val'ter for his constant interest and attention to this work.

[16] H. S. W. Massey and E. H. S. Burhop, *Electronic and Ionic Impact Phenomena*, Oxford, 1952

Translated by M. J. Stevenson
175

Further Discussion on Fluctuations in Gravitating Systems

IA. P. TERLETSKII
Moscow State University
(Submitted to JETP editor November 22, 1954)
J. Exper. Theoret. Phys. USSR **29**, 237-241 (1955)

IN connection with the objections[1] relative to the conclusions arrived at by me in references 2 and 3, I must necessarily write some explanation verifying the correctness of these conclusions.

In a note and at a meeting we have pointed out that in sufficiently large gravitating systems the magnitude of fluctuations increases with increasing dimensions of the system. This statement was proved with the aid of the simplified model of the isothermal ideal gas, occupying a volume V for a constant external pressure P and temperature T (for example, an ideal gas in a container, closed by a piston on which a constant force is applied). An analogous model is used for calculating the value of the fluctuations in a real gas at the critical point, as is done, for example, by Leontovich[4].

For the proof we used the relations

$$(\overline{\Delta V})^2 = -kT\frac{\partial V}{\partial P}, \qquad (1)$$

$$P = \frac{NkT}{V} - \frac{\partial U}{\partial V}, \quad U = -\alpha\frac{\varkappa M^2}{V^{1/3}},$$

the first of these can be proved as a rigorous theorem of the Gibbs statistical mechanics and hence is used only for systems in thermodynamic equilibrium; the expression for the potential energy U has the same validity as the law of gravitation of Newton.

From Eq. (1) the relative volume fluctuations of gravitating systems was derived as

$$\frac{(\overline{\Delta V})^2}{V^2} = \frac{1}{N}\left(1 - \frac{4\alpha}{9}\frac{\varkappa m^2}{kT}\frac{N}{V^{1/3}}\right)^{-1}, \qquad (2)$$

where m is the mass of the gas molecules, N is the total number of molecules in the system, κ is the gravitational constant and α is the numerical coefficient of the order of unity*. Since the last formula is used only for systems in thermodynamic equilibrium, the condition of applicability is

$$\partial P/\partial V < 0, \qquad (3)$$

precisely as for the analysis of the fluctuations at the critical point [see Eq. (32.1) in reference 4].

According to Eq. (3), formula (2) can be applied to an ideal gravitating gas, enclosed in a shell under a sufficiently large positive external pressure ($P > NkT/V$), but is inapplicable to a confined gaseous cloud, occupying a volume V and located in an infinite empty space, since in this case $P = 0$, from which, according to Eq. (1), $\partial P/\partial V > 0$ and, consequently, condition (3) is not satisfied. Formula (2) is also inapplicable to the ideal gravitating gas, filling all of infinite space, since such a system obeys Newton's law of gravitation and is not thermodynamically stable.

Thus, if for the nature of the rough model of the real gravitating system of galactic (or metagalactic) form, we assume a gravitating ideal gas, enclosed in a shell, subjected to an external pressure (Model I) then, starting from formula (2), the applicability of which in the given case cannot be disputed, we come to the conclusion of increasing magnitude of fluctuations with increasing number of particles as the system approaches a gravitating unstable state. If as the model of a real gravitating system we use one gravitating according to the Newtonian law for an ideal gas filling all of infinite space (model II), then, by virtue of the Newtonian law of gravitation, such a system can not be in thermodynamic equilibrium, and, hence, formula (2) is inapplicable. If, finally, as the model of a real gravitating system we choose a spatially bounded gaseous cloud in an infinite empty space (Model III) then the system cannot be stable because of the condition $P = 0$ at the boundaries of the cloud. Clearly, such a model is unstable for an ideal non-gravitating gas, and can-

[1] M. I. Shakharonov, J. Exper. Theoret. Phys. USSR 27, 646 (1954)

[2] Ia. P. Terletskii, J. Exper. Theoret. Phys. USSR 22, 507 (1952)

[3] Ia. P. Terletskii, Proceedings of the Second Conference on the Problems of Cosmogony, Acad. Sci. USSR, 1953, p. 507

[4] M. A. Leontovich, *Statistical Physics*, Govt. Technical Printing Office, 1944, p. 124

* We note that in reference 3 this formula is given with two misprints. The accurate expression was derived in reference 2.

not be considered as a model of a real universe.

It is entirely obvious that in our notes[2,3] we implied Model I, and not models II or III, because only in the case of Model I is it valid to use formula (2) to fulfill the condition: $dP/dV < 0$ or consequently, $P > [(NkT)/(4V)]$. At first sight, Model II seems more accurate because the external shell of Model I is clearly an artificial structure. However, Model II results in a gravitationally unstable universe, and, hence, the usual laws of thermodynamics and statistical mechanics of systems in equilibrium are inapplicable. With Model II the assertions of the correctness of the thermodynamic laws or the small value of the fluctuations in macroscopic systems has as little basis as for its opposite. This model prohibits any theoretical analysis of thermodynamic or statistical questions regarding the universe because there does not exist a statistical mechanics or thermodynamics for absolutely nonequilibrium systems*.

It is known that a gravitationally unstable model of the universe is always inadequate, and repeated attempts were made to set aside the instability by generalizations from Newton's law of gravitation. It is not difficult to see that the instability of Model II is caused by a very rapid decrease of the potential energy of any part of the system as its dimensions increase. Actually, for the uniformly dense gas $\sigma = mN/V$, the potential energy of a part of the gas, enclosed in a volume V, can be expressed as $U = -a\kappa\sigma V^{5/3}$, while its kinetic energy $({}^3/_2)NkT = (3\sigma kT/2m)V$ and consequently, for sufficiently large parts of the system the potential energy may exceed the kinetic energy by an arbitrary amount. However, a system is known to be unstable if the potential energy taken with a minus sign is greater than one-and-a-half times the kinetic energy, and, because of Eqs. (3) and (1), the system of a gravitating ideal gas can be stable only by fulfilling the condition

$$\frac{NkT}{V^2} + \frac{\partial^2 U}{\partial V^2} > 0, \tag{4}$$

and by virtue of Eq. (1),

$${}^3/_2({}^3/_2 NkT) + U > 0. \tag{5}$$

Obviously, the stability of an unbounded system of an ideal gas may be guaranteed if we assume a violation of the Newtonian law of gravitation for very large systems and imagine, for example, above a critical value V_{cr} the potential energy of an isolated volume of a homogeneous gas increases not as $V^{5/3}$, but simply proportional to V. In this case, condition (4) is always fulfilled for sufficiently large systems. Thus, it is possible to have another model (Model IV) of a large gravitating system, in which the gas fills up all of infinite space, as in Model II, but in which the universe is gravitationally stable, as in Model I, as a result of the breakdown of Newton's law of gravitation for sufficiently large systems.

It is easy to see that for Model IV the fluctuations of the volume of any isolated part of the gas may be calculated from Eq. (2) if its volume does not exceed the critical volume V_{cr}, because in this case the law of gravitation has the Newtonian form. For volumes larger than V_{cr}, it is necessary to use another expression for U, and consequently, the expression for the fluctuations is different from Eq. (2). Thus, in the same domain where Newton's law of gravitation is fulfilled, the fluctuations can be calculated with the aid of Model I.

It is not difficult to cite a concrete example of Model IV. It is well-known that the Poisson equation for the gravitational potential φ does not have a finite solution for a uniformly distributed density for all space. In Einstein's theory of gravitation there occurs an analogous difficulty. It is known that this difficulty is removed in the classical Newtonian theory as well as in the more

---

* In his critical note, M. I. Shakharonov arbitrarily assumed that we considered Model II or Model III, as this may otherwise be understood from the reference to the formula which Shakharonov refers to as the virial theorem. We notice that Eq. (2) does not apply in these cases (in the first case this is obvious, owing to the gravitational instability of an unbounded system obeying Newton's law; in the second case, it is a consequence of the condition $P = 0$ at the boundary of the cloud). Shakharonov denies the correctness of my conclusions for the macroscopic character of the fluctuations in sufficiently large gravitating systems and the possibility of significant spontaneous departure from a state of thermodynamic equilibrium in a system of galactic dimensions. Denying our conclusions, Shakharonov considers the widespread opinion " that the fluctuations may not lead to a breakdown of thermodynamic equilibrium on a macroscopic scale" to be correct. Shakharonov does not note, however, the internal inconsistency of his conclusion. Using Model II, Shakharonov acknowledges a gravitationally unstable universe. But in this case it is impossible to come to any conclusions about the magnitude of the fluctuations, inasmuch as thermodynamics and statistical mechanics are inapplicable. The use of Model III is inconsistent as we demonstrated above because of the inevitable condition $P = 0$ and not by virtue of the virial theorem, as was maintained by Shakharonov. The virial theorem is in general inapplicable in the case of Model III, since the system of an ideal gas without an external potential barrier is unbounded.

precise theory of Einstein by means of the introduction of an additional term (the so-called cosmological term [see, for example, reference 5)]. It is easy to show that with the introduction of an additional term in the gravitational equations it is possible to eliminate the gravitational instability of an infinite gravitational system. Since we are concerned with the principal aspects of the problem, we will consider only the simplest generalization of Newton's theory, suggested by Neiman, according to which, in place of Poissons's equation, we postulate the equation of the form

$$\nabla^2\varphi - \lambda^2\varphi = 4\pi\sigma, \tag{6}$$

where $\lambda^2\varphi$ is the cosmological term.

According to Eq. (6) the potential energy of matter distributed with a density $\sigma(\mathbf{r})$ in a volume V can be expressed as:

$$U = -\frac{\varkappa}{2}\int_V\int_V \frac{\sigma(\mathbf{r})\,\sigma(\mathbf{r}')}{|\mathbf{r}-\mathbf{r}'|}\, e^{-\lambda|\mathbf{r}-\mathbf{r}'|}\, d\mathbf{r}d\mathbf{r}', \tag{7}$$

where $d\mathbf{r}$ and $d\mathbf{r}'$ are elements of volume.

For small volumes, where $V^{1/3} \ll \lambda^{-1}$, the exponential factor inside the integral expression can be neglected and in this case, for a system of mass M, we obtain the result of the Newtonian theory, that is, $U \sim M^2 V^{-1/3}$. For larger volumes, when $V^{1/3} \gg \lambda^{-1}$, then, according to Eq. (7) we obtain $U \sim M^2 V^{-1}$. For example, for the case of a volume filled with matter of uniform density $\sigma = M/V$, we calculate

$$U = -\frac{\varkappa M^2 2\pi}{\lambda^2 V} \text{ при } V^{1/3} \gg \lambda^{-1}. \tag{8}$$

Consequently, for a universe that is filled uniformly with matter, the potential energy taken with a minus sign for a sufficiently large portion, increases proportionally with the volume, as well as does the kinetic energy. Thus, an ideal gas, gravitating according to Eq. (6), and filled uniformly to an infinite extent, can be considered as an example of Model IV.

Model IV may be rather somewhat of an approximation to the real universe, if we consider not an ideal, but a real gas, obeying Van der Waals equation and gravitating according to Eq. (6). For such a gas, for $V^{1/3} \ll \lambda^{-1}$, according to Eq. (8), we have

$$P = \frac{N(kT)}{(V-\Lambda b)} - \frac{aN^2}{V^2} - \frac{2\pi\varkappa m^2 N^2}{\lambda^2 V^2}, \tag{9}$$

i.e., written differently, the gas obeys Van der – Waals equation and has a constant a, equal to

$$A = a + \frac{2\pi\varkappa m^2}{\lambda^2}. \tag{10}$$

It is obvious that the question of stability of the model chosen is the same as for a real gas, obeying Van der Waal's equation, and the expression for the relative volume fluctuations has the form

$$\frac{\overline{(\Delta V)^2}}{V^2} = \frac{1}{N}\left[\frac{1}{\left(1-\frac{Nb}{V}\right)^2} - \frac{2aN}{\Theta V}\right]^{-1}. \tag{11}$$

It is obvious that the latter formula stands on the same basis in this case as in the case of an ordinary real gas.

From the point of view of Model IV the Boltzmann fluctuation hypothesis is more likely to be valid. Let the average density of the universe be such that on the average it is found in the gaseous phase and, according to Eq. (11), for sufficiently large volumes macroscopic fluctuations are possible. If fluctuations of gigantic dimensions are realized with increasing density in a definite portion of the universe, then in this region a condensed phase is developed, i.e., the formation of stars, planets, etc., results. In the course of time, however, this fluctuation is resolved, i.e., the density begins to decrease because the mass leaves the center of the fluctuation. After the transition to a sufficiently rarefied state there remains a region of condensed material (for example, a planet) which is gradually transformed into the gas phase owing to the statistical instability of such gravitating systems. In this manner, this portion of the universe is finally returned to its initial condition. Parallel to the fluctuations changing the volume on a macroscopic scale are changes in entropy, and, consequently, the law of monotonic increase in entropy is violated in a large part of the universe. Clearly, what this picture describes is only a roughly simplified model of an endlessly complicated phenomenon in a bounded portion of an infinite universe. However, it is not excluded that in this model there are shown features of cosmological processes in the course of large intervals of time in systems on a metagalactic scale.

An analysis of the methodological significance of the Boltzmann fluctuation hypothesis is given in articles in references 6 and 7 and in a monograph[8]

[5] D. Ivanenko and A. Sokolov, *Classical Theory of Fields*, GITTL, 1951, p. 70

[6] Ia. P. Terletskii, Dokl. Akad. Nauk SSSR **72**, 1041 (1950)

[7] Ia. P. Terletskii, *Problems of Philosophy*, No. 5, 1951, p. 180

[8] Ia. P. Terletskii, *Dynamic and Statistical Laws of Physics*, IZD, Moscow State University, 1950

Another article[9] is devoted to a related problem. As for the paper of M. I. Shakharonov in the Reports of the Moscow University[10], which he cites in reference 1 as if it contains a philosophic analysis of Boltzmann's hypothesis and in which he draws a conclusion about the supposedly idealistic character of Boltzmann's theory, it cannot be regarded as convincing, especially in view of an evaluation of Boltzmann, given by V. I. Lenin[11], as a materialist who struggled systematically against Machism. It is strange that Shakharonov arrives at the conclusions of Boltzmann's idealism from numerous quotations of Engels, which merely give witness to the direct bond between the fluctuation hypothesis of Boltzmann and the exposition of the qualitative indestructibility of motion as developed by Engels.

[9] Ia. P. Terletskii, J. Exper. Theoret. Phys. USSR 17, 837 (1947)

[10] M. I. Shakharonov, Reports, Moscow State University 6, 15 (1953)

[11] V. I. Lenin, *Collected Works*, 4th printing, vol. 14, pp. 274-276

Translated by B. Hamermesh
178

Photoelectron Emission in a Ferromagnetic

A. Z. VEKSLER
Institute for the Physics of Metals, Ural Affiliate, Academy of Sciences, USSR
(Submitted to JETP editor May 10, 1954)
J. Exper. Theoret. Phys. USSR **29**, 201-208 (August, 1955)

A formula is derived which determines the velocity distribution of photoelectrons and the temperature dependence of the photocurrent in the neighborhood of the Curie point. The calculations are carried out on the basis of the $s-d$ exchange model[1], with the periodic potential of the lattice being taken account of by the method of variation of parameters. It is shown that the photocurrent depends quadratically on the magnetization, in accordance with the results of Cardwell's work[2].

1. INTRODUCTION

THE theory of photoelectronic emission in a ferromagnetic is given in reference 3, where a formula for the photocurrent at a light frequency in the neighborhood of threshold and in a temperature region in the neighborhood of the Curie point is derived. A simplified theory of the photoeffect[4,5] was used in the derivation of this formula, as was the $s-d$ exchange model, taking account of the interaction of the s electron with the d electrons, thanks to which one is able to connect the electrical, thermal and mechanical properties of a ferromagnetic with its magnetic state. Failure to take account of the interaction of the s electrons within the framework of the $s-d$ exchange model would certainly be a defect; hence, it must be considered as one of the stages in the development of a consistent theory of ferromagnetics.

The use in reference 3 of a theory of the photoeffect which does not take account of the periodic potential is inappropriate, since special features of the motion of the electrons in ferromagnetics depend upon their interaction, which is but weakly connected with the properties of the limiting boundary. Hence, the motion of the electrons is not to be described as the sum of two plane waves[5,6], but more correctly as a function of the form:

$$\psi(\mathbf{r}) = e^{i\mathbf{kr}} u_{\mathbf{k}}(\mathbf{r}),$$

in which

$$u_{\mathbf{k}}(\mathbf{r}) = u_{\mathbf{k}}(\mathbf{r} + \mathbf{n}a),$$

where a is the lattice parameter. In this case there is no necessity of dividing the photoeffect into two parts: volume and surface. Moreover, the results obtained in the present work show that the photocurrent consists of two similar parts. Thus, the usual theory of the photoeffect is substantiated. Taking account of the periodic potential in a systematic way leads to the fact that the velocity distribution of the photoelectrons is different from that resulting from a theory of the photoeffect which does not take account of this potential.

2. THE WAVE FUNCTION OF THE ELECTRON

Let the metal occupy the half space $x<x_0$ and let the region $x \geq x_0$ be vacuum. Let us consider the emission of s-electrons from the metal which is produced by the absorption of light.

The wave function of the electron is determined by the equation:

$$\Delta\psi_1 + \frac{2m}{\hbar^2}[E - V(x, y, z)]\psi_1 = 0 \qquad (2.1)$$

for $x<x_0$,

$$\Delta\psi_2 + \frac{2m}{\hbar^2}\left[E + \frac{e^2}{4x}\right]\psi_2 = 0 \qquad (2.1')$$

for $x \geqslant x_0$,

where $V(x, y, z)$ is a periodic function. The solution of Eq. (2.1) has the following form:

$$\psi_1 = \sum_n \{a_n \exp[i(g_x + q_{n_1})(x - x_0)] \qquad (2.2)$$

$$+ b_n \exp[-i(g_x + q_{n_1})(x - x_0)]\}$$

$$\times \exp\{i[(g_y + q_{n_2})y + (g_z + q_{n_3})z]\},$$

where $q_{n_i} = 2\pi n_i / a$, n_i is an integer, g_x, g_y, g_z are the components of the quasi-momentum of the

[1] S. V. Vonsovskii, J. Exper. Theoret. Phys. USSR **16**, 981 (1946)

[2] A. B. Cardwell, Phys. Rev. **76**, 125 (1949)

[3] S. V. Vonsovskii and A. V. Sokolov, Dokl. Akad. Nauk SSSR **76**, 197 (1951)

[4] I. E. Tamm, Z. Phys. **68**, 97 (1931)

[5] R. H. Fowler, Phys. Rev. **38**, 45 (1931)

[6] K. Mitchell, Proc. Roy. Soc. (London) **A153**, 513 (1936)

electron.

The second equation can be solved by the method of separation of variables, setting

$$\psi_2 = f_1(x) f_2(y) f_3(z).$$

Then, on putting ψ_2 into Eq. (2.1′), we obtain

$$f_2(y) = e^{if_y y}, \quad f_3(z) = e^{if_z z}, \tag{2.3}$$

while $f_1(x)$ satisfies the equation

$$\frac{d^2 f_1}{dx^2} + \frac{2m}{h^2}\left(\frac{h^2 f_x^2}{2m} + \frac{e^2}{4x}\right) f_1 = 0, \tag{2.4}$$

and we have

$$\frac{h^2}{2m}(f_x^2 + f_y^2 + f_z^2) = E. \tag{2.5}$$

The general solution of Eq. (2.1′) has the form:

$$\psi_2(x, y, z) \tag{2.6}$$
$$= \sum_{f_x, f_y, f_z} C_f f_1(x) \exp\{i(f_y y + f_z z)\}.$$

The coefficients C_f are determined by the boundary conditions

$$\psi_1|_{x=x_0} = \psi_2|_{x=x_0}, \quad \psi_1'|_{x=x_0} = \psi_1'|_{x=x_0}. \tag{2.7}$$

In the present instance the prime indicates differentiation with respect to x. These conditions can be satisfied if Eqs. (2.2) and (2.6) are compared with each other term by term. In this case identity results on fulfillment of the equations

$$f_y = g_y + q_{n_2}, \quad f_z = g_z + q_{n_3}. \tag{2.8}$$

Taking account of relation (2.5), we find

$$f_x^2 = \frac{2m}{h^2} E - (g_y + q_{n_2})^2 - (g_z + q_{n_3})^2. \tag{2.9}$$

Thus, the summation in Eq. (2.6) is to be carried out over n_2 and n_3

$$\psi_2(x, y, z) \tag{2.6′}$$
$$= \sum_{n_2, n_3}' C_{n_2 n_3} f_1(x) \exp\{i[(g_y + q_{n_2}) y + (g_z + q_{n_3}) z]\}.$$

At great distances from the dividing boundary this function must have the form:

$$\psi_2(x, y, z) \tag{2.10}$$
$$= \sum_{n_2 n_3} C_{n_2 n_3} \exp\{i[f_x x + (g_y + q_{n_2}) y + (g_z + q_{n_3}) z]\}$$

or

$$\psi_2(x, y, z) \tag{2.10′}$$
$$= \sum_{n_2 n_3} C_{n_2 n_3} \exp\{-\varkappa_n x + i[(g_y + q_{n_2}) y + (g_z + q_{n_3}) z]\},$$

where $\kappa_x = -if_x$ if f_x is an imaginary number.

States of the electron which are described by the function (2.10) will be referred to in what follows as "free", while those described by the function (2.10′) will be called "bound". A finite nonzero probability of finding the electron at an arbitrarily large distance from the dividing boundary corresponds to the first case. The corresponding current is also different from zero. In the second case, the current is equal to zero, and the probability of finding the electron at a very great distance from the dividing boundary is small and tends to zero with increasing x.

Calculation of the current and averaging it over the coordinates gives for the first case the expression

$$j_x = \frac{eh}{m} \sum_{n_2 n_3} |C_{n_2 n_3}|^2 f_x. \tag{2.11}$$

The photoeffect for light of frequency near the threshold will be considered below. In this case, the overwhelming majority of the photoelectrons leaving the metal have an energy of the order of thermal. As was shown in reference 7, formula (2.11) then is simplified and takes the form

$$j_x = \frac{eh}{m} |C_{0,0}|^2 f_x. \tag{2.12}$$

3. THE CURRENT OF PHOTOELECTRONS

The wave function describing the state of the photoelectrons is the solution of the equation

$$\frac{h^2}{2m}\Delta u = \frac{h}{i}\frac{\partial u}{\partial t} - W(x, y, z) u \tag{3.1}$$
$$- \frac{eh}{imc}(\mathbf{A}\vec{\nabla}) u;$$

$$\mathbf{A} = 2\mathbf{a} \cos\left[\omega\left(t - \frac{x\cos\theta + y\sin\theta}{c}\right)\right], \tag{3.2}$$

where $W(x, y, z)$ is the periodic potential in the region of the metal, with $W = -e^2/4x$ for the region outside the metal.

Ordinarily the term standing at the right in Eq. (3.1) is small in comparison with the term on the

---

[7] A. V. Sokolov and A. Z. Veksler, J. Exper. Theoret. Phys. USSR 25, 215 (1953)

left side. Hence, Eq. (3.1) may be solved by the method of perturbation theory.

We seek a solution of Eq. (3.1) in the form

$$u = u_g + v, \tag{3.3}$$

where

$$u_g = \psi(x, y, z) \exp\{-iE_g t/\hbar\}, \tag{3.4}$$

subject to the condition $|u_g| \gg |v|$.

On substituting Eq. (3.3) into Eq. (3.1) and discarding the term containing $(\mathbf{A}\vec{\nabla})v$, we obtain

$$\frac{\hbar^2}{2m}\Delta v + \frac{h}{i}\frac{\partial v}{\partial t} - W(x, y, z)u = \frac{eh}{imc}(\mathbf{A}\vec{\nabla})u_g. \tag{3.5}$$

We seek the solution of this equation in the form of an expansion in terms of the integral of the eigenfunctions of the unperturbed problem:

$$v = \iint_{-\infty}^{+\infty} dg_y dg_z \Big\{ \int_0^{\infty} c_g^+(t)\, u_g^+(t)\, dg_x + \int_0^{\infty} c_g^-(t)\, u_g^-(t)\, dg_x \Big\}, \tag{3.6}$$

where

$$u^-_{g_x, g_y, g_z} = u^+_{-g_x, g_y, g_z} = u_{-g_x, g_y, g_z}.$$

On putting Eq. (3.6) into Eq. (3.5), multiplying once by u_g^{+*} and again by u_g^{-*}, and integrating, we find

$$\iint_{-\infty}^{+\infty} dg_y dg_z \Big\{ \int_0^{\infty} dg_x \frac{dc_g^+(t)}{dt} \int d\tau\, u_g^+ u_g^{\alpha *} + \int_0^{\infty} dg_x \frac{dc_g^-(t)}{dt} \int d\tau u_g^- u_g^{\alpha *} \Big\} = \frac{e}{mc} \int u_g^{\alpha *} (\mathbf{A}\vec{\nabla}) u_g\, d\tau, \tag{3.7}$$

where the index α takes on the values plus (+) or minus (–).

In virtue of the orthogonality of the functions u_g, we obtain

$$\int d\tau\, u_g^+ u_{g'}^{+*} = \int d\tau\, u_g^- u_{g'}^{-*} = N_g^{(1)} \delta(\mathbf{g} - \mathbf{g}'), \tag{3.8}$$

$$\int d\tau\, u_g^+ u_{g'}^{-*} = \int d\tau\, u_g^{+*} u_{g'}^- = N_g^{(2)} \delta(\mathbf{g} - \mathbf{g}'),$$

where $\delta(\mathbf{g} - \mathbf{g}')$ is the usual δ function. Hence, Eq. (3.7) can be written in the form: (3.9)

$$N_g^{(1)} \frac{dc_g^+(t)}{dt} + N_g^{(2)} \frac{dc_g^-(t)}{dt} = \frac{e}{mc} \int d\tau\, u_g^{+*} (\mathbf{A}\vec{\nabla}) u_{g'},$$

$$N_g^{(2)} \frac{dc_g^+(t)}{dt} + N_g^{(1)} \frac{dc_g^-(t)}{dt} = \frac{e}{mc} \int d\tau\, u_g^{-*} (\mathbf{A}\vec{\nabla}) u_g.$$

Eliminating dc_g/dt and integrating with respect to the time, we obtain

$$c_g^{\pm}(t) = \frac{\exp[(i/\hbar)(E_g + h\omega - E_{g'})t] - 1}{(i/\hbar)(E_g + h\omega - E_{g'})} (\mathbf{g}\,|\,\mathbf{a}\,|\,\mathbf{g}')^{\pm}, \tag{3.10}$$

where

$$(\mathbf{g}\,|\,\mathbf{a}\,|\,\mathbf{g}')^{\pm} = \frac{(e/mc)}{[N_g^{(1)}]^2 - [N_g^{(2)}]^2} \int d\tau\, [(\mathbf{a}\vec{\nabla})\psi_{g'}] [N_g^{(1)} \psi_g^{\pm *} - N_g^{(2)} \psi_g^{\mp *}]. \tag{3.11}$$

In the calculation, the term containing $\exp[i(E_g + h\omega - E_{g'})(t/h)]$, which corresponds to radiation, is discarded. Moreover, the factor $\exp[i\omega \frac{x\cos\theta + y\sin\theta}{c}]$ is omitted, since the case under consideration is that for which the frequency of the light is near threshold, in virtue of which $\omega/c \ll g$.

The energy connected with the quasi-momentum function[1] is

$$E = B + B'y + (C + C'_y)(\cos g_x a + \cos g_y a + \cos g_z a), \tag{3.12}$$

where y is the magnetization; B, B', C, C' are parameters depending on the energy of interaction of the s and d electrons and the energy of exchange of the s electrons. From this it is readily found that

$$N_g^{(1)} = \frac{(2\pi)^3 h^2}{2m(C + C'y)\sin g_x a} \Big\{ \sum_{n, n'} (2ag_x + 2\pi n_1 + 2\pi n_1')(a_n a_{n'}^* - b_n b_{n'}^*) + \sum_{n_1 n_2} |C_{n_1 n_2}|^2 afx \Big\}; \tag{3.13}$$

$$N_g^{(2)} = \frac{(2\pi)^3 h^2}{2m(C + C'y)\sin g_x a} \Big\{ \sum_{n, n'} (2ag_x + 2\pi n_1 + 2\pi n_1')(a_n b_{n'}^* + a_{n'}^* b_n) \Big\}.$$

On putting Eq. (3.10) into Eq. (3.6) and carrying out the integration, we find

$$v = \frac{(2\pi)^3 (\mathbf{g} \mid \mathbf{a} \mid \mathbf{g}_1)^+}{(C + C'y)\, a \sin g_{1x} a} u_{g_1}(x, y, z), \quad (3.14)$$

where $\mathbf{g}_1$ is the magnitude of g′ corresponding to the equalities:

$$E_{g_1} = E_g + h\omega; \quad (3.15)$$
$$g_{1y} = g_y + \frac{2\pi n_2}{a}, \quad g_{1z} = g_z + \frac{2\pi n_3}{a}.$$

The matrix element $(\mathbf{g} \mid \mathbf{a} \mid \mathbf{g}_1)$ breaks down into two parts, one of which corresponds to the region inside the metal, the other to the region external to it. On carrying out the integration over the basic region, we find that the part of the matrix element which is connected with the wave function of the electron in the metal is equal to

$$(\mathbf{g} \mid \mathbf{a} \mid \mathbf{g}_1)_1^+ \quad (3.16)$$
$$= a_x \Bigg\{ N_g^{(1)} \sum_{n_1, n_1'} (g_{1x} + q_{n_1}) \Bigg[\frac{a_n^* a_{n'} + b_n b_{n'}^*}{g_x + q_{n_1} - g_{1x} - q_{n_1'}} - \frac{a_n^* b_{n'} + a_{n'} b_n^*}{g_x + q_{n_1} + g_{1x} + q_{n_1'}} \Bigg]$$
$$+ N_g^{(2)} \sum_{n_1, n_1'} (g_{1x} + q_{n_1'}) \Bigg[\frac{a_n^* a_{n'} + b_n^* b_{n'}}{g_x + g_{n_1} + g_{1x} + q_{n_1'}} - \frac{a_n^* b_{n'}' + b_n^* a_{n'}}{g_x + q_{n_1} - g_{1x} - q_{n_1'}} \Bigg] \Bigg\},$$

where a_x is the component of the vector a along the x axis.

The calculation of the matrix element for the region inside the metal is extremely difficult. Hence, we shall limit ourselves merely to a determination of its dependence on the wave function f and the parameter κ. In the calculation of the matrix element we can use in place of the wave function of the bound state its asymptotic representation[6]

$$f_\varkappa(x) = b_\varkappa e^{-\varkappa x} (2\varkappa x)^{s/\varkappa}, \quad (3.17)$$

where $s = me^2/4h^2$. If $\kappa \geq 10^8$ cm^{-1}, then such a substitution is valid down to $x = (3 - 4)\, 10^{-8}$ cm.

An asymptotic decomposition of the type of Eq. (3.17) is not valid for the wave functions of the free states in view of the fact that at light frequencies near threshold the component of the wave vector f_x has an order of magnitude of 10^7 cm^{-1}. Instead of the asymptotic decomposition we can make use of the result of the work of reference 6, where it is shown that for frequencies in the neighborhood of threshold,

$$f_{f_x}(x) = \lambda(x) \; ; \quad (3.18)$$

to first approximation, this does not depend on f_x. Thus, the part of the matrix element for the region outside the metal and for a light frequency in the neighborhood of the critical point can be written in the form

$$(\mathbf{g} \mid \mathbf{a} \mid \mathbf{g}_1)_2 = a_x b_x \Big[N_g^{(1)} - N_g^{(2)} \Big] \int_{x_0}^{\infty} \lambda^*(x) \frac{d}{dx} \left\{ e^{-\varkappa x} (2\varkappa x)^{s/\varkappa} \right\} dx. \quad (3.19)$$

The term corresponding to the equality

$$g_{1x} = g_x + q_{n_1} - q_{n_1'}, \quad (3.20)$$

which, because of the zonal periodicity of the energy

$$E(\mathbf{g} + \mathbf{q}_n) = E(\mathbf{g}) \quad (3.21)$$

is not in conformity with the law of conservation of energy (3.15), has been dropped in Eq. (3.16). It can occur only for an excitation of the electron such that the latter goes over into the next zone. In view of the fact that in the present work we are considering the emission of photoelectrons for a light frequency near threshold, the number of electrons going over into the next zone is small, and hence the term corresponding to the condition (3.20) may be neglected.

The member in the matrix element, the x component of the quasi-momentum of which satisfies Eq. (3.20), corresponds to the "volume" photoeffect. The selection rules for the electron here are the same as for optical transitions. Ordinarily, the "volume" photoeffect is considered separately from the "surface" photoeffect. The calculation of the photocurrent in the present work does not require such a separation. Both kinds of transitions of the electrons are obtained automatically as component parts of the matrix element.

Calculation of the current with the aid of Eqs. (2.10) and (3.14) leads to the following result:

$$j_x = \frac{(2\pi)^6 e\hbar \mid (\mathbf{g} \mid \mathbf{a} \mid \mathbf{g}_1)^+ \mid^2}{m (C + C'y)^2 a^2 \sin^2 g_{1x} a} f_x \mid C_{0,0} \mid^2. \quad (3.22)$$

As was shown in reference 7, $f_x \mid C_{0,0} \mid^2$ does not depend on f_x. Let us designate

$$f_x \mid C_{0,0} \mid^2 = A(g_{1x}). \quad (3.23)$$

Then

$$j_x = \frac{(2\pi)^6 e\hbar \mid (\mathbf{g} \mid \mathbf{a} \mid \mathbf{g}_1) \mid^2 A(g_{1x})}{m (C + C'y)^2 a^2 \sin^2 g_{1x} a} \quad (3.24)$$

Integrating over the initial states, we find the complete current

$$I_x = \frac{1}{8\pi^3} \int_{-\pi/a}^{+\pi/a} dg_y \int_{-\pi/a}^{+\pi/a} dg_y \times \int_{f_x=0}^{\infty} dg_x j_x \frac{1}{\exp[(E-\varepsilon_0)/kT]+1} \quad (3.25)$$

We expand $\frac{1}{\exp[(E-\epsilon_0)/kT]+1}$ as a series in powers of $\exp[\frac{E-\epsilon_0}{kT}]$. If $E > \epsilon_0$, then

$$\frac{1}{\exp[(E-\varepsilon_0)/kT]+1} = \sum_n (-1)^n \exp\left\{-(n+1)\frac{E-\varepsilon_0}{kT}\right\} \quad (3.26)$$

For $E < \epsilon_0$ we obtain

$$\frac{1}{\exp[(E-\varepsilon_0)/kT]+1} = \sum_n (-1)^n \exp\left\{n\frac{E-\varepsilon_0}{kT}\right\}. \quad (3.26')$$

We make use of the equality

$$E = \frac{h^2}{2m}(f_x^2 + g_y^2 + g_z^2) - h\omega$$

and make a change of the variables of integration: in place of g_x, g_y, g_z we take

$$\rho^2 = g_y^2 + g_z^2, \quad \theta = \arctan(g_y/g_z) \text{ and } f_x.$$

Taking outside the integral sign those factors which are only weakly dependent of ρ and f_x, we obtain for $E > \epsilon_0$

$$I_x = -\frac{(2\pi)^4 mek^2T^2 |(\mathbf{g}|\mathbf{a}|\mathbf{g}_1)^+|^2}{h^3(C+C'y)^3 a^3 \sin^3 g_{1x}a} A(g_{1x}) \times \sum_n \frac{(-1)^n \exp\{(n+1)(h\omega+\varepsilon_0)/kT\}}{(n+1)^2} \quad (3.27)$$

If the frequency of the light is sufficient to knock out electrons with energy $E < \epsilon_0$, then in this case the region of integration can properly be divided into two: $E < \epsilon_0$ and $E > \epsilon_0$. As a result of the calculation we obtain the following expression:

$$I_x = -\frac{(2\pi)^4 mek^2T^2 |(\mathbf{g}|\mathbf{a}|\mathbf{g}_1)^+|^2 A(g_{1x})}{h^3(C+C'y)^3 a^3 \sin^3 g_{1x}a} \times \left\{\frac{\pi^2}{6} + \frac{(\varepsilon_0+h\omega)^2}{2k^2T^2} + \sum_n \frac{(-1)^n \exp\{-n(h\omega+\varepsilon_0)/kT\}}{n^2}\right\}. \quad (3.27')$$

It should be remarked that $\epsilon_0 < 0$ and is equal to the work of emission with sign reversed[7]. The expression obtained for the photocurrent has the same temperature dependence as that given in reference 4. If is fully confirmed by experimental results.

Using the Eq. (2.14) of reference 7 it is not difficult to find an expression for the total photocurrent in the neighborhodd of the Curie point (in the approximation of a weakly filled zone)

$$I_x = I_x^+ + I_x^- = (A_0 + B_0 y^2) T^2 \Phi_{1,2}\left[\frac{\varepsilon(\omega)+\beta_1 y^2}{kT}\right], \quad (3.28)$$

where

$$A_0 = -\frac{(2\pi)^4 mek^2A}{h^2a^4\alpha_1^{5/2}} M_0 \sum_{n_1} |a_{n,\,00}|^2 (\gamma_1 + q_{n_1}),$$

$$B_0 = -\frac{16\pi^4 mek^2A}{h^2a^4\alpha_1^{5/2}} \times \sum_{n_1}\left\{M_0\gamma_3 + \left(M_1 - \frac{3}{2}\frac{\alpha_2}{\alpha_1}M_0\right)\gamma_2 + \left[\left(\frac{15}{8}\frac{\alpha_2^2}{\alpha_1^2} - \frac{3}{2}\frac{\alpha_3}{\alpha_1}\right)M_0 - \frac{3}{2}M_1\frac{\alpha_2}{\alpha_1}\right](\gamma_1+q_{n_1})\right\}|a_{n,\,00}|^2;$$

$$\Phi_1(x) = \sum_n \frac{(-1)^{n+1}}{(n+1)^2} e^{(n+1)x}$$

for the case described by formula (3.27),

$$\Phi_2(x) = \left[\frac{x^2}{2} + \frac{\pi^2}{6} + \sum \frac{(-1)^n e^{-nx}}{n^2}\right]$$

for the case described by formula (3.27'); M_0, M_1 and M_2, are, respectively, the first, second and third coefficients in the expansion of the squared modulus of the matrix element in powers of y:

$$|(\mathbf{g}|\mathbf{a}|\mathbf{g}_1)|^2 = M_0 + M_1 y + M_2 y^2;$$

I_x^+ and I_x^- are the total currents of electrons with right and left orientations of mechanical moment, respectively;

$$\alpha_1 = B^2 + 3C^2 + \varepsilon^2(\omega) + 4BC - 2(B+2C)\varepsilon(\omega);$$

$$\alpha_2 = 2CC' + 2\varepsilon(\omega)(B'+2C');$$

$$\alpha_3 = 3C'^2 + B'^2 + 4B'C' + \beta'(B + 2C);$$

$$\gamma_1 = \arccos \xi_0; \quad \gamma_2 = \frac{\beta_2}{(1-\xi_0^2)^{1/2}};$$

$$\gamma_3 = -\frac{\xi_0 \beta_2^2}{(1-\xi_0^2)^{3/2}} - \frac{\beta_3}{(1-\xi_0^2)^{1/2}};$$

$$\xi_0 = \frac{\varepsilon(\omega) - (B+2C)}{C}; \quad \beta_2 = \frac{B' + 2C'}{C} + \xi_0 \frac{C'}{C};$$

$$\beta_3 = \xi_0 \frac{C'^2}{C^2} + \frac{B' + 2C'}{C^2} C' + \frac{\beta_1}{C};$$

$$\varepsilon(\omega) = \alpha + a^2 (3\pi^2 n)^{2/3} \beta + h\omega;$$

$$\beta_1 = a^2 (3\pi^2 n)^{2/3} k_1 \left(\frac{3}{8} k_1 \beta + \frac{3}{2} \beta' \right).$$

The symbols α, α', β, β', n, k_1 are taken from the work of Vonsovskii[1]. Formula (3.28) can obviously be used for nonferromagnetic metals if $\gamma = 0$ is inserted in it.

In this case, there results a temperature dependence of the same form as in the simplified theory of the photoeffect which does not take account of the periodic potential. The distinction between the simplified view of the photoeffect and the more coherent one is especially noticeable on comparison of the expressions determining the velocity distribution of the photoelectrons [Eq. (3.24)]. This dependence is more complicated than in the simplified theory, which, apparently, is what actually occurs.

If the photoeffect produced by light of frequency much greater than threshold is considered, then the second component of the matrix element, corresponding to the so-called "volume" effect, must also be taken into account.

A comparison of Eq. (3.28) for the photocurrent with the well-known relation determining its temperature dependence shows that the work of emission must be equal to $-\epsilon_0$. This result can be substantiated not only by a formal comparison, but also on the basis of thermodynamic relations[7].

In conclusion, the author expresses his profound gratitude to A. V. Sokolov for a number of valuable suggestions and to S. V. Vonsovskii for a discussion of the present work.

Translated by Brother Simon Peter, F. S. C.
174

SOVIET PHYSICS VOLUME 2, NUMBER 2 MARCH, 1956

International Values for the Thermal Cross Section of Fissionable Isotopes

At the session of August 17* of the International Conference on the Peaceful Application of Atomic Energy, a large amount of declassified data was presented on the effective neutron cross sections of the fissionable isotopes U-233, U-235 and Pu-239. In the low energy region, for which a large number of measurements was reported, excellent agreement was obtained for these isotopes, which play important roles in reactor installations. At the initiation of the Chairman, the scientists of France, Great Britain, the USSR and the USA met after the official session to consider the effective cross sections of absorption and fission of these isotopes by thermal neutrons (with velocities of 2200 m/sec). It was decided to develop a system of international mean values for these effective cross sections. Such values would contribute to agreement of reactor calculations based on these constants. The errors in the mean international values listed here are based on the scatter of reported values and in some instances exceed the errors of particular individual measurements.

	absorption in barns	fission in barns
U-233	593 ± 8	524 ± 8
U-235	698 ± 10	590 ± 15
Pu-239	1032 ± 15	729 ± 15

* Session 17A, August 17, 1955. "The Effective Cross Section of Fissionable Isotopes." Chairman, D. Hughes (USA), Vice-chairman, D. Popovich (Yugoslavia).

Translated by R. T. Beyer
237

The Mechanism of the Formation of Anode Layers in Molded Dielectrics

IA. N. PERSHITS
Pskov State Teacher's Institute

(Submitted to JETP editor March 6, 1954)
J. Exper. Theoret. Phys. USSR 29, 362-368 (September, 1955)

It is established that the mechanism of formation of electrode-attached layers is identical in dielectrics with various structures. By means of a comparative study of the electrode-attached effects in various dielectrics, it is shown that the mechanism of formation suggested by Warburg[1,2] is unsatisfactory.

DURING the electrolysis of many dielectrics, there appears a gradual decrease of current, associated with the formation of an electrode-attached (anode) layer of high resistance. Molded dielectrics possess unipolar conductivity: the flow of current in the "easy" direction is considerably greater than the flow of current in the "hard" direction, coinciding with the direction of the molding current. It has been shown[3,4] that for the dielectrics investigated (fused quartz, porcelain, eternit, mica, asbestos, alkali-haloid crystals) there appear the peculiarly typical curves of the time dependence of the "hard" current following the transient passage of the "easy" current (reference 4, Figs. 1,2). For all the dielectrics investigated, the curves of "hard" current have a point of inflection; moreover, the rate of decrease of the current in the "hard" direction is shown to depend on the duration of the current in the "easy" direction. Conformance with this behavior always indicates the presence of an unstable electrode-attached layer of high resistance in the dielectric.

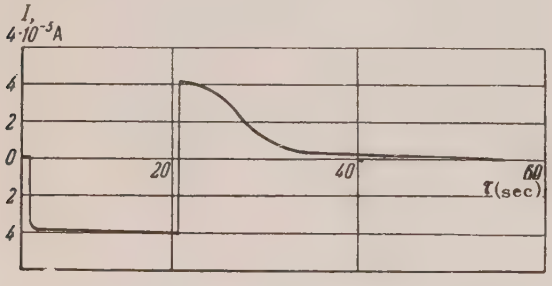

FIG. 1. Time dependence of current for molded glass

In the present work, glass was investigated. As is well-known, a molded layer is also created in glass as a result of electrolysis. The study of the character of the "easy" and "hard" currents in glass was conducted with a view to the establishment of a common mechanism of formation of the electrode-attached layer in glass and in dielectrics investigated previously. During the investigation of glass, it was discovered that the state of the surface of the dielectric has a considerable influence on the effects associated with the formation and destruction of electrode-attached layers.

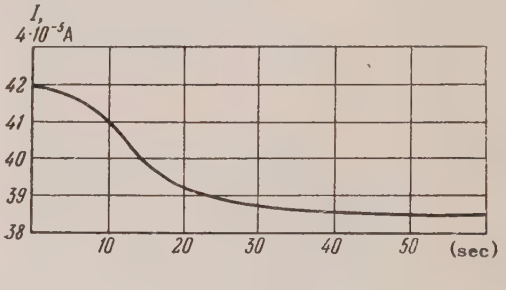

FIG. 2. Variation of the current in the "hard" direction for rock salt.

If the casting of the glass is carried out with the use of the usual metal electrodes at a comparatively high temperature (250 – 400° C), then at the change in the direction of the field, the destruction of the electrode-attached (anode) layer of high resistance at one electrode and the formation of a layer at the other electrode take place extremely rapidly, as disclosed by the corresponding change in the current. In this connection, it is important as to whether the metal electrodes are placed on the usual smooth surface of the glass, or, on a surface worked with sandpaper (made opaque). Under identical experimental conditions, the decrease of current following the change of direction of the field in a cast sample takes place more slowly in the second case than in the first, which indicates the influence of the state of the surface of the dielectric on the conditions for the formation of the electrode-attached layer. Using graphite

[1] E. Warburg, Wied. Ann. 21, 622(1884)

[2] E. Warburg and F. Tegetmeier, Wied. Ann. 32, 442 (1887); 35, 445 (1888)

[3] Ia. N. Pershits, J. Exper. Theoret. Phys. USSR 17, 251 (1947)

[4] Ia. N. Pershits, J. Exper. Theoret. Phys. USSR 28, 181 (1955); Soviet Phys. 1, 110 (1955)

electrodes, it was found possible, even for glass, to obtain curves fully coinciding with those presented in reference 4, Figs. 1,2,5. These curves differ from those obtained for glass with metal electrodes, in that here it is found that the "easy" current passes through a maximum, i.e., following the change in direction of the field, the "easy" current increases during a certain period of time. In one of the experiments, the sample of glass ($6cm^2 \times 0.4$ cm), furnished with graphite electrodes, was subjected to electrolysis at a temperature of 250 °C. The casting was performed during the course of one hour. The change in the direction of the field following the protracted electrolysis gave the usual picture (as, for example, in porcelain and eternit) of the increase of the "easy" current, and subsequent to the switching a smaller growth and then a constant current. A similar change of the "easy" current was described earlier for eternit (reference 4, Fig. 5). In Fig. 1, a curve is presented showing the time dependence of the flow of current in the "easy" and "hard" directions for the present sample of glass at a temperature of 210 °C. This curve differs from the curves obtained, for example, for quartz, only by the considerably large coefficient of unipolarity. In the present case, the coefficient of unipolarity is $K \sim 200$.

It has been noted[4] that the heat treatment of the sample has considerable influence on the stability of the electrode-attached layer. A decrease in the temperature of the cast sample leads to an increase of the stability of the electrode-attached layer, which is manifested in the character of the curves of the "easy" current. Cooling the sample, with a subsequent warming up to the temperature at which the casting was performed, stimulates a substantial increase of the stability of the electrode-attached layer and an increase of the resistance of the sample for current in the "easy" and "hard" directions. The procedure of cooling and subsequent heating of the dielectric leads to the same change in the character of the time dependence of the current, as does a protracted electrolysis.

The influence of cooling on glass was investigated in the same way as for the other dielectrics[4]. A frame with the sample cast at a high temperature was removed from the furnace, and, after complete cooling, was again placed in the furnace and heated to the previous temperature. For these investigations, use was made of a special arrangement in the form of a sled, with which the frame with the dielectric was moved. This device guaranteed the rigorously identical position of the dielectric in the furnace during the two successive measurements of the current. The constancy of the temperature was carefully controlled with the use of a thermocouple, included in a compensating system. Furthermore, during the series of observations, an electronic temperature regulator was used, which helped to maintain a constant temperature in the furnace and automatically effected the locking of the dielectric bonds at the given temperature.

In one of the experiments, the sample of glass was cast for a long time at a temperature of 250 °C. After cooling, it was again introduced into the furnace and was subjected to an extremely short electrolysis at a temperature of 250 °C, after which the direction of the field was changed. The "easy" current (increasing), recorded at the instant the field was switched, comprised only 60% of the current obtained in the same direction before the cooling of the sample (0.65×10^{-3} A and 0.36×10^{-3} A). Figure 1 refers to a sample subjected to such a procedure and then cooled down to 210 °C.

Comparing the character of the time and temperature dependence of the current in glass and in other dielectrics[4] previously investigated, we see that they are completely identical. This allows us to think that in all of the dielectrics investigated, we have to do with one and the same mechanism of formation and destruction of electrode-attached layers.

At the present time, the generally accepted mechanism of formation is that proposed by Warburg[1,2]. It is assumed that the molded layer in solid dielectrics represents simply a region with a deficiency of mobile positive ions[5,6]; but this is completely incapable of accounting for the processes taking place in the layer under the action of an electric field and heat. A study of the conditions of formation of electrode-attached layers in dielectrics has shown[4] that these processes must be taken into account in the explanation of the molding effects.

It should be noted that the shortcomings of the mechanism of formation suggested by Warburg also follow from the experiments of Kosman and Sozina[7], who investigated polarization effects in cast glass. It was established by them that there is a nonlinear dependence in glass of the effective thickness of the polarized layer on the amount of electricity that has flowed past. Kosman and Sozina showed that the thickness of the layer

---

[5] A. Venderovich and B. Lapkin, Zh. Tekhn. Fiz. 9, 46 (1939)

[6] Ia. M. Ksendzov, Zh. Tekhn. Fiz. 18, 3 (1948)

[7] M. S. Kosman and N. N. Sozina, J. Exper. Theoret. Phys. USSR 17, 340 (1947)

that is formed does not increase proportionately to the amount of electricity gone by, but that in a sizable formation the accumulation of the electrode-attached layer, in general, practically ceased. In order to bring these results into conformance with the classical mechanism of formation proposed by Warburg, Kosman and Sozina put forward the hypothesis that there exists in glass a substantial electronic composition of the current. However, it is necessary to keep in mind that the limitation of the thickness of the layer that is formed also takes place in dielectrics for which there is no basis for the assumption of electronic conductance, as for example, in alkali-haloid crystals.

In alkali-haloid crystals, the currents in the "hard" and "easy" directions generally differ by only 5-10%. Figure 2 shows the diminishing part of the curve of the current in the "hard" direction, obtained following a protracted electrolysis (10 hours) of natural rock salt (using iron electrodes) at a temperature of 600 °C. In the "easy" direction the current continued for 20 seconds, and during this time remained unchanged. As is evident in the figure, the coefficient of unipolarity in this case is $K = 1.1$. This leaves no doubt that the mechanism of formation of electrode-attached layers in alkali-haloid crystals is the same as in the other dielectrics investigated. Since the effects associated with the formation and destruction of electrode-attached layers are more graphically displayed by large differences of "hard" and "easy" currents, we strove to obtain the largest possible coefficient of unipolarity. By gradually decreasing the temperature of the molded crystal of rock salt, and from time to time switching the field, it was possible to observe the increase of the coefficient of unipolarity from $K = 1.1$ to $K = 1.43$ (at $T = 350$ °C).

Under these circumstances, however, in order to maintain the relatively large value of K, it was necessary to make sure that the temperature did not change during the course of the experiment. If the temperature fell to a lower value than that at which the measurement was made (350 °C), then, even at the given temperature (350 °C) the coefficient of unipolarity was reduced, and its value could be restored only by a repetition of the casting at a higher temperature, and a new lowering of the temperature to 350 °C. This extremely complex temperature dependence of the coefficient of unipolarity was not observed in the other dielectrics investigated. We pressume that this is connected with the special conditions of penetration and binding of the admixtures in alkali-haloid crystals. Since in the majority of dielectrics the casting effects are associated with always having admixtures in the dielectric, it may be conjectured that in alkali-haloid crystals the basic role is played by admixtures diffusing in the sample at the high temperature. This question must be subjected to special study in the future. A further increase of the coefficient of unipolarity to $K \sim 2$ in the same crystal was obtained by means of a decrease of the difference of potential applied to the sample. The increase of the coefficient of unipolarity at reduced field intensities is explained in that for molded crystals, Ohm's law is obeyed for current in the "easy" direction, but is not obeyed for current in the "hard" direction.

The investigation of cast samples of rock salt indicated that in them as in other dielectrics, there is a sharp increase of the "easy" current following the change in direction of the electric field. Hence, it follows that the electrode-attached layer in rock salt, for instance, and in glass, has little stability and is easily destroyed by a field in the opposite direction. But if the limitation of the growth of the thickness of the layer in glass could be explained by the layer having a very large resistance, so that in the course of time the current would become negligibly small, such an explanation would not be possible in the present case. It is evident from the experiments that for the complete formation of the layer in rock salt it is sufficient to conduct the electrolysis for one hour. If in reality an anode layer of high resistance would be created by the simple uncompensated departure of cations of the admixtures, then we would obtain as a result of an extremely protracted electrolysis, a layer of such thickness that it could not remain in the same way with little stability, as in glass, and with a change of the direction of the field, there would be observed a gradual, and not an abrupt change of current. At the same time, it is of course not possible to explain the limitation of the growth of the layer in alkali-haloid crystals, as was proposed in reference 7 for glass, by electronic conduction.

If there had been electronic conduction in alkali-haloid crystals, or if it had appeared as a result of electrolysis, it would have provoked a coloring of the crystal, since the movement of electrons in alkali-haloid crystals is accompanied by the formation of F-centers.

2. A time dependence of current completely analogous to that which is observed in solid dielectrics at high temperatures has been successfully disclosed also at low temperatures (10-15 °C) at which, in such objects, it hardly has meaning to speak of electronic conductivity. At room temperature, the molding effects accompanied by the formation of an anode layer of little stability are easily detected in eternit, which is a hydro-

philic dielectric;in a humid atmosphere, it may possess considerable conductivity, which disappears after warming. In eternit the curves of the time dependence of current at low temperatures are completely the same as those at high temperatures[4], and besides, a considerable coefficient of unipolarity is observed (at $T = 10\,°C$, $K \sim 50$). The possibility of observing molding effects at low temperatures renders their investigation exceptionally easy.

Using a plate of eternit supplied with clamps to serve as electrodes, the effects observed in glass and other dielectrics at high temperatures were successfully reproduced with the clarity of a demonstration experiment. Here, it is particularly easy to ascertain the role of the anode layer. If one of the electrodes on the border of the dielectric is moistened with a liquid electrolyte, the character of the curves is changed, so that at once the role of the anode in the process of the formation of the layer is disclosed.

Effects, quite analogous to those studied in other dielectrics, are also observed during the electrolysis of skin. The tissues of a living organism represent an extremely complex electrolytic conductor, consisting of liquid and semiliquid media. The greatest resistance is possessed by dry skin, especially the horny layer. When metal electrodes are used, complicated processes take place in the tissues at the points of contact, associated with the electrolysis of tissue fluid and the subsequent formation of secondary chemical unions. As a result of these processes, oxygen is isolated at the anode and hydrogen at the cathode.

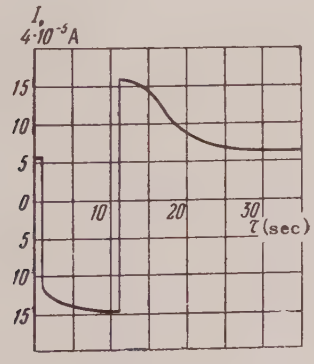

FIG3. Time dependence of current for formed skin (dry anode).

Here, as our observations have shown, an electrode-attached layer arises at the anode, quite the same as in other dielectrics, as for example, in glass and in alkali-haloid crystals. This circumstance, it appears, introduces interest in that relation, which will permit a deeper understanding of the electro-physiological tissue electro-conductivity studied, especially if it is taken into account that analogous effects could take place on the borders of cells, and also on the surfaces separating different tissues.

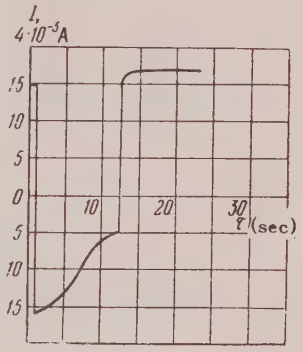

FIG. 4. Time dependence of current for skin (moist anode).

To study this effect, circular metallic electrodes ($d = 3$ mm) were placed on the ends of fingers ($V = 75\,V$). As was to be expected, the character of the effects taking place were essentially dependent on the state of the electrodes (dry or moist). During the passage of current, as is well-known, the resistance of skin decreases; therefore, when using dry electrodes, the current gradually increases. Here, however, an electrode-attached layer of high resistance is created at the anode. This layer is easily disclosed by means of successive changes of the direction of the electric field. The formation of an anode layer follows from the character of the curve of current in the "hard" direction, which appears quite the same as for other dielectrics. In conformance with this, in considering the dependence on the state of the electrodes, it is necessary to distinguish two cases: a) during the initial imposition of the field, the border of the anode is dry skin, and the border of the cathode is moist skin; b) during the initial imposition of the field, the border of the anode is moist skin, and the border of the cathode is dry skin. In the first case, in spite of the increase of the conductivity of the skin during the imposition of the field, a drop in the current is observed as a consequence of the rapid formation of an electrode-attached layer. With the change of direction of the field, an increasing current is observed, and with a repeated change of the direction we obtain the usual characteristic curve (Fig. 3). In the second case, when the anode is moist, the formation of a layer of high resistance

at the anode does not take place (as for example, also in eternit) and during the imposition of the field, a considerable increase of current is disclosed. At the change of direction of the field the current is diminished as a consequence of the formation of a layer at the new anode (dry), and with a repeated change of direction of the field, the current is almost constant. This is fully understandable, because the layer formed at the dry anode is destroyed, and no layer is created at the moist electrode (Fig. 4).

It should be noted that during the conditions of formation of the anode layer, the observed dependence of the curve of diminishing current in the "hard" direction from the time of the passage of current in the "easy" direction is completely the same as described for other dielectrics [3,4]. The corresponding curves, obtained with the aid of a cathode ray oscillograph, are presented in Fig. 5.

Thus, there is a basis for the assertion that in all of the cases we have to do with the identical physical process.

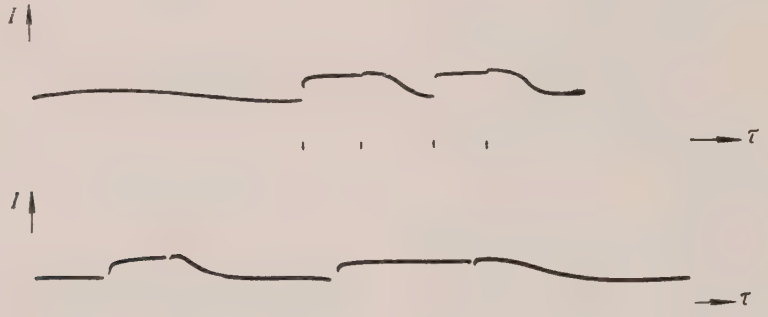

FIG. 5. Dependence of the "hard" current from the time of the passage of the "easy" current during the electrolysis of skin. The increasing curves represent the "easy" current, and the decreasing curves represent the "hard" current.

CONCLUSION

As a result of investigations conducted with various dielectrics we come to the following conclusions: 1) the character of the electrode-attached effects is the same for all the dielectrics investigated, and it is possible also for all molded dielectrics; 2) these effects cannot be explained by a simple uncompensated motion of cations. It appears that to a considerable degree, the effects are conditioned by processes in which anions are involved.

Taking into account the extraordinary generality of the effects in the different dielectrics, it may be conjectured that in the formation of the layer a particular role is played by oxygen produced at the anode during electrolysis. This is all the more probable since for many dielectrics, and in the first place for glass, the production of hydrogen is associated with the transfer of cations[8,9,10]. In glass for example, the reaction assumed at the anode is

$$Na_2SiO_3 = 2\dot{N}a + SiO_2 + O''.$$

The question of the character of the changes taking place in the electrode-attached layer under the action of a field and of temperature requires still further investigations. The experimental and theoretical data of the majority of authors[11,12,13] leads to the conclusion that in glass there exists purely ionic conductivity. It would be important to establish whether the purely cationic conductivity is maintained in the electrode-attached layer in glass, or whether the anions possess a certain mobility in the layer. The clarification of this question is necessary for the theoretical investigation of the disclosed time dependence of the current.

As concerns the role of electronic conductivity, it is impossible to deny that it takes place in the actual electrode-attached layer, because very

[8] M. Le Blanc and F. Kerschbaum, Z. Phys. Chem. 72, 468 (1910)

[9] G. Schulze, Ann. Physik 37, 435 (1912)

[10] P. P. Kobeko and I. V. Kurchatov, Dokl. Akad. Nauk USSR 1, 187 (1928)

[11] H. Schiller, Ann. Physik 83, 137 (1927)

[12] A. M. Venderovich and V. I. Chernykh, Tr. Sib. FTI 24, 156 (1947)

[13] V. A. Presnov, Tr. Sib. FTI 30, 175 (1950)

strong fields are created therein To assume that electronic conduction must exist in the whole volume of the molded dielectric[7] does not have satisfactory grounds in our opinion, because such an assumption is found to be in contradiction with experimental data.

Translated by D. Lieberman
204

SOVIET PHYSICS JETP VOLUME 2, NUMBER 2 MARCH, 1956

Investigation of the Isotope Effect in the Uranium Spectrum

A. R. STRIGANOV AND L. A. KOROSTYLEVA

(Submitted to JETP editor May 10, 1955)
J. Exper. Theoret. Phys. USSR 29, 393-405 (October, 1955)

The isotope shift in the spectrum of uranium has been measured for 346 lines among the components of the isotopes U^{238} and U^{235}. The regularities obtained in the isotope shift have been employed for the extension of the classification of the uranium spectrum and for the establishment of the isotope shift in several terms of U I and U II.

Starting from the shift of the terms $5f^4\,7s^6\,I_{9/2}$ and $5f^3\,7s^2\,{}^4I_{9/2}$, it is found that the lowest electron configuration for U II is $5f^4 7s$.

THE isotope effect in the spectrum of uranium was first discovered by Anderson and White[1] and was later studied by a number of other investigators[2-4], including ourselves. As the problem of the present research, which was carried out in 1951, a much more complete investigation was conducted of the isotope shift in the lines of uranium, with the aim of establishing the dependence of the isotope shift on the electron configuration and the determination of the shift in the terms. It was also desirable to establish the presence of even-odd shift, which had not yet been observed in the uranium spectrum at that time. The results of these investigations are given below.

1. EXPERIMENTAL PART

Three spectrographs were used for the investigation of the isotope shift in the spectrum of uranium. The spectral region 2300-2700 A was obtained with the help of a large Hilger quartz spectrograph whose dispersion in this region ranged from 2.3 to 3.1 A/mm. The interval 3900-4400 A was spectrographed by means of a Zeiss three prism glass spectrometer with an autocollimating chamber $f = 1300$ mm. The dispersion of this apparatus in the given region varied from 1.3 to 2.6 A/mm. The intervals 2700-3900 A and 4400-6600 A were obtained with a Baird diffraction spectrograph with a concave grating of radius of curvature 3 m, with 600 lines/mm. Some parts of these intervals were spectrographed in second order (dispersion 2.6 A/mm) and some in third order (dispersion 1.8 A/mm).

An arc of variable current between graphite electrodes was used as an excitation source. The arc was fed by a generator DG-1. The current strength was 5 A.

In the investigations we used samples of enriched uranium which represented a mixture of two isotopes, U^{238} and U^{235}, and also samples of a three isotope mixture, U^{238}, U^{235}, U^{233}, or U^{238}, U^{235}, U^{234}. In addition to the spectra of these samples, we recorded the spectra of natural uranium and of iron. For a survey of the spectra of uranium from mixed oxides, we prepared aqueous solutions of uranium nitrate from a calculation of 0.06 cm^3 of distilled water per milligram of salt. This sample, in the form of an aqueous solution, was applied on the tips of the upper and lower graphite electrodes (length 50 mm, diameter, 5 mm) and dried out on the slab. For the survey of each spectrum we used 2 milligrams of material, the time of

[1] D. E. Anderson and H. E. White, Phys. Rev. 71, 911 (1947)

[2] L. E. Burkhart, G. L. Stukenbrocker and S. Adams, Phys. Rev. 75, 83 (1949)

[3] J. K. McNally, J. Opt. Soc. Am. 39, 271 (1949)

[4] D. D. Smith, G. L. Stukenbrocker and J. K. McNally, Phys. Rev. 84, 383 (1951)

exposure being 2-3 minutes. In the case of the diffracting spectrograph, third order spectrum, the sample was increased to 6 milligrams, which were applied to the two pairs of graphite electrodes. Each pair of electrodes was arranged in series and was employed for the survey of a single spectrum; the total exposure was increased to 14 minutes for certain regions of the spectrum.

The isotope shift in the uranium spectrum was determined by linear interpolation between two nearby lines of iron. The mean relative error was approximately ±5%.

2. THE RELATION OF THE ISOTOPE SHIFT TO THE ELECTRON CONFIGURATIONS OF U I AND U II

Making use of the spectrum of the two isotope sample (U^{238} and U^{235}) with 50% of each isotope, we measured the isotope shift for 346 lines. It turned out that of all the lines measured, 301 had negative shift (the component of the lighter isotope shifted in the direction of higher wave number) and 45 lines had a positive shift. Of the 45 positive shifts, 34 were in the visible portion of the spectrum. Of the most sensitive lines of uranium, two spark lines, 4244.372 A, ($\Delta\lambda = 0.246$ A) and 4689.074 A, ($\Delta\lambda = 0.219$ A) underwent significant shifts.

TABLE I

Arc Lines of Uranium

Line wavelength in Angstroms	Classification of the line[5]	Intensity		Shift $\Delta(U^{238}-U^{235})$	
		Arc	Spark	A	cm^{-1}
3454.617	$5f^36d7s^2\ {}^5K_5^0 - 295_6$	10	—	—0.058	—0.48
3489.371	$5f^36d7s^2\ {}^5L_6^0 - 287_5$	20	1	—0.059	—0.48
3644.245	$5f^36d7s^2\ {}^5K_5^0 - 280_6$	18	2	—0.044	—0.33
3679.375	$5f^36d7s^2\ {}^5K_5^0 - 278_5$	2	—	—0.050	—0.37
3904.299	$5f^36d7s^2\ {}^5K_5^0 - 262_6$	8	15	—0.062	—0.40
3918.065	$5f^36d7s^2\ {}^5K_6^0 - 297_7$	3	—	—0.086	—0.56
3923.054	$5f^36d7s^2\ {}^5K_5^0 - 261_6$	15	6	+0.110	+0.71
4246.261	$5f^36d7s^2\ {}^5L_6^0 - 235_7$	30	2	—0.051	—0.28
4266.331	$5f^36d7s^2\ {}^5L_6^0 - 234_5$	15	—	—0.082	—0.46
5329 223	$5f^36d7s^2\ {}^5L_6^0 - 187_6$	10	1	—0.118	—0.42
6395.446	$5f^36d7s^2\ {}^5L_6^0 - 156_7$	100	—	+0.117	+0.29
6502.59	$5f^36d7s^2\ {}^5K_6^0 - 196_5$	15	—	—0.089	—0.24
		Average		—0.071*	—0.40*
4285.232	$5f^36d7s\ {}^7K_6^0 - 301_6$	10	1	—0.098	—0.54
5997.329	$5f^36d7s\ {}^7M_6^0 - 229_7$	25	—	+0.106	+0.30
6246.550	$5f^36d7s\ {}^7K_6^0 - 217_6$	6	—	—0.146	—0.37
		Average		—0.122*	—0.44*

* The average value of the shift is taken without regard to sign.

[5] C. O. Kiss, C. Hymphreys and D. D. Laun, J. Res. Nat. Bur. Stand. **37**, 57 (1946)

TABLE II

Spark Lines of Uranium

Line wavelength in Angstroms	Classification of the line[6]	Intensity		Shift $\Delta(U^{238}-U^{235})$	
		Arc	Spark	A	cm^{-1}
2556.194	$5f^37s^2\ {}^4I^0_{9/2} - 391_{11/2}$	15	12	—0.081	—1.24
2865.679	$5f^37s^2\ {}^4I^0_{9/2} - 349_{11/2}$	30	50	—0.080	—0.98
2923.174	$5f^37s^2\ {}^4I^0_{9/2} - 342_{11/2}$	8	10	—0.071	—0.84
2962.207	$5f^37s^2\ {}^4I^0_{9/2} - 337_{11/2}$	6	4	—0.074	—0.85
3216.201	$5f^37s^2\ {}^4I^0_{9/2} - 311_{11/2}$	5	3	—0.109	—1.06
3325.658	$5f^37s^2\ {}^4I^0_{9/2} - 300_{11/2}$			—0.104	—0.94
3339.446	$5f^37s^2\ {}^4I^0_{9/2} - 299_{11/2}$	5	1	—0.059	—0.52
3399.958	$5f^37s^2\ {}^4I^0_{9/2} - 294_{11/2}$	6	3	—0.07	—0.60
3476.293	$5f^37s^2\ {}^4I^0_{9/2} - 287_{11/2}$	4	3	—0.126	—1.05
3497.067	$5f^37s^2\ {}^4I^0_{9/2} - 286_{11/2}$	3	3	—0.123	—1.00
3550.822	$5f^37s^2\ {}^4I^0_{9/2} - 281_{11/2}$	12	20	—0.072	—0.64
3654.294	$5f^37s^2\ {}^4I^0_{9/2} - 272_{11/2}$	3	4	—0.141	—1.05
3895.272	$5f^37s^2\ {}^4I^0_{11/2} - 301_{11/2}$	12	20	—0.145	—0.96
3899.097	$5f^37s^2\ {}^4I^0_{11/2} - 300_{11/2}$	5	3	—0.149	—0.98
3918.065	$5f^37s^2\ {}^4I^0_{11/2} - 299_{11/2}$	3	8	—0.086	—0.56
3933.030	$5f^37s^2\ {}^4I^0_{9/2} - 254_{9/2}$	5	10	—0.097	—0.62
3989.953	$5f^37s^2\ {}^4I^0_{11/2} - 294_{13/2}$	4	6	—0.145	—0.91
4033.427	$5f^37s^2\ {}^4I^0_{11/2} - 292_{11/2}$	12	10	—0.140	—0.86
4050.039	$5f^37s^2\ {}^4I^0_{9/2} - 247_{9/2}$	25	35	—0.107	—0.65
4062.549	$5f^37s^2\ {}^4I^0_{9/2} - 246_{11/2}$	12	18	—0.120	—0.72
4088.254	$5f^37s^2\ {}^4I^0_{9/2} - 244_{9/2}$	25	18	—0.186	—1.11
4106.931	$5f^37s^2\ {}^4I^0_{9/2} - 243_{7/2}$	25	10	—0.102	—0.61
4116.097	$5f^37s^2\ {}^4I^0_{9/2} - 243_{11/2}$	25	35	—0.173	—1.02
4244.372	$5f^37s^2\ {}^4I^0_{9/2} - 235_{11/2}$	25	25	—0.249	—1.38
4287.869	$5f^37s^2\ {}^4I^0_{9/2} - 233_{9/2}$	15	18	—0.141	—0.76
4301.470	$5f^37s^2\ {}^4I^0_{9/2} - 232_{11/2}$	15	15	—0.081	—0.44
4415.241	$5f^37s^2\ {}^4I^0_{9/2} - 226_{11/2}$	12	12	—0.200	—1.02
4510.320	$5f^37s^2\ {}^4I^0_{9/2} - 222_{9/2}$	20	30	—0.187	—0.92
4689.074	$5f^37s^2\ {}^4I^0_{9/2} - 213_{7/2}$	30	40	—0.219	—1.00
4755.729	$5f^37s^2\ {}^4I^0_{9/2} - 210_{7/2}$	8	15	—0.178	—0.79
4769.260	$5f^37s^2\ {}^4I^0_{9/2} - 209_{7/2}$	6	15	—0.178	—0.78
4819.544	$5f^37s^2\ {}^4I^0_{4/2} - 251_{13/2}$	12	12	—0.209	—0.90
4859.750	$5f^37s^2\ {}^4I^0_{9/2} - 205_{7/2}$	8	8	—0.207	—0.88

[6] J. C. van den Bosch, Physica 15, 503 (1949)

TABLE II (continued)

Line wavelength in Angstroms	Classification of the line[6]	Intensity		Shift $\Delta(U^{238}-U^{235})$	
		Arc	Spark	A	cm^{-1}
4933.657	$5f^37s^2\ {}^4I^0_{11/2}-247_{9/2}$	8	8	—0.151	—0.62
5311.881	$5f^37s^2\ {}^4I^0_{11/2}-232_{11/2}$	18	18	—0.113	—0.40
		Average		—0.135	—0.84
3222.293	$5f^36d7s\ {}^4L^0_{13/2}-373_{13/2}$	8	3	—0.049	—0.47
3370.134	$5f^36d7s\ {}^6L^0_{15/2}-349_{13/2}$	6	4	—0.053	—0.47
3496.415	$5f^36d7s\ {}^6L^0_{13/2}-303_{15/2}$	8	15	—0.059	—0.48
3826.514	$5f^36d7s\ {}^6L^0_{11/2}-264_{13/2}$			—0.06	—0.41
3890.364	$5f^36d7s\ {}^6L^0_{11/2}-260_{13/2}$	35	30	—0.055	—0.35
3978.159	$5f^36d7s\ {}^6L^0_{13/2}-269_{11/2}$	4	—	—0.151	—0.95
3985.795	$5f^36d7s\ {}^6L^0_{15/2}-303_{15/2}$	25	30	—0.089	—0.56
4004.063	$5f^36d7s\ {}^6L^0_{13/2}-267_{13/2}$	15	20	—0.082	—0.51
4234.688	$5f^36d7s\ {}^4L^0_{13/2}-253_{11/2}$	10	8	—0.114	—0.63
4297.112	$5f^36d7s\ {}^6L^0_{11/2}-235_{11/2}$	18	18	—0.121	—0.66
4553.858	$5f^36d7s\ {}^6K^0_{9/2}-228_{9/2}$	4	1	—0.085	—0.41
4584.847	$5f^36d7s\ {}^6L^0_{13/2}-235_{11/2}$	10	15	—0.109	—0.52
4651.546	$5f^36d7s\ {}^6L^0_{13/2}-232_{11/2}$			+0.096	+0.42
4702.517	$5f^36d7s\ {}^6K^0_{11/2}-235_{11/2}$	10	20	—0.112	—0.50
4772.701	$5f^36d7s\ {}^6K^0_{11/2}-232_{11/2}$	6	18	+0.077	+0.33
5247.352	$5f^36d7s\ {}^6I^0_{7/2}-244_{9/2}$	6	6	—0.118	—0.43
5321.605	$5f^36d7s\ {}^6H^0_{7/2}-244_{9/2}$	6	3	—0.099	—0.35
5400.951	$5f^36d7s\ {}^6I^0_{7/2}-239_{9/2}$	10	6	—0.107	—0.36
5551.441	$5f^36d7s\ {}^6I^0_{9/2}-244_{9/2}$	8	5	—0.133	—0.43
5581.610	$5f^36d7s\ {}^6L^0_{11/2}-182_{9/2}$	12	5	+0.230	+0.74
5723.632	$5f^36d7s\begin{cases}{}^6I^0_{9/2}-239_{9/2}\\ {}^6I^0_{7/2}-228_{9/2}\end{cases}$	15	1	—0.159	—0.49
5843.294	$5f^36d7s\ {}^6I^0_{9/2}-235_{11/2}$	3	—	—0.200	—0.58
5952.053	$5f^36d7s\ {}^6I^0_{9/2}-232_{11/2}$	3	—	+0.121	+0.35
6087.338	$5f^36d7s\ {}^6I^0_{9/2}-228_{9/2}$	10	—	—0.227	—0.61
		Average		—0.114*	—0.51*
3924.272	$5f^36d^2\ {}^6M^0_{13/2}-300_{11/2}$	15	15	+0.059	+0.38
3943.498	$5f^36d^2\ {}^6M^0_{13/2}-299_{11/2}$	6	10	+0.124	+0.8
4241.669	$5f^36d^2\ {}^6M^0_{13/2}-281_{11/2}$	40	50	+0.069	+0.38
4992.940	$5f^36d^2\ {}^6M^0_{13/2}-246_{11/2}$	4	4	+0.138	+0.55

TABLE II (continued)

Line wavelength in Angstroms	Classification of the line[6]	Intensity		Shift $\Delta(U^{238}-U^{235})$	
		Arc	Spark	A	cm^{-1}
5405.996	$5f^36d^2\ {}^6M^0_{15/2} - 269_{15/2}$	5	6	+0.152	+0.52
5837.707	$5f^36d^2\ {}^6M^0_{13/2} - 217_{13/2}$	30	1	+0.145	+0.42
		Average		+0.114	+0.51
3605.823	$5f^47s\ {}^6I_{9/2} - 287^0_{11/2}$	8	8	−0.136	−1.05
3904.299	$5f^47s\ {}^6I_{11/2} - 299^0_{11/2}$	8	15	−0.062	−0.40
3951.553	$5f^47s\ {}^4I_{9/2} - 290^0_?$	1	8	−0.106	−0.67
3992.539	$5f^47s\ {}^4I_{9/2} - 260^0_{9/2}$	10	8	−0.149	−0.93
		Average		−0.113	−0.76
5480.275	$5f^46d\ {}^6L_{11/2} - 260^0_{9/2}$	15	25	+0.115	+0.38
5527.848	$5f^46d\ {}^6L_{11/2} - 259^0_{9/2}$	25	40	+0.107	+0.35
6181.369	$5f^46d\ {}^6K_{9/2} - 277^0_{7/2}$	2	—	+0.214	+0.56
		Average		+0.145	+0.43

* The average value of the shift is taken without regard to sign.

The isotope shift for the classified lines of U I and U II, which are subdivided into groups according to the electron configurations of the lower term, are given in Tables I and II. It should be noted that the electron configurations of the higher terms have not yet been established. Therefore, these terms are denoted by the first three digits of their calculated value in cm^{-1} and the small interlinear number is their internal quantum number. The isotope shift for the unclassified lines is given in the separate table in the Appendix.

The average, maximum and minimum shift in the uranium lines for each electron configuration of the lowest term is given in Table III. The mean shift for all lines of the ionized atom amounts to 0.67 cm^{-1}, while the mean shift for the lines of the neutral atom amounts to 0.41 cm^{-1}. An especially large difference is observed for lines which refer to the terms of the lowest electron configuration of U II ($5f^3\,7s^2$, $5f^4\,7s$) and of U I ($5f^3\,6d\,7s^2$). The mean values of the shift of the lines of the two electron configurations

TABLE III

State of the atom and electron configuration of the lower term	$\Delta\nu\ (U^{238}-U^{235})$ in cm^{-1}		
	Mean	Maximum	Minimum
U I $5f^36d7s^2$	−0.40	−0.56	−0.24
U I $5f^36d^27s$	−0.44	−0.54	−0.37
U II $5f^37s^2$	−0.84	−1.37	−0.40
U II $5f^36d7s$	−0.51	−0.95	−0.35
U II $5f^36d^2$	+0.51	+0.80	+0.38
U II $5f^47s$	−0.76	−1.05	−0.40
U II $5f^46d$	+0.43	+0.56	+0.35

for U I ($5f^3 6d 7s^2$, $5f^5 6d^2 7s$) differ slightly from one another. The great majority of the lines connected with the two configurations have negative shift, and only three lines have a positive shift. The group of lines in U II which are related to the lowest configuration $5f^3 7s^2$ in system B with penetrating s^2 electrons undergo a very large average shift, equal to 0.84 cm^{-1}, while the shift for all the lines is directed one way, without exception. In system A the lines of the lowest configuration $5f^4 7s$ with a single penetrating s electron also have a large mean shift, equal to 0.76 cm^{-1}. All the lines of this configuration have a negative shift. The lines of the higher configurations ($5f^3 6d 7s$, $5f^3 6d^2$, $5f^4 6d$) of both systems, including the non penetrating d electron, have smaller and approximately uniform shift. The overwhelming majority of lines belonging to the configuration $5f^3 6d 7s$ have a negative shift and only four lines have a positive shift. All the lines of the two other higher configurations $5f^3 6d^2$ and $5f^4 6d$ with non penetrating d and f electrons have positive shifts.

These regularities in the isotope shift can serve for the further extension of the classification of the uranium spectrum. It is evident from the Table that all the lines of uranium with negative shift exceeding 0.56 cm^{-1} in absolute value belong to lines of the ionized atom. Furthermore, the lines with negative shift exceeding 1.05 cm^{-1} belong to the electron configuration $5f^3 7s^2$. Lines with negative shift which lie in the interval from 0.95 cm^{-1} to 1.05 cm^{-1} belong to one of the two lowest configurations $5f^3 7s^2$, $5f^4 7s$. Lines which undergo a positive shift belong generally to the two electron configurations $5f^3 6d^2$ and $5f^4 6d$ of the ionized atom, while those of them which have a positive shift greater than 0.56 cm^{-1} belong to the configuration $5f^3 6d^2$.

On the basis of the isotope shift we have once again established the connection of 220 lines to the ionized atom and have also determined the electron configuration of the lowest term for 153 transitions. These results are given in a Table (see Appendix), where the lines analyzed are designated in the fourth column either by the single symbol II (which denotes that the line belongs to the ion) or by this symbol and the electron configuration to which the lowest term of the given line belongs. It should be noted, however, that excitation in the levels has not been taken into account in establishing electron configurations by this method, so that errors are possible.

3. ISOTOPE SHIFT IN THE TERMS

Relying on the extensive experimental material on the isotope shift in the uranium spectrum, we have succeeded in determining the isotope shift

TABLE IV

Isotope Shift of the Terms of U I

Electron configuration and term	Shift $\Delta T(U^{238}-U^{235})$ in cm^{-1}	Initial term	Electron configuration and term	Shift $\Delta T(U^{238}-U^{235})$ in cm^{-1}	Initial term
$5f^3 6d 7s^2\ {}^5L_6^0$	0.48	287_5	234_5	0.02	287_5
$5f^3 6d 7s^2\ {}^5K_5^0$	0.48	295_6	235_7	0.20	287_5
$5f^3 6d 7s^2\ {}^5K_6^0$	0.56	297_7	261_6	1.19	295_6
$5f^3 6d^2 7s\ {}^7K_6^0$	0.54	301_6	262_6	0.08	295_6
$5f^3 6d^2 7s\ {}^7M_6^0$	$\simeq 0.5$	—	278_5	0.11	295_6
156_7	0.77	287_5	280_6	0.15	295_6
187_6	0.06	287_5	287_5	0	
196_5	0.32	297_7	295_6	0	
217_6	0.17	301_6	297_7	0	
229_7	$\simeq 0.8$	${}^7M_6^0$	301_6	0	

TABLE V

Isotope Shift of the Terms of U II

Electron configuration and terms [6]	Shift $\Delta T(U^{238}-U^{235})$ in cm^{-1}	Initial term	Electron configuration and terms [6]	Shift $\Delta T(U^{238}-U^{235})$ in cm^{-1}	Initial term
			System *A*		
$5f^4 7s\ {}^6I_{9/2}$	1.31	$^6L_{11/2}$	$260^0_{9/2}$	0.38	$^6L_{11/2}$
$5f^4 6d\ {}^6K_{9/2}$	0		$277^0_{7/2}$	0.56	$^6K_{9/2}$
$5f^4 6d\ {}^6L_{11/2}$	0		$287^0_{11/2}$	0.26	$^6L_{11/2}$
$259_{9/2}$	0.35	$^6L_{11/2}$	$290^0_?$	0.64	$^6L_{11/2}$
			System *B*		
$5f^3 7s^2\ {}^4I^0_{9/2}$	1.30	$^6M^0_{13/2}$	$244_{9/2}$	0.44	$^6M^0_{13/2}$
$5f^3 7s^2\ {}^4I^0_{11/2}$	1.30	$^6M^0_{13/2}$	$246_{11/2}$	0.57	$^6M^0_{13/2}$
$5f^3 6d7s\ {}^6I^0_{7/2}$	0.57	$^6M^0_{13/2}$	$247_{9/2}$	0.67	$^6M^0_{13/2}$
$5f^3 6d7s\ {}^6I^0_{9/2}$	0.51	$^6M^0_{13/2}$	$251_{13/2}$	0.40	$^6M^0_{13/2}$
$5f^3 6d7s\ {}^6K^0_{9/2}$	0.49	$^6M^0_{13/2}$	$254_{9/2}$	0.68	$^6M^0_{13/2}$
$5f^3 6d7s\ {}^6K^0_{11/2}$	0.48	$^6M^0_{13/2}$	$260_{13/2}$	0.24	$^6M^0_{13/2}$
$5f^3 6d7s\ {}^6K^0_{13/2}$	>0.35	$325_{13/2}$	$264_{13/2}$	0.18	$^6M^0_{13/2}$
$5f^3 6d7s\ {}^6L^0_{11/2}$	0.59	$^6M^0_{13/2}$	$267_{13/2}$	−0.06	$^6M^0_{13/2}$
$5f^3 6d7s\ {}^6L^0_{13/2}$	0.46	$^6M^0_{13/2}$	$269_{11/2}$	−0.50	$^6M^0_{13/2}$
$5f^3 6d7s\ {}^6L^0_{15/2}$	0.53	$^6M^0_{13/2}$	$269_{15/2}$	0.52	$^6M^0_{15/2}$
$5f^3 6d7s\ {}^6H^0_{7/2}$	0.49	$^6M^0_{13/2}$	$272_{11/2}$	0.25	$^6M^0_{13/2}$
$5f^3 6d^2\ {}^6M^0_{13/2}$	0		$281_{11/2}$	0.38?	$^6M^0_{13/2}$
$5f^3 6d^2\ {}^6M^0_{15/2}$	0		$286_{11/2}$	0.30	$^6M^0_{13/2}$
$182_{9/2}$	1.33	$^6M^0_{13/2}$	$287_{9/2}$	0.69	$^6M^0_{13/2}$
$205_{7/2}$	0.42	$^6M^0_{13/2}$	$287_{11/2}$	0.25	$^6M^0_{13/2}$
$209_{7/2}$	0.52	$^6M^0_{13/2}$	$292_{11/2}$	0.44	$^6M^0_{13/2}$
$210_{7/2}$	0.51	$^6M^0_{13/2}$	$294_{11/2}$	0.70	$^6M^0_{13/2}$
$213_{7/2}$	0.30	$^6M^0_{13/2}$	$294_{13/2}$	0.33	$^6M^0_{13/2}$
$217_{13/2}$	0.42	$^6M^0_{13/2}$	$299_{11/2}$	0.77	$^6M^0_{13/2}$
$222_{9/2}$	0.38	$^6M^0_{13/2}$	$300_{11/2}$	0.35	$^6M^0_{13/2}$
$226_{11/2}$	0.28	$^6M^0_{13/2}$	$301_{11/2}$	0.34	$^6M^0_{13/2}$
$228_{9/2}$	0.08	$^6M^0_{13/2}$	$303_{15/2}$	−0.03	$^6M^0_{13/2}$
$232_{11/2}$	0.86	$^6M^0_{13/2}$	$311_{11/2}$	0.24	$^6M^0_{13/2}$
$233_{9/2}$	0.54	$^6M^0_{13/2}$	$337_{11/2}$	0.45	$^6M^0_{13/2}$
$235_{11/2}$	−0.07	$^6M^0_{13/2}$	$342_{11/2}$	0.46	$^6M^0_{13/2}$
$239_{9/2}$	0.21	$^6M^0_{13/2}$	$349_{11/2}$	0.32	$^6M^0_{13/2}$
$243_{7/2}$	0.69	$^6M^0_{13/2}$	$349_{13/2}$	0.06	$^6M^0_{13/2}$
$243_{11/2}$	0.28	$^6M^0_{13/2}$	$391_{11/2}$	0.06	$^6M^0_{13/2}$

in the terms. The so-called initial terms were selected for this purpose. These terms take part in transitions in the case of certain spectral lines, but are known not to undergo isotope shift, or to undergo a shift which is small and, for all practical purposes, equal to zero. The isotope shift of the other term is completely determined in this case by the shift in the line. The relative shifts for the other terms have been found for other lines with measured isotope shift and with a known shift of one term, connected with this line. In order to obtain the correct sign, use is made of the relation

$$\Delta\nu = \Delta T_h - \Delta T_l$$

where $\Delta\nu$ is the shift in the line, ΔT_h and ΔT_l are the shifts in the higher and lower terms.

For initial terms among the arc lines, we used the highest part of the upper terms: 287_5, 295_6, 297_7, 301_6. The normalized results are given in Table IV, where the isotope shift for 20 terms of the neutral uranium atom are listed. For the spark spectra, ${}^6K_{9/2}$, ${}^6L_{11/2}$ were taken for the initial terms in system A and ${}^6M^0_{13/2}$, ${}^6M^0_{15/2}$ in system B. These terms do not undergo any noticeable

TABLE VI

Isotope Shift for the Line 4244.372 A

Isotope	Our results		Reference 3		Reference 4	
	$\Delta\lambda$(Å)	$\Delta\nu$ (cm^{-1})	$\Delta\lambda$ (Å)	$\Delta\nu$ (cm^{-1})	$\Delta\nu$ (Å)	$\Delta\nu$ (cm^{-1})
U^{238}	0.000	0.00	0.000	0.00	0.000	0.00
U^{236}	—	—	—	—	0.147	0.82
U^{235}	0.246	1.37	0.248	1.37	0.251	1.39
U^{234}	0.303	1.69	—	—	0.298	1.66
U^{233}	0.386	2.15	0.373	2.07	0.396	2.20

TABLE VII

Isotope Shift Per Unit Mass

wavelength of line in Angstroms	$\Delta\nu$ (U^{238}—U^{235}) in cm^{-1}	$\Delta\nu$ (U^{235}—U^{233}) in cm^{-1}	wavelength of line in Angstroms	$\Delta\nu$ (U^{238}—U^{236}) in cm^{-1}	$\Delta\nu$ (U^{236}—U^{233}) in cm^{-1}
3895.272	0.32	0.23	4088.254	0.37	0.41
3899.097	0.33	0.24	4225.369	0.39	0.36
3906.525	0.28	0.24	4231.676	0.26	0.22
3911.673	0.39	0.34	4234.688	0.21	0.38
3919.719	0.36	0.35	4244.372	0.46	0.38
3221.550	0.24	0.25	4252.426	0.29	0.22
3947.959	0.36	0.31	4261.505	0.36	0.28
3988.644	0.29	0.26	4422.984	0.40	0.32
4023.170	0.40	0.43			

isotope shift since they belong to the electron configurations $5f^4 6d$ and $5f^3 6d^2$, in which penetrating s electrons are absent. The isotope shift for 64 terms of single ionized uranium is listed in Table V. The isotope shift in the terms is established most reliably for the system B in U II.

A comparison of the lowest terms of U I and U II which belong to configurations with s^2 electrons ($5f^3 6d 7s^2$ and $5f^3 7s^2$), show that the isotope shift in the terms of the ionized atom is about 2.5 times larger than in the terms of the neutral atom. The largest shift in the limits of the system B is undergone by the term which belongs to the configuration with penetrating s^2 electrons. In comparison with these, the terms of configurations with a single s electron have about 2.5 times smaller shift. Most of the terms undergo a positive shift. This demonstrates that the term of the lighter isotope lies lower than the term of the heavier one.

It should be noted that, on the basis of these results, it is possible to establish a quantitative

connection between the systems of terms A and B of the ionized atom. Actually, inasmuch as one of the lowest terms of the system A ($5f^4 7s^6 I_{9/2}$) in the presence of a single s electron, undergoes the same isotope shift as does the lowest term of the system B ($5f^3 7s^2 4I_{9/2}$) with two s electrons, then, in accord with the data of Schurmans[7], we can regard the lowest electron configuration to be $5f^4 7s$. Hence, the ground state for U II is $5f^4 7s^6 I_{7/2}$.

It must be noted that the magnitude of the isotope shift of the higher terms of uranium fluctuates widely, reaching comparatively large and comparatively small values. Furthermore, in system B of U II, there are 4 terms with negative shift for which the levels of the lighter isotope are higher. The difference in the shift of the higher term is by itself not unexpected. It is explained by the connection of the terms with different types of electron configurations and by the decrease in the shift with increasing principal quantum number n. However, to the anomalies in the form of very large or very small shift in the neighboring terms, and also their inverse distribution one must add the interaction of the close lying levels, of a similar quantum nature. This interaction reduces to the excitation of terms which have a significant effect on the magnitude of the shift, decreasing or increasing the purely isotope shift. By way of an example of strongly excited levels, we have the higher terms of U I: 156_7, 229_7, 261_6, 262_6 and of U II: $182_{9/2}$, $228_{9/2}$, $233_{9/2}$, $232_{11/2}$, $235_{11/2}$, $269_{11/2}$, $272_{11/2}$. Evidently, all the cases of positive shift that we have discovered in the lines for the configurations $5f^3 6d 7s^2$ and $5f^3 6d^2 7s$ (U I), and also $5f^3 6d 7s$ (U II) are related to transitions from the higher excited levels.

On the basis of the results that we have obtained from the shift of the terms, it is not difficult to see that all the negative shifts in the uranium lines are occasioned either by transitions from the less shifted higher terms to the more shifted lower terms, or by transitions from the higher inverted terms to the lower normal ones. All the positive shifts are obtained for transitions from the higher shifted (among these, the excited) terms to the lower, unshifted or less shifted term. The different cases of transitions are shown in Fig. 1. These permit the explanation of the isotope structure in the uranium spectrum.

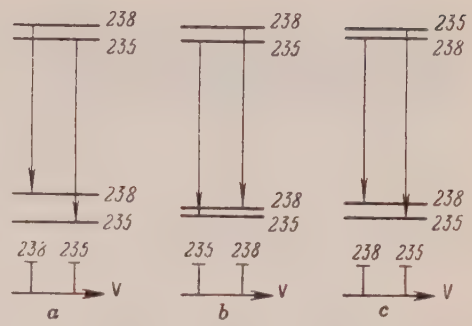

FIG. 1. Different cases of transitions between terms: a and c --- negative shift, b --- positive shift.

Comparison of the isotope shift in the terms of uranium with the shift in the terms of neighboring heavy elements (Hg, Tl, Pb) shows that the isotope shift for uranium is approximately twice as great. Thus, in accordance with our data, the isotope shift in the terms of U II which are related to the electron configurations $5f^3 7s^2$, is equal on the average to 0.42 cm^{-1} per unit atomic mass. The isotope shift in the terms of Hg II and Pb II for the configurations $5d^9 6s^2$ and $6s^2 7p$ are, respectively, 0.26 cm^{-1} and 0.22 cm^{-1} per unit mass[8]. Such a relatively large isotope shift in the terms of uranium cannot be fully explained by the single increase in charge and volume of the charge. Here, evidently, there is, along with the volume effect, an additional effect connected with large deformation of the shape of the nucleus[9]

4. THE ADDITIONAL EVEN-ODD SHIFT

For the detection of the even-odd shift, the spectra of three isotope samples (U^{238}, U^{235} and U^{233}) were photographed on the three prism spectrograph with the autocollimating chamber $f = 130$ cm, and measurements of the interval between the shifted components of the three isotopes were made on a series of lines. For measurement of the intervals a dispersion curve was constructed along the spectrum of iron. The position of each line was measured tenfold on a comparator with accuracy ± 0.004 A (± 0.02 cm^{-1}). One of the spectrograms is reproduced in Fig. 2 with the isotope structure of the line of U II 4244.372 A; the three components U^{238}, U^{235} U^{233} are clearly evident. A microphotometer trace of these lines is shown in Fig. 3.

[7] Ph. Schurmans, Physica 11, 419 (1946); Ph. Schurmans, J. C. van den Bosch and Dijkwol, Physica 13, 117 (1947)

[8] P. Brix and H. Kopfermann (see Landolt-Börnstein, Vol. 1, part 5, pp. 1-59, Berlin, 1952)

[9] L. Wilets, D. L. Hill and W. Ford, Phys. Rev. 66, 1041 (1953); A. R. Bodmer, Proc. Phys. Soc. (London) A67, 622 (1954)

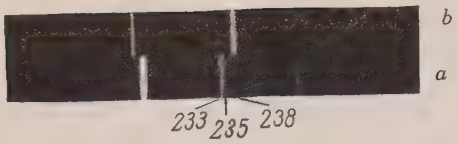

FIG. 2. The U II line 4244.372 A with components of three isotopes: *a*--- spectrum of a mixture of three isotopes of uranium, *b*--- spectrum of natural uranium.

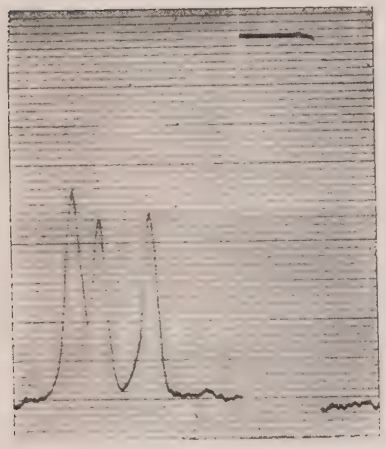

FIG. 3. Microphotograph of the U II line 4244.372 A.

The isotope structure of the line 4244.372 A of the three isotope sample U^{238}, U^{235}, U^{234} was spectrographed for the detection of the component of the isotope U^{234}. The shift between the components U^{235} and U^{234} was measured directly on the spectrum with the aid of a comparator, and then checked on a microphotogram obtained on a recording microphotometer. This shift was equal to 0.030 ±0.002 mm. If we take into consideration the dispersion in this region (1.907 A/mm), then the magnitude of the shift will be equal to 0.057 ±0.004 A or 0.32 ±0.013 cm^{-1}.

The results are given in Table VI along with the data of other investigators[3,4]. Comparing the isotope shift of the even isotopes with the odd, it can be noted that in the uranium spectrum the lines of odd isotopes undergo an additional shift (in comparison with the lines of the even isotopes) in the direction of the components of the isotopes of lower mass number. This additional shift, equal to 0.04 cm^{-1} (per unit mass) in the case of the U II line 4244.372 A shows that the *s* electrons of the odd isotope have a somewhat larger binding energy with the nucleus than the electrons of even isotopes.

The isotopes shifts referred to unit mass, for 17 lines between the isotopes $U^{238} - U^{235}$ and $U^{235} - U^{233}$, are given in Table VII. For the major share of the lines, the magnitude of the isotope shift per unit mass between the even isotope U^{238} and the odd isotope U^{235} is larger than the corresponding magnitude of the shift between the odd isotopes U^{235} and U^{233}. This also points to the presence in the isotope shift in the case of the uranium spectrum of an additional even-odd shift. For five lines of uranium the shifts $\Delta\nu(U^{238}-U^{235})$ and $\Delta\nu(U^{235}-U^{233})$ per unit mass appeared to be approximately equal or, on the other hand, the shift between odd isotopes $U^{235} - U^{233}$ was larger than the shift between the isotopes U^{238}-U^{235} It can be assumed that these deviations from the usually ovserved regularities in the isotope shift for the spectra of the heavy elements are explained by excitations of close lying levels in the uranium atom.

CONCLUSIONS

1. Comparison of the isotope shift of the lines of uranium with the electron configuration of the lower term leads to the following conclusions:

a) The average shift of the lines of the ionized atom is larger than the average shift of the lines of the neutral atom.

b) The lines of the ionized atom, which are related to the lower configurations $5f^3 7s^2$ and $5f^4 7s$ have a negative and, on the average, a small shift; the lines belonging to the higher configurations $5f^3 6d^2$ and $5f^4 6d$ have a smaller and only positive shift; the lines which are related to the configuration $5f^3 6d 7s$ have, as a rule, a negative shift and only four lines have a positive shift.

2. On the basis of the isotope shift, 220 lines of uranium have been associated with U II; the electron configurations of the lower terms have beer found for 153 lines and the shift in the terms have been established for U I and U II.

3. The isotope shift in the terms of U II is generally 2.5 times larger than the shift in the terms of U I. I f we exclude excited levels, then the terms undergo the largest shift which belong to configurations with s^2 electrons. The terms of configurations with a single *s* electron undergo a shift which is about 2.5 times smaller.

4. From the data obtained on the shift of the terms

it follows that all the negative shifts in the lines of uranium are determined either by transitions to a greater shifted lower term or to transitions from higher "inverted" terms to lower normal terms. All the positive shifts are obtained for transitions from higher shifted terms to lower unshifted or slightly shifted terms.

5. With the help of the investigation of isotope structure of the U II line 4244.372 A the presence of an additional shift of the components of even-odd isotopes in the direction of the isotopes of lower mass number has been established.

APPENDIX

Spectral Lines of Uranium with Isotope Shift ∓

wavelength of line in Angstroms	Shift $\Delta\nu$ (U^{238}—U^{235}) in cm^{-1}	Electron configuration and atomic state, according to our results	wavelength of line in Angstroms	Shift $\Delta\nu$ (U^{238}—U^{235}) in cm^{-1}	Electron configuration and atomic state, according to our results
2390.11	—1.64	II, f^3s^2	2698.452	1.73	II, f^3s^2
2390.97	—1.28	II, f^3s^2	2700.96	—1.21	II, f^3s^2
2402.159*	—1.1	II, f^3s^2	2706.95	—1.12	II, f^3s^2
2407.599*	—1.59	II, f^3s^2	2733.772	—1.22	II, f^3s^2
2409.558*	—1.02	II, f^3s^2 or f^4s	2734.964	+1.84	II, f^3d^2
2414.56	—1.48	II, f^3s^2	2735.580	—0.96	II, f^3s^2 or f^4s
2419.573	—1.14	II, f^3s^2	2743.40	—1.17	II, f^3s^2
2424.971	—1.36	II, f^3s^2	2747.15	—1.09	II, f^3s^2
2427.454	—0.94	II	2747.362	—1.27	II, f^3s^2
2432.461*	—0.91	II	2757.554	—1.12	II, f^3s^2
2435.05*	—1.4	II, f^3s^2	2761.18	—1.34	II, f^3s^2
2438.007*	—1.8	II, f^3s^2	2765.40	—1.18	II, f^3s^2
2441.399*	—1.37	II, f^3s^2	2766.875	—1.19	II, f^3s^2
2442.895	—1.70	II, f^3s^2	2770.044	—1.06	II, f^3s^2
2448.931	—1.14	II, f^3s^2	2780.040	—1.10	II, f^3s^2
2450.443	—1.33	II, f^3s^2	2784.919	—0.85	II
2454.367	—1.26	II, f^3s^2	2831.169	+1.95	II, f^3d^2
2460.86	—1.17	II, f^3s^2	2840.940	—1.09	II, f^3s^2
2463.695*	—1.55	II, f^3s^2	2841.17	+1.54	II, f^3d^2
2468.261	—1.62	II, f^3s^2	2845.959	+1.32	II, f^3d^2
2470.645	—1.14	II, f^3s^2	2857.93	—1.04	II, f^3s^2 or f^4s
2477.178	—1.76	II, f^3s^2	2858.903	—0.91	II
2490.928	—1.24	II, f^3s^2	2865.14	—1.14	II, f^3s^2
2498.829	—1.68	II, f^3s^2	2866.986	—1.24	II, f^3s^2
2500.864	—1.24	II, f^3s^2	2873.298	—1.03	II, f^3s^2 or f^4s
2505.289	—1.58	II, f^3s^2	2874.083	—1.23	II, f^3s^2
2514.768	—1.71	II, f^3s^2	2877.569	—0.99	II, f^3s^2 or f^4s
2518.974	—1.31	II, f^3s^2	2878.2	+2.39	II, f^3d^2
2524.311	—2.05	II, f^3s^2	2880.4	—0.96	II, f^3s^2 or f^4s
2528.77	—2.16	II, f^3s^2	2882.345	—1.02	II, f^3s^2 or f^4s
2537.296	—1.58	II, f^3s^2	2882.741	—1.15	II, f^3s^2
2538.430	—1.25	II, f^3s^2	2887.907	—1.06	II, f^3s^2
2541.370	—1.29	II, f^3s^2	2888.380	—1.26	II, f^3s^2
2547.998	—1.88	II, f^3s^2	2888.741	—0.88	II
2548.328	—1.49	II, f^3s^2	2908.275	—0.78	II
2549.296	—1.59	II, f^3s^2	2910.201	—1.72	II, f^3s^2
2562.841	—1.76	II, f^3s^2	2931.891	—0.97	II, f^3s^2 or f^4s
2565.406	—1.33	II, f^3s^2	2935.615	—0.93	II
2567.108	—1.66	II, f^3s^2	2943.405	—1.08	II, f^3s^2
2567.955	—1.96	II, f^3s^2	2944.637	—0.93	II
2569.712	—1.6	II, f^3s^2	2946.772	—0.70	II
2583.480	—2.02	II, f^3s^2	2947.653	+0.92	II, f^3d^2
2584.420	—1.57	II, f^3s^2	2948.936	—0.82	II

∓ The wavelengths of most of the lines are taken from the tables of Harrison. Lines not in these tables were either measured again (single asterisk) or taken from the tables of van der Bosch (double asterisk). Lines marked with a triple asterisk were referred[5] to arc lines while by our research they belong to spark lines. For all these lines the configuration of the lower term has not yet been established[5].

APPENDIX (continued)

wavelength of line in Angstroms	Shift $\Delta\nu$ (U^{238}—U^{235}) in cm^{-1}	Electron configuration and atomic state, according to our results	wavelength of line in Angstroms	Shift $\Delta\nu$ (U^{238}—U^{235}) in cm^{-1}	Electron configuration and atomic state, according to our results
2591.252	—1.46	II, f^3s^2	2951.07	—1.18	II, f^3s^2
2592.572	—1.54	II, f^3s^2	2956.060	—0.76	II
2593.571	—1.41	II, f^3s^2	2957.229	—1.22	II, f^3s^2
2597.689	—1.28	II, f^3s^2	2960.942	—1.28	II, f^3s^2
2624.915	—1.29	II, f^3s^2	2991.248	—0.92	II
2628.504	—1.32	II, f^3s^2	2993.355	—0.86	II
2628.928	—1.3	II, f^3s^2	3002.645	—0.61	II
2635.528	—1.25	II, f^3s^2	3009.42	—0.88	II
2648.789	—1.63	II, f^3s^2	3013.370	—1.05	II, f^3s^2 or f^1s
2652.828	—1.66	II, f^3s^2	3017.351	—1.09	II, f^3s^2
2691.038	—0.68	II	3022.753	—1.00	II, f^3s^2 or f^1s
2692.365	—0.98	II, f^3s^2 or f^1s	3025.406	—1.36	II, f^3s^2
3033.77	—1.23	II, f^3s^2	3733.752	—0.39	
3038.047	—1.08	II, f^3s^2	3761.961	—0.59	II
3049.584	—1.23	II, f^3s^2	3769.535	—0.42	
3050.198	—1.09	II, f^3s^2	3906.525	—0.85	II
3066.286	—1.14	II, f^3s^2	3911.673	—1.17	II, f^3s^2
3081.188	—0.78	II	3919.719	—1.09	II, f^3s^2
3081.666	—1.03	II, f^3s^2 or f^1s	3921.550	—0.71	II
3088.731	—1.16	II, f^3s^2	3930.982	—0.81	II
3090.554	—1.02	II, f^3s^2 or f^1s	3937.068	—0.84	II
3113.637	—0.93	II	3947.959	—1.08	II, f^3s^2
3115.795	—0.58	II	3973.234	+0.51	II, f^3d^2 or f^1d
3120.866	—0.42		3974.975	—1.05	II, f^3s^2 or f^1s
3121.330	—1.02	II, f^3s^2 or f^1s	3977.064	—0.92	II
3133.641	—1.28	II, f^3s^2	3988.644	—0.89	II
3138.513	—1.03	II, f^3s^2 or f^1s	4023.170	—1.2	II, f^3s^2
3153.120	—0.76	II	4026.999	+0.67	II, f^3d^2
3157.446	—0.96	II, f^3s^2 or f^1s	4064.165	—0.96	II, f^3s^2 or f^1s
3173.706	—1.08	II, f^3s^2	4071.108	+0.64	II, f^3d^2
3184.406	—1.26	II, f^3s^2	4086.145	+0.57	II, f^3d^2
3193.226	—0.92	II	4106.416	—0.69	II, f^3s^2
3203.223	—0.58	II	4128.336	—1.03	II, f^3s^2 or f^1s
3221.103	—1.18	II, f^3s^2	4225.369***	—1.16	II, f^3s^2
3224.261	—0.50		4231.676***	—0.78	II
3229.502	—0.78	II	4252.426	—0.89	II
3239.614	—0.97	II, f^3s^2 or f^1s	4253.848	—0.76	II
3244.165	—0.40		4261.505	—1.09	II, f^3s^2
3253.351	—0.55		4263.419	—0.67	II
3267.638	—0.77	II	4270.89	—0.69	II
3279.096	—0.59	II	4289.556	—0.88	II
3280.004	—0.41		4313.147***	—0.65	II
3282.542	—0.81	II	4399.631	—1.00	II, f^3s^2 or f^1s
3284.368	—0.85	II	4405.952	—1.44	II, f^3s^2
3287.448	—0.43		4422.984	—1.21	II, f^3s^2
3288.209	—0.47		4468.895	—1.45	II, f^3s^2
3291.335	—0.62	II	4493.044	—1.08	II, f^3s^2
3322.350*	—0.75	II	4511.158	—1.09	II, f^3s^2
3337.929	—0.53		4513.373	—0.91	II
3367.896	—1.16	II, f^3s^2	4611.436	—1.17	II, f^3s^2
3371.292	—0.61	II	4614.678	—1.00	II, f^3s^2 or f^1s
3380.700	—0.74	II	4637.940	—1.05	II, f^3s^2
3381.95	—0.80	II	4684.644	—0.89	II
3401.213	—0.76	II	4713.943	—0.93	II
3403.546	—0.30		4844.716	—0.69	II
3424.810	—0.69	II	4911.668	—0.65	II
3426.393	—0.79	II	4934.105*	—0.69	II
3454.228	—0.31		5030.738	—1.17	II, f^3s^2
3455.742	—0.52		5200.667	—0.92	II
3458.683	—0.56		5204.316	+0.33	II, f^3d^2 or f^1d
3472.107	—0.80	II	5290.505	—0.34	

APPENDIX (continued)

wavelength of line in Angstroms	Shift $\Delta\nu$ (U^{238}—U^{235}) in cm^{-1}	Electron configuration and atomic state, according to our results	wavelength of line in Angstroms	Shift $\Delta\nu$ (U^{238}—U^{235}) in cm^{-1}	Electron configuration and atomic state, according to our results
3480.359	—0.67	II	5298.81	—1.01	II, f^3s^2 or f^4s
3488.815	—0.53		5310.038	—0.40	
3495.748	—0.29		5313.722	—0.84	II
3513.370	—0.50		5349.917	—0.99	II, f^3s^2 or f^4s
3591.560	—0.84	II	5352.320	+0.54	II, f^3d^2 or f^4d
3630.733	—0.35		5371.835	—0.79	II
3638.200***	—0.47		5409.096	—0.44	
3640.757	—0.81	II	5413.947	—0.81	II
3672.579	—0.42		5455.499	+0.43	II, f^3d^2 or f^4d
3697.93	—0.50		5479.935	+0.36	II, f^3d^2 or f^4d
3701.522	—0.35		5491.236	—0.38	
3704.099	—0.92	II	5513.386	+0.50	II, f^3d^2 or f^4d
3705.983	—0.74	II	5564.187***	—0.37	
3715.470	—0.27		5567.343	+0.70	II, f^3d^2
3733.069	—0.51		5733.262	—1.12	II, f^3s^2
5832.389	—0.51		6298.551***	—0.65	II
5845.272	+0.37	II, f^3d^2 or f^4d	6322.368	—0.71	II
5853.930	+0.42	II, f^3d^2 or f^4d	6347.671*	+0.57	II, f^3d^2
5986.122***	—0.34		6390.943	—0.37	
6051.745	+0.43	II, f^3d^2 or f^4d	6428.396*	+0.50	II, f^3d^2 or f^4d
6067.229	+0.36	II, f^3d^2 or f^4d	6428.870*	+0.35	II, f^3d^2 or f^4d
6132.613	—0.41		6465.005***	—0.44	I
6215.397***	—0.46		6470.550	+0.39	II, f^3d^2 or f^4d
6255.852*	+0.38	II, f^3d^2 or f^4d	6511.136*	+0.39	II, f^3d^2 or f^4d
6258.836*	—0.87	II	6557.581	+0.22	
6291.484	+0.35	II, f^3d^2 or f^4d			

Translated by R. T. Beyer
219

Real Spinors in Curvilinear Coordinates and Pseudo-Riemannian Space

G. A. ZAITSEV
Ivanova, USSR

(Submitted to JETP editor May 21, 1954)
J. Exper. Theoret. Phys. USSR 29, 345-353 (September, 1955)

Properties of matrix-tensors are utilized for the investigation of real spinors in curvilinear coordinates. It is shown that one need not replace ordinary derivatives of spinors by more general derivatives. In connection with this, contrary to the opinion that is widely held, the equations of Dirac and other analogous relativistically invariant differential equations, by nature, do not change their form in transformation into curvilinear coordinates. The problem of generalization to the case of pseudo-Riemannian space is considered. It is significant that one can explain the appearance of a term with the factor $m_0 c / \hbar$ in the equation of Dirac, if we regard the space, not as pseudo-Euclidian, but as pseudo-Riemannian.

1. INTRODUCTION

IN earlier publications[1-3], it is shown that real spinors, applied to the description of the state of individual elementary particles, must be examined as parameters defined by certain primary tensors. Thus, in order for it to be possible to write down appropriate equations in curvilinear coordinates, and in order to discover ways of possible generalization, it is necessary to examine the question of real spinors in curvilinear coordinates and pseudo-Riemannian space. The method by which it is possible to do this is based on the law of transformation of a component tensor under change from one coordinate system to another, provided that the appropriate related matrix is employed. It is necessary to go into some detail on this point, if only for the reason that the results obtained in this case are essentially different from the results of a series of authors who have attempted to generalize the equations of Dirac[4-10].

The question of writing the equations for elementary particles, containing real spinors, in curvilinear coordinates and consequent generalizations in the case of pseudo-Riemannian space should present considerable physical interest. The general theory of relativity showed that mass, energy and momentum appear to be related to the properties of space. Various investigators[11] hold that the general theory of relativity is, above all, a theory of gravitation. It is impossible to agree with such an opinion. The fundamental meaning of the general theory of relativity consists of the following: it permits us to find important properties of energy (and mass) and momentum, and to display the close connection between these and the properties of four-dimensional space-time. We should consider the theory of gravitation and certain confirmations of the general theory of relativity, of an experimental character, as confirmation of the correctness of the geometric treatment of important physical quantities--components of the energy tensor--momentum. As for the theory of elementary particles, it appears characteristic that the question of the more profound nature of mass, energy and momentum remains unclear. Thus, for instance, in the equation for the electron the rest mass m_0 is introduced in a purely formal way, but its real meaning is obscure, etc. Inasmuch as the geometric nature of quantities of such a type is confirmed for macroscopic phenomena, then, in their consideration in the theory of microphenomena, it is necessary to take into account the possibility of their connection with the geometric characteristics of space. This question must be examined carefully in each case, in any re-examination of the basic foundations of the theory of microphenomena.

---

[1] G. A. Zaitsev, J. Exper. Theoret. Phys. USSR **25**, 653 (1953)

[2] G. A. Zaitsev, J. Exper. Theoret. Phys. USSR **25**, 667 (1953)

[3] G. A. Zaitsev, J. Exper. Theoret. Phys. USSR **29**, 166 (1955); Soviet Phys. **2**, 240 (1956)

[4] V. A. Fock, Z. Physik **57**, 261 (1929); Zh. Ros. Fiz.-Khim. Ob., Fiz. Ch. **62**, 133 (1930)

[5] H. Weyl, Z. Physik **56**, 330 (1929)

[6] E. Schrodinger, Sitzungsb. Preus. Akad. **105** (1932)

[7] V. Bargmann, Sitzungsb. Preus. Akad. **346** (1932)

[8] L. Infeld and B. L. van der Waerden, Sitzungsb. Preus. Akad. **380** (1933)

[9] J. A. Schouten, J. Math. Phys. **10**, 239 (1931)

[10] E. Cartan, *Leçons sur la theorie des spineurs*, Paris, Hermann and Cie., 1938

[11] V. A. Fock, J. Exper. Theoret. Phys. USSR **9**, 375 (1939)

2. MATRIX-TENSORS IN CURVILINEAR COORDINATES

Let us examine some properties of matrix-tensors in curvilinear coordinates. Just because of a lack of knowledge of these properties various misunderstandings may arise in the discussion of questions concerning real spinors.

For definiteness, we shall distinguish quantities, expressed in orthogonal coordinates and investigated in previous discussions[2], that will carry on the right hand the index zero, for instance, $g^0_{\alpha\beta}$, x^α_0, R^0_α, J_0, etc. To transform to curvilinear coordinates $x^\alpha = x^\alpha(x^1_0, x^2_0, x^3_0, x^4_0)$ it is necessary to replace R^0_α by R_α according to the formula

$$R_\alpha = \frac{\partial x^\beta_0}{\partial x^\alpha} R^0_\beta, \tag{1}$$

in such a way that $R_\alpha = \partial X / \partial x^\alpha$, where $X = x^\beta_0 R^0_\beta = x^\beta R_\beta$ is a matrix-vector. Further, we have

$$\tfrac{1}{2}(R_\alpha R_\beta + R_\beta R_\alpha) = g_{\alpha\beta} \tag{2}$$

$$= \frac{\partial x^\gamma_0}{\partial x^\alpha}\frac{\partial x^\delta_0}{\partial x^\beta} g^0_{\gamma\delta}, \; R^\gamma = g^{\gamma\alpha}R_\alpha$$

$$\tfrac{1}{2}(R_\beta R^\gamma + R^\gamma R_\beta) = \delta^\gamma_\beta,$$

$$\tfrac{1}{2}(R^\alpha R^\beta + R^\beta R^\alpha) = g^{\alpha\beta}.$$

From Eqs. (1) and (2) we see that matrices R_α and R^α, under transformation from one system of coordinates to another, transform formally as components of a covariant and contravariant vector. As far as matrix-tensors are concerned, in general they do not vary under these transformations, for instance,

$$F = \tfrac{1}{2} F^0_{\alpha\beta} R^\alpha_0 R^\beta_0 = \tfrac{1}{2} F_{\alpha\beta} R^\alpha R^\beta \tag{3}$$

etc.

Consider further in what form the matrix J must be defined in curvilinear coordinates. It is expedient to write the formula for J_0 in the form

$$J_0 = R^1_0 R^2_0 R^3_0 R^4_0 = -\frac{1}{4!}\varepsilon_{\alpha\beta\gamma\delta} R^\alpha_0 R^\beta_0 R^\gamma_0 R^\delta_0. \tag{4}$$

The minus sign is related to the fact that we assume $\epsilon^{1234} = 1$, while $\epsilon_{1234} = -1$. It is then clearly necessary to define J in the general case as

$$J = -\frac{1}{4!}\varepsilon_{\alpha\beta\gamma\delta} R^\alpha R^\beta R^\gamma R^\delta. \tag{5}$$

Further, making use of the fact that

$$g = |g_{\alpha\beta}| = \left|\frac{\partial x^\gamma_0}{\partial x^\alpha}\frac{\partial x^\delta_0}{\partial x^\beta} g^0_{\gamma\delta}\right| = \left|\frac{\partial x^\beta_0}{\partial x^\alpha}\right|^2 g_0, \tag{6}$$

$$g_0 = -1,$$

and likewise that

$$\varepsilon_{\alpha\beta\gamma\delta}\frac{\partial x^\alpha_0}{\partial x^{\alpha'}}\frac{\partial x^\beta_0}{\partial x^{\beta'}}\frac{\partial x^\gamma_0}{\partial x^{\gamma'}}\frac{\partial x^\delta_0}{\partial x^{\delta'}} = \left|\frac{\partial x^\mu_0}{\partial x^{\nu'}}\right| \varepsilon_{\alpha'\beta'\gamma'\delta'}$$

[see reference 12, Eq. (14)] and

$$R^\alpha_0 = \frac{\partial x^\alpha_0}{\partial x^\beta} R^\beta \quad \left(R^\beta = \frac{\partial x^\beta}{\partial x^\gamma_0} R^\gamma_0\right), \tag{7}$$

from Eqs. (4) and (5) we obtain

$$J_0 = \sqrt{-g}\, J, \; J = (1/\sqrt{-g})\, J_0. \tag{8}$$

And, as in reference 2, it is necessary to obtain the formulas for the result of multiplying J by other matrices. For instance,

$$R_\alpha J = -JR_\alpha = -\frac{1}{3!}\varepsilon_{\alpha\beta\gamma\delta} R^\beta R^\gamma R^\delta \tag{9}$$

etc. As a demonstration it suffices to transform to orthogonal coordinates and make use of the corresponding formulas from Veblen[12].

Taking into account the fact that R^α or R_α appear as linear combinations of the four constant matrices R^α_0, and considering that explicit expressions for matrices are defined according to Veblen, we obtain

$$R'_\alpha R_0 = R_0 R_\alpha, \; (R^\alpha)' R_0 = R_0 R^\alpha, \tag{10}$$

$$J' R_0 = R_0 J \qquad (R_0 = R^1_0 R^2_0 R^3_0),$$

whence the matrix R_0 has one and the same value at any point of space.

In conformity with the well-known formulas for differentiation of fundamental vectors in curvilinear coordinates of pseudo-Euclidian space (see reference 13, Sec. 77) we will have

$$dR_\alpha = \Gamma^\gamma_{\alpha\beta} R_\gamma \, dx^\beta, \quad \partial R_\alpha / \partial x^\beta = \Gamma^\gamma_{\alpha\beta} R_\gamma, \tag{11}$$

where

$$\Gamma^\gamma_{\alpha\beta} = \tfrac{1}{2} g^{\gamma\delta}\left[(\partial g_{\delta\alpha}/\partial x^\beta) + (\partial g_{\delta\beta}/\partial x^\alpha) - (\partial g_{\alpha\beta}/\partial x^\delta)\right].$$

---

[12] O. Veblen, *Invariants of Quadratic Differential Forms*, Cambridge Univ. Press, 1927

[13] P. K. Rashevskii, *Riemannian Geometry and Tensor Analysis*, State Publishing House of Technical-Theoretical Literature, 1953

From Eq. (11) it follows also that

$$dR^{\alpha} = -\Gamma^{\alpha}_{\gamma\beta} R^{\gamma} dx^{\beta}, \quad \partial R^{\alpha} / \partial x^{\beta} = -\Gamma^{\alpha}_{\gamma\beta} R^{\gamma}. \quad (12)$$

Equations (11) and (12) permit us to find differentials and derivatives of matrix-tensors, with components expressed in curvilinear coordinates. In this case there occurs an important property of such differentials and derivatives which we consider in the example of a matrix-tensor of the second rank $F = \frac{1}{2} F^{\alpha\beta} R_{\alpha} R_{\beta}$. According to Eq. (11) we have

$$dF = \frac{1}{2} \left(\frac{\partial F^{\alpha\beta}}{\partial x^{\delta}} R_{\alpha} R_{\beta} + F^{\alpha\beta} \Gamma^{\gamma}_{\alpha\delta} R_{\gamma} R_{\beta} + F^{\alpha\beta} R_{\alpha} \Gamma^{\gamma}_{\beta\delta} R_{\gamma} \right) dx^{\delta} = \frac{1}{2} (DF^{\alpha\beta}) R_{\alpha} R_{\beta}, \quad (13)$$

where

$$DF^{\alpha\beta} = [(\partial F^{\alpha\beta} / \partial x^{\gamma}) + \Gamma^{\alpha}_{\delta\gamma} F^{\delta\beta} + \Gamma^{\beta}_{\delta\gamma} F^{\alpha\delta}] dx^{\gamma}. \quad (14)$$

We see that $DF^{\alpha\beta}$ is the absolute differential of $F^{\alpha\beta}$. Hence, it follows that the ordinary derivative of a matrix-tensor is expressed by covariant derivatives of its components according to formulas of the type

$$\partial F / \partial x^{\gamma} = \frac{1}{2} (F^{\alpha\beta})_{\gamma} R_{\alpha} R_{\beta}. \quad (15)$$

In obtaining our formulas, the concrete form of the matrix R_{α} was not defined. It is only important to emphasize that, for convenience in the choice of matrices, R^{0}_{α} must be constant. This corresponds to that fact that, for a given constant vector at any point of space there must correspond the very same matrix, i.e., the law of correspondence between matrices and tensors must be one and the same throughout all space*.

Finally, making use of Eq. (8), we find the expression for the differentiation of the matrix J

$$\frac{\partial J}{\partial x^{\alpha}} = -\frac{1}{2} \frac{\partial \ln g}{\partial x^{\alpha}} J = -\Gamma^{\beta}_{\beta\alpha} J. \quad (16)$$

* If we define the law of correspondence in various forms for different points of space, then a set of completely indeterminate conditions would enter. Thus, speaking no longer of the fact that it is necessary to take this into account in the differentiation of matrices, in ordinary cases we should not obtain either the results of reference 2 or of other works, since the fundamental matrices were considered constant here.

3. REAL SPINORS IN CURVILINEAR COORDINATES

In reference 2, the components of a real spinor ψ were defined as parameters which were characterized by the assignment of an anti-symmetric tensor of the second rank, for which both invariants equal zero. Then ψ is found from

$$F_0^{\alpha\beta} = -\psi' R_0 R_0^{\alpha} R_0^{\beta} \psi. \quad (17)$$

Real spinors can also be defined by starting from the assignment of other primary tensors (see reference 3)*. For definiteness, we restrict ourselves to Eq. (17) and by its help take up the question of real spinors in curvilinear coordinates, although we would obtain other results if we were to examine, for instance, systems of other real spinors defined by certain tensors (as in reference 3). Transforming to curvilinear coordinates, in accordance with Eq. (3) we obtain

$$F^{\alpha\beta} = \frac{\partial x^{\alpha}}{\partial x_0^{\gamma}} \frac{\partial x^{\beta}}{\partial x_0^{\delta}} (-\psi' R_0 R_0^{\gamma} R_0^{\delta} \psi) = -\psi' R_0 R^{\alpha} R^{\beta} \psi. \quad (18)$$

We can also employ this formula for the definition of ψ in generalized coordinates.

In the transformation to curvilinear coordinates, the matrices R_0^{α} in expressions for components of tensors are replaced by R^{α}, but the corresponding real spinors remain invariant. Also, the matrix R_0 does not change**.

* We note that in the literature the term "real spinors" is already used, although their treatment differs from ours. That is, matrices R_0^{α}, $R_0^{\alpha} R_0^{\beta} (\alpha \neq \beta)$, etc. form the idea of hyper-complex systems of numbers (sedenions). The space in which this representation is realized, is often called spinor, but the tensors of this space, according to van der Waerden, are also called spinors (or also wave tensors). If the matrices R_0^{α} have real elements, then spinors with real elements are called real spinors (see reference 14, J. A. Schouten and D. v. Dantzig, Z. Physik 78, 639 (1932), p. 657]. For our definition of real spinors, as parameters characterizing primary tensors, some of the properties coincide with the attributes of spinors, as defined above. But there are differences connected with the fact that a perfectly definite meaning is attached to our real spinors. Thus, components of a real spinor are transformed only in rotations or reflections of all space, but not in changes of the choice of the system of coordinates. In a symmetric transformation the general multiplier i can appear; otherwise, the problem arises as to transformation to a description in curvilinear coordinates, etc.

** Moreover, these statements also apply in the case of double real spinors, defined in correspondence to the assignment of certain tensors.

[14] J. A. Schouten and D. v. Dantzig, Z. Physik 78, 639 (1932)

The problem of differential operations does not present complications, since expressions for the transformation of matrices R^α (or R_α) are known. Making use of Eq. (11), for instance, we obtain the ordinary differential of $F^{\alpha\beta}$:

$$dF^{\alpha\beta} = (\partial F^{\alpha\beta} / \partial x^\gamma)\, dx^\gamma$$

$$= [-(\partial\psi' / \partial x^\gamma) R_0 R^\alpha R^\beta \psi$$

$$- \psi' R_0 R^\alpha R^\beta (\partial\psi / \partial x^\gamma)$$

$$+ \Gamma^\alpha_{\delta\gamma}\psi' R_0 R^\delta R^\beta \psi + \Gamma^\beta_{\delta\gamma}\psi' R_0 R^\alpha R^\delta \psi]\, dx^\gamma,$$

i.e.,

$$DF^{\alpha\beta} = -(d\psi') R_0 R^\alpha R^\beta \psi - \psi' R_0 R^\alpha R^\beta d\psi, \quad (19)$$

where the quantity on the left is the absolute differential of $F^{\alpha\beta}$. If we introduce the concept of "covariant derivative" of real spinors $(\psi)_\gamma$ in conformity with the formula

$$(F^{\alpha\beta})_\gamma = -(\psi)'_\gamma R_0 R^\alpha R^\beta \psi - \psi' R_0 R^\alpha R^\beta (\psi)_\gamma, \quad (20)$$

where $(F^{\alpha\beta})_\gamma$ are ordinary covariant derivatives of tensors, then we get from Eq. (19)

$$(\psi)_\gamma = \partial\psi / \partial x^\gamma, \quad (21)$$

so that "covariant derivatives" of real spinors coincide with ordinary derivatives. Hence, there follows, in particular, an important consequence, that $R^\alpha_0 (\partial\psi / \partial x^\alpha_0)$, for transformation into curvilinear coordinates, is replaced by $R^\alpha(\partial\psi/\partial x^\alpha)$, i.e., in spite of long-standing notions, it has in essence the same form (only now the matrices R^α are no longer constant). Thus, for instance, Maxwell's equations for the radiation field with a fixed direction of propagation, written in the form of reference 15, have, in curvilinear coordinates, the form of

$$R^\alpha \frac{\partial\psi}{\partial x^\alpha} = 0 \left(\psi' R_0 \frac{\partial\psi}{\partial x^\alpha} = 0, \quad \psi' R_0^4 \frac{\partial\psi}{\partial x^\alpha} = 0\right). \quad (22)$$

From Eq. (22) one may conversely obtain the corresponding Maxwell equations in the customary form but in curvilinear coordinates. Thus, multiplying Eq. (20) on the left by $\psi' R_0 R^\beta$, and the transposed equation on the right by $R_0 R^\beta \psi$, consolidating the resulting expressions, and making use of Eqs. (2), (10) and (20), there results

$$(F^{\beta\alpha})_\alpha = 0$$

etc. Likewise it would have been possible to write the equations of Dirac (expressed as equations for two real spinors, see reference 16) in curvilinear coordinates, etc.

Note that the equation of Dirac, written in the form indicated above, will have a different appearance from the Dirac equations in curvilinear coordinates, obtained by the method of other authors, inasmuch as more general expressions are used in them in place of the derivatives $\partial\psi/\partial x^\alpha$. Therefore, we shall consider this problem in some detail.

It is a characteristic feature of researches concerned with the equations of Dirac in curvilinear coordinates and pseudo-Riemannian space that (if one looks at spinors from our point of view) there are various ideas mixed together: the transformation from one system of coordinates to another and the transformation from one isomorphic correspondence between matrices and tensors to others. As an example of this kind, consider the work of Fock [4], since the views set forth there have received wide distribution and have had significant influence on other work*. Fock introduces at every point of four-dimensional space an orthogonal reference system and refers the components of the four-dimensional vector current to this reference system. Components of vectors in such a local system of coordinates are expressed by components of spinors and constant matrices, the same for all reference systems. Making use of our notation, this means that the matrices R^0_α, corresponding to the basic vectors of reference system, are considered constant at every point of space. But since the vasic vectors of the reference system, under transformation from one point to another, are changed, then in the use of curvilinear coordinates in pseudo-euclidean space, the matrices R^0_α are no longer the same at any point, and are linked to one another by an appropriate transformation. In other words, different matrices correspond at each point to the same constant vector of pseudo-

---

[15] G. A. Zaitsev, J. Exper. Theoret. Phys. USSR 25, 675 (1953)

* Detailed accounts of these views are contained in reference 17.

[16] G. A. Zaitsev, J. Exper. Theoret. Phys. USSR 29, 176 (1955); Soviet Phys. 2, 140 (1956)

[17] A. P. Sokolov and D. D. Ivanenko, *Quantum field theory*, State Publishing House of Technical-Theoretical Literature, 1952

euclidian space, whence the law of correspondence that depends on what form is chosen for the local reference system. For just this reason, our way of writing the equation of Dirac in curvilinear coordinates differs from the writings of Fock.

Similar considerations apply also to other researches to which we have referred.

4. TRANSFORMATION IN PSEUDO-RIEMANNIAN SPACE

Separate formulas, written for curvilinear coordinates, are correct in the more general case of pseudo-Riemannian space. Here also for every point of space it is necessary to introduce matrices R^α or R_α, with the help of which the expressions for matrix-tensors are written out. Eqs. (1) to (9) apply here as before for the corresponding matrices. But it is necessary to keep in mind that, insofar as the space is no longer pseudo-euclidian, the matrices R_0^α, R_0, J_0 will now characterize some locally-Galilean systems of coordinates, whereupon they can no longer be considered constant for all space (if only not to confuse a transformation from one system of coordinates to another, and the different character of an isomorphic correspondence between matrices and tensors). So far as the operation of differentiation is concerned, the situation is considerably more complicated. If we write

$$\partial' R^\alpha / \partial x^\beta_{,} = -\Gamma^\alpha_{\gamma\beta} R^\gamma, \tag{23}$$

then the right side will not be an absolute derivative of the matrices R^α) (A prime is written to denote this case.) In fact, from Eq. (23) we obtain

$$\frac{\partial'}{\partial x^\gamma}\left(\frac{\partial' R^\alpha}{\partial x^\beta}\right) - \frac{\partial'}{\partial x^\beta}\left(\frac{\partial' R^\alpha}{\partial x^\gamma}\right) = B^\alpha_{\delta\gamma\beta} R^\delta, \tag{24}$$

where $B^\alpha_{\delta\gamma\beta} = \partial\Gamma^\alpha_{\delta\gamma}/\partial x^\beta - \partial\Gamma^\alpha_{\delta\beta}/\partial x^\gamma + \Gamma^\epsilon_{\delta\gamma}\Gamma^\alpha_{\epsilon\beta} - \Gamma^\epsilon_{\delta\beta}\Gamma^\alpha_{\epsilon\gamma}$ are components of the curvature tensor*. Therefore, $\partial' R^\alpha / \partial x^\beta$ can be derived only if $B^\alpha_{\delta\gamma\beta} = 0$, i.e., if the space is pseudo-euclidean. For absolute derivatives we must write the expression

$$\partial R^\alpha / \partial x^\beta = -\Gamma^\alpha_{\gamma\beta} R^\gamma + \overline{Y}^\alpha_\beta, \tag{25}$$

where matrices Y^α_β characterize the departure of the space from pseudo-euclidian and for the latter must revert to zero.

* Various authors denote components of the full curvature tensor differently. Our notation corresponds to that of reference 12.

Real spinors in pseudo-Riemannian space must be defined as in curvilinear coordinates, i.e., from relations of the type $F^{\alpha\beta} = -\psi' R_0 R^\alpha R^\beta \psi$, etc., but the matrix R_0 will now, generally speaking, be different for different points, and the question of differentiation and of differential equations, containing real spinors, becomes considerably complicated. Therefore, we limit ourselves to the selection of a special case, when the matrices R^α at any point of space are linear combinations of the five *constant* matrices $R^\alpha_{(0)}$ and $J_{(0)}$. (We assume $R^\alpha_{(0)}$ and $J_{(0)}$ are such that Eq. (10) is satisfied.) In this case the matrix R_0 will also be constant. The meaning of the limitation that we have placed on the matrices R^α is that pseudo-Riemannian space is considered as a certain surface in five-dimensional pseudo-Euclidean space, for which there are constant basic matrices --either $R^\alpha_{(0)}$ or $J_{(0)}$ (i.e., it will be a space of the first class in space, see reference 18). In connection with this, the derivatives of R^α will be linear combinations of the matrices $R^\alpha_{(0)}$ and $J_{(0)}$ or R^β and J,

$$\partial R^\alpha / \partial x^\beta = -\Gamma^\alpha_{\gamma\beta} R^\gamma + \pi^\alpha_\beta J, \tag{26}$$

i.e., where the nonvanishing character of π^α_β is connected with the non-Euclidean nature of the space.

It is not difficult to show that if Eq. (26) is satisfied,

$$[(R^\alpha + dR^\alpha)(R^\beta + dR^\beta) + (R^\beta + dR^\beta)(R^\alpha + dR^\alpha)] - [R^\alpha R^\beta + R^\beta R^\alpha] = 2\frac{\partial g^{\alpha\beta}}{\partial x^\gamma} dx^\gamma, \quad dR^\alpha = \frac{\partial R^\alpha}{\partial x^\gamma} dx^\gamma, \tag{27}$$

The deviation of the space from pseudo-Euclidean will be shown by the nature of the differential equations that contain real spinors. It is necessary to examine how equations for primary tensors, which are written, however, in original form, and properties of space will influence the nature of transformation from equations for tensors into equations for spinors.

Let us consider the case where the primary tensors are vectors and pseudovectors with components $P^\alpha_{(+)}$ and n^α and the invariants and pseudo-invariants Ω_1 and Ω_2, connected with the cor-

[18] L. P. Eisenhart, *Riemannian Geometry*, Princeton Univ. Press, 1926

responding relations (see references 3 and 16). n^α is expressed by the real spinors ψ_1 and ψ_2 in the form

$$n^\alpha = \sqrt{-g}\,\psi'_{(2)} R_0 R^\alpha \psi_{(1)}. \qquad (28)^*$$

For abbreviation we will make use of the components $Q^\alpha = (1/\sqrt{-g})\, n^\alpha$ in place of the components vector of the pseudovector.

Suppose that we have the relativistically invariant differential equation

$$(Q^\alpha)_\alpha = 0. \qquad (29)$$

If the space be pseudo-Euclidean, then Eq. (29) would be obtained, in particular, from the following relativistically invariant equations for ψ_1 and ψ_2:

$$R^\alpha \frac{\partial}{\partial x^\alpha}\psi_{(1)} = 0; \qquad (30)$$

$$R^\alpha \frac{\partial}{\partial x^\alpha}\psi_{(2)} = 0. \qquad (31)$$

For pseudo-Riemannian space Eq. (29) no longer follows from Eqs. (30) and (31).

Supposing that Eq. (26) holds, we consider the problem of the form to which it is necessary to generalize Eqs. (30) and (31), so that as before there will be equivalence with Eq. (29). From Eqs. (26) and (28) results

$$(Q^\alpha)_\alpha = \frac{\partial Q^\alpha}{\partial x^\alpha} + \Gamma^\alpha_{\gamma\alpha} Q^\gamma \qquad (32)$$

$$= \frac{\partial \psi'_{(2)}}{\partial x^\alpha} R_0 R^\alpha \psi_{(1)} + \psi'_{(2)} R_0 R^\alpha \frac{\partial \psi_{(1)}}{\partial x^\alpha} + \pi^\alpha_\alpha \psi'_{(2)} R_0 J \psi_{(1)}.$$

Consequently, in order that Eq. (29) hold for the operator it is necessary to add $\frac{1}{2}\pi^\alpha_\alpha J$ to the operator $R^\alpha(\partial/\partial x^\alpha)$ so that Eqs. (30) and (31) become

$$R^\alpha \frac{\partial}{\partial x^\alpha}\psi_{(1)} + {}^1/_2 \pi^\alpha_\alpha J \psi_{(1)} = 0; \qquad (33)$$

$$R^\alpha \frac{\partial}{\partial x^\alpha}\psi_{(2)} + {}^1/_2 \pi^\alpha_\alpha J \psi_{(2)} = 0. \qquad (34)$$

In fact, to obtain Eq. (29) it is necessary to multiply Eq. (33) on the left by $\psi'_2 R_0$, but the equation transformed into Eq. (34), on the right by $R_0 \psi_{(1)}$, and to add the result.

Equations (33) and (34) will be the equations of Dirac without an external field (see reference 16) if we merely set

$$-{}^1/_2 \pi^\alpha_\alpha = m_0 c / \hbar. \qquad (35)$$

Thus, it seems that the appearance of a term proportional to the rest mass in the equations for elementary particles can be connected with the curvature of four-dimensional space. This result presents great interest of a fundamental nature, since it shows how a term characterizing the mass of a particle can appear in the transition from tensor equations in non-Euclidean space into equations containing spinors. Already at that time, possibly, it has only approximate significance, and in the future theory of the internal structure of elementary particles, one must expect essential changes and refinements.

In conclusion, we shall derive a formula relating π^α_β with components of the curvature tensor. From Eqs. (26) and (5), taking account of Eq. (9), we obtain, after some computation,

$$\frac{\partial J}{\partial x^\beta} = -{}^1/_2 \frac{\partial \ln g}{\partial x^\beta} J - \frac{\pi_{\alpha\beta}}{g} R^\alpha \qquad (36)$$

$$(\pi_{\alpha\beta} = g_{\alpha\gamma}\pi^\gamma_{,\beta}).$$

Taking into account that $\partial^2 R^\alpha / \partial x^\gamma \partial x^\beta = \partial^2 R^\alpha / \partial x^\beta \partial x^\gamma$, we obtain the formula relating matrices Y^α_β [see Eq. (25)] with components of the curvature tensor

$$\frac{\partial Y^\alpha_\gamma}{\partial x^\beta} - \frac{\partial Y^\alpha_\beta}{\partial x^\gamma} + \Gamma^\alpha_{\delta\beta} Y^\delta_\gamma - \Gamma^\alpha_{\delta\gamma} Y^\delta_\beta = B^\alpha_{\delta\gamma\beta} R^\delta. \qquad (37)$$

Hence, using Eqs. (26) and (36) for examination of our case, we obtain the following equations which π^α_β must obey:

$$\frac{\partial \pi^\alpha_\gamma}{\partial x^\beta} + \Gamma^\alpha_{\delta\beta}\pi^\delta_\gamma - \Gamma^\delta_{\gamma\beta}\pi^\alpha_\delta - {}^1/_2 \frac{\partial \ln g}{\partial x^\beta}\pi^\alpha_\gamma \qquad (38)$$

$$= \frac{\partial \pi^\alpha_\beta}{\partial x^\gamma} + \Gamma^\alpha_{\delta\gamma}\pi^\delta_\beta - \Gamma^\delta_{\gamma\beta}\pi^\alpha_\delta - {}^1/_2 \frac{\partial \ln g}{\partial x^\gamma}\pi^\alpha_\beta;$$

$$\frac{1}{g}(\pi^\alpha_\beta \pi_{\delta\gamma} - \pi^\alpha_\gamma \pi_{\delta\beta}) = B^\alpha_{\delta\gamma\beta} \qquad (39)$$

This is found to be in complete agreement with the theory of space of the first class [see reference 18, p. 238, Eqs. (59.3) and (59.4)].

We see that the π^α_β are not related to the components of the curvature tensor in exactly the same way as the components of tensors of energy-momentum in the corresponding form in the general

* The presence on the right side of Eq. (28) of factor $\sqrt{-g}$, which is equal to unity in the particular case of orthonormal basic vectors, is related to certain requirements for the quantities $\psi_{(1)}$, $\psi_{(2)}$. We examine just this case, therefore, which here is especially easy to show, in what form terms which conserve the rest mass appear in the equations for $\psi_{(1)}$, $\psi_{(2)}$. Although the situation is actually more complicated, the principle of the problem remains the same.

theory of relativity. But, it is necessary to keep in mind that for elementary particles the concrete character of the connection between the mass and the properties of space does not necessarily have to correspond to the particular requirements of the theory, which are confirmed only for macrophenomena.

Translated by D. E. Spencer
202

SOVIET PHYSICS JETP VOLUME 2, NUMBER 2 MARCH, 1956

Phenomena in the Vicinity of Detonation Formation in a Gas

K. I. SHCHELKIN
Institute of Chemical Physics, Academy of Sciences, USSR
(Submitted to JETP editor May 10, 1954)
J. Exper. Theoret. Phys. USSR 29, 221-226 (August, 1955)

Phenomena in the vicinity of a detonation are discussed. It is shown in particular that in accordance with a previously developed theory[1,2] explaining how slow burning combustion turns into a detonation, a detonation can occur in gas both at some distance in front of the slow combustion as well as in its immediate vicinity.

INTRODUCTION

THE mechanism whereby slow combustion of a gas in a tube turns into a detonation was discussed earlier[1,2] and can be summarized briefly as follows: The expansion of the slowly-burning mixture causes motion and turbulence of the unburned gases. The turbulence increases the velocity of propagation of the combustion relative to the gas, and this in turn causes an increase in the velocity of the gas--the combustion accelerates progressively.

The accelerating combustion, acting like a piston moving in a gas-filled tube, produces an adiabatic-compression wave. The slope of the adiabatic-compression wave front increases progressively until a state and velocity discontinuity occurs in the gas. At the instant that the discontinuity occurs, its surface separates the undisturbed and uncompressed adiabatically compressed gas, the velocity of which is readily computed from the velocity of sound in the gas on both sides of the discontinuity.

From the theory of random discontinuities[3] it is known that such a discontinuity of state and velocity cannot propagate in the gas; it breaks into a shock wave, which travels through the unperturbed gas, and a rarefaction wave, which propagates in the opposite direction, through the adiabatically-compressed gas. At the place of shock-wave formation the gas experiences a density and temperature discontinuity, the surface of which is stationary relative to the gas. The gas temperature in the shock wave rises sharply because of the non-adiabatic shock compression. This leads to a detonative ignition of the uncombusted gas--to the formation of a detonation.

Once certain assumptions are made, the entire process lends itself readily to analysis; this was done with an accuracy to within constant multipliers in the reference quoted[2]. The fact that in most cases the explosion actually occurs not in a single plane but over a certain length of the tube does not affect the argument substantially. It produces no change whatever in the qualitative picture of the detonation phenomenon and reduces only insignificantly the accuracy of the computation of the distance between the ignition point and the location where the detonation occurs.

In principle it is possible also to suggest another mechanism for the pre-detonation acceleration of the combustion in the tube, proposed by L. D. Landau, and based on the instability of the plane combustion front and the self-turbulence of the gas in the region of the flame. In tubes, however, it is the turbulence produced by the walls that always precedes the self-turbulence and determines the acceleration of the flame. To observe the self-turbulence it becomes necessary to employ special measures to prevent formation of turbulence due to the walls[4].

[1] K. I. Shchelkin, Dokl. Akad. Nauk SSSR 23, 636 (1939)

[2] K. I. Shchelkin, J. Exper. Theoret. Phys. USSR 24, 589 (1953)

[3] Ia. B. Zel'dovich and K. I. Shchelkin, J. Exper. Theoret. Phys. USSR 10, 569 (1940)

[4] Kh. A. Rakipova, Ia. K. Troshin and K. I. Shchelkin, Zh. Tekhn. Fiz. 17, 1397 (1947)

The above brief description of the elementary theory of the transition from slow combustion into detonation does not lead to any essential or fundamental objections. There exist, however, contradictions between theory and experiment, and these call for a special analysis and for more rigor in the elementary theory developed earlier. This contradiction is due to the following: From the scheme described above it follows that the detonation should always occur at a certain distance forward of the accelerating-flame front. This follows directly from the mechanism by which the discontinuity forms forward of the front of the accelerating combustion. In fact, however, the detonation occurs almost always directly at the accelerating-flame front. Regardless of the theory, a detonation that forms forward of the accelerating combustion front is observed only in rare cases; for example, in mixtures of carbon monoxide and oxygen.

This article is devoted principally to an analysis of the above contradiction. Clarifying this contradiction requires analysis of the phenomena occurring near the site of the detonation, which is equivalent to analysis of several cases where a slow combustion changes into a detonation.

1. OCCURRENCE OF DETONATION AT A CERTAIN DISTANCE FORWARD OF A SLOW-COMBUSTION FRONT

The analysis is best carried out by using a numerical example. Let the acceleration of a slow combustion in a diatomic gas, which is initially at atmospheric pressure, result in an adiabatic-compression wave of finite pressure, say 10 atmospheres (Fig. 1 *a*), and let an increase in the slope of the wave turn its front into a discontinuity at section *A* of the tube.

If we represent the adiabatic wave as a sum of low-intensity compression waves rapidly following each other (Fig. 1 *b*), then the discontinuity will occur in Section *A* of the tube at the instant when all the low-intensity waves catch up with each other and combine at section *A* (Fig. 1 *c*). At the instant the discontinuity is formed, the gas is adiabatically compressed to ten atmospheres on the left of the explosion plane and is at the initial atmospheric pressure on the right of the explosion plane. The values of the densities, temperatures and velocities of the gas in both sides of the explosion are given in Fig. 1 *c*.

Figure 2 shows the picture of the phenomenon some time Δt after the discontinuity has formed. The discontinuity plane A_0 has moved during the time Δt at a distance $\Delta t \times 2.05\ c_0$ to position *A*, where c_0 is the velocity of sound in the uncompressed gas. The discontinuity is broken up into a shock wave, the front *C* of which, with a pressure of 9.1 atmospheres, has moved through the tube a distance $\Delta t \times 2.82\ c_0$, and into a rarefaction wave, the front of which is located at the time Δt in plane *B*. At the same instant that the adiabatic

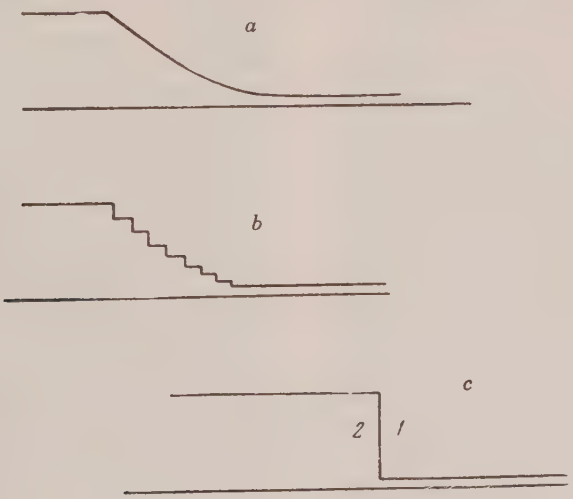

FIG. 1. Formation of state and velocity discontinuity in gas.
a--adiabatic compression wave at $p = 10$ atmospheres;
b--the same wave, represented as a sum of weak compression waves;
c--adiabatic discontinuity of state: *1*--$p_1 = 1$ atm, $w_0 = 0$, ρ_0, T_0, c_0: *2*-- $p = 10$ atm, $w = 1.95\ c_0$, $\rho = 5.16\rho_0$, $T = 1.93\ T_0$.

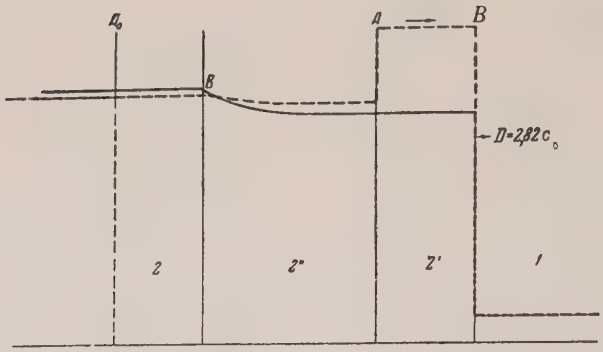

FIG. 2. Separation of discontinuity into a shock wave and rarefaction wave. Solid line = pressure; dashed line = temperature. *1*--unperturbed gas at p_0, T_0, c_0 and ρ_0; *2'*--state of gas in shock wave moving at a velocity D: $p = 9.1\ p_0$, $w = 2.05\ c_0$, $\rho = 3.8\ \rho_0$, $T = 2.46\ T_0$; *2''*--state of gas in rarefaction wave: $p = 9.1\ p_0$, $w = 2.05\ c_0$, $\rho = 4.84\ \rho_0$, $T = 1.88\ T_0$: *2*--adiabatic discontinuity of state: $p = 10\ p_0$, $w = 1.95\ c_0$, $\rho = 5.16\ \rho_0$, $T = 1.93\ T_0$.

discontinuity breaks up and the shock wave is formed, a gas density and temperature discontinuity is formed in plane A_0; this discontinuity is at rest relative to the gas and moves with the gas and at the same velocity as the gas behind the front of the shock wave. At the instant Δt the plane of this discontinuity is located in position A. The values of the velocity, temperature and density in various locations in the tube are given in Fig. 2.

As already indicated the gas can ignite and detonate at the site of the shock wave formation. The ignition can occur either practically instantaneously, or after the lapse of a certain ignition delay time τ_0. In Fig. 3, point A represents the site of the discontinuity formation, line A_0B the motion of the shock-wave front, and line A_0A the motion of the temperature and density discontinuity. Line A_0C of the same figure represents the motion of the front of the flame.

Point D in the figure shows the detonation ignition of the gas, occurring at a time t after the formation of the discontinuity at point A_0 and at a distance l forward of the slow-combustion front. At point D, in addition to the detonation wave DO which moves forward, there also occurs a compression wave, partly caused by the detonation wave DR, which moved backwards, opposite to the slow flame. It is evident that only by coincidence will the delay time τ be such that the detonation occurs at the instant the front of the flame arrives at the discontinuity plane A.

It is interesting to note that after forming at point D (Figs. 3 and 4), the detonation moves through the compressed and moving gas to the intersection with line A_0B. In this section the speed of the detonation relative to the tube walls is often experimentally observed to be considerably greater than after the detonation moves into the gas at rest beyond the line AC.

2. FORMATION OF DETONATION NEAR THE SLOW-COMBUSTION FRONT

From the preceding Section it follows that the detonation can occur at a distance forward of the flame before the slow combustion arrives at the discontinuity plane (at line A_0B, Fig. 3). However, it may happen that no detonation ignition occurs in the shock wave. What will occur if the temperature in the shock wave is not high enough to cause detonation ignition of the gas?

In this case the flame, in the final analysis, will catch up with the plane of the temperature and density discontinuity A (Fig. 2), and after passing through the temperature discontinuity plane, will move from a colder medium to one heated to a considerably higher temperature. In Fig. 4 the intersection between the flame and the discontinuity plane is shown by the intersection between the line $B'D$ of the front of the flame and line A_0A. In the example given above, the flame passes from a medium with an approximate temperature of 290° C into a medium with an approximate temperature of 450° C.

It is natural to expect the speed of propagation of the flame at such a transition at point D to increase sharply (with a jump) so that a second shock wave DM forms in the adiabatically-compressed and heated gas, propagates through the

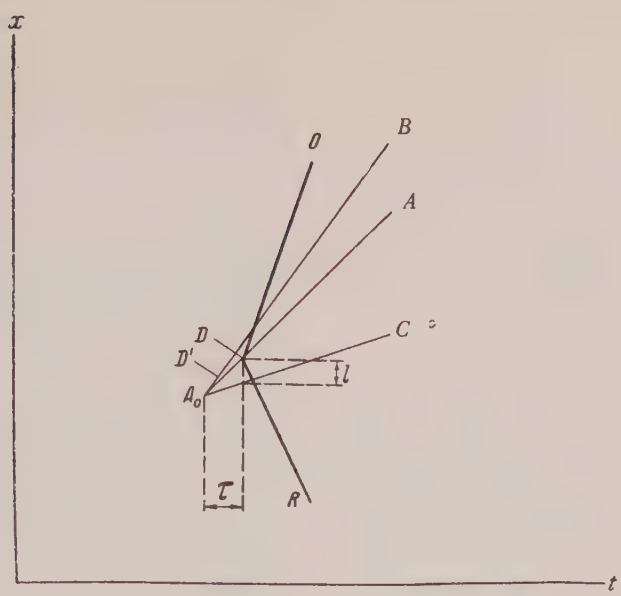

FIG. 3. Appearance of detonation forward of the flame front.

gas compressed by shock wave A_0B (Fig. 4), and heats the gas further. This additional acceleration of the combustion and the resulting additional increase in temperature of the uncombusted gas can lead to a detonation ignition of the gas at point D or in its vicinity on line DM, and to the formation of a detonation wave DO (Fig. 4). If even this temperature rise in the second wave DM is insufficient for detonation ignition of the gas, the detonation will not occur at all under the given conditions.

The description above explains quite clearly the origin of the second shock wave, which plays a substantial role in the formation of the detonation in the case when the detonation does not originate in the first wave A_0B. Thus, a second wave is possible only in the presence of the fundamental shock wave (A_0B in Fig. 4). In other words, its formation is possible only if the speed of propagation of the undetonated flame suddenly increases at point D, i.e., if the velocity of the pre-detonation combustion turbulence increases with the temperature of the gas. According to the elementary theory of turbulent combustion, the speed of a flame in a strongly turbulent stream is independent of the normal speed of the flame with an accuracy to within a slowly-varying function and is consequently independent of the temperature. However, the strong (quadratic) dependence of the normal speed on the temperature ($\sim T^2$) causes a considerable acceleration of the flame both here and also when the speed of the turbulent combustion does not depend strongly on the normal speed. Therefore, in the case under consideration the slowly variable function in the relationship between the turbulent and normal speeds of the flame cannot be neglected, nor can the possibility of such an acceleration be denied thereby. For quantitative evaluation of the intensity of the second shock wave, occurring at point D of Fig. 4, it would be very important to know the form of this slowly-varying function.

3. PHENOMENON OF "DRAWING" THE FLAME TO THE SITE OF THE DETONATION

It is important to note that before the appearance of the detonation at point D of Fig. 4, the flame experiences an acceleration relative to the tube walls at section B'-D. This acceleration is due to the flame falling into the rarefaction wave, the front of which moves against the flame, while the gas velocity is directed along the motion of the flame. Because of this, the flame is accelerated in the rarefaction wave. In the actual example (Fig. 2) the speed of gas in the rarefaction wave from the plane B to the plane A increases by several dozens of meters per second (by approximately $0.1\ c_0$).

It is possible that in this case, gas turbulence causes the flame not merely to travel faster, but also to overtake the gas itself. In view of the short time involved, the turbulence may not propagate from the walls over the entire section of the tube, and the flame may move more rapidly along the walls of the tube, in the zone where the turbulence is higher.

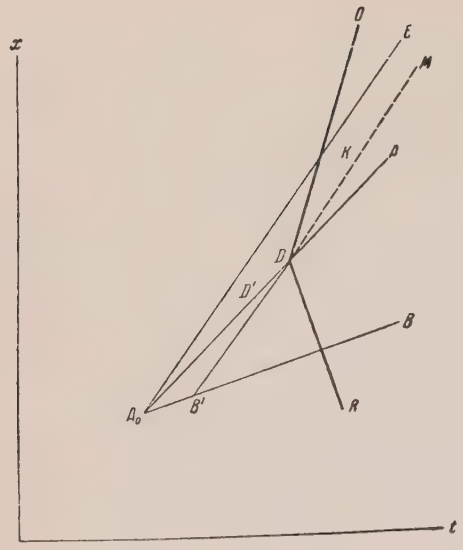

FIG. 4. Formation of second shock wave and appearance of detonation in the immediate vicinity of the flame front.

In view of the above, the acceleration of the flame in the rarefaction wave may contribute somewhat to the formation of the detonation. In certain cases the detonation may occur even before the front of the flame arrives at the temperature discontinuity (to line A_0B of Fig. 4) for example, in point B', at a certain small distance forward of the front of the flame.

4. FORMATION OF DETONATION IN THE PRESENCE OF UNEVENNESS OR ROUGHNESS

The entire detonation picture changes substantially in a tube that is uneven or rough inside. Roughness in the initial portion of the tube contributes strongly to the acceleration of the slow combustion, and to the formation of the shock wave A_0B. This problem was discussed earlier[1,2].

In addition to affecting the acceleration of the slow flame, roughness (as was already indicated earlier) can contribute to the transformation of a slow combustion into a detonation, because the gas temperature rises sharply wherever the shock wave front strikes a projection (a roughness). The temperature rise in a shock wave reflected from an obstacle depends on the intensity of the wave and can easily be computed.

In the case shown in Fig. 3, the detonation may be caused by local overheating of the gas when the shock wave is reflected from a rough or uneven spot, for example, at point D'. The delay period of the detonation combustion in this case cannot be long, since the gas will not stay very long at the location where the shock wave is reflected by the rough spot, but it will be swept away by the stream and will be diluted by gas that is less heated. The delay period is therefore not shown in Fig. 3.

In the case shown in Fig. 4, the second shock wave DK occurs at the point D as a result of the transformation of the flame into heated gas. If this wave is incapable of initiating the detonation at point D, the motion of its front, as mentioned above, can be represented by line DM of Fig. 4. The reflection of the second wave from the rough spot or obstacle, say at point K, can also cause detonation provided, naturally, that it has not occurred earlier.

In conclusion, it must be noted that when the shock wave is formed not in a single plane (point A_0 of Figs. 3 and 4), but over a certain length of the tube, as is more likely, the qualitative picture of all these phenomena in the vicinity of the detonation does not change substantially.

It must also be pointed out that the arguments given in this work supplement rather than change those conclusions made earlier[1,2] and mentioned briefly in the beginning of this article concerning the mechanism by which slow combustion transforms into detonation.

Translated by J. G. Adashko
176

Delayed Neutrons Which Accompany Photofission of Uranium and Thorium

L. E. LAZAREVA, B. S. RATNER AND I. V. SHTRANIKH
P. N. Lebedev Institute of Physics, Academy of Sciences, USSR
(Submitted to JETP editor May 31, 1955)
J. Exper. Theoret. Phys. USSR **29**, 274-279 (September, 1955)

Decay curves and yield were obtained from delayed neutron radiation accompanying the photofission of uranium and thorium. The delayed neutrons represent 0.41 ± 0.02% and 0.18 ± 0.01%, respectively, of all the neutrons emitted in photofission of uranium and thorium.

AT the present time, there are many papers available devoted to the investigation of delayed neutrons which accompany the fission of U^{236}, U^{239} and Th^{233} isotopes, produced during irradiation of uranium and thorium with neutrons. There is in the literature no study of delayed neutrons in photofission of uranium and thorium, where fission of the primary isotopes of U^{235}, U^{238} and Th^{232} takes place. In 1950 such a work was performed in the laboratory of V. I. Veksler on samples of natural uranium and thorium.

Photofission cross sections of U^{235} and U^{238} differ from each other by a factor of 1.5-2[1,2]. Therefore, the delayed neutron radiation obtained by irradiation, with x-rays, of uranium sample composed of the natural isotopic mixture pertains almost entirely to the U^{238} isotope, the content of which is 99.3% in natural uranium.

Measurements were performed with the synchrotron at the x-ray energy $E_{max} = 18.5$ mev. The mean excitation energy of fission nuclei,

$$E = \int_{E_{thr}}^{E_{max}} E\sigma_f(E) f(E)\, dE \Big/ \int_{E_{thr}}^{E_{max}} \sigma_f(E) f(E)\, dE$$

[E is the energy of photons; $f(E)$ is the number of photons having energy $E + dE$; σ_f is the photofission cross section; E_{thr} is the energy corresponding to the photofission threshold], calculated in accordance with available curves obtained by I. V. Chuvilo, which represent photofission cross sections as a function of photon energy, is equal to 12-12.5 mev, for uranium and thorium, at $E_{max} = 18.5$ mev.

The irradiated samples of uranium and thorium, in the form of discs 4 cm in diameter, were placed in the center of a large paraffin block. The γ-rays striking the samples passed through a round canal 5 cm in diameter made in paraffin. The delayed and the "instantaneous" neutrons ejected at the instant of photosplitting, were registered in the ionization chamber KH-14, filled with BF_3 after having been slowed down in paraffin. In Fig. 1 are illustrated the plots of the decreasing activity of delayed neutrons, which accompany the photofission of uranium and thorium, against time. The curves were obtained from a great number of sample irradiation cycles followed by the registration of neutrons. In each cycle, samples were irradiated with γ-rays for 3 min, then the irradiation was interrupted and after 1/2 sec, the registration of neutrons started and was continued for 5 min. From Fig. 1 it is seen that in the case of uranium, and thorium as well, the activity of delayed neutrons decreases rapidly with time. The character of this decrease of neutron activity indicates that most of the delayed neutrons have decay half-periods of less than 30 sec.

The exact determination of the decay periods and their relative yields was difficult due to the small cross section of the photofission. For uranium the following decay half-periods were established:

$$T_1 = 58 \text{ sec} \pm 8 \text{ sec}; \quad T_2 = 22 \text{ sec} \pm 3 \text{ sec};$$
$$T_3 = 5.5 \text{ sec}; \quad T_4 \sim 2 \text{ sec}.$$

The yield of delayed neutrons with a 22 sec period was several (about six) times greater than the yield of neutrons with the period of 58 sec. The correlation of the periods obtained, with the half-decay periods of the delayed neutrons which accompany the fission under the action of

[1] J. McElhinney and W. E. Ogle, Phys. Rev. **81**, 342 (1951)

[2] J. R. Huizenga, J. E. Gindler and R. B. Duffield, Phys. Rev. **95**, 1009 (1954)

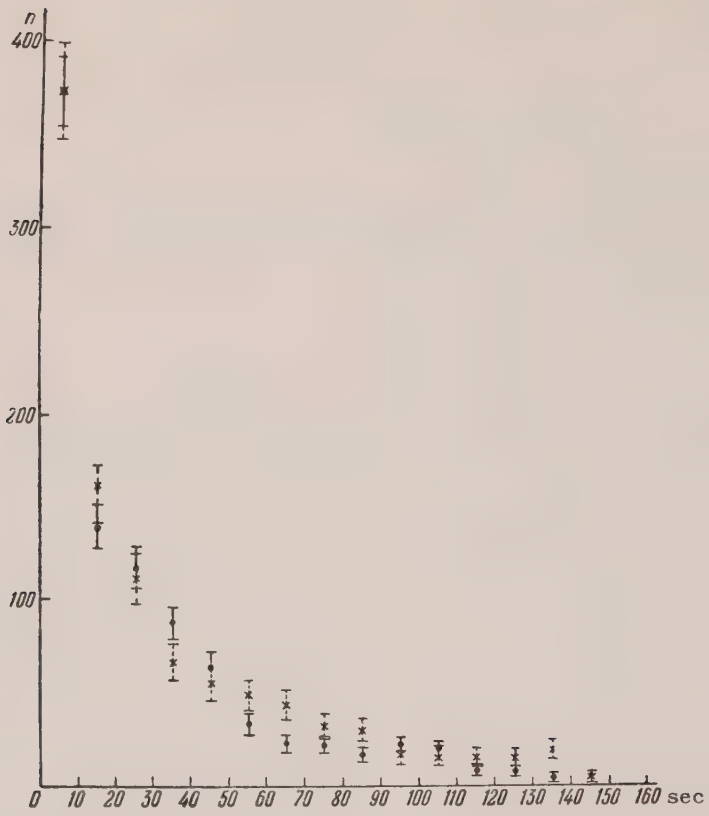

FIG. 1. Decay curve for delayed neutrons of photofission of uranium and thorium. ● – uranium, × – thorium, n – number of delayed neutrons.

neutrons [3,4] permits us to assume that in photofission there are formed the same neutron-active nuclei as in the case of neutron-induced fission.

YIELD OF DELAYED NEUTRONS

a) *Method of measurement.* The yield of delayed neutrons relative to the total yield of photoneutrons emitted in photofission of uranium and thorium was measured by a method which could be applied because of the pulse character of the accelerator. The synchrotron with which the measurements was made, produces γ-pulses of about 20 μ-sec duration, and frequency of 150 pulses/sec (the interval between γ-pulses being 6,667 μ sec). A special electronic circuit was developed which allowed the neutron pulses leaving the ionization chamber to be recorded in various time intervals between γ-pulses. Pulses from the ionization chamber were fed into a preamplifier consisting of two amplifying stages. Through the inverting stage with a double triode, 6N7, pulses were transmitted from the preamplifier in opposite phase, using a double-shielded symmetric twin-conductor cable (in order to reduce the amount of pick-up of electric disturbances), to the main amplifier, where they were recombined in proper phase.

All three preamplifier tubes were mounted in the lower part of a pipe, 5 cm in diameter, at the end of which, chamber KN-14 was placed. This setup was very convenient in working with a paraffin block. As the main amplifier, type ZH was used (amplification band up to $3 - 5 \times 10^6$ cps) with its agram slightly changed to suit the given problem. In order to decrease the charging time of the amplifier, at the instant of γ-pulse, a relatively small resistance of the order of 1 MΩ was included in the chamber circuit. For the purpose of decreasing recovery time of the system, which is dependent on grid currents during charging of the amplifier, the

[3] D. J. Hughes, J. Dabbs, A. Cahn and D. Hall, Phys. Rev. 73, 111 (1948)

[4] K. H. Sun, R. A. Charpie, F. A. Pecjak, B. Jennings, J. F. Nechaja and A. J. Allen, Phys. Rev. 79, 3 (1950)

time constant, *RC*, of grid circuits of the amplifier tubes was also reduced to 1 μsec. Moreover, in order to eliminate the secondary pulses, which were obtained due to multi-differentiation, diodes were included in two stages, which cut off the pulses from repeatedly entering.

Thus, the system recovered within a period of time of the order of 1 μsec. After amplification, pulses from the ionization chamber passed through a control circuit, resulting in time selection of pulses. The working principle of the control circuit was the following:

1) Pulses from the amplifier entered the grid of the input tube and then were transferred through a noise reducing diode into a fast counting system.

2) The diode was closed or opened depending on the voltage on the control grid of the special modulating tube which was also connected to the anode of the input tube.

3) Associated with the instant of the exclusion of high-frequency voltage on the "endo"-vibrator and preceeding each γ-pulse, the control pulse which is connected with the moment of switching off the high-frequency voltage on the vibrator, and which precedes each γ-pulse, traversing the system of vibrators, there is applied to the grid of the modulating tube a selective rectangular pulse, the width and position of which, relative to the control pulse, could be changed by means of potentiometers in the circuits of univibrators.

4) The diode was open for pulses from the amplifier only at the instant of arrival of the selective pulse. Pulses from the output of the diode were fed to the fast counting system throughout the duration of the rectangular pulse. The duration of the rectangular pulse--a measurable interval--determined the "gating" of the arrangement, and its position relative to the γ-pulse (the initial rise) determined the "delay" relative to the γ-pulse. The gating and delay were established by means of the timing pips on the ocsilloscope and could be changed within rather wide limits, from 50 to 7000 μ sec.

5) The by-pass capacitor of the main diode, through which the differentiated fronts of the selective pulse had to pass, was compensated by means of a second selective pulse which had opposite phase. This pulse was passed through the by-pass capacitor of the auxiliary diode (second half of the envelope) into the output circuit of the main diode.

The time distribution of the number of instantaneous photoneutrons in lead upon photodisintegration is plotted in Fig. 2. The abscissa gives the time in microseconds, and the ordinate gives the logarithm of the counter number of neutrons, measured at constant gating of 200 μ sec, and with various delays. As follows from Fig. 2, the neutron density decreases with time according to the law e^{-t/τ_0}, where $\tau_0 = 183 \pm 3$ μ sec. After a time $t = 2000$ μ sec, the photoneutrons are practically completely absorbed in the paraffin. Therefore, the "instantaneous" neutrons were recorded during the first 2000 μ sec after the γ-pulse. To eliminate the strong pulse of γ-rays, the instantaneous neutrons were recorded with a 20 μ sec delay. Correction was made for the number of neutrons in the first 20 μ sec after the γ-pulse.

Table I gives the number of neutrons recorded at the various delays indicated in the first line, with a constant gating of 500 μ sec for uranium, thorium and lead. The number of the instantaneous neutrons of lead, recorded with this arrangement, drops by a factor of 15 when the delay is changed to 500 μ sec, which is in complete agreement with the measured lifetime of neutrons in paraffin. As a consequence of the rapid decrease in the intensity of the neutrons, about 94% of the total number of neutrons are recorded in a 500 μ sec delay. Only 0.03% are recorded for 1540 μ sec delay, while for a 2000 μ sec delay, the counted number of neutrons drops to zero.

A similar drop of the instantaneous neutrons with time was obtained by us for copper and zinc.

The initial intensities for all three samples--uranium, thorium and lead--were of the same order; therefore, because of the absence of delayed neutron radiation in uranium and thorium, neutrons should not have been recorded after 2000 μ sec from the γ-pulse, just as in lead. However, it is seen from Table I that, from the 2000 μ sec time to the next γ-pulse, constant neutron activity was observed for uranium and thorium, corresponding to delayed neutron radiation. Simultaneous recording of the neutrons in the first 2000 μ sec after the γ-pulse and of the delayed neutrons in the interval from 2000 to 6000 μ sec after the γ-pulse allows the determination of the ratio of the delayed neutrons to the total number of photoneutrons. This method of recording the neutrons is very effective, since it permits the recording of the delayed neutron radiation for 2/3 of the time at saturated activity, which yields a several fold increase in the statistics. Large samples had to be used because of the high background of instantaneous neutrons from the synchrotron and

TABLE I

Delay (in μsec)	40	540	1040	1540	2040	2540	3040	3540	4040	4540	5040	5540	6040
Uranium	65520 ∓230	4622 ∓50	309 ∓17	56 ∓6	43 ∓2	42 ∓3.5	41 ∓3.5	42 ∓3.5	48 ∓3.7	40 ∓3.5	45 ∓5	40 ∓5	47 ∓2.5
Thorium	20952 ∓105	1394 ∓28	89 ∓7	8 ∓1.7	5 ∓0.9	6 ∓1.2	8 ∓1.4	5 ∓1.1	5 ∓1.1	6 ∓1.2	6 ∓1.3	6 ∓1.2	6 ∓1.2
Lead	28023 ∓109	1729 ∓33	120 ∓8	8 ∓2	1 ∓1	0	0	0	0	0	0	0	0

because of the small output of delayed neutrons. In order to maintain the same conditions of neutron absorption in background determination, the samples were placed in small cadmium boxes (wall thickness ½ mm), the same empty cadmium box being put in place of the sample in background measurements. The sample of uranium weighed 284 gm, that of thorium 120 gm. The background of instantaneous neutrons amounted to ~ 10% in the uranium case and ~ 20% for thorium. In the measurement of delayed neutrons, the background was practically equal to zero, since the neutron background from spontaneous fission was negligibly small.

Comparison of the number of incident neutrons recorded in a 500 μ sec interval and for various delays from 2000 μ sec to 6000 μ sec (Table I) shows that the intensity of the radiation of the delayed neutrons is constant to within a few percent in the time interval from 2000 to 6000 μ sec. This means that there is no appreciable number of nuclei with a decay period of the order of a few milliseconds among the neutron active nuclei formed during photo-fission.

Yields of instantaneous and delayed neutrons were measured for a fixed position of the ionization chamber in paraffin. In the calculation of the ratio of the delayed neutrons to the instantaneous neutrons, corrections were made for the different space distributions of the densities $\rho(r)$ of the delayed and instantaneous neutrons of uranium. The curves in Fig. 3 show the spatial distribution $\rho(r)\,r^2$ for delayed and instantaneous neutrons of uranium. Similar curves were obtained for thorium. The curves meet at 5 = 10 cm, where the chamber was placed for the measurements. As is seen from these curves, the spectrum of the delayed neutrons is appreciably softer. The curves that have been obtained permit us to estimate the mean energy of the delayed and instantaneous neutrons.

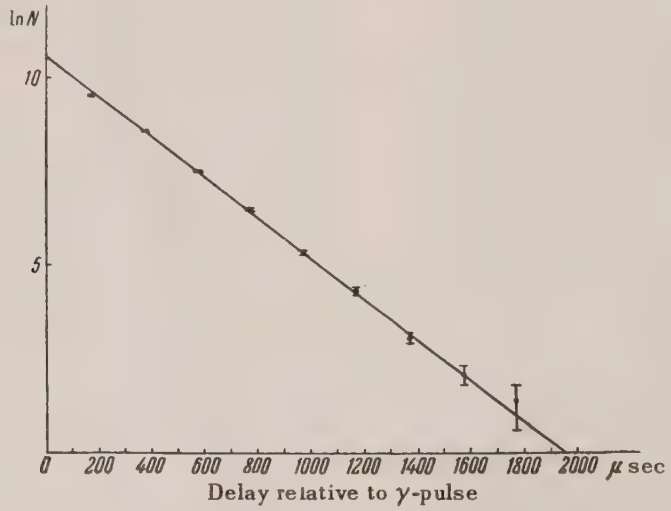

FIG. 2. Number of photoneutrons of lead N, recorded in paraffin, at constant gating (200 μsec) and various delays relative to the γ-pulse; $\tau_0 = 183 \pm \mu$sec.

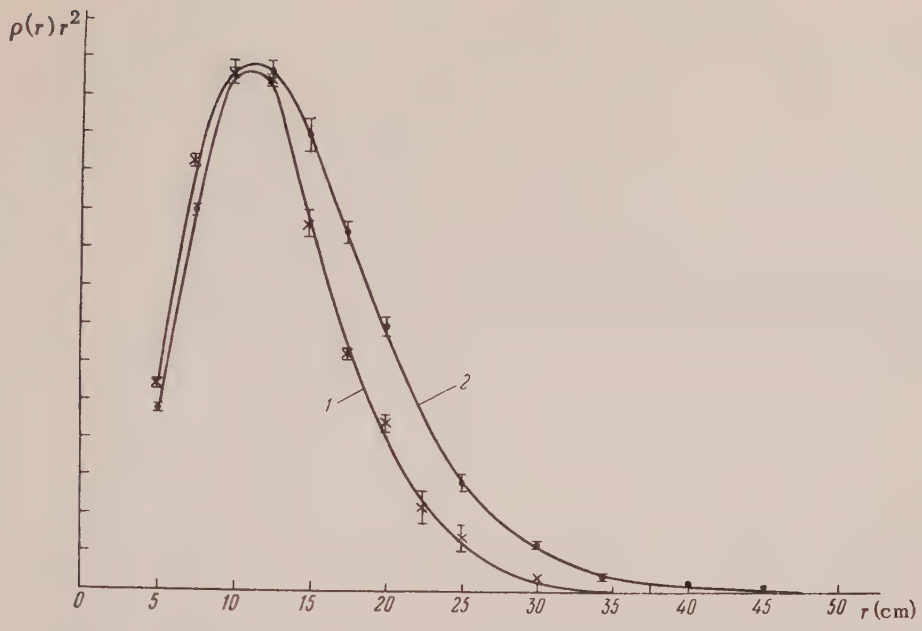

FIG. 3. Space distribution of the delayed and instantaneous neutrons of uranium in paraffin. *1.* delayed neutrons, *2.* instantaneous neutrons.

TABLE II

	Source (Ra_α+Be)	Photoneutrons of uranium	Photoneutrons of thorium	Delayed neutrons of Uranium	Photoneutrons (Na_γ^{24}+Be)
$\overline{r^2}$, cm^2	362	259	243	185	199
$\sqrt{\overline{r^2}}$, cm	19.0	16.1	15.6	13.6	14.1
Mean energy, mev	5 4	2.5 2.1	2.1 1.8	0.4 0.5	0.83 ∓ 0.04

Table II lists the mean square distance from the sample, which was the neutron source, for instantaneous neutrons of uranium and thorium, and delayed neutrons of uranium. In the same Table the values of the quantity $\overline{r^2}$ are given for photoneutrons of a $(Na_\gamma^{24} + Be)$ source and $(Ra_\alpha + Be)$ source, measured for calibration purposes. The $(Na_\gamma^{24} + Be)$ source emits monochromatic neutrons with energies 0.83 ± 0.04 mev.

The mean neutron energy of the source $(Ra_\alpha + Be)$ is 4-5 mev according to various data in the literature. The mean energy of the instantaneous neutrons of uranium and thorium is about 2 mev and of the delayed neutrons of uranium, ~ 0.5 mev. The measured mean energy of the delayed neutrons, brought about by photofission of uranium, coincides with the mean energy of the delayed neutrons emitted in the fission of U^{235} under the action of slow neutrons (515 ± 60 kev).

a) *Yield of delayed neutrons.* For uranium, the yield of delayed neutrons, relative to all neutrons emitted in photodisintegration, amounted to $0.41 \pm 0.02\%$; for thorium, $0.18 \pm 0.01\%$.

In the photodisintegration of uranium and thorium by γ-bremsstrahlung with $E_{max} = 18.5$ mev, four reactions involving neutron emission are energetically possible: (γ, f), (γ, n), (γ, nf) and $(\gamma, 2n)$. Thus the yield of delayed neutrons is larger relative only to the neutrons which accompany photofission. In 1951-1952, measurements were made, with this same arrangement, on the average number of neutrons ν, relative to a single fission, in the

photodisintegration of uranium and thorium by γ-rays with $E_{max} = 18.5$ mev[5]. The following values of ν were obtained:

uranium 6.2 ± 0.5;

thorium 14.2 ± 1.2.

If in accord with the results of this research, we assume the average number of neutrons emitted immediately in photofission to be equal to 3, then the percent of delayed neutrons (relative to instantaneous neutrons of photofission for U^{238} and Th^{232} at a mean excitation energy of ~ 12 mev) is equal to $\sim 0.8\%$.

[5] B. N. Valuev, B. I. Gavrilov, G. N. Zatsepina and L. E. Lazareva, J. Exper. Theoret. Phys. USSR **29**, 280 (1955); Soviet Phys.

Translated by A. Cybriwsky
192

Loss of Two Electrons by Negative Ions in Collisions with Atoms and Molecules

V. M. DUKEL'SKII AND N. V. FEDORENKO
Leningrad Physico-Technical Institute
(Submitted to JETP editor May 27, 1954)
J. Exper. Theoret. Phys. USSR 29, 473-478 (October, 1955)

The appearance of positive ions was detected in simple collisions of Cl^-, Br^-, I^-, Na^-, Sb^-, Bi^- and Sb_2^- ions (at an energy of 5 to 17.5 kev) with helium and argon atoms, and also with nitrogen and hydrogen molecules. They were formed by the loss of two electrons by the positive ions. The cross section for this process is about 10^{-17} to 10^{-16} cm^2. In the case of Sb_2^- and Bi_2^- ions, dissociation was observed with the appearance of not only negative but also of positive atomic ions.

1. INTRODUCTION

NEGATIVE ions with energies of about 1000 ev easily lose their extra electron in collisions with the atoms of a gas[1]. Being engaged in an investigation of this phenomenon, we performed the following experiment. A beam of negative iodine ions traversed a chamber filled with argon at a pressure of 3×10^{-3} mm Hg and thereupon entered the space between the plates of a parallel plate condenser. In the field of the condenser the beam (whose emitted light it was possible to observe) was divided into two separate beams. One of them (the beam of negative ions) was deflected toward the positive plate, the other passed through the condenser without being deflected. This undeflected beam consisted of neutral iodine atoms, formed by neutralization of negative ions in collisions with argon atoms.

The appearance of a third beam was detected upon increasing the argon pressure to 1×10^{-2} mm. It was deflected toward the side lying opposite from that toward which the negative ions were deflected. Obviously, this third beam could be only a beam of positive ions. In order to explain its appearance, it was necessary to suppose that in collisions with argon atoms a portion of the negative iodine ions could lose two electrons and be converted into positive ions.

Upon decreasing the argon pressure the beam of positive ions became weaker but remained perceptible to about 10^{-3} mm. At that pressure the stripping of two electrons in two successive collisions was improbable. Therefore, one might think that the negative iodine ions had lost two electrons in a single collision with an argon atom.

2. APPARATUS. METHOD OF OBSERVATION

The method of the double mass spectrometer[2] is well suited to the study of the charge exchange of ions in collisions with atoms. In this apparatus a homogeneous beam of ions, prepared by a mass monochromator, is incident upon a gas cell. Ions, whose charge or mass has been changed in collisions but whose velocity has been almost fully conserved, are then analyzed by means of a second mass spectrometer (mass analyzer).

The double mass spectrometer used by us has been described in detail by Fedorenko[2]. It is shown schematically in Fig. 1. The ion source with a solid working substance was used. Sodium halide salts were used for producing sodium and halogen ions; antimony and bismuth ions were obtained from a discharge in vapors of these metals.

The experiments for the detection of positive ions, which are formed from negative ions in collisions with the atoms of a gas, were performed as follows. The apparatus was evacuated to a pressure of 10^{-5} mm Hg, and a beam of negative ions of the chosen element was emitted with a given energy into the gas cell. The magnet of the mass analyzer was then turned on and adjusted until near a certain value H_A the negative-ion beam fell onto the detector Φ_2. The gas was then admitted into the gas cell; thereupon, the current of negative ions into the detector dropped, as a portion of the ions was scattered and destroyed in the gas cell. After changing the direction of the magnetic field in the mass analyzer we found the positive ions by varying the magnetic field slowly about the value H_A. In the first experiment with a beam of I^- ions (ion energy 10 kev; the gas cell

[1] V. M. Dukel'skii and E. Ia. Zandberg, J. Exper. Theoret. Phys. USSR 21, 1270 (1951)

[2] N. V. Fedorenko, Zh. Tekhn. Fiz. 24, 769 (1954)

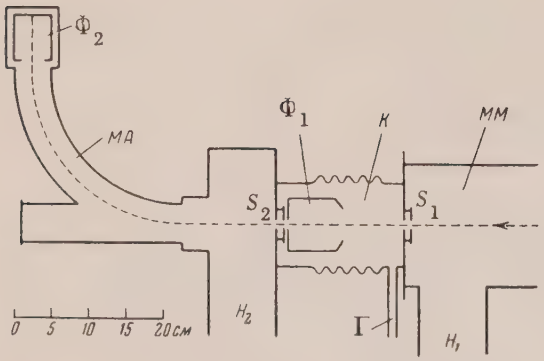

FIG. 1. Schematic drawing of the double mass spectrometer. *MM*, tube of the mass monochromator; *K*, gas cell; *MA*, mass analyzer; Φ_1, detector for measuring the current in the primary ion beam; Φ_2, detector for ions that have traversed the mass analyzer; S_1 and S_2, slits; H_1 and H_2, pipes to the vacuum pumps; Г, gas inlet.

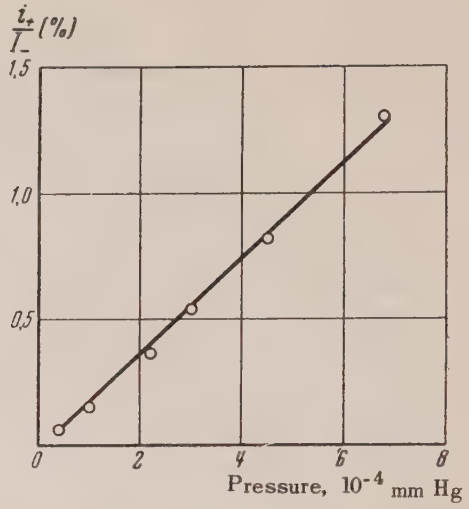

FIG. 2. Conversion of negative into positive ions as a function of gas pressure. I^- ions (10 kev; argon).

was filled with argon at 3×10^{-4} mm.) we found a sharp "line" of positive ions; it was observed at the same magnetic field intensity (within the limits of accuracy of the measurement) as the primary beam of I^- ions. We were able to interpret the observed effect as a conversion, brought about by collisions of I^- ions with argon atoms, of I^- into I^+ ions without a perceptible change of energy.

By deflecting the mass analyzer through small angles out of the null position (up to 5°), we discovered that the positive-ion beam diverged more than the negative-ion beam from which it was formed. This showed that the conversion of I^- into I^+ ions could be accompanied by a perceptible scattering of the ions coming out.

3. RESULTS OF THE MEASUREMENTS

A process of conversion, entirely like that described for the I^- ions, was detected also in all other cases investigated by us. The conversion appeared for Cl^-, Br^-, Na^-, Sb^-, Bi^- and Sb_2^- ions with the gas cell filled with argon, helium, hydrogen and nitrogen.

In the different cases the current in the primary ion beam varied from 2×10^{-10} to 2×10^{-9} amp. The magnitude of the effect depended on the kind and energy of the negative ions, and on the kind and pressure of the gas. In most cases the positive-ion current became measurable at an energy of the primary beam of about 5 kev and grew with increasing energy. The positive ion current was of the order of 10^{-12} amp at energies from 10 to 15 kev and a gas-cell pressure of 3 to 4×10^{-4} mm. The upper limit of ion energy was 17.5 kev in our experiments.

It was very important to ascertain that the appearance of positive ions did not result from a successive stripping of two electrons in two successive collisions (first of a negative ion, next of the neutral atom thus formed) with atoms of the gas. In this case the dependence of the effect upon the pressure in the gas cell was measured in a series of experiments. As an example, a curve showing this dependence for the conversion $I^- \rightarrow I^+$ in argon at 10 kev is displayed in Fig. 2. The abscissa represents the pressure of argon, and the ordinate the ratio of the current i_+ of secondary positive ions to the current I_- of the primary beam of negative ions. As is evident from the figure, the dependence upon pressure is linear in the interval from 1×10^{-4} to 7×10^{-4} mm. In the other cases investigated by us the effect of ion conversion (at gas pressures of about 10^{-4} mm) also was proportional to pressure or increased more slowly than the pressure. It was thus verified that under the conditions of our experiments the positive ions appeared as a result of single collisions of negative ions with atoms or molecules.

Having measured the current ratio i_+/I_- at a given pressure of the gas in the gas cell, we were able to effect an approximate determination of the cross sections Q for collisions accompanied by a conversion of negative into positive ions. The inaccuracy of these determinations is connected with the fact that not all the positive ions produced in the gas cell entered the detector of the mass analyzer, because of the scattering of the

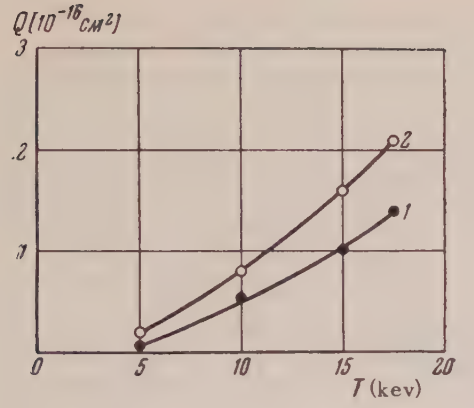

FIG. 3. Cross section for the conversion $I^- \rightarrow I^+$ as a function of ion energy. *1*, argon at 3.3×10^{-4} mm; *2*, nitrogen at 3.5×10^{-4} mm.

ions in the conversion process. Another source of error was the indefiniteness of the length l of the effective volume of gas; we took this length as equal to the distance between the slits S_1 and S_2 (Fig. 1).

The magnitude of the cross section Q was calculated by means of the approximate formula

$$Q = \frac{i_+}{I_- nlk},$$

where n is the number of atoms (molecules) per cm^3 of the gas in the gas cell, and k is the "coefficient of admission" of the mass analyzer for the primary ion beam. The quantity k (the ratio of the number of ions traversing the mass analyzer to the number of ions entering the gas cell) was measured for several primary ions at a residual pressure in the apparatus of 10^{-5} mm and was shown equal to 0.5. The values of Q calculated by this method must be less than the actual ones since the quantity k for secondary positive ions probably is considerably smaller that for the primary negative-ion beam and may depend upon the ion energy.

In Figs. 3, 4 and 5 are shown several of the curves obtained by us. They show the dependence of the cross section Q upon the ion energy T. The curves in Fig. 3 refer to the conversion $I^- \rightarrow I^+$ in collisions of I^- ions with argon atoms and molecules. At an energy of 5 kev of the I^- ions, Q is about 10^{-17} cm^2. With increasing energy Q increases and attains a value of about 10^{-16} cm^2 at 17.5 kev. Figure 4 shows curves for the conversion $Br^- \rightarrow Br^+$; the order of magnitude of Q and the character of the energy dependence in this case are similar to those for the conversion $I^- \rightarrow I^+$. The curves in Fig. 5 apply to the con-

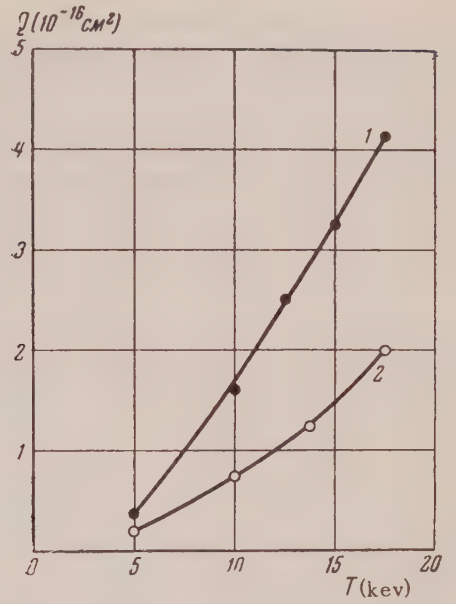

FIG. 4. Cross section for the conversion $Br^- \rightarrow Br^+$ as a function of ion energy. *1*, argon at 4.0×10^{-4} mm; *2*, nitrogen at 3.8×10^{-4} mm.

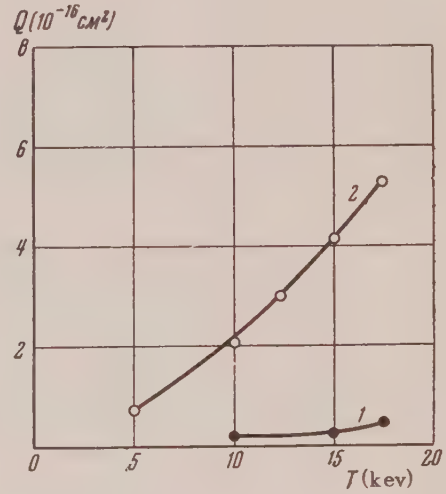

FIG. 5. Cross section for the conversion $Na^- \rightarrow Na^+$ as a function of ion energy. *1*, argon at 5.4×10^{-4} mm; *2*, nitrogen at 4.0×10^{-4} mm.

version $Na^- \rightarrow Na^+$; in this case Q for argon atoms is small (10^{-17} cm^2) and increases comparatively slowly with energy. For the conversion $Cl^- \rightarrow Cl^+$ in argon and nitrogen, Q has a value of about 10^{-16} cm^2 and in the interval 5-17.5 kev increases to several times that value. For the conversions $Sb^- \rightarrow Sb^+$ and $Bi^- \rightarrow Bi^+$ the energy dependence

passed through because of insufficient intensity of the primary negative-ion beam. In both cases Q is about 10^{-16} cm^2 at 10 kev.

The conversion process was also observed for Sb_2^- ions. An Sb_2 ions can be converted into an Sb_2^+ ion in collisions with argon atoms and nitrogen molecules. In the case of argon the process is detected with difficulty because of the small cross section.

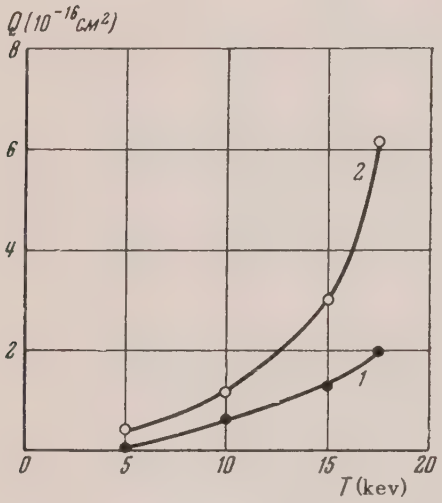

FIG. 6. Cross section for the process $Bi_2^- \rightarrow Bi^+ + Bi + 2e$ as a function of the energy of the Bi_2^- ions. *1*, argon at 2.5×10^{-4} mm; *2*, nitrogen at 2.5×10^{-4} mm.

At 10 kev we were unable to detect the conversion $Bi_2^- \rightarrow Bi_2^+$ either in nitrogen or argon.

In the case of hydrogen and helium the cross sections for conversions in most cases were smaller than in the case of argon or nitrogen, but were of the same order of magnitude (10^{-17} to 10^{-16} cm^2) and also increased with the ion energy.

Performing experiments with a beam of Sb_2^- ions we discovered two more secondary lines: one negative (Sb^-), the other positive (Sb^+), with an energy equal to half the energy of the primary Sb_2^- ions. Sb^- ions could appear as the result of a dissociation of an Sb_2^- ion into an Sb^- ion and a neutral Sb atom (in collisions with atoms of the gas). The cross section for the process $Sb_2^- \rightarrow Sb^- + Sb$ depended little on the ion energy (5-17.5 kev) and was about 10^{-17} cm^2 in argon as well as in nitrogen. The appearance of the Sb^+ ions indicated the possibility of a conversion complicated by dissociation. Evidently the Sb^+ ion appeared as the result of the loss of two electrons by the Sb_2^- ion, in which the newly formed Sb_2^+ ion disintegrated into an Sb^+ ion and an Sb atom*. The process $Sb_2^- \rightarrow Sb^+ + Sb + 2e$ appeared in argon and nitrogen. The cross section of this process increased rapidly with the primary-ion energy, attaining several units $\times 10^{-16}$ cm^2 at 17.5 kev.

In the case of Bi_2^- ions we observed the same phenomena of dissociation and of dissociation with appearance of positive ions. The curves in Fig. 6 show the dependence of the cross section Q for the process $Bi_2^- \rightarrow Bi^+ + Bi + 2e$ in argon and nitrogen upon the energy T of the primary ions. As is evident from the figure, Q increases rapidly with T.

We also observed the conversion of negative into positive iodine ions spectrographically. A beam of negative iodine ions (beam current 3×10^{-6} amp, ion energy 7.5 kev) was incident on the gas cell filled with argon at 5×10^{-3} mm. The weak light emitted by the beam was analyzed by means of a sensitive glass spectrograph. On the spectrograms we obtained the spectral lines of the iodine atom (JI), $\lambda = 5235$, 5119, 4917, 4862 Å, and others; but besides these also the lines $\lambda = 5497$, 5465, 5438-5436, 5407-5405, 5338, 5161 Å, and others belonging to the spectrum of the I^+ ion (JII). The lines JI obviously appear as the result of the stripping of the extra electron from the I^- ions in collisions with argon atoms and of simultaneous excitation of the iodine atoms being formed. The appearance of the lines JII can be explained as the result of the conversion of a portion of the negative iodine ions into positive ones with simultaneous excitation of the I^+ ions. The intensity of the observed JII lines was comparable with that of the JI lines. Upon decreasing the argon pressure to 2×10^{-3} mm and increasing it to 8×10^{-3} mm, the relative intensity of the lines JI and JII changed little. This showed that the excitation of the JII lines occurred as the result of single collisions of I^- ions with argon atoms, but not in a stepwise fashion.

---

* It seems that another process, namely, $Sb_2^- \rightarrow Sb^+ + Sb^- + e$, which could also lead to the appearance of Sb^+ ions did not take place in our experiments since the number of Sb^- ions always was considerably less than the number of Sb^+ ions.

4. CONCLUSION

The loss of two electrons by a negative ion in a single collision with an atom represents a process analogous to the two-step ionization of atoms by electrons. The ionization of atomic particles in collisions becomes possible at lower velocities than in the case of ionization by electrons, but because of the large difference between the masses of the electron and the atom it requires that the particles possess a considerably larger kinetic energy of relative motion. For stripping two electrons from a negative ion it is necessary to expend an energy equal to the sum of the energy of the electron affinity and the energy of the first ionization of the atom. This sum is always less than the energy of the two-step ionization of any neutral atom or of the more positive ion. Thus, it is explained that is is possible to observe two-step ionization of negative ions at comparatively low ion energies (beginning with 5 kev), at which practically no stripping of two electrons from neutral atoms or from positive ions takes place*.

For all ion-atom pairs investigated by us, the cross section for the conversion of negative into positive ions increased with the ion energy. The energy interval (5-17.5 kev) investigated by us was, however, too small, and the inaccuracy of the determination of the cross sections was too great to conclude anything about the form of the function $Q(T)$.

The large values of the cross sections for the conversion process--several units $\times 10^{-16}$ cm^2 at 10 to 15 kev--deserve to be noted. Since our method of measurement yielded values that are too small, the true values of the cross sections must be even larger.

As our preliminary experiments show, in the energy interval 5-17.5 kev the stripping of a single electron continues to be the fundamental process occurring in collisions of negative ions with atoms. For instance, for I^- ions with an energy of 15 kev and argon atoms the cross section for this process is about 1×10^{-15} cm^2; but the cross section for conversion into positive ions is about 1×10^{-16} cm^2.

In the region of low energies (of the order of 100 to 1000 ev) the process of stripping a single electron serves as the sole source of the appearance of slow electrons in collisions of negative ions with atoms. Therefore, by measuring the number of slow electrons it is possible to determine the cross section for this process[1,3] In applying this method in the region of energies above 5 kev, it is necessary to remember the existence of the process of conversion of negative into positive ions. At these energies the measurements with utilization of the slow electrons yield a total cross section into which the doubled cross section for the loss of two electrons enters together with the cross section for the stripping of a single electron.

* One of us (N.V.F.) has discovered the stripping of two electrons from Ba and A ions (at 20 kev) in collisions with argon atoms and nitrogen molecules[2].

[3] J. B. Hasted, Proc. Roy. Soc. (London) A212, 235 (1952)

Translated by J. W. Heberle
227

The Theory of the Propagation of Gamma Rays through Matter

V. I. OGIEVETSKII

(Submitted to JETP editor June 25, 1954)
J. Exper. Theoret. Phys. USSR 29, 454-463 (October, 1955)

The angular and energy distribution of gamma radiation is found as a function of depth of penetration into matter, for an initial energy of the order of several mev.

THE investigation of the energy spectrum and angular distribution of gamma rays as a function of depth of penetration in matter is of interest both for theory and for many experiments and applications, among which we may mention various questions concerning dosimetry, design of gamma-ray filters, etc.

In the present paper the following question is considered. A parallel beam of monochromatic γ - radiation is incident perpendicular on the plane surface of a layer of matter. How will the distribution of the γ - radiation in energy and angle change, as a function of depth, initial energy, and the properties of the material?

The energy spectrum of the scattered radiation has been found for several cases, without any simplifications, by a numerical method[1].

In contrast to this work, an analytic method is developed in the present paper for determining not only the energy spectrum, but also the angular distribution of the scattered γ - radiation. The calculations developed in the work are based on an equation of radiative transfer of the Boltzmann type. The angles of scattering are assumed to be small, as is the case for energies of the order of several mev. For the Klein-Nishina-Tamm cross section, we use an approximate formula which gives a good fit to the true cross section. No other omissions or simplifications are contained in the work.

In the special case where the absorption coefficient of the γ - rays can be taken as constant, this problem has been solved previously[2,3] by another method, more complicated than that applied here.

1. INTRODUCTION

During the passage of γ - rays through matter, absorption and scattering occur as a result of the following three fundamental processes: a) photoeffect, b) Compton effect, c) production of electron-positron pairs.

The photoeffect predominates at low energies. With increasing energy, the Compton scattering becomes important. For still higher energies, the probability of photo-and Compton effects decreases, while the probability of pair formation increases, so that pair formation begins to play the major role.

The energy interval within which the Compton effect is dominant is quite wide for light elements (0.03-25 mev for carbon, 0.05-15 mev for aluminum) and becomes narrower with increasing atomic number (0.2 -12 mev for copper, 0.6-5 mev for lead).

The intensity of the unscattered monochromatic radiation decreases exponentially during its passage through matter[4]

$$J = J_0 e^{-\tau x}, \qquad (1)$$

where τ is the total absorption coefficient. Figure 1 (which is taken from reference 4) shows the dependence of the total absorption coefficient on energy for several elements. We note that for light elements, in the high energy region, (for example, for aluminum with $h\nu \gtrsim 10\, m_0 c^2$), τ can be taken as approximately constant.

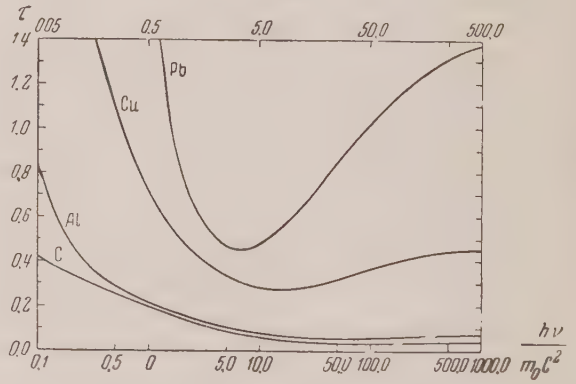

FIG. 1. Energy dependence of γ - ray absorption coefficient

[1] L. Spencer and U. Fano, Phys. Rev. 81, 464(1951); J. Res. Nat. Bur. Stand. 46, 446 (1951)

[2] L. L. Foldy, Phys. Rev. 81, 395,400 (1951)

[3] L. L. Foldy, Phys. Rev. 82, 927 (1951)

[4] W. Heitler, *Quantum Theory of Radiation*

In the energy range in which the Compton scattering is most important, we can neglect the radiation from photoelectrons, Compton recoils and pair particles.

We introduce certain formulas concerning the theory of Compton scattering. It is well known that the Compton effect is the incoherent scattering of γ - radiation by free electrons. Applying the laws of conservation of energy and momentum leads to the following expression for the wavelength of a photon scattered through an angle θ:

$$\lambda' = \lambda + 1 - \cos\theta, \qquad (2)$$

where λ' and λ are, respectively, the wavelengths of the scattered and initial photon, expressed in units of the Compton wavelength ($\lambda = m_0 c^2/h\nu$).

The Klein-Nishina-Tamm formula, giving the probability that a photon of wavelength λ, in passing through a one centimeter layer of material, collides with an electron and is deflected through an angle θ while its wavelength becomes λ', is conveniently written in the form

$$dW_K(\lambda, \lambda', \theta) = n\pi r_0^2 \left(\frac{\lambda}{\lambda'}\right)^2 \left[\frac{\lambda}{\lambda'} + \frac{\lambda'}{\lambda} - \sin^2\theta\right] \qquad (3)$$

$$\times \frac{1}{2\pi}\delta(1 - \cos\theta - \lambda' + \lambda)\, d\lambda' d\Omega,$$

where n is the number of electrons per cc, r_0 is the classical electron radius, $d\Omega$ is the element of solid angle, and $\delta(\alpha)$ is the delta function.

In this form, $dW_K(\lambda, \lambda', \theta)$ automatically becomes zero if condition (2) is not satisfied.

We should emphasize that for gamma rays with an energy of the order of several mev, scattering through large angles, which is accompanied by large energy loss, is improbable compared to scattering through small angles. We may therefore neglect the $\sin^2\theta$ term in (3).

For our later work we also replace the factor $\frac{1}{2}(\lambda/\lambda')^2[(\lambda/\lambda') + (\lambda'/\lambda)]$ in (3) by $(\lambda/\lambda')^k$. If we determine the exponent k by the method of least squares, k turns out to be 1.69. Since our main concern is with values of λ' close to λ, we have chosen $k = 1.8$. In reference 2, k was taken equal to unity. In a note by the same author[3], the possibility of choosing k different from unity is pointed out. From. Fig. 2 it is clear that our choice gives a good fit to the true cross section. The expression for dW_K becomes:

$$dW_K(\lambda, \lambda', \theta) \qquad (3')$$

$$= a(\lambda/\lambda')^k (1/2\pi)\delta(1 - \cos\theta - \lambda' + \lambda) d\Omega d\lambda',$$

where $k = 1.8$ and $a = 2\pi n r_0^2$.

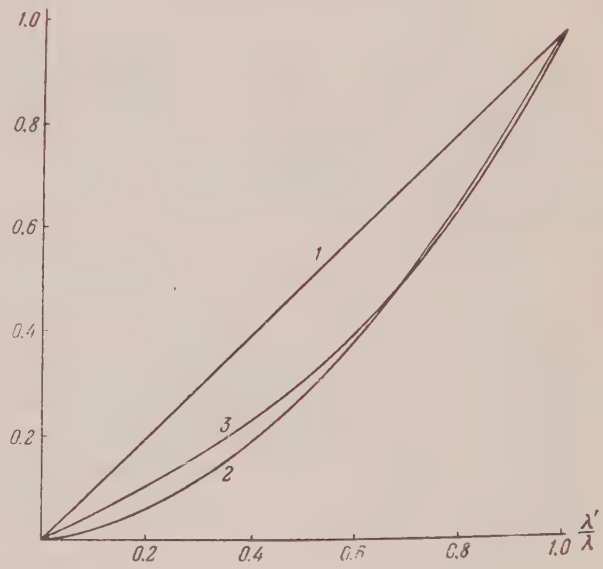

FIG. 2. Approximate replacements for the Klein-Nishina-Tamm formula. *1* - replacement of the factor $\frac{1}{2}(\lambda'/\lambda)^2[(\lambda'/\lambda) + (\lambda/\lambda')]$ by (λ'/λ); *2*- replacement of the same factor by $(\lambda'/\lambda)^{1.8}$, which is used in this paper; *3*- exact value.

The values of the constant a for various elements are given in the following table.

Values of the constant a in cm^{-1}

	C	Al	Fe	Cu	Pb
a	0.3435	0.3885	1.095	1.215	1.3425

The distribution of once-scattered radiation was found in reference 5.

It is obvious that for a monochromatic unidirectional source, the distribution of unscattered radiation can be given in the form

[5] L. Cave, J. Corner and R. Liston, Proc. Roy. Soc. (London) **A204**, 223 (1950)

$$\Gamma^0(x, \lambda, \theta) = (1/2\pi)\,\delta(1-\cos\theta)\,\delta(\lambda-\lambda_0)\,e^{-\tau(\lambda_0)x}, \quad (4)$$

where λ_0 is the wavelength of the primary radiation.

One then finds[5], for the distribution in angle and energy of the once-scattered radiation (in our notation), the following expression:

$$\Gamma^1(x, \lambda, \theta)\,d\Omega d\lambda = d W_K(\lambda_0, \lambda, \theta)\,e^{-\tau(\lambda_0)x} \times \frac{1-\exp\left\{-\dfrac{\tau(\lambda)-\tau(\lambda_0)\cos\theta}{\cos\theta}\,x\right\}}{\tau(\lambda)-\tau(\lambda_0)\cos\theta}. \quad (5)$$

Calculation by the method of reference 5 of higher orders of scattering becomes, even for the second, extremely involved, and is practically impossible. We therefore turn to the general equation of radiative transfer.

2. THE EQUATION OF RADIATIVE TRANSFER

We denote by $\Gamma(x, \lambda, \theta)$ the photon distribution function in wavelenght λ, angle θ with respect to the normal to the surface of the material , and depth x in cm. Then if the primary radiation has wavelength λ_0 and is incident perpendicular to the surface of the material, the change in $\Gamma(x, \lambda, \theta)$ is given by the equation

$$\cos\theta\,\frac{\partial\Gamma(x,\lambda,\theta)}{\partial x} = -\tau(\lambda)\,\Gamma(x,\lambda,\theta) + \int_{\lambda_0}^{\lambda}\int_{4\pi}\Gamma(x,\lambda',\theta')\,d W_K(\lambda',\lambda,\theta_1) + \frac{1}{2\pi}\,\delta(1-\cos\theta)\,\delta(\lambda-\lambda_0)\,\delta(x), \quad (6)$$

where

$$\cos\theta_1 = \cos\theta\cos\theta' + \sin\theta\sin\theta'\cos(\varphi-\varphi').$$

Equation (6) can be described in words as follows:

The change in the distribution function $\Gamma(x,\lambda,\theta)$ (the left side of the equation) is caused by absorption (first term on the right), scattering (second term), and by newly arriving photons from the source (last term on the right).

We note that we could have omitted the source term in the equation, and taken account of it by a boundary condition at $x = 0$. Clearly, in our case the distribution function does not depend on azimuth.

We expand $\Gamma(x,\lambda,\theta)$ in a series of Legendre polynomials

$$\Gamma(x, \lambda, \theta) = \frac{1}{2\pi}\sum_{l=0}\frac{2l+1}{2}\,\Gamma_l(x, \lambda)\,P_l(\cos\theta). \quad (7)$$

Using Eqs. (6) and (3′), we obtain the following infinite system of equations for $\Gamma_l(x,\lambda)$:

$$\frac{l+1}{2l+1}\,\frac{\partial\Gamma_{l+1}(x,\lambda)}{\partial x} + \frac{l}{2l+1}\,\frac{\partial\Gamma_{l-1}(x,\lambda)}{\partial x} + \tau(\lambda)\,\Gamma_l(x,\lambda) = a\int_{\lambda_0}^{\lambda}\left(\frac{\lambda'}{\lambda}\right)^{1,8} P_l(1-\lambda+\lambda')\,\Gamma_l(x,\lambda')\,d\lambda' + \delta(x)\,\delta(\lambda-\lambda_0). \quad (8)$$

In deriving this system of equations, we have expanded the delta function which appears in the transfer equation (6) in a series of Legendre polynomials and have used the addition theorem for Legendre polynomials.

The solution of this system of equations in the general case is very difficult. But, as already mentioned, the scattering through small angles is much more probable than scattering through large angles, especially for γ - rays of high energy (3-4 mev and greater). We may therefore assume that the angle θ is small. Since, for small angles, the terms in (7) with large l are most important, the expansion (7) in Legendre polynomials agrees approximately with the expansion in Bessel functions of zero order (Hankel transformation). We mention that this fact was first used in studying the scattering of electrons, by Kompaneets[6]:

$$T(x, \lambda, \theta) = (1/2\pi)\int_0^{\infty} J_0(l\theta)\,\Gamma_l(x, \lambda)\,l\,dl. \quad (9)$$

where we have used the relation

$$\lim_{l\to\infty} P_l\left(\cos\frac{\theta}{l}\right) = J_0(\theta). \quad (10)$$

For large l the system of equations (8) reduces approximately to the equation

---

[6] A.S. Kompaneets, J. Exper. Theoret. Phys. USSR 15, 235 (1945)

$$\frac{\partial \Gamma_l(x,\lambda)}{\partial x} + \tau(\lambda)\Gamma_l(x,\lambda) \tag{11}$$
$$= a\int_{\lambda_0}^{\lambda} J_0\left(l\sqrt{2(\lambda-\lambda')}\right)\left(\frac{\lambda'}{\lambda}\right)^{1,8}\Gamma_l(x,\lambda')\,d\lambda' + \delta(x)\,\delta(\lambda-\lambda_0).$$

Equation (11) is the definitive equation which we wanted to get for the distribution function of scattered γ - radiation in angle and energy.

3. SOLUTION OF THE EQUATION OF RADIATIVE TRANSFER

We expand the absorption coefficient $\tau(\lambda)$ in powers of $(\lambda-\lambda_0)$:

$$\tau(\lambda) = \tau_0 + \tau_1(\lambda-\lambda_0) + \tau_2(\lambda-\lambda_0)^2 + \ldots, \tag{12}$$

multiply Eq. (11) by $(\lambda/\lambda_0)^{1\cdot 8}\exp[-(\lambda-\lambda_0)\,s]$ and integrate with respect to λ from λ_0 to ∞. We then get

$$\frac{\partial F_l(x,s)}{\partial x} + \tau_0 F_l - \tau_1\frac{\partial F_l}{\partial s} + \tau_2\frac{\partial^2 F_l}{\partial s^2} - \ldots \tag{13}$$
$$= \left(\frac{a}{s}\right)\exp[-l^2/2s]\,F_l(x,s) + \delta(x),$$

where $F_l(x,s)$ is related to $\Gamma_l(x,\lambda)$ by a Laplace transformation:

$$F_l(x,s) \tag{14}$$
$$= \int_{\lambda_0}^{\infty} (\lambda/\lambda_0)^{1,8}\,\Gamma_l(x,\lambda)\exp(-(\lambda-\lambda_0)\,s)\,d\lambda.$$

Clearly, the unknown distribution function $\Gamma(x,\lambda,\theta)$ is expressed as:

$$\Gamma(x,\lambda,\theta) = \frac{1}{2\pi i}\left(\frac{\lambda_0}{\lambda}\right)^{1,8} \tag{15}$$
$$\int_{\delta-i\infty}^{\delta+i\infty}\exp[(\lambda-\lambda_0)s]\,ds\,\frac{1}{2\pi}\int_0^{\infty}F_l(x,s)\,J_0(l\theta)\,l\,dl.$$

To solve Eq. (13), we look for $\Gamma_l(x,s)$ in the form

$$F_l(x,s) = e^{-\tau_0 x}\sum_{n=0}^{\infty} m_n(s,l)\,x^n. \tag{16}$$

We obtain the recursion relation

$$(n+1)\,m_{n+1}(s,l) = \frac{a}{s}\exp\left(-\frac{l^2}{2s}\right)m_n(s,l) \tag{17}$$
$$+\tau_1\frac{\partial m_n(s,l)}{\partial s} - \tau_2\frac{\partial^2 m_n(s,l)}{\partial s^2} + \ldots$$

for $m_n(s,l)$.

Clearly, $m_0(s,l) = 1$. The expressions for $m_n(s,l)$ are sums of terms of the type

$$\frac{l^{2k}}{s^p}\exp\left(-r\,\frac{l^2}{2s}\right) \tag{18}$$

so that we can easily construct Laplace and Hankel transforms.

If we are interested only in the energy spectrum

$$\Gamma_0(x,\lambda) = 2\pi\int_0^{\infty}\Gamma(x,\lambda,\theta)\,\theta\,d\theta, \tag{19}$$

then the quantities $m_n^{(0)}(\lambda)$ in the expansion

$$\Gamma_0(x,\lambda) = \left(\frac{\lambda_0}{\lambda}\right)^{1,8}e^{-\tau_0 x}\sum_{n=0}^{\infty} m_n^{(0)}(\lambda)\,x^n \tag{20}$$

will be connected by the recursion relations:

$$(n+1)\,m_{n+1}^{(0)}(\lambda) \tag{21}$$
$$= a\int_{\lambda_0}^{\lambda} m_n^{(0)}(\lambda')\,d\lambda' - [\tau(\lambda)-\tau_0]\,m_n^{(0)}(\lambda),$$

where $m_0^{(0)}(\lambda) = \delta(\lambda-\lambda_0)$. One can similarly obtain expansions for the angular moments.

We note that, by the method described above, we can find the angular distribution and energy spectrum not only by expanding the absorption coefficient $\tau(\lambda)$ in powers of $(\lambda-\lambda_0)$, but also if we replace it in any manner whatsoever, e.g. by a sum of exponentials

$$\tau(\lambda) = a\exp(b\lambda) + c\exp(d\lambda).$$

The expansions obtained for the distribution of scattered γ - radiation in energy and angle (16), and for the energy spectrum (20), converge rapidly, especially when the scattered radiation is softer than the unscattered (i.e., when the absorption coefficient does not decrease with decreasing energy). If the absorption coefficient increases with decreasing energy, we should replace

$\exp(-\tau_0 x)$ in the expansions (16) and (20) by $\exp(-\tau_m x)$, where τ_m is the absorption coefficient for the hardest component of radiation. This is easily done. It increases the rapidity of convergence for relatively large depths of penetration.

Clearly, in practical cases, in order that the calculation should not become too complicated, it is convenient to approximate the absorption coefficient by a simple formula of the type $\tau(\lambda) = \sum_{i=0}^{n} \tau_i (\lambda - \lambda_0)^i$, with small n.

Let us consider some simple cases.

4. THE CASE OF CONSTANT ABSORPTION COEFFICIENT

The calculations are most easily done when the absorption coefficient can be regarded as independent of energy, which is the case, as already mentioned above, in light elements at high energies: in carbon, for $h\nu \gtrsim 8\, m_0 c^2$; in aluminum, for $h\nu \gtrsim 10\, m_0 c^2$, etc.

In this case we can find all the terms in the expansion (16) and, taking Laplace and Hankel transforms, get the following expression for the distribution function of the scattered radiation in angle and energy:

$$\Gamma(x, \lambda, \theta) = \frac{1}{2\pi}\left(\frac{\lambda_0}{\lambda}\right)^{1,8} e^{-\tau_0 x}\left\{\delta(\lambda - \lambda_0)\,\delta\left(\frac{\theta^2}{2}\right)\right. \quad (22)$$

$$+ \frac{\rho^2}{4(\lambda - \lambda_0)}\,\delta\left(\lambda - \lambda_0 - \frac{\theta^2}{2}\right)$$

$$+ \frac{1}{(\lambda - \lambda_0)^2} \sum_{n=2}^{\infty} \frac{n-1}{(n!)^2}\left(\frac{\rho}{2}\right)^{2n}$$

$$\left. \times \quad \left(1 - \frac{\theta^2}{2n(\lambda - \lambda_0)}\right)^{n-2} u\left(\lambda - \lambda_0 - \frac{\theta^2}{2}\right)\right\},$$

where

$$\rho = 2\sqrt{ax(\lambda - \lambda_0)}, \quad (23)$$

and $u(x)$ is the unit step function

$$u(x) = \begin{cases} 1, & x > 0, \\ 0, & x < 0. \end{cases} \quad (24)$$

The solution has the form of a power series in the depth of penetration of the γ - radiation in the matter, multiplied by the exponential $\exp(-\tau_0 x)$ which describes the absorption of the unscattered radiation. Each term of the series has a simple physical meaning. The first term describes the radiation which has not undergone scattering. The second term represents the once-scattered radiation. It is clear from the relation between angle and wavelength that the succeeding terms represent the fractions of γ - radiation which have been Compton-scattered 2,3,... times.

As was to be expected, the maximum angle of deviation for twice-scattered radiation is $\theta^{(2)}_{max} = \sqrt{4(\lambda - \lambda_0)}$, for thrice-scattered radiation $\theta^{(3)}_{max} = \sqrt{6(\lambda - \lambda_0)}$, for radiation scattered n times – $\theta^{(n)}_{max} = \sqrt{2n(\lambda - \lambda_0)}$.

The intensity of the unscattered radiation is given by the product of two delta functions, that of the once-scattered radiation by a single delta function; the intensity of the twice-scattered radiation has a discontinuity at $\theta = \theta^{(2)}_{max}$, the intensity of the thrice-scattered radiation is continuous but has a discontinuous first derivative, the intensity of the radiation which has been scattered n times has a discontinuity in its $(n-2)$ nd derivative. The curve describing the intensity of the radiation which has been scattered n times naturally become smoother with increasing n. The angular distribution of γ-radiation which is scattered two or more times has a characteristic step function form.

These considerations about the continuity of the intensity of multiply scattered radiation are valid for any absorption coefficient.

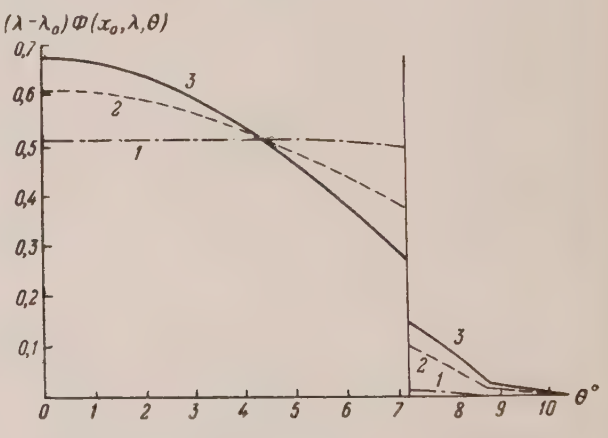

FIG. 3. Evolution of the angular distribution of scattered γ - radiation in the case of constant absorption coefficient. Normalized angular distributions are shown for radiation scattered more than once, at depths $\rho = 1.4$ and 6; $\lambda_0 = 1/34$, $\lambda = 1/30$. The discontinuities at $\theta = 7.1°$ and the kink at $\theta = 8.8°$ are caused, respectively, by the twice-and thrice-scattered radiation. With increasing depth of penetration, the distribution becomes smoother. Curve *1* - $\rho = 1$; *2* - $\rho = 4$; *3* - $\rho = 6$.

With increasing depth of penetration, the higher orders of scattering begin to be more and more important, the angular distribution becomes smoother and, as will be shown later, approaches a Gaussian $\exp[-\theta^2/2(\lambda-\lambda_0)]$.

The evolution of the angular distribution is shown in Fig 3.

To get the energy spectrum we must integrate Eq. (22) over all angles:

$$\Gamma_0(x,\lambda) = \delta(\lambda-\lambda_0)\,e^{-\tau_0 x} + \left(\frac{\lambda_0}{\lambda}\right)^{1.8}\frac{e^{-\tau_0 x}}{(\lambda-\lambda_0)}\left(\frac{\rho^2}{4}+\frac{1}{2}\left(\frac{\rho}{2}\right)^4 + \ldots + \frac{1}{n!\,(n-1)!}\left(\frac{\rho}{2}\right)^{2n}+\ldots\right) = e^{-\tau_0 x}\left\{\delta(\lambda-\lambda_0)+\left(\frac{\lambda_0}{\lambda}\right)^{1.8}\frac{\rho}{2(\lambda-\lambda_0)}I_1(\rho)\right\}, \tag{25}$$

where $I_1(\rho)$ is the Bessel function of first order and imaginary argument.

The physical meaning of the expansion (25) for the energy spectrum is the following: the n-th term refers to the n-times scattered radiation. This enables us to evaluate the contributions to the energy spectrum of multiply scattered radiations at different depths.

Thus, for $\rho = 1/2$, the intensity of once-scattered radiation makes up 96.95% of the total intensity of scattered radiation.

For $\rho = 1$, the once-scattered radiation contributes 88.5%, twice-scattered radiation gives 11.1%.

For $\rho = 2$, the intensity of once-scattered radiation drops to 62.9%, the intensities of twice- and thrice-scattered radiations are 31.4% and 5.2%.

For $\rho = 4$, the intensities of radiations scattered one, two, three and four times make up, respectively, 20.5, 41, 27.3 and 9.1% of the total intensity of scattered radiation.

For $\rho = 1$, it is already necessary to take into account the twice-scattered radiation. For initial energy $h\nu_0 = 12 m_0 c^2$ and final energy $h\nu = 10 m_0 c^2$, in carbon $\rho = 1$ corresponds to 44 cm, $\rho = 2$ to ~ 1.76 m.

As indications of the rapidity of convergence of the expansion (22), we may mention the following data: for $\rho = 2$ (an extremely great depth!), the third term is 4.5 times as small as the second, the fourth is 10.7 times as small as the third, etc.

In reference 2, an expression identical with Eq. (22) was obtained by another, more complicated, method. The physical meaning of the energy spectrum was not made clear in that reference.

5. VARIABLE ABSORPTION COEFFICIENT

Let us consider the case where the absorption coefficient is a quadratic function of the wavelength:

$$\tau(\lambda) = \tau_0 + \tau_1(\lambda-\lambda_0) + \tau_2(\lambda-\lambda_0)^2. \tag{26}$$

We can approximate the absorption coefficient by an expression of the type of Eq. (26) both for light and heavy elements in various energy regions, including the neighborhood of the minimum absorption coefficient (cf. Fig. 1).

For the distribution of γ - radiation in energy and angle, we get

$$\Gamma(x,\lambda,\theta) = \Gamma^0(x,\lambda,\theta) + \Gamma^1(x,\lambda,\theta) + \frac{e^{-\tau_0 x}}{2\pi}\left(\frac{\lambda_0}{\lambda}\right)^{1.8} \times\left\{\frac{a^2}{2!2}u\left(1-\frac{\alpha}{2}\right)x^2 + \left[\frac{a^3}{3!3\cdot 1!}\left(1-\frac{\alpha}{3}\right)u\left(1-\frac{\alpha}{3}\right) - \frac{a^2\tau_1}{8}u\left(1-\frac{\alpha}{2}\right) - \frac{a^2\tau_2}{96}(10+2\alpha-\alpha^2) \times(\lambda-\lambda_0)\,u\left(1-\frac{\alpha}{2}\right)\right](\lambda-\lambda_0)\,x^3+\ldots\right\}, \tag{27}$$

where $\alpha \approx \theta^2/2(\lambda-\lambda_0)$, $\Gamma^0(x,\lambda,\theta)$ is the angular distribution (4) for unscattered radiation, $\Gamma^1(x,\lambda,\theta)$ is the angular distribution (5) for once-scattered radiation. The energy spectrum is given by

$$\Gamma_0(x,\lambda) = \Gamma_0{}^0(x,\lambda) + \Gamma_0{}^1(x,\lambda) + \left(\frac{\lambda_0}{\lambda}\right)^{1.8}e^{-\tau_0 x} \times\left\{\frac{a^2}{2}(\lambda-\lambda_0)\,x^2 + \frac{1}{6}\left[\frac{a^3}{2} - \frac{3}{2}a^2\tau_1 - \frac{4}{3}a^2\tau_2(\lambda-\lambda_0)\right](\lambda-\lambda_0)^2\,x^3+\ldots\right\}, \tag{28}$$

where $\Gamma_0^0(x,\lambda)$ and $\Gamma_0^1(x,\lambda)$ are the energy spectra of unscattered and once-scattered radiation, respectively, and are easily gotten from Eqs. (4) and (5).

Actually two more terms were calculated in the expansions (27) and (28), but these have not been given because of their complexity.

The distribution in energy and angle for the case of constant absorption coefficient (22) is obtained from (27) for $\tau_1 = \tau_2 = 0$.

In light elements, over a wide energy interval, the absorption coefficient may be assumed to be

linearly dependent on wavelength: $\tau(\lambda) = \tau_0 + \tau_1 \times (\lambda - \lambda_0)$. Correspondingly, one should set $\tau_2 = 0$ in Eqs. (27) and (28).

In this case the expression for the energy spectrum is obtained in closed form:

$$\Gamma_0(x, \lambda) = e^{-\tau_0 x}\left\{\delta(\lambda - \lambda_0) + ax\left(\frac{\lambda_0}{\lambda}\right)^{1.8} \times {}_1F_1\left(1 - \frac{a}{\tau_1}; 2; -\tau_1(\lambda - \lambda_0)x\right)\right\}, \quad (29)$$

where ${}_1F_1(\alpha; \beta; x)$ is the confluent hypergeometric function. The energy spectrum for the case of a linear absorption coefficient was found in reference 7; our spectrum (29) coincides with the spectrum given there if we take into account the difference in the approximations used for the differential scattering cross section.

We now turn to a discussion of the general expression (27) for the distribution of scattered γ - radiation in angle and energy, and the energy spectrum (28).

First of all, it is easy to establish the physical meaning of these expansions: terms containing a to the nth power correspond to n-fold scattered radiation.

We have already dealt with the continuity properties of the intensity of the n-fold scattered radiation in Section 5: the intensity of the n-fold scattered radiation has a discontinuity in its $(n-2)$nd derivative; with increasing order of scattering, the angular distribution becomes smoother.

For energies less than that at which the absorption coefficient reaches its minimum value (left of the minimum in Fig. 1), the primary radiation is more penetrating than the scattered radiation.

Photons deflected through large angles will have less energy, and will therefore suffer stronger absorption than photons scattered through small angles. With increasing depth of penetration, the angular spread of the γ - radiation will become narrower than in the case of constant absorption coefficient. The expansions for the angular distribution and energy spectrum will converge rapidly even for relatively large depths of penetration.

If, on the other hand, the initial energy is above the energy for minimum absorption, the primary radiation will be softer than the scattered radiation. With increasing depth of penetration the angular distribution will become diffuse.

The expansions (27) and (28) will converge well only for not too large depths of penetration. The rapidity of convergence can be somewhat increased by introducing $\exp(-\tau_m x)$ in place of $\exp(-\tau_0 x)$ and making corresponding changes in all the expansions, which is not hard to do. Figure 4 shows a sketch of the normalized angular distribution of the radiation, having energy 10.2 mev ($\lambda = 1/20$), which has been scattered two or more times in copper, at a depth of 30 cm, if the initial energy was 12.75mev ($\lambda_0 = 1/25$). Here $\tau_0 = 0.30\ \text{cm}^{-1}$, $\tau_1 = -4\ \text{cm}^{-1}$; $\tau_2 = 200\ \text{cm}^{-1}$; $\tau_m = 0.28\ \text{cm}^{-1}$.

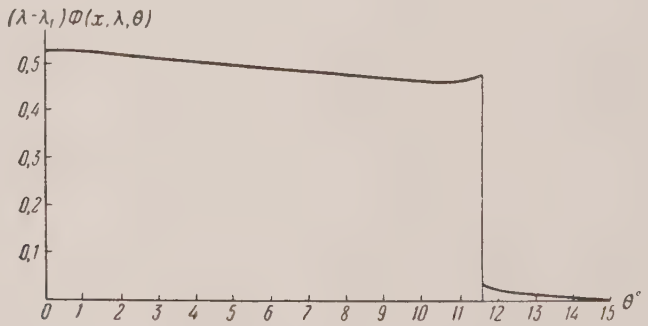

FIG. 4. Normalized angular distribution of γ -radiation of energy 10.2 mev, scattered two or more times in copper. The depth of penetration is 30 cm, the primary energy 12.75 mev.

[7] S. Z. Belen'kii, *Shower Processes in Cosmic Rays*, Gov't. Publ. House, Moscow-Leningrad, 1948

To characterize the convergence in this case, we give the following: the second term in the sum in (27) is 2.5 times smaller than the first, the

third term is 4.4 times smaller than the second, etc. At greater depths, the convergence is much poorer.

From Figure 4 we see that at $\theta = 11.5°$, (just before the twice scattered radiation drops out), the curve for the angular distribution actually rises a little, which can be explained by the methods given above.

The investigation of the angular distribution and energy spectrum of scattered γ - radiation at great depths of penetration in matter will be carried out in another paper.

In conclusion, I must express my profound gratitude to Prof. S. Z. Belen'kii for valuable suggestions, and to Acad. I. E. Tamm and Prof. E. L. Feinberg for supervising the work.

Translated by M. Hamermesh
225

SOVIET PHYSICS JETP VOLUME 2, NUMBER 2 MARCH, 1956

Angular Distribution of Gamma Rays at Great Depths of Penetration in Matter

V. I. OGIEVETSKII

(Submitted to JETP editor June 25, 1954)
J. Exper. Theoret. Phys. USSR 29, 464-472 (October, 1955)

The angular and energy distribution of γ-rays at great depths of penetration in matter is found for the cases of constant and linear dependence of the absorption coefficient on wavelength. The passage of γ-rays through an inhomogeneous medium is examined.

1. THE qualitative nature of the angular distribution at great depths of penetration depends strongly on the behavior of the γ-ray absorption coefficient. If the initial energy of the γ-ray is less than that at which the absorption coefficient is a minimum, then on the average, γ-rays scattered through small angles will be more penetrating than those scattered through large angles. With increase in the depth of penetration, the angular distribution will become narrower, or at any rate no wider. The small angle approximation applicable to scattering at energies of the order of several mev remains valid for great depths of penetration.

In the other case, where the absorption coefficient increases with energy, photons scattered through large angles will be more penetrating than those scattered through small angles. As the depth of penetration increases, the angular distribution will be smeared out, and the small angle approximation for each Compton scattering becomes incorrect.

In this respect, the results of reference 1, where the γ-ray energy spectrum at great depths of penetration is calculated using the small angle approximation, arouse some doubt.

In the present article, using the polynomial expansion of Spencer and Fano [2], the energy and angular distribution of γ-rays at great depths of penetration are found for the case of constant absorption coefficient (γ-rays of high energy in light elements, see reference 3), and for an absorption coefficient which increases linearly with wavelength. In these cases the small angle approximation is applicable, as can be seen from the final result.

In the case of constant absorption coefficient, the angular distribution tends to a gaussian one, although the approach to a gaussian distribution takes place significantly slower than indicated in reference 4. At the end of the article these results and those of reference 3 are generalized for an inhomogeneous medium. Below we shall use equations of radiation transport and the notation of the preceeding article [3].

[1] U. Fano, Phys. Rev. **76**, 739 (1949); U. Fano, H. Hurwitz, Jr. and L. V. Spencer, Phys. Rev. **77**, 425 (1950)

[2] L. V. Spencer and U. Fano, Phys. Rev. **81**, 464 (1951); J. Research, Nat. Bur. Stand. **46**, 446 (1951)

[3] V. I. Ogievetskii, J. Exper. Theoret. Phys. USSR **29**, 454 (1955); Soviet Phys. **2**, 312 (1956)

[4] L. Foldy, Phys. Rev. **81**, 395, 400 (1951)

2 In the preceeding article[3], the energy and angular distribution function of scattered γ-rays was found in the form of a rapidly converging series in powers of the depth of penetration, multiplied by an exponential which describes the damping of the most penetrating radiation.

The moments of the angular distribution may be obtained in closed form from Eq. (13) of reference 3, as will be shown below, for the cases of constant and linear dependence of the absorption coefficient on wavelength. It also can be shown that at great depths in the constant absorption coefficient case, the angular distribution will be close to the gaussian: $\exp[-\theta^2/2(\lambda-\lambda_0)]$.

It is well known[5] that the values of all moments of a distribution function in principle determine the function (the Stieltjes problem). However, since it is necessary to know every moment in a more or less simple analytic form, then in our case, as well as many others, this method of finding the distribution function from the moments is impractical.

As shown in reference 2, a knowledge of the moments frequently allows finding the distribution function as a rapidly converging series in some well-chosen set of orthogonal polynomials. The method of expansion in polynomials consists of the following[2].

Let the distribution function $f(x)$ be defined in the interval $(0, \infty)$. For an arbitrary function $\varphi(x)$, such that $\int_0^\infty \varphi(x)\, x^n\, dx$ exists for all n, it is possible to construct a set of polynomials $P_0(x)$, $P(x)$, . . . , orthonormal on the interval $(0, \infty)$ with weight $\varphi(x)$:

$$\int_0^\infty \varphi(x)\, P_n(x)\, P_m(x)\, dx = \delta_{mn}. \tag{1}$$

Let us examine the expansion of $f(x)$ in the following form

$$f(x) = \varphi(x) \sum_{n=0}^{\infty} b_n P_n(x). \tag{2}$$

From the values of the first m moments $a_m = \int_0^\infty f(x)\, x^m\, dx$, using the orthogonality of the polynomial set $P(x)$, it is possible to find the first m coefficients b_m of expansion (2).

It often happens that certain characteristics of the distribution function are known, or even that there is an approximate expression for $f(x)$. Physical considerations may sometimes determine the behavior of $f(x)$ for very large x, or, as in our case, the distribution function depends both on depth of penetration and on the energy, so that one may suppose that at great depths of penetration the angular distribution will be gaussian.

Let us choose a weighting function $\varphi(x)$ which reflects the properties of $f(x)$, and can thus be used as a first approximation to $f(x)$. Then the first and second terms of the polynomial expansion (2) can be considered corrections; the nth correction changes the nth moment, and does not affect the preceeding approximations. If the weight function has been well chosen, then the expansion (2) converges rapidly. Conversely, the rapidity of convergence of expansion (2) allows evaluation of the quality of the first approximation $\varphi(x)$.

The method of polynomial expansion has considerable generality, and can also be used in other branches of physics, for example, in the calculation of the spatial distribution of (cosmic-ray) shower particles.

3. In accordance with the above let us calculate the moments of the angular distribution. In the case of linear dependence of the absorption coefficient on wavelength $\tau(\lambda) = \tau_0 + \tau_1(\lambda - \lambda_0)$ the kinetic radiation transport equation in the variables s and l [reference 3, Eq. (13)] has the solution:

$$F_l(x, s) = \exp[-\tau_0 x] \exp\left\{a \int_0^x \frac{\exp\left[-\frac{l^2}{2(s-\tau_1 y)}\right]}{s-\tau_1 y}\, dy\right\}, \tag{3}$$

where the desired energy and angular distribution of the γ radiation are related to $F_l(x, s)$ by [Eq. (15), reference 3]

$$\Gamma(x, \lambda, \theta) = \left(\frac{\lambda_0}{\lambda}\right)^{1.8} \frac{1}{2\pi i} \int_{\delta-i\infty}^{\delta+i\infty} e^{(\lambda-\lambda_0)s}\, ds\, \frac{1}{2\pi} \int_0^\infty F_l(x, s)\, J_0(l\theta)\, l\, dl, \tag{4a}$$

$$F_l(x, s) = \int_{\lambda_0}^\infty d\lambda \left(\frac{\lambda}{\lambda_0}\right)^{1.8} \exp[-(\lambda-\lambda_0)s]\, ds\, 2\pi \times \int_0^\infty \Gamma(x, \lambda, \theta)\, J_0(l\theta)\, \theta\, d\theta. \tag{4b}$$

[5] Titchmarsh, *Theory of Fourier Integrals*

Direct Laplace and Hankel transformation (on variables s and l) without expansion in powers of x is very difficult[3]. However, the moments can be determined. Since

$$J_0(l\theta) = \sum_{m=0}^{\infty} \frac{(-1)^m (i\theta)^{2m}}{2^{2m}(m!)^2}, \tag{5}$$

then

$$\overline{\theta^{2n}}(x,\lambda) = 2\pi \int_0^{\infty} \Gamma(x,\lambda,\theta)\,\theta^{2n}\,\theta d\theta \tag{6}$$

$$= \left(\frac{\lambda_0}{\lambda}\right)^{1,8} \frac{1}{2\pi i} \int_{\delta-i\infty}^{\delta+i\infty} \exp[(\lambda-\lambda_0)s]\,ds$$

$$\times \left[(-1)^n 2^{2n} n! \left(\frac{\partial}{\partial(l^2)}\right)^n F_l(x,s)\right]_{l=0}$$

To make this convincing, the operator in the square brackets of Eq. (6) can be applied to Eq. (4b). A somewhat more difficult method to determine the moments in the case of a Hankel transform is used in reference 6, p. 167.

Substituting Eq. (3) into Eq. (6), and applying a Laplace transform, we obtain for the first few moments:

$$\overline{\theta^0}(x,\lambda) = e^{-\tau_0 x}\left\{\delta(\lambda-\lambda_0)\right. \tag{7a}$$

$$\left. + ax\left(\frac{\lambda_0}{\lambda}\right)^{1,8} {}_1F_1\left(1-\frac{a}{\tau_1};2;-\tau_1 x(\lambda-\lambda_0)\right)\right\},$$

$$\overline{\theta^2}(x,\lambda) = 2ax(\lambda-\lambda_0)\left(\frac{\lambda_0}{\lambda}\right)^{1,8} e^{-\tau_0 x} \tag{7b}$$

$$\times\ {}_1F_1\left(1-\frac{a}{\tau_1};2;-\tau_1 x(\lambda-\lambda_0)\right),$$

$$\overline{\theta^4}(x,\lambda) = 8ax(\lambda-\lambda_0)^2\left(\frac{\lambda_0}{\lambda}\right)^{1,8} e^{-\tau_0 x} \tag{7c}$$

$$\times\left\{{}_1F_1\left(1-\frac{a}{\tau_1};2;-\tau_1 x(\lambda-\lambda_0)\right)\right.$$

$$\left. + \frac{1}{2\tau_1(\lambda-\lambda_0)x}\left[{}_1F_1\left(2-\frac{a}{\tau_1};2;-\tau_1 x(\lambda-\lambda_0)\right)\right.\right.$$

$$\left.\left. - {}_1F_1\left(-\frac{a}{\tau_1};2;-\tau_1 x(\lambda-\lambda_0)\right)\right]\right\},$$

$$\overline{\theta^6}(x,\lambda) = 48ax(\lambda-\lambda_0)^3\left(\frac{\lambda_0}{\lambda}\right)^{1,8} e^{-\tau_0 x} \tag{7d}$$

$$\times\left\{\frac{1}{3!}\,{}_1F_1\left(1-\frac{a}{\tau_1};4;-\tau_1 x(\lambda-\lambda_0)\right)\right.$$

$$+ \frac{(3a-\tau_1)\,x(\lambda-\lambda_0)}{4!}$$

$$\times\ {}_1F_1\left(2-\frac{a}{\tau_1};5;-\tau_1(\lambda-\lambda_0)x\right)$$

$$+ \frac{(\lambda-\lambda_0)^2 x^2 (2\tau_1^2 - 9a\tau_1 + 6a^2)}{6!}$$

$$\left.\times\ {}_1F_1\left(3-\frac{a}{\tau_1};6;-\tau_1(\lambda-\lambda_0)x\right)\right\},$$

where ${}_1F_1(\alpha;\beta;z)$ is a degenerate hypergeometric function.

For the transition to the case of constant absorption coefficient $\tau(\lambda) = \tau_0$, substitute $\tau_1 = 0$ into (3). Then

$$F_l(x,s) = \exp[-\tau_0 x]\exp\left\{\frac{ax}{s}\exp\left(-\frac{l^2}{2s}\right)\right\}. \tag{8}$$

Using Eq. (6) for the moments of the angular distribution we obtain:

$$\overline{\theta^0}(x,\lambda) = e^{-\tau_0 x}\left\{\delta(\lambda-\lambda_0) + \left(\frac{\lambda_0}{\lambda}\right)^{1,8} 2\frac{ax}{\rho} I_1(\rho)\right\}, \tag{9a}$$

$$\overline{\theta^2}(x,\lambda) = 4\left(\frac{\lambda_0}{\lambda}\right)^{1,8} e^{-\tau_0 x}\frac{ax(\lambda-\lambda_0)}{\rho} I_1(\rho), \tag{9b}$$

$$\overline{\theta^4}(x,\lambda) = 16 e^{-\tau_0 x}\left(\frac{\lambda_0}{\lambda}\right)^{1,8}\frac{ax(\lambda-\lambda_0)^2}{\rho} \tag{9c}$$

$$\times\left\{I_1(\rho) - 2\frac{I_0(\rho)}{\rho} + 4\frac{I_1(\rho)}{\rho^2}\right\},$$

$$\overline{\theta^6}(x,\lambda) = 96\left(\frac{\lambda_0}{\lambda}\right)^{1,8} e^{-\tau_0 x}\frac{ax(\lambda-\lambda_0)^3}{\rho} \tag{9d}$$

$$\times\left\{I_1(\rho) - \frac{6}{\rho} I_1(\rho) + \frac{28}{\rho^2} I_1(\rho)\right.$$

$$\left. - \frac{64}{\rho^3} I_0(\rho) + \frac{128}{\rho^4} I_1(\rho)\right\},$$

where $I_\nu(\rho)$ is a ν-th order Bessel function of an imaginary argument, and as in reference 3, $\rho = 2\sqrt{ax(\lambda-\lambda_0)}$.

The moments (9) for the case of a constant absorption coefficient can also be obtained from the moments (7) by the limiting process $\tau_1 \to 0$. The zero moments are energy spectra, and were calculated in several ways in reference 3.

---

[6] S. Z. Belen'kii, *Avalanche Processes in Cosmic Rays*, Gov. Tech. Publishers, USSR, 1948

We note that the mean square of the angular deviation is:

$$\langle\theta^2\rangle = \frac{\overline{\theta^2}(x, \lambda)}{\overline{\theta^0}(x, \lambda)} = 2(\lambda - \lambda_0) \qquad (10)$$

and does not depend on the depth of penetration. This is also correct for an arbitrary absorption coefficient in the small angle approximation.

The moments have now been found, and to construct the distribution function we must choose a weighting function.

4. The angular and energy distribution functions for γ-radiation scattered two or more times, for the case of constant absorption coefficient, was found in the form [reference 3, Eq. (22)]:

$$\Gamma(x, \lambda, \theta) = \frac{1}{2\pi}\left(\frac{\lambda_0}{\lambda}\right)^{1,8} \frac{e^{-\tau_0 x}}{(\lambda - \lambda_0)^2} \sum_{n=2}^{\infty} b_n,$$

where

$$b_n = \frac{(n-1)}{(n!)^2}\left(\frac{\rho}{2}\right)^{2n} \times \left(1 - \frac{\theta^2}{2n(\lambda - \lambda_0)}\right) u\left(1 - \frac{\theta^2}{2n(\lambda - \lambda_0)}\right). \qquad (11)$$

At large depths of penetration ($\rho \gg 1$) the main contributions to expansion (11) come from terms with large n, and b_n may then be approximated as:

$$\tilde{b}_n = \frac{n-1}{(n!)^2}\left(\frac{\rho}{2}\right)^{2n} \exp\left\{-\frac{\theta^2}{2(\lambda - \lambda_0)}\right\}. \qquad (12)$$

Recalling that the Bessel function of an imaginary argument has the expansion [7]:

$$I_0(\rho) = \sum_{n=0}^{\infty} \frac{1}{(n!)^2}\left(\frac{\rho}{2}\right)^{2n}; \quad I_1(\rho) = \frac{dI_0(\rho)}{d\rho},$$

the distribution function (11) at great depths of penetration may be approximated by

$$\Gamma(x, \lambda, \theta) \sim \frac{1}{2\pi}\left(\frac{\lambda_0}{\lambda}\right)^{1,8} \frac{e^{-\tau_0 x}}{(\lambda - \lambda_0)^2} \times \left[\frac{\rho}{2} I_1(\rho) - I_0(\rho) + 1\right] \exp\left[-\frac{\theta^2}{2(\lambda - \lambda_0)}\right]. \qquad (13)$$

The substitution of $\tilde{b}_n$ for b_n is also possible for $\theta^2 / 2(\lambda - \lambda_0) \ll 1$, i.e., for angles considerably smaller than the mean square. The similarity of the angular distribution of multiply scattered radiation to a gaussian distribution was pointed out by Foldy [4], in whose paper the angular distribution is approximated in a different but equally valid way. From Eq. (13), or from the corresponding approximation of reference 4, it follows only that the angular distribution tends to a gaussian, while an investigation of this trend, as done by Foldy, is impossible if only because the approximate substitution is not single valued [in Eq. (13), for example, we immediately obtained a gaussian exponential]. As will be shown below, the gaussian distribution is attained considerably more slowly than claimed by Foldy.

5. Thus, to find the angular and energy distributions in the case of constant absorption coefficient at great depths of penetration, it is natural to set the weight function equal to

$$\theta \exp\left[-\theta^2 / 2(\lambda - \lambda_0)\right].$$

The corresponding set of orthonormal polynomials are those of Chebishev-Laguerre

$$L_n\left[\frac{\theta^2}{2(\lambda - \lambda_0)}\right]$$

$$L_n(\alpha) = \frac{1}{n!} e^{\alpha} \frac{d^n}{d\alpha^n}(e^{-\alpha}\alpha^n). \qquad (14)$$

With the help of the polynomial expansion method, using the moments (9), we obtain the γ-radiation distribution function in the form:

$$\Gamma(x, \lambda, \theta) = \frac{4a^2x^2}{\pi}\left(\frac{\lambda_0}{\lambda}\right)^{1.8} \times \exp\left[-\tau_0 x\right] \exp\left[-\frac{\theta^2}{2(\lambda - \lambda_0)}\right] \times \left\{\frac{1}{\rho^3} I_1(\rho) - \frac{2}{\rho^4}\left[I_0(\rho) - \frac{2}{\rho} I_1(\rho)\right] L_2\left(\frac{\theta^3}{2(\lambda - \lambda_0)}\right) - \frac{16}{\rho^5}\left[I_1(\rho) - \frac{4}{\rho} I_0(\rho) + \frac{8}{\rho^2} I_1(\rho)\right] \times L_3\left(\frac{\theta^2}{2(\lambda - \lambda_0)}\right) + \ldots\right\}. \qquad (15)$$

The term which describes unscattered radiation in (15) is omitted. The ratios of successive coefficients of Chebishev-Laguerre polynomials fall off as $1/\rho$, i.e., Eq. (15) is valid for $\rho \gg 1$. This is quite natural, since it is at great depths that the chosen weighting function (a gaussian exponent) closely describes the angular distribution. Expression (15) is valid for all materials in which, at the given energy, the absorption coefficient can be considered constant (the variable ρ depends on the constant a which varies with material).

Figure 1 shows normalized angular distributions of multiply scattered γ-radiation with, initial

[7] H Watson, *Theory of Bessel Functions*

energy 17.34 mev at depths of $\rho = 4.8$ and 16 at an energy 9.18 mev. The curve for $\rho = 4$ is not certain, since the expansion (15) converges poorly for this ρ.

Figure 1 clearly shows the trend to a gaussian distribution as the depth of penetration increases.

For $\rho = 4$, $\Gamma(x, \lambda, \theta)$ increase with θ for small θ. This is also, although to a lesser extent, true for $\rho = 8$. It is explained by the influence of single scattered radiation at these depths.

For $\rho = 16$ the angular distribution is already very close to gaussian.

Figure 2 shows the evolution of the angular distribution of multiply scattered γ-radiation with increasing depth of penetration. The curves for $\rho = 1$, 4 and 6 were calculated by the method used in reference 3, the curve for $\rho = 16$ was calculated by the method of polynomial expansion. A gaussian distribution is shown for comparison. Thus, for the case of constant absorption coefficient we have accounted for all depths.

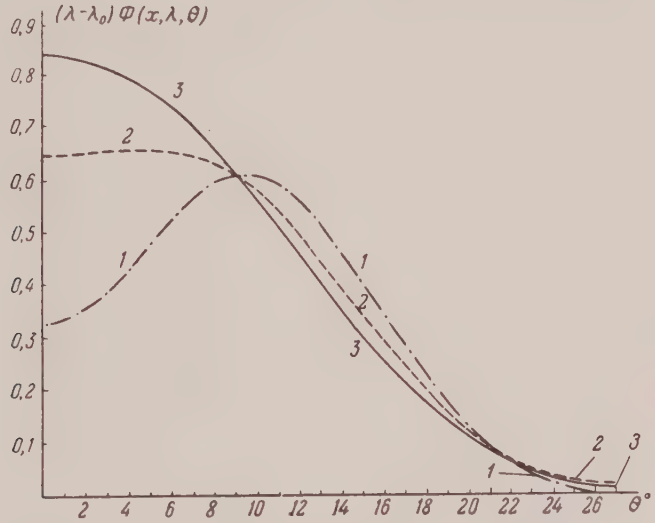

FIG. 1. Normalized angular distributions of multiply scattered γ-radiation of energy 9.18 mev. Initial energy 17.34 mev. *1.* $\rho = 4$; *2.* $\rho = 8$; *3.* $\rho = 16$.

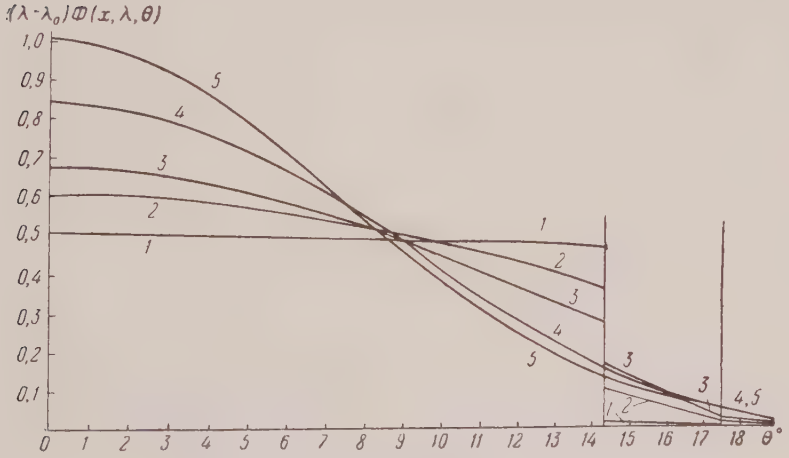

FIG. 2. Evolution of the angular distribution of γ-rays with increase in depth of penetration. Normalized angular distributions of 9 mev radiation scattered two or more times. Initial energy 12.5 mev. *1.* $\rho = 1$; *2.* $\rho = 4$; *3.* $\rho = 6$; *4.* $\rho = 16$; *5.* $\exp\left[-\theta^2/2(\lambda-\lambda_0)\right]$.

6. Let us now consider the case of a linear absorption coefficient $\tau(\lambda) = \tau_0 + \tau_1(\lambda - \lambda_0)$. Here, as was discussed in Sec. 1, the angular distribution does not tend to a gaussian with increase in the depth of penetration. But if τ_1 is positive, then the angular distribution is already gaussian, and if $\tau_1 \ll 1$, the distribution will not differ strongly from a gaussian. This gives the basis for the selection of the same weighting function as for the case of constant absorption coefficient: $\theta \exp[-\theta^2/2(\lambda - \lambda_0)]$. The final result will allow us to judge the success of this choice.

The moment expression (7) is very clumsy; since we are interested in great depths, we shall use an asymptotic expansion of the moments in our calculation. This is obtained from the known asymptotic expansion of the degenerate hypergeometric function [8]

$$
\begin{aligned}
{}_1F_1(\alpha;\gamma;z) \sim{}& \frac{\Gamma(\gamma)}{\Gamma(\gamma-\alpha)}(-z)^{\alpha} \\
&\times {}_2F_0(\alpha;\ \alpha-\gamma+1;\ -z) \\
&+ \frac{\Gamma(\gamma)}{\Gamma(\alpha)} e^z z^{\alpha-\gamma} {}_2F_0(1-\alpha;\ \gamma-\alpha;\ z),
\end{aligned}
\tag{16}
$$

where $\Gamma(\gamma)$ is the gamma function, and

$$
{}_2F_0(\alpha;\gamma;z) = 1 + \frac{\alpha\gamma}{1!\,z} + \frac{\alpha(\alpha+1)\gamma(\gamma+1)}{2!\,z^2} + \ldots
$$

has asymptotic meaning (the series diverges for any z as long as α or γ are not negative integers).

In this case we obtain the energy and angular distributions at great depths in the form:

$$
\begin{aligned}
\Gamma(x,\lambda,\theta) = {}& \left(\frac{\lambda_0}{\lambda}\right)^{1.8} \frac{ax\exp[-\tau_0 x]}{2\pi(\lambda-\lambda_0)} \frac{v^{a/\tau_1-1}}{\Gamma\left(1+\frac{a}{\tau_1}\right)} \\
&\times \left\{1 + \frac{a(a-\tau_1)}{\tau_1^2 v} + \frac{a(a^3-4a^2\tau_1+5a\tau_1^2-2\tau_1^3)}{2\tau_1^4 v^2}\right. \\
&- \left[\frac{\tau_1}{2(a+\tau_1)} + \frac{a\tau_1}{2\tau_1^2 v} + \frac{a\tau_1(a^2-a\tau_1-2\tau_1^2)}{4\tau_1^4 v^2}\right] \\
&\times L_2\left(\frac{\theta^2}{2(\lambda-\lambda_0)}\right) \\
&- \left[\frac{4\tau_1^2}{3(a+\tau_1)(a+2\tau_1)} + \frac{4a\tau_1^2}{3(a+\tau_1)\tau_1^2 v} + \frac{2a\tau_1^2(a-\tau_1)}{3\tau_1^4 v^2}\right] \\
&\left. \times L_3\left(\frac{\theta^2}{2(\lambda-\lambda_0)}\right) + \ldots\right\},
\end{aligned}
\tag{17}
$$

where

$$
v = \tau_1(\lambda - \lambda_0)x.
$$

In contrast to the case of constant absorption coefficient, the coefficient ratio of adjacent Chebishev-Laguerre polynomials in Eq. (17) does not tend to zero with increasing x. The reason for this has already been considered: photons scattered through large angles have a larger absorption probability than photons scattered through small angles. The "homogeneity" of absorption is destroyed, and the angular distribution must fall off more steeply than a gaussian. Similarly, if $0 < \tau_1 < a$ expression (17) can be used. Thus if 1.5 mev γ-rays are incident on carbon ($\lambda_0 = 1/3$, $\tau_1 = 0.15\ \text{cm}^{-1}$), then at a depth of $v = 20$, the coefficient of the second polynomial is less than one sixth the coefficient of the zeroth polynomial.

The condition $\tau_1 < a$ is satisfied in a wide energy interval for light elements, in the interval 0.5-3 mev for medium elements, and not at all for the heavy elements. Figure 3 shows a graph of the normalized angular distributions at two depths of penetration. The small rise in the $v = 10$ curve depends on singly scattered radiation.

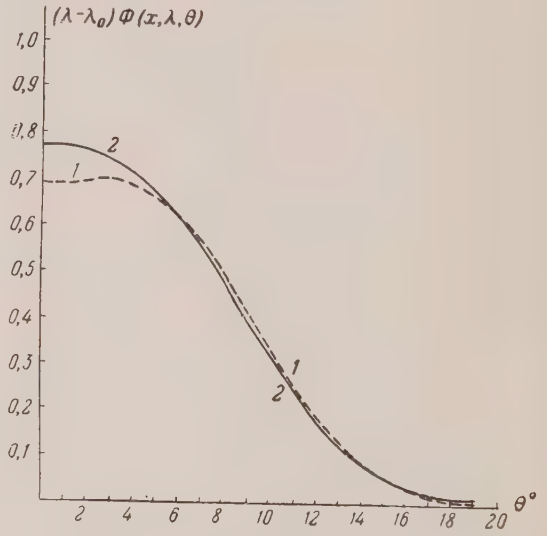

FIG. 3. Normalized angular distributions of scattered γ-radiation of energy 2.8 mev in carbon at depths of $v = 10$ and $v = 40$. Initial energy is 3 mev, $\tau_1 = 0.12\ \text{cm}^{-1}$. *1.* $v = 10$. *2.* $v = 40$.

7. In the above, and in reference 3 we have considered the propagation of γ-rays in a homogeneous medium. The problem of multiple γ-ray scattering in an inhomogeneous medium is of interest (the atmosphere, transition effects at counter walls, etc.).

[8] L. D. Landau and E. M. Lifshitz, *Quantum Mechanics*, Gov. Publisher USSR, 1948, p. 557

Let us examine the passage of a parallel monochromatic bundle of γ-rays through a medium which consists of plane parallel layers of various materials; the absorption coefficient can be considered independent of energy in each material. For simplicity let the medium consist of two layers: the first of material A ($\tau_0 = \tau_A$, $a = a_A$) thickness and the second of material B ($\tau_0 = \tau_B$, $a = a_B$). The absorption coefficient and constant a both depend on the material, and can be conveniently written:

$$a = a_A + (a_B - a_A)\, u(x - x_A), \qquad (18)$$

$$\tau_0 = \tau_A + (\tau_B - \tau_A)\, u(x - x_A);$$

where $u(x)$ is a unit step function.

The kinetic equation in variables l and s [reference 3, Eq. (13)] is written:

$$\frac{\partial F_e(x, s)}{\partial x} \qquad (19)$$

$$+ [\tau_A + (\tau_B - \tau_A)\, u(x - x_A)]\, F_e(x, s)$$

$$= \frac{a_A + (a_B - a_A)\, u(x - x_A)}{s}\, F_e(x, s) + \delta(x).$$

The solution of this equation differs from Eq. (8) in that the exponential describing the damping of the unscattered radiation has the argument $\tau_A x_A + \tau_B (x - x_A)$ instead of $\tau_0 x$, while the exponential describing the scattered radiation has the argument $a_A x_A + a_B (x - x_A)$ instead of ax. Analogously, if the medium consists of layers: A thickness x_A, B thickness x_B, . . . , M thickness x_M, then substitutions must be made in the homogeneous medium equations:

$$\tau_A x_A + \tau_B x_B + \ldots + \tau_M x_M \text{ for } \tau_0 x$$

and

$$a_A x_A + a_B x_B + \ldots + a_M x_M \text{ for } ax. \qquad (20)$$

Thus, in the case of constant absorption coefficient, the final result of multiple scattering does not depend on the order of layers, and the layers may be shuffled. This is not true for an arbitrary absorption coefficient.

Let us now examine the passage of γ-rays through a medium whose density is a function of the depth of penetration x: $\rho(x) = f(x)$. The atmosphere will serve as an example. Since the absorption coefficient and the number of electrons are both proportional to the density of the material in the energy region where Compton scattering predominates over photoeffect and pair production, we can write

$$\tau(\lambda, x) = \overline{\tau(\lambda)}\, f(x); \quad a(x) = \bar{a} f(x). \qquad (21)$$

It is easy to show that in this case we may use the results for a homogeneous medium with the substitutions $\overline{\tau(\lambda)}$ and $\bar{a}$ for $\tau(\lambda)$ and a, and $z = \int_0^x f(x)\, dx$ for the depth of penetration x.

In conclusion, I would like to express gratitude to Prof. C. Z. Belen'kii for valuable comments, and to Academician I. E. Tamm and Prof. E. L. Feinberg for interest in this work.

Translated by G. L. Gerstein
226

Letters to the Editor

On the Theory of Langmuir Probes

IU. M. KAGAN AND V. I. PEREL'
Karelo-Finnish State University
(Submitted to JETP editor March 9, 1955)
J. Exper. Theoret. Phys. USSR 29, 261-263
(August, 1955)

IN the last few years there have appeared a number of articles[1-3] in which several premises of the theory of Langmuir probes have been subject to criticism. The purpose of the present paper is to compare Langmuir's theory with the exact theory of spherical probes developed in reference 4 for low pressures and for the condition of negative probe potential. Under these conditions, Langmuir's basic assumptions[5,6] are as follows:

1) The actual potential distribution is replaced by potential $\varphi(r)$ which differs from zero in a certain range of radius r_s (in the sheath), and equals zero in the remaining space. Plasma outside the sheath is undisturbed.

2. Within the sheath there are only ions. This determines the sheath boundary. Potential distribution inside the sheath is in accordance with the three-halves-power law with zero initial velocities.

3. Pressure is assumed to be low and, for given probe potential, whether a particle arrives at the probe is determined by the threshold parameter p and by particle velocity at the sheath boundary. If r_m is the minimum distance from the probe reached by an ion, then

$$p^2(r_m v) = r_m^2\left[1 - \frac{2e\varphi(r_m)}{Mv^2}\right]. \qquad (1)$$

where e and M are ion charge and mass. In the case of attraction, $e\varphi(r_m) < 0$. In accordance with assumption 1, $p = r_m$ when $r_m > r_s$. Depending on $\varphi(r)$ and v, the relation between p and r_m may be monotonic or nonmonotonic. This is shown in the graph for a fixed $\varphi(r)$ and for several values of v, where curves a, b, c, d correspond to descending values of v. The graph shows that above a certain velocity the curves exhibit a minimum which lies within the sheath. The variable p which is determined by Eq. (1) acts as a target parameter only to the minimum point; and only the right side of the $p(r_m)$ curves has a physical meaning. If the target parameter is smaller than the minimum value of Eq. (1), then the motion is of threshold value, and the particles are captured by the probe. The radius of the threshold sphere, r_0, (i.e., the value of r_m at which Eq. (1) is at a minimum), differs from probe radius and is a function of velocity v.

It is shown in reference 4 that for any (monotonic) potential, current into the probe is determined by the minimum value of Eq. (1), and equals

$$F = \int_0^\infty 4\pi p^2(r_0 v)\, f(v)\, v^3\, dv, \qquad (2)$$

where $f(v)$ is the number of ions in a unit phase volume at a large distance from the probe.

In Langmuir theory[5], current to the probe is determined by probe potential and sheath dimensions, and is independent of potential within the sheath. This is a consequence of the assumption that when the square of the radial velocity of an ion, formally calculated on the basis of the law of conservation, is not negative on the probe surface, then it is also not negative elsewhere. This in turn leads to the assumption that Eq. (1) has a minimum on the probe surface, i.e., that there is no threshold motion. However, in Langmuir's model with a sheath, Eq. (1) is known not to be monotonic, and its minimum is not located on the probe, at least at sufficiently small velocities (threshold motion). This contradiction in Langmuir theory becomes obvious from the fact that, to assure a particle reaching the probe, aside from the requirement that the square of radial velocity on the probe surface must be positive, the additional independent requirement is needed that radial velocity on sheath surface must be positive. The first condition is equivalent to p^2 being smaller than the right side of Eq. (1) on the surface of the probe; and the second, that p^2 is smaller on sheath surface. If the minimum value of Eq. (1) occurred on the probe, then the second condition would be a consequence of the first condition. Actually, during derivation, occasions arise when the second condition is met but not the first. This is especially clearly brought out in the form of Langmuir theory used in reference 6, where the expression for ion probe current is based on the assumption that all ions may be divided into two groups:

$$v > \sqrt{-2e\varphi(a)/M\left[\left(\frac{r_s}{a}\right)^2 - 1\right]} \qquad (3a)$$

(for these velocities an absence of threshold motion is assumed, i.e., $r_0 = a$); and

$$v < \sqrt{-2e\varphi(a)/M\left[\left(\frac{r_s}{a}\right)^2 - 1\right]} \qquad (3b)$$

(for these velocities it is assumed that the motion has a threshold value, and that the threshold sphere coincides with sheath boundary r_s).

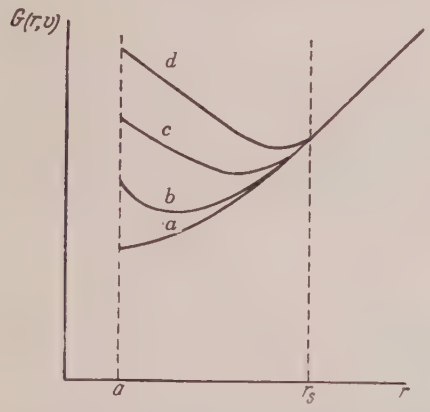

Condition (3a) leads to the conclusion that $p(r_s) > p(a)$. Curves a and b in the graph satisfy this condition. However, with curve b there is threshold motion, and $r_0 > a$. From condition (3b) it follows that $p(r_s) < p(a)$. Curves c and d satisfy this requirement. It is obvious from the curves that in this case $r_0 < r_s$. Since for curves of type b, $p^2(r_0 v) < p^2(av)$, and for curves of type c, $p^2(r_0 v) < p^2(r_s v)$, therefore Eq. (2) shows that calculation of current F in a Langmuir model with a sheath, using the above method, results in values of ion probe current known to be too high. As a matter of fact, even calculations using Langmuir's equations result in ion current values smaller than those obtained by experiment. This is due to the fact that assumption 1, which does not allow for a field outside the sheath, and which assumes that ion velocity at the sheath boundary is equal to velocity at a large distance from the probe, constitutes a poor approximation for ions. An approximate expression for ion current, taking into account the field outside the sheath, is given in reference 3.

Assumption of three-halves-power law potential distribution inside the sheath is proper when ions inside the sheath are moving radially. Since, in Langmuir's model, the threshold sphere lies within the sheath, use of the three-halves-power law is not proper. At the same time, for assumptions made in reference 3, the threshold sphere lies outside the charged sheath, and three-halves-power law can be applied.

[1] R. Boyd, Proc. Roy. Soc. (London) A201, 329 (1950)
[2] F. Wenzl, Z. angew. Phys. 2, 59 (1950)
[3] Iu. M. Kagan and V. I. Perel', Dokl. Akad. Nauk SSSR 91, 1321 (1953)
[4] Iu. M. Kagan and V. I. Perel', Dokl. Akad. Nauk SSSR 95, 765 (1954)
[5] H. Mott-Smith and I. Langmuir, Phys. Rev. 28, 727 (1952)
[6] V. L. Granovskii, *Electric Current Flow in a Gas*, GITTL, 1952

Translated by K. V. Amatneek
189

Adiabatic Process at High Temperatures

I. L. Aptekar' and B. L. Timan
Dneperpetrovsk Mining Institute

(Submitted to JETP editor November 22, 1954)
J. Exper. Theoret. Phys. USSR 28, 758-759 (June, 1955)

In connection with the effect of thermal ionization on the thermal properties of gases at high temperatures[1], it is of interest to consider an an adiabatic process, taking the thermal ionization into account. In this case, the original equation for an adiabatic process will have the following form:

$$pdV + dU' + I_1 dN_1 = 0 \qquad (1)$$

where dV is the increase in volume, I_1 is the energy of single ionization, dU' is the increase in internal energy of the gas, dN_1 the increase in the number of ions in the heating of the gas.

The expression pdV can be found from the Mendeleev-Clapeyron equation:

$$pdV = \frac{(N + N_1)\, kT dV}{V}. \qquad (2)$$

The internal energy of the gas can be written in the following form:

$$U' = 3/2\,(N + N_1)kT. \qquad (3)$$

Denoting the degree of ionization by $x = N_1/N$ and substituting Eqs. (2), (3) in Eq. (1), we obtain the equation

$$\frac{3}{2}(1+x)\frac{dT}{T} + \left(\frac{3}{2} + \frac{I_1}{kT}\right)dx + (1+x)\frac{dV}{V} = 0. \qquad (4)$$

At the same time, the formula of Sack, which characterizes the degree of ionization of the gas at a given temperature and pressure, can be written in the form[2]

$$\frac{1-x^2}{x^2} = p\frac{c'}{T^{5/2}}\exp\left\{\frac{I_1}{kT}\right\} = \frac{(1+x)\,c''}{VT^{3/2}}\exp\left\{\frac{I_1}{kT}\right\}.$$

Taking the logarithm of both sides and differentiating this expression, we get

$$-\frac{dx}{1-x} - \frac{2dx}{x} + \frac{3}{2}\frac{dT}{T} + \frac{dV}{V} + \frac{I_1}{kT^2}dT = 0. \quad (5)$$

Multiplying this equation by $(1+x)$ and subtracting the result from Eq. (4), we have

$$\frac{1+x}{1-x}dx + \frac{2dx}{x} + \left(\frac{7}{2} + \frac{I_1}{kT}\right)dx - \frac{I_1 dT}{kT^2}(1+x) = 0. \quad (6)$$

Upon integrating this equation, we find the dependence on temperature of the degree of ionization of the gas in an adiabatic process:

$$\frac{5}{2}x - 2\ln\frac{(1-x)}{x} + \frac{I_1}{kT}(1+x) = C \quad (7)$$

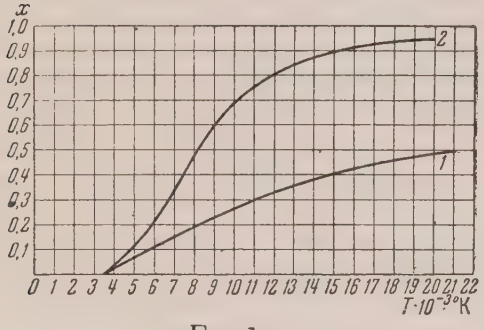

FIG. 1

Curve 1 in Fig. 1 represents the dependence on temperature of the degree of ionization x of Cs vapor for an adiabatic process, taking ionization during the process into account. For comparison, there is drawn in the same figure the dependence on temperature of the degree of ionization, if the pressure is expressed in terms of the temperature in Sack's formula, making use of the equation for an adiabatic process without taking ionization into account. It is evident that curve *1*, which corresponds to the actual case (with ionization), lies below curve *2*, the calculation of which ignored the effect of ionization during the process.

We now investigate how the thermal ionization during an adiabatic process affects the dependence of the pressure on the temperature. From Sack's equation it follows that

$$\frac{p}{T^{5/2}} = \frac{1}{c'}\frac{1-x^2}{x^2}\exp\left\{-\frac{I_1}{kT}\right\}.$$

Expressing the ratio I_1/kT by x from Eq. (7), and substituting in the latter equation, we get

$$\frac{p}{T^{5/2}} = \frac{x^{2/(1+x)}}{x^2}\frac{(1-x^2)}{(1-x)^{2/(1+x)}} \times \exp\left\{\frac{5}{2}x\right\}\frac{1}{c'C^{1/(1+x)}}. \quad (8)$$

This equation characterizes the effect of ionization on the temperature dependence of the pressure during an adiabatic process.

We shall now consider Eq. (8). As $x \to 0$, Eq. (8), as should be expected, undergoes a transition to the usual equation for an adiabatic process:

$$\frac{p}{T^{5/2}} = \frac{1}{Cc'} = \text{const}. \quad (9)$$

As $x \to 1$, which corresponds to complete ionization, Eq. (8) becomes

$$\frac{p}{T^{5/2}} = 2\frac{1}{C^{1/2}c'}\exp\left\{\frac{5}{2}\right\}. \quad (10)$$

It is clear from the latter equation that, at a high degree of ionization of the gas, a much lower temperature corresponds to a given pressure in comparison with the case which obtains in the absence of ionization.

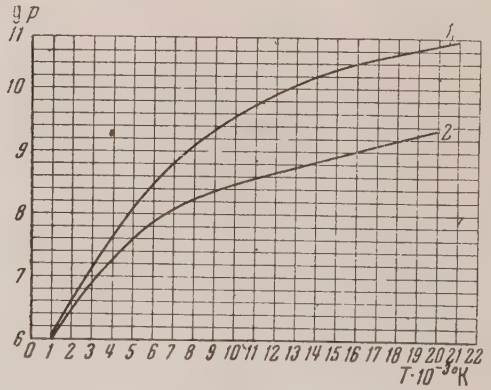

FIG. 2

We compare the dependence $p(T)$ from Eq. (8) with Eq. (9). The dependence of $p(T)$ is plotted in Fig. 2. Curve *1* corresponds to Eq. (8), curve *2*, to Eq. (9). As can be seen from Fig. 2, the curve which corresponds to Eq. (8) lies above the curve corresponding to the adiabatic process, for which ionization is not taken into account. This is evidently explained by the fact that with an

increase in temperature in the adiabatic process, the number of particles in the system increases as a result of the ionization. This effect, in turn, increases the pressure of the gas. The figure shows that at high temperatures, the pressure in an adiabatic process, computed by Eq. (9) is almost 100 times smaller than the pressure computed by the equation in which ionization has been considered. This circumstance should be very significant for the consideration of adiabatic processes in gases taking place at high temperatures.

[1] B. L. Timan, J. Exper. Theoret. Phys. USSR **27**, 2 (1954)

[2] L. D. Landau and E. M. Lishitz, *Statistical Physics*, GITTL, Moscow, 1952

Translated by R. T. Beyer
144

Stable Dipole Moment of Aerosol Particles

A. A. SPARTAKOV AND N. A. TOLSTOI
Leningrad Technical Institute

(Submitted to JETP editor May 12, 1955)
J. Exper. Theoret. Phys. USSR **29**, 385
(September, 1955)

NEW methods of investigation of electro-optical phenomena in hydrophobic colloids[1,2] based on the measurement of the modulation of light passing perpendicularly to the lines of the electric field through a parallel plate condenser (Fig. 1, *b, c*) upon which a square-wave voltage is impressed, show that the colloidal particles in aqueous media possess a stable dipole moment of a very considerable magnitude[2]. It is assumed that this stable dipole moment is caused by spontaneous orientation of water molecules possessing a stable dipole adsorbed on the surface of the particle[2]. The unipolarity (in the mean effect) of this orientation makes it possible to treat the film of water adsorbed on the particle as a surface electret[2].

We have carried out an analogous experiment with an aerosol. Light, passing through 3–5 cm of tobacco smoke is modulated by the field of a square-wave voltage (see Figure). The modulation curve shows a periodic decrease in the transparency of the medium. This effect can be observed for any direction of polarization of light. Each reversal of the field produces a reiteration of the modulation wave. Since the field intensity E in the condenser (of the order of 300 v/cm) is of constant magnitude ($E^2 = \text{const}$), the re-orientation of smoke particles brought about by light modulation is possible only when the smoke particle is itself polar, i.e. it possesses a stable dipole moment.

The electro-optical properties of smoke may therefore be similar to those of hydrophobic colloids. It should be mentioned that, for the case of smoke, modulation of light is maintained up to much higher frequencies than is the case for an aqueous colloid. Undoubtedly, this is connected with the difference in viscosity of the respective media. It is our opinion that the origin of the stable dipole moment of smoke particles is likewise connected with the orientation of adsorbed polar molecules on the surface of particles. The influence of moisture on the magnitude of the observed effect implies that, in this case also, polar molecules of water are involved.

The establishment of polarity of smoke particles may be important in the explanation of aggregation mechanism of uncharged particles in smoke.

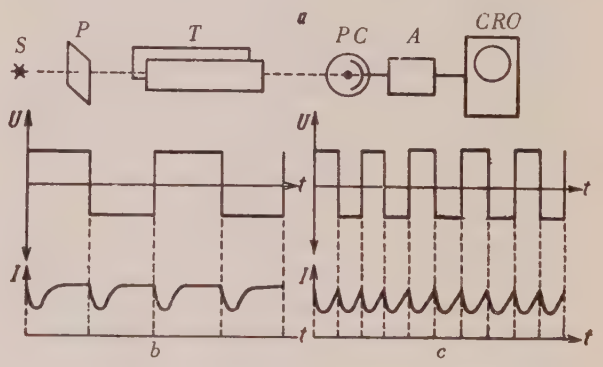

FIG. 1. *a)* Simplified diagram of the experimental set-up: S-light source; P-polaroid; T-tank with the parallel plate condenser, filled with tobacco smoke; PC-photoelectric cell; A-amplifier; CRO-cathode ray oscilloscope (Russian type EO-7).

b) Modulation of light by low-frequency square-wave (10-100 cps): U-voltage on the condenser; I-intensity of passing light.

c) Modulation of light by high-frequency square-wave (~ 1000 cps).

[1] N. A. Tolstoi and P. P. Feofilov, Dokl. Akad. Nauk SSSR **66**, 617 (1949)

[2] N. A. Tolstoi, Dokl. Akad. Nauk SSSR **100**, 893 (1955)

Translated by H. Kasha
214

Fluctuating Structure in the Absorption Spectrum of Ruby

B. N. Grechushnikov and P. P. Feofilov
Institute of Crystallography
Academy of Sciences, USSR
(Submitted to JETP editor May 19, 1955)
J. Exper. Theoret. Phys. USSR 29, 384
(September, 1955)

IT was theoretically demonstrated in the works of Pekar and Krivoglaz[1,2] that the form of the light absorption band by admixtures in the dielectrics can be expressed, within the limits of definite assumptions, as a product of two functions of frequency. The first factor, presented as a function of frequency, produces a smooth, bell-like curve and delineates the general contours of the absorption spectrum. The second factor, representing a rapidly oscillating function, shows the "structure" of the absorption band. In a case in which the dispersion of frequencies of normal fluctuations is small, the absorption band breaks into a series of fine lines. These are separated from one another by a distance ω_0, which is equal to the threshold frequency of longitudinal polarization fluctuations.

The absorption spectrum of ruby at the temperature of liquid nitrogen has been investigated in reference 3. Earlier, the influence of temperature upon the ruby spectrum had been studied by Gibson[4]. However, since the determinations obtained in these works pertained to separate wavelengths, the structure of the absorption spectrum did not become apparent. Photographs of the absorption spectrum at the temperature of liquid nitrogen have shown that the structure is clearly discernible at the long wave side of the broad absorption band. The graph shows the absorption spectrum of ruby obtained with a spectrograph ISP-51 at the temperature of liquid nitrogen and raised in optical density by means of blackening. At the long wave side of the absorption band we can see five subordinate maxima (indicated by arrows), separated by almost identical distances from one another. These are: 16,780, 16, 900, 17,200, 17,410 and 17,640 mc^{-1}. Distances between the adjacent maxima are on the average 215 cm^{-1}.

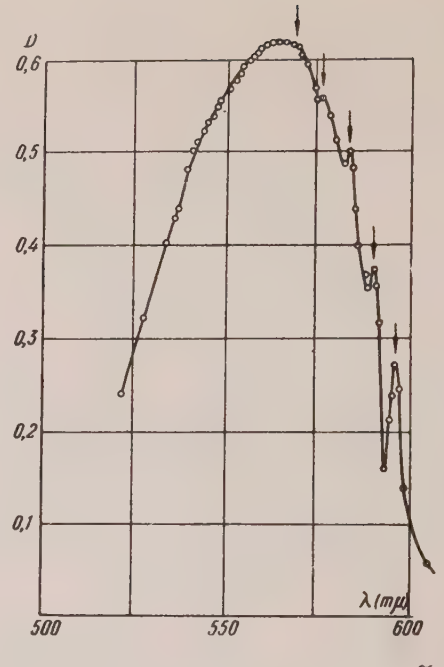

Absorption spectrum of ruby (Al_2O_3 --- 0.1% Cr_2O_3) for an ordinary wave, at the temperature of – 190° C.

The structure of the wide absorption band appears only in the spectrum of the ordinary wave. That is, polarization in the narrow absorption bands is the same as in the basic wide band. As the temperature increases, the subordinate maxima gradually fade and disappear completely at – 100° C. The structure does not appear at the short wave side of the wide absorption band. The distance between the subordinate maxima is comparable to the fluctuation frequency of 194 cm^{-1} discovered in the infrared absorption spectrum of ruby[5].

In this way, the observed structure of the wide absorption band of ruby can be construed to be the result of interaction between optical electrons at the "center of absorption" and the fluctuations of crystalline lattice.

---

[1] S. I. Pekar, J. Exper. Theoret. Phys. USSR 22, 641 (1952)

[2] M. A. Krivoglaz and S. I. Pekar, Trudy Fiz. Inst. Akad. Nauk SSSR 4, 37 (1954)

[3] B. N. Grechushnikov, Dokl. Akad. Nauk SSSR 99, 707 (1955)

[4] K. S. Gibson, Phys. Rev. 8, 38 (1916)

[5] Krishnan, Proc. Ind. Soc. 26A, 6, 450 (1947)

Translated by R. G. Huzarski

Temperature Dependence of the Relaxation Time of Luminescence of Platino Cyanides of Barium and of Potassium, and of Fluorite Activated with Europium

N. A. Tolstoi, A. M. Tkachuk
and N. N. Tkachuk

(Submitted to JETP editor May 27, 1955)
J. Exper. Theoret. Phys. USSR 29, 386-387
(September, 1955)

BY employing the method of the ultra-taumeter[1], we have succeeded in investigating for the first time the kinetics of the photoluminescence of several substances with relaxation time lying in the time interval of 10^{-7} - 10^{-5} sec. It was the absence of data pertaining to the relaxation of photoluminescence that had at one time caused Vavilov to call this interval the "white spot" in the luminescence[2].

1. Platino Cyanide of Barium (yellow-green variety, commercial product). The relaxing and lighting of luminescence are exponential $[I_{rel} \sim I_0 e^{-t/\tau}, I_{light} \sim I_0(1 - e^{-t/\tau})]$. Within the range of temperatures from - 183° C to - 80° C, $\tau = 8 \times 10^{-7}$ sec = const. Brightness of the luminescence is also constant. As the temperature continues to increase, the substance loses two molecules of its water of crystallization and ceases (irreversibly) to luminesce.

2. Platino Cyanide of Potassium (commercial product). Relation of τ and I_0 to the temperature is shown in Fig. 1. It can be seen here that τ and I_0 do not follow the simple law of relaxation $I_0 \sim \tau \sim 1/(1 + Ce^{-U/kT})$.

Light spectra of both platino cyanides are shown in Fig. 2. As the temperature decreases, the light band of each substance narrows and moves toward the long wave side.

Khvostikov[3], working on the basis of his measurements of light depolarization in solutions, arrived indirectly at the value of τ for platino cyanide of potassium. According to him, when the relaxation does not occur, $\tau = 5.6 \times 10^{-9}$ sec. It can be seen from Fig. 1 that direct measurements differ greatly from his value.

3. Calcium Fluoride activated with bivalent europium[4], $CaF_2(Eu^{++})$, produces a purely exponential luminescence. Relation of τ and I_0 to the temperature is shown in Fig. 3. Ratio of I_0/τ shows no dependence on the temperature. Both I_0 and τ follow the simple law of relaxation. Activation energy of relaxation is $U = 0.75$ ev.

For all three substances the brightness of luminescence is proportional to the intensity of

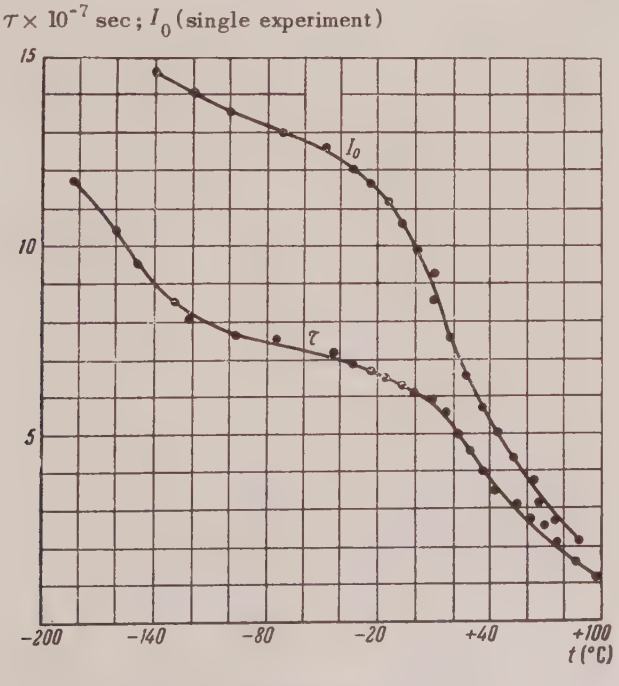

FIG. 1. $K_2[Pt(CN)_4] \cdot 3H_2O$

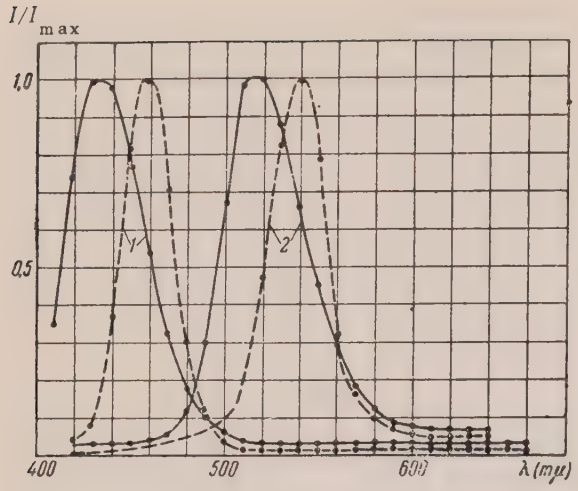

FIG. 2. *1.* Potassium; *2.* Barium. Continuous curves were obtained at $t = 20°$ C, curves shown in dashes were obtained at $t = -183°$ C.

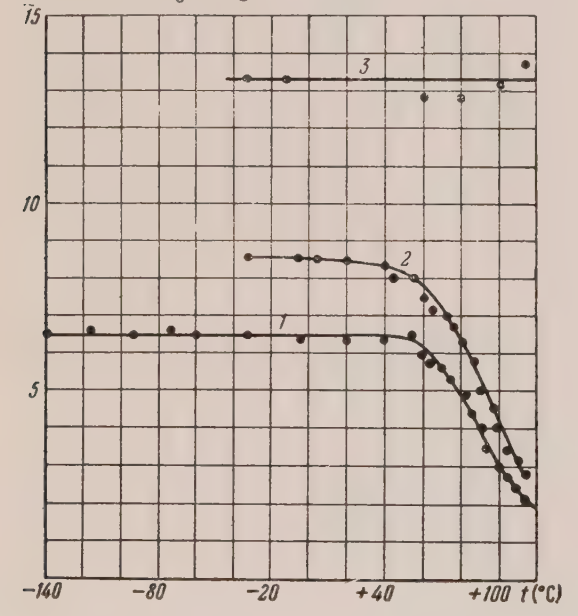

FIG. 3. $CaF_2(Eu^{++})$. *1.* τ; *2.* I_0; *3.* I_0/τ.

excitation, E, while the time necessary for relaxing and lighting does not depend on E. It can be seen from the above that in the case of all three substances we are dealing with a monomolecular process representing a relatively slow fluorescence.

[1] N. A. Tolstoi, Dokl. Akad. Nauk SSSR 102, 935 (1955)

[2] S. I. Vavilov, Izv. Akad. Nauk SSSR, Ser. Fiz. **13**, 216 (1949)

[3] I. A. Khvostikov, Trudy G.O.I. **12**, 104, 3 (1937)

[4] P. P. Feofilov, Dokl. Akad. Nauk SSSR **99**, 731 (1954)

Translated by R. G. Huzarski
215

The Measurement of the Specific Charge of Conduction Electrons

V. M. IUZHAKOV
Leningrad Industrial Correspondence Institute
(Submitted to JETP editor November 15, 1954)
J. Exper. Theoret. Phys. USSR **29**, 388-390
(September, 1955)

IN the development of the theory of metals and semiconductors there arises the problem of the experimental determination of the ratio e/m and the effective mass of conduction electrons.

As is well-known, Mandel'shtam and Papaleski[1] were the first to show the inertia for transport of charges in metals experimentally, but, because of the beginning of the war in 1914, they were not able to complete their work. In 1916-1926, Tolman and his co-workers proved conclusively, in a series of papers, that the transport of charges in metals was due to electrons. The value of e/m obtained in this work and the corresponding value for free electrons in a vacuum were, however, different from each other. This difference could be explained by inaccuracies in the theory.[2] Thus, assuming that the acceleration of the electron with respect to the conductor is equal to the acceleration of the conductor, with opposite sign, the value of e/m found in the later papers of this series can be interpreted as an overestimate of the electrons' acceleration. The sign of e/m obtained, in the first paper, by braking a rotating coil can be explained in terms of the disregard of capacitative currents and self-induction. Heat due entirely to electronic motion was also not taken into account. In what degree the various simplifications of the theory affected the result has not been established[3]. Planned extensions of the research have not occurred.

In future measurements of the ratio e/m of conduction electrons, we require both improvement in experimental techniques and the use of new methods, and also simpler and more accurate interpretation of the experiments. If the Coriolis effect

is used as an inertial effect, we can evidently approach this goal closely. The fact is that the Coriolis forces act on the electrons in the rotating conductor in a fashion completely analogous to a Lorentz force. They can, therefore, equalize or balance it. Consequently, null methods are possible. In these, the electron will generally not be accelerated with respect to the conductor; the theory of such methods is extremely simple, since one proceeds only from the equality of the Coriolis and Lorentz forces. We note that all the effects caused by magnetic fields and explained by Lorentz forces must, because of the Coriolis force, also cause rotations. In particular, there must be a phenomenon of electron inertia induction, analogous to electromagnetic induction, acting on the rotation of a current bearing conductor. Such an effect would be similar to that of a magnetic field acting on current bearing conduction, to the Hall effect, and to others. Comparison or mutual compensation of some similar effects of rotation in a magnetic field will allow determination of e/m for conduction electrons.

As an example, we consider a generator, equipped with a special device permitting it to be driven in rotation about an axis parallel to the direction of the magnetic lines of force. Thus, the rotor of the generator performs two rotating motions about the mutually perpendicular axes. An electromotive force will then be generated in its windings even when the magnetic field is turned off. This emf will be called inertial, since it is generated by Coriolis forces. Let o be the angular velocity of rotation of this assembly, and let ω be the angular velocity of rotation of the rotor, which we shall consider to be at right angles to the frame of N turns of wire. Two sides of the frame (each of length l) are active; two others with length b connect them. The linear velocity of the leads will be $v = \omega b/2$, while the electrons experience the Coriolis force

$$2mvo \sin \omega t = m\omega ob \sin \omega t,$$

which corresponds to the voltage

$$(m/e)\, \omega ob \sin \omega t.$$

In order to find the electromotive force U_{inertia} that is produced in the rotor, it is necessary to multiply the last expression by $2l$ times the number of turns N; then, taking into account that $bl = S$, the area of the frame, we get

$$U_{\text{inertia}} = 2\,(m/e)\, No\omega S \sin \omega t. \tag{1}$$

The centrifugal forces which act on the electron have the same direction in the opposite leads of each coil; their actions, therefore, are mutually compensated; therefore, they do not enter into the calculation for the computation of U_{inertia}.

The emf produced in the generator under the action of a magnetic field is determined by

$$U_{\text{mag}} = \frac{1}{c}\, NHS\omega \sin \omega t \tag{2}$$

(c = velocity of light, H = magnetic field strength). From Eqs. (1) and (2) we obtain

$$\frac{U_{\text{inertia}}}{U_{\text{mag}}} = \frac{2}{(e/cm)}\,\frac{o}{H}. \tag{3}$$

We can so choose the magnetic field that $U_{\text{mag}} = U_{\text{inertia}}$; the condition is

$$o = (e/2cm)\, H. \tag{4}$$

Equation (4) is the expression for the Larmor precession. As we know, the Larmor precession frequency is approximate, the degree of accuracy depending on how the centrifugal force compares with the Coriolis force. But, as is evident from our previous conclusion, Eq. (4) is exact in our case. This behavior is evidently connected with the absence of the effects of centrifugal force.

Upon obtaining equality for U_{inertia} and U_{mag}, we can determine e/mc from Eq. (4).

It is understood that a special generator must be prepared for experiments on the determination of e/m. The rotor must contain as large coils as possible, with very fine wire. The inductor can be replaced by a solenoid surrounding the assembly. The earth's magnetic field must be carefully removed. As a control, the rotor should be operated in each of its two rotations separately, for different positions of the rotor; elimination of the earth's field will be considered sufficient only when there exists no emf in the rotor in these preliminary experiments. The effect of a small residual field could be removed if the direction of rotation was changed in these experiments. The rotor resembles a precessing gyrocsope, the axes of precession being perpendicular to the axes of rotation. The leads from the frame can be connected to a copper commutator which rolls on a copper brush. Since the current is alternating, the effect of thermoelectric forces arising in the brushes can be eliminated.

Let the coil consist of $N = 10^4$ turns of copper wire of diameter 0.2 mm, the area of the loop S be 10^3 cm^2. Assume $o = \omega = 100/\text{sec}$ and $e/m = 5 \times 10^{17}$ cgs units/gm. The amplitude of U_{inertia} is then 10^{-4} volt, the internal resistance of the rotor about 10^4 ohms. The large internal resistance makes insignificant the variable resistance

at the moving contacts. The measurement can be obtained with the aid of a ballistic galvanometer and amplifier. With the estimated magnitudes above, this apparatus ought to give the value of e/m for conduction electrons with an error not exceeding 1%.

[1] N. D. Papaleksi, *Collected Works*, p. 379, Academy of Sciences Publishing House, Moscow, 1948

[2] Handbuch d. Experim. Phys. vol. 11, pt. 2, 1935

[3] R. C. Tolman and L. M. Mott-Smith, Phys. Rev. 28, 794 (1926)

Translated by F. A. Metz
217

The Radiation of a Rapidly Moving Electric Image of a Uniformly Moving Charge

G. A. Askar'ian

(Submitted to JETP editor April 25, 1955)
J. Exper. Theoret. Phys. USSR 29, 388
(September, 1955)

Of the wide class of problems on radiation effects accompanying the rapid passage of charges near conducting or dielectric surfaces of given arbitrary form, we consider the simplest concrete example: the calculation of the radiation caused by the change of the image of a charge with non-relativistic but sufficiently large velocity falling upon a conducting sphere of radius R. In the non-relativistic case we can employ certain formulas of electrostatics connected with the magnitude and coordinates of the inducing charge and the image charges: $x_1x_0 = R^2$; $e_1 = -e_0R/x_0 = -e_2$; $x_2 = 0$ (origin of coordinates measured from the center of the sphere, and the zero subscript denoting quantities relating to the inducing charge).

The dipole moment of the image charge is equal to the induced dipole moment of the sphere $p = e_1x_1 = e_0R^3/x_0^2$, and has a second derivative with respect to time, different from zero even for $\dot{x}_0 = -\beta_0 c = \text{const}$. The total energy radiated for the change of dipole moment, due to the motion of the inducing change from infinity to the surface of the sphere, is

$$\Delta\mathcal{E} = \frac{2}{3c^3}\int \ddot{p}^2 dt = \frac{24}{7}\frac{e_0^2}{R}\beta_0^3.$$

Such energy of the first burst of radiation precedes the radiation of the transient decelerating source (concerning transient radiation for a plane boundary, see references 1 and 2). We compare the received radiation of the image with the radiation of a charge in complete braking in the electric field of a parallel plate condenser. For the path of charge parallel to the field

$$\delta\mathcal{E} = \frac{2}{3}\frac{e_0^3E\beta_0}{m_0c^2},$$

$$\frac{\Delta\mathcal{E}}{\delta\mathcal{E}} = \frac{36}{7}\frac{m_0c^2\beta_0^2}{e_0ER} = \frac{72}{7}\frac{\mathcal{E}_{\text{kin}}}{e_0ER};$$

for $eER = \mathcal{E}_{\text{kin}}$; $\Delta\mathcal{E} \simeq 10\,\delta\mathcal{E}$.

It is evident that by suitable choice of the form (concave or convex) of the conducting surface, an accelerated or "super light" collapse of the field can be realized, redistributing the charge, even for a constant velocity of motion of the inducing charge (not exceeding that of light).

The employment of a bunch of charged particles as an inducing charge can increase the radiation effect by many orders of magnitude.[3] This justifies the interest in the study of the potentialities of transformation of the velocities and accelerations of image charges, and in the investigation of annihilation radiation associated with the uniting of the bunch with the induced charge.

[1] B. L. Ginzburg and I. M. Frank, J. Exper. Theoret. Phys. USSR 16, 15 (1946)

[2] H. P. Klepikov, Vest. Moscow State Univ. 8, 61 (1951)

[3] B. L. Ginzburg, Izv. Akad. Nauk SSSR, Ser. Fiz. 11, 165 (1947)

Translated by F. A. Metz.
216

On the Problem of Rotational Levels and the Spectra of Heavy Nuclei. II

S. G. Ryzhanov
Kishinev State University

(Submitted to JETP editor September 8, 1954)
J. Exper. Theoret. Phys. USSR 29, 247-249
(August, 1955)

In the present communication, calculations concerning the relative intensities of α-particle groups from RdAc → AcX, based on the model of nuclear rotators[1], are presented, and are compared with experimental data[2,3]. The quantum-mechanical theory of α-decay, presented in

Bethe's monograph[4], is placed in the framework of the calculation. According to this theory, the probability of emission of an α-particle with reduced kinetic energy (reduced because of the excitation ΔE of the daughter nucleus) is equal to the probability of emission to the ground state multiplied by a factor approximately equal to

$$\exp(-170\Delta E\, E_{\alpha m}^{-3/2}), \qquad (1)$$

where $E_{\alpha m}$ is the maximum disintegration energy, expressed (as is ΔE) in mev. If the α-particle carries an orbital angular momentum $l\hbar$, then the probability for its emission from the nucleus is decreased by

$$\exp\left[\frac{2l(l+1)}{g}\sqrt{1-x}\right]. \qquad (2)$$

For a heavy nucleus, $g \approx 12$, $x = E_\alpha / E_0$, where E_α is the disintegration energy for the particular group and $E_0 = 2Ze^2/R_c \approx 25$ mev. The calculation of the relative intensity of a given α-group (characterized by a particular excitation energy ΔE) leads to the multiplication of the factor (2) by the corresponding normalization of the statistical weight of the chosen l, and summed over all l possible for the group being investigated, with the consequent multiplication by the factor (1). In order to compare these intensities with the intensity of the ground state group (the normal state of the daughter nucleus), it is necessary to divide them by factor (2) for the ground state, which is assigned a statistical weight of one. In order to find the various l's possible for each group considered, and to calculate the corresponding "statistical weights", the following nuclear model is used: the nucleons, forming closed (or rather, almost closed) shells, distribute themselves into groups, forming "rotators"[5]. In addition to these groups, there are a small number of non-shell nucleons (formed, so to speak, by the nuclear atmosphere), for which the corresponding individual energy levels can be represented by Heisenberg's scheme[6]. The nuclear rotators and the non-shell nucleons are treated below as almost independent subsystems. The calculation of the non-shell nucleons is necessary in order to obtain the correct value for the ground state spins of heavy nuclei. In α-decay, the formation of α-particles in the nucleus leads to the regrouping of non-shell nucleons, whose energy enters as a very small part in the maximum disintegration energy.

The simplest regrouping consists in the jump of one nucleon between neighboring levels, near the direct transitions in the middle part of the scheme[6]. The resulting momentum of the α-particle can be obtained by the addition of the rotator momenta and the changed momenta of the non-shell nucleons participating in the energy and momentum balance of the nucleus. Such an addition of momenta is carried out according to the known quantum mechanical law[7]. Each possible value j of the sum of the momenta j_1 and j_2 being added has a definite "statistical weight" expressed by Wigner's well-known formula[8]. Using the notation of the monograph cited earlier (Bethe's), one can obtain the desired statistical weight of a given j by adding the $|C^{j}_{m_1 m_2}|^2$ (over all possible $m_1 m_2$ and $m = m_1 + m_2$ corresponding to the j_1, j_2 and j_3 permitted by selection laws). Selection laws consist of the law of conservation of parity and the selection law for the numbers m of rotators. The latter derives from the type of rotation symmetry of the electric quadrupole moments of the rotators (when some rotator is excited, its m can change either by 0 or ± 2 or by ± 1, depending upon the type of symmetry)*.

It is not without interest to bring in some concrete data in the disintegration RdAc → AcX being investigated, according to the scheme presented as Fig. 3 in reference 1. With the best agreement with the empirical data, it is assumed that the change Δj for the non-shell nucleons in a wide range ΔE (from 32 to 280 kev) is equal to three momentum units:

a) The ground state group, $E_{\alpha m} = 6.16$ mev, $\Delta E = 0$. The rotator is not excited.

The non-shell nucleon, participating in the momentum balance, changes by $\Delta j = 3$; this momentum value leads to an α-particle with $l = 3$.

b) The group with $\Delta E = 32$ kev. One rotator, B_1, is excited and gets a momentum $J = 1$. In this case $\Delta j = 3$. The possible values for the momentum of the α-particle are $l = 2$ and 4. Their statistical weights are in the ratio 3 to 6.

c) The group with $\Delta E = 62$ kev. Two rotators (of the B_1 type) are excited, each with a momentum $J = 1$. The resulting momentum can have the values 0 and 2. Adding these momentum values with $\Delta j = 3$, we obtain $l = 1$, 3 and 5 with a multiplicity 1 for $l = 1$ and 5 and a multiplicity 2 for $l = 3$, and statistical weights in the ratios 3:8:10.

d) The group with $\Delta E = 84$ kev. Two rotators are also excited (B_1 and B_3, each with $j = 1$) and the calculation is analogous to the previous

one, with but one change, however: the rotator B_3 has a different rotation symmetry than B_1. For the case under consideration m can take values 1 and - 1 and then, as in the previous case, this quantity can have values +2, 0 and - 2, which carry almost twice as much statistical weight.

e) The group with $\Delta E = 129$ kev. Three rotators (B_1, B_2, B_3), each with $J = 1$, are excited. Their resulting momentum has values of 1 or 3. Essentially, the maximum statistical weight has to be one. The addition with Δj virtually leads to case c).

The analysis of the remaining groups is carried out in similar fashion.

Figure 1 shows two experimental curves of the dependence of the intensity of the α-groups on the excitation energy (the shape of the α-spectrum), drawn according to the data of Rasetti[2] and Bethe[3] (dotted lines). The solid line gives the calculated dependence. All three curves are normalized to the same total number of α-particles Taking into account the rather large scattering of the experimental data, one must admit that the agreement with the theory presented is satisfactory. Better agreement can be attained only on the basis of a more complete theory of α-decay, founded on the quantum many-body problem, instead of the present theory which is "one-bodied" in essence.

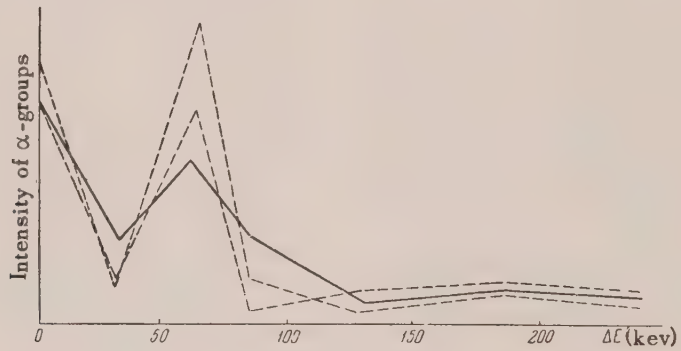

FIG. 1

The experimental data[2,3] show that, starting with $\Delta E = 290$ kev and higher (up to 380 kev) the shape of the α-spectrum almost perfectly reproduces its shape in the interval 0-290 kev. According to Bethe[4] the influence of factor (1), leading to a sharply decreasing intensity, can be compensated by a slight increase in the radius of the potential well for the α-particles, due to the fact that the α-particle already interacts with a relatively highly excited nucleus. The shape of the curve further on can be obtained excellently on the basis of the model of nuclear rotators developed here, if one assumes that the change in momentum of the non-shell nucleons $\Delta j = 1$. Indeed, the group $\Delta E = 290$ kev is connected with the excitation of two rotators: A_2 with $J = 3$ and B_3 with $J = 1$. The addition of the momenta of these two rotators leads to case (b) and gives a resulting momentum of four which, when added to $\Delta j = 1$, leads to a momentum of 3 (which has an overwhelmingly large "statistical weight"). Therefore, this group finally leads to case (a). The following group with $\Delta E = 312$ kev is connected with the excitation of one rotator B_3 with $J = 3$, the addition of which to $\Delta j = 1$ gives, in accordance with (b), a resulting momentum of four. This group is a repetition of the group with $\Delta E = 32$ kev. The group $\Delta E = 337$ kev (rotators B_1 with $J = 2$ and B_3 with $J = 3$), as can be easily shown, repeats the group with $\Delta E = 62$ kev. More interesting is the last group with $\Delta E = 383$ kev. This value of ΔE can be split into 312 kev (rotator B_3 with $J = 3$), 40 kev (rotator B_2 with $J = 1$) and 31 kev (rotator B_4 with $J = 1$). The addition of the first two momenta gives, according to (b), a resulting momentum of four, which, when added to the momentum of the third rotator ($J = 1$), gives with overwhelming probability the resulting momentum of three. Its addition to $\Delta j = 1$ leads to case (b) and this group repeats the groups with $\Delta E = 32$ kev and $\Delta E = 120$ kev.

Analogous calculations have been performed for two α-groups ThC $\rightarrow$ ThC'' with satisfactory agree-

ment with experimental data. It is of interest to look over the scheme of the α-decay ThC → ThC″ (Fig. 2) in accordance with the newest experimental data compiled in Selinov's monograph[9]. These data are in much better agreement than the previous ones with the scheme of nuclear rotators. For the interpretation of some even newer empirical data[10] it turns out to be necessary to introduce yet a fourth rotator with a rotation constant $B = 33$ kev. This constant, just as the first three, agrees with the simple natural proportion ($B_1 : B_2 : B_3 : B_4 = 3 : 4 : 5 : 6$) pointed out in our earlier paper**[1].

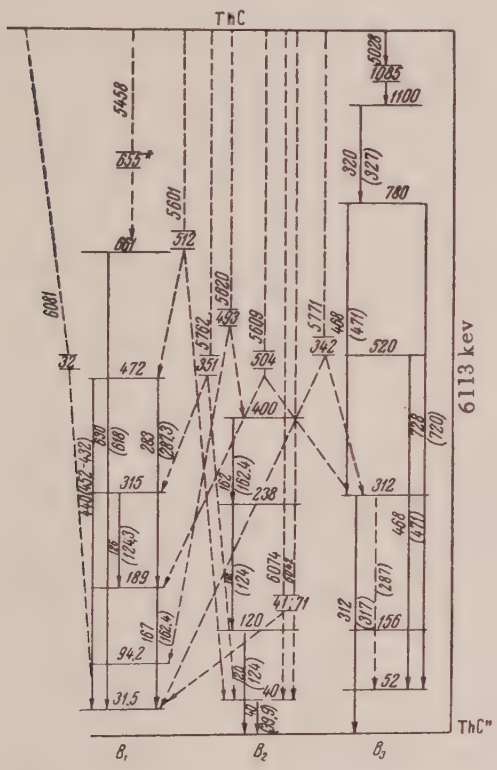

FIG. 2. The α-particle decay ThC $\xrightarrow{\alpha}$ ThC″. The assignment of excitation energies of ThC″ by rotators and the resulting emission of γ-quanta. Full lines: γ-rays; dashed lines: α-particles. Numbers between horisontal lines: excitation energy of ThC″ in kev; numbers above lines: energy of α-particles in kev*.

* $\Delta E = 655$ kev can also be explained by the scheme $520 + 94 + 40$ (B_3, B_1, B_2).

The fact that much experimental information on the α- and γ-spectra of naturally radioactive elements can be interpreted theoretically on the basis of the scheme of nuclear rotators indicates that this scheme is of some significance.

* In connection with Wigner's formula, it is conveniento remove from the statistical weight $(2j + 1)$ that statistical weight which corresponds to forbidden m.

** The quadrupolarity of the γ-rays can be explained, in connection with Fig. 1 (of the previous paper[1]), by the unity spin of the γ-photon and the circularly polarized radiation.

[1] S. G. Ryzhanov, J. Exper. Theoret. Phys. USSR 23, 417 (1952)

[2] F. Rasetti, *Elements of Nuclear Physics*, p. 92 (read in U. S. edition)

[3] H. Bethe, *Physics of the Nucleus*, Part 2, p. 194 (published in U. S.)

[4] See reference 3, p. 178-198

[5] S. G. Ryzhanov, J. Exper. Theoret. Phys. USSR 24, 361 (1953)

[6] W. Heisenberg, *Theory of the Atomic Nucleus*, p. 38

[7] L. D. Landau and E. M. Lifshitz, *Quantum Mechanics*, I, pp. 123-126 (OGIZ, 1948)

[8] See reference 7, pp. 404-409

[9] I. P. Selinov, *Atomic Nuclei and Nuclear Transmutations*, I, p. 198 (GITTL, 1951)

[10] F. Rasetti and E. C. Booth, Phys. Rev. 91, 315 (1953)

Translated by F. Ajzenberg-Selove
182

Green's Function in Scalar Electrodynamics in the Region of Small Momenta

A. A. LOGUNOV
Moscow State University

(Submitted to JETP editor June 24, 1955)
J. Exper. Theoret. Phys. USSR 29, 871-874
(December, 1955)

IN the usual perturbation theory, in addition to the fundamental divergences which occur at high energies of the virtual quanta, there arise divergences in the integration over the virtual quanta with q^2, close to zero. This divergence bears the name of the infrared "catastrophe", and is connected with the improper application of perturbation theory to the given processes. The study of any particular process presents no difficulty if the Green's function and the operator of the peak part are computed. Inasmuch as we do not have to take into account the virtual electron-positron pairs at $k^2 \sim m^2$, the photon Green's function will be the Green's functions of the free photon field.

In this note we investigate the behavior of the Green's function of the particle when $k^2 \sim m^2$ in the case of scalar electrodynamics:

$$\left\{M^2 - \left[i\frac{\partial}{dx^k} + \sqrt{4\pi}\,eA_k(x) + i\sqrt{4\pi}\,e\int \mathfrak{G}_{\beta,k}(\xi, x \mid A)\frac{\delta}{\delta A_\beta(\xi)}\right]^2\right\} G(x, y \mid A) = \delta(x-y), \tag{1}$$

$\mathfrak{G}_{\beta,k}(\xi, x \mid A)$ is the Green's function of the photon. Representing $G(x, y \mid A)$ in the form

$$G(x, y \mid A) = \sum_n \frac{1}{n!}\int G_n(x, y \mid x_1 \ldots x_n)\, A(x_1)\ldots A(x_n)\, dx_1 \ldots dx_n,$$

where G_n, by virtue of the homogeneity of the space, is translationally invariant:

$$G_n(x, y \mid x_1, \ldots x_n) = G_n(x+a, y+a; x_1+a, \ldots, x_n+a),$$

we have

$$G(x, y \mid A) = G(y-x \mid T_x A) = T_x G(y-x \mid A),$$

where

$$T_x A(\xi) = A(\xi + x).$$

Since

$$G(y-x \mid A) = \frac{1}{(2\pi)^4}\int e^{ik(y-x)} G(k \mid A)\, dk,$$

we get

$$i\frac{\partial}{\partial x^\nu} G(x, y \mid A) = T_x \frac{1}{(2\pi)^4}\int e^{ik(y-x)}\left[k^\nu g^{\nu\nu} + \int p^\nu g^{\nu\nu} A_\nu(p)\frac{\delta}{\delta A(p)}\, dp\right] G(k \mid A)\, dk. \tag{2}$$

After substituting Eq. (2) in Eq. (1) and making several elementary computations, we get

$$\left\{M^2 - \left[k + \Pi + g\int A(p)\, dp + ig\int \mathfrak{G}(p \mid A)\frac{\delta}{\delta A(p)}\, dp\right]^2\right\} G(k \mid A) = 1, \tag{3}$$

where

$$g^{00} = 1,\ g^{ii} = -1,$$

$$\Pi_\nu = \int p^\nu g^{\nu\nu} A_\alpha(p)\frac{\delta}{\delta A_\alpha(p)}\, dp;\ g = \frac{\sqrt{4\pi}\,e}{(2\pi)^2}.$$

Carrying out the renormalization of Eq. (3), we get

$$\left\{M^2 - \left[k + \Pi + g\int A(p)\, dp + ig\int \mathfrak{G}(p \mid A)\frac{\delta}{\delta A(p)}\, dp\right]^2\right\} G(k \mid A) = Z_2^{-1} \tag{4}$$

In our approximation we can take for $\mathfrak{G}(p \mid A)$ [2]

$$\mathfrak{G}_{\alpha\beta}(p) = \frac{1}{p^2}\left[d_l(p^2)\left(-g^{\alpha\beta} + g^{\alpha\alpha} g^{\beta\beta}\frac{p^\alpha p^\beta}{p^2}\right) - d_l(p^2) g^{\alpha\alpha} g^{\beta\beta}\frac{p^\alpha p^\beta}{p^2}\right]. \tag{5}$$

Making use of the method of proper time [1] we can rewrite Eq. (4) in the form

$$i\frac{\partial U(\nu, k|A)}{\partial \nu} = (M^2 - \hat{\mathscr{H}})\, U(\nu, k|A), \tag{6}$$

$$U(0, k|A) = -Z_2^{-1};\quad G(k|A) = -i\lim_{\varepsilon \to 0}\int_0^\infty e^{-\varepsilon\nu} U(\nu, k|A)\, d\nu.$$

Limiting ourselves to terms no higher than second order in g^2 and linear in $A_\alpha(p)$, we obtain

$$\hat{\mathscr{H}} = k^2 + \int dp\,[2(kp) + p^2] A_\alpha(p)\frac{\delta}{\delta A_\alpha(p)} + g\int dp\,(2k+p) A(p) + ig\int dp\,[2k^\beta + p^\beta]\,\mathfrak{G}_{\alpha\beta}(p)\frac{\delta}{\delta A_\alpha(p)} + ig^2\int dp\, g^{\alpha\alpha}\mathfrak{G}_{\alpha\alpha}(p). \tag{7}$$

The constants M, Z_2^{-1} in our approximation are represented with an accuracy which does not exceed g^2. We have

$$U(\nu, k|A) = -Z_2^{-1} \exp\{iS(\nu, k|A)\}.$$

Then:

$$\frac{\partial S(\nu,k|A)}{\partial \nu} = (k^2 - M^2 + g\int dp\,(2k+p)\,A(p) \tag{8}$$

$$+ ig^2 \int dp g^{\alpha\alpha}\,\mathfrak{G}_{\alpha\alpha}(p) + i\int dp\,[2(kp)+p^2]\,A_\alpha(p)$$

$$\times \frac{\delta}{\delta A_\alpha(p)} S(\nu,k|A) + ig^2 \int dp\,\mathfrak{G}_{\alpha\beta}(2k^\beta + p^\beta)\frac{\delta S}{\delta A_\alpha(p)}$$

We set

$$\frac{\delta S(\nu,k|A)}{\delta A_\alpha(p)} = \tau^\alpha(\nu,k,p).$$

Then, by varying Eq. (8) we obtain

$$\frac{\delta \tau^\alpha(\nu,k,p)}{\delta \nu} = g(2k^\alpha + p^\alpha) \tag{9}$$

$$+ i[2(kp)+p^2]\,\tau^\alpha(\nu,k,p),\ \tau^\alpha(0,k,p) = 0,$$

whence

$$\tau^\alpha(\nu,k,p) = ig\frac{(2k^\alpha + p^\alpha)}{2(kp)+p^2} \tag{10}$$

$$\times \quad (1 - \exp\{i\nu[2(kp)+p^2]\}),$$

and, consequently,

$$S(\nu, k|A) = \int_0^\nu H(\nu, k|A)\,d\nu, \tag{11}$$

$$H(\nu, k|A) = k^2 - M^2 + ig^2\int dp\,g^{\alpha\alpha}\,\mathfrak{G}_{\alpha\alpha}(p)$$

$$+ g\int dp\,(2k+p)\,A(p)$$

$$+ i\int dp\,[2(kp)+p^2]\,A_\alpha(p)\,\tau^\alpha(\nu,k,p)$$

$$- g\int dp\,\mathfrak{G}_{\alpha\beta}(p)\,(2k^\beta + p^\beta)\,\tau^\alpha(\nu,k,p).$$

Substituting Eq. (10) in (11) and assuming

$$d_l(p^2) = \int_0^\infty e^{i\gamma p^2} v_l(\gamma)\,d\gamma, \tag{12}$$

$$d_t(p^2) = \int_0^\infty e^{i\gamma p^2} v_t(\gamma)\,d\gamma,$$

we obtain, after some computation,

$$H(\nu,\ k|0) = k^2 - M^2 + ig^2\int dp g^{\alpha\alpha}\,\mathfrak{G}_{\alpha\alpha}(p) \tag{13}$$

$$+ ig^2 A(0) - ig^2 A(\nu) - 4g^2\int_0^\nu F(\nu)\,d\nu,$$

$$A(\nu) = -\frac{\pi^2}{\nu^2}\int_0^1 d\omega\, e^{-\nu k^2\omega}\,\omega\,[2i\nu k^2 \tag{14}$$

$$+ 2 - i\nu k^2\omega]\int_0^{(\nu/\omega)-\nu} d\beta \int_0^\beta v_l(\gamma)\,d\gamma,$$

$$F(\nu) = \frac{3}{2}\frac{\pi^2}{\nu^2}k^2\int_0^1 e^{-i\nu k^2\omega}\omega\,d\omega \int_0^{(\nu/\omega)-\nu} d\beta\int_0^\beta v_t(\gamma)\,d\gamma, \tag{15}$$

whence

$$U(\nu, k|0) = -Z_2^{-1}\exp\left[i\left(k^2 - M^2\right.\right. \tag{16}$$

$$\left. + ig^2\int dp g^{\alpha\alpha}\mathfrak{G}_{\alpha\alpha}(p) + ig^2 A(0)\right)\nu$$

$$\left. + g^2\int_0^\nu A(\nu)\,d\nu - 4ig^2\int_0^\nu d\beta\int_0^\beta F(\gamma)\,d\gamma\right].$$

Carrying out renormalization of the mass we obtain

$$U(\nu, k|0) = -Z_2^{-1}\exp\left[i\,(k^2 - m^2 - ig^2\int_0^\nu A(\nu)\,d\nu\right. \tag{17}$$

$$\left. + 4g^2\int_0^\nu d\beta\int_\beta^\infty F(\gamma)\,d\gamma\right],$$

and hence

$$G(k|0) = iZ_2^{-1} \lim_{\varepsilon \to 0} \int_0^\infty e^{i\Phi(\nu)} d\nu; \qquad (18)$$

$$\Phi(\nu) = (k^2 - m^2)\nu + i\varepsilon\nu - ig^2 \int_0^\nu A(\nu)\, d\nu + 4g^2 \int_0^\nu d\beta \int_\beta^\infty F(\gamma)\, d\gamma.$$

We now write the integral in Eq. (18) in the form

$$\lim_{\varepsilon \to 0} \int_0^\infty e^{i\Phi(\nu)} d\nu = i\xi_0 e^{i\Phi(i\xi_0)} \int_0^\infty \exp\left\{ -i\xi_0^2 \int_1^\lambda \Phi''(i\xi_0\omega)(\lambda - \omega)\, d\omega \right\} d\lambda,$$

where $\Phi'(i\xi_0) = 0$. But, since

$$A(\nu) \underset{|\nu| \to \infty}{\sim} -\frac{2\pi^2}{\nu} d_e(0), \quad F(\nu) \underset{|\nu| \to \infty}{\sim} -i\frac{3}{2}\frac{\pi^2}{\nu^2} d_t(0), \qquad (19)$$

then for $k^2 \sim m^2$,

$$\xi_0 = 2\pi^2 g^2 \frac{[3d_t(0) - d_l(0)]}{k^2 - m^2},$$

and, consequently, for the corresponding choice of constant Z_2^{-1}, we obtain [3]

$$G(k|0) = \sim [m^2 - k^2]^\gamma,$$

$$\gamma = -1 - \frac{e^2}{2\pi}[3d_t(0) - d_l(0)].$$

The increase of the singularity of the Green's function for $k^2 \sim m^2$ in comparison with the Green's functions of the free scalar field lead to the conclusion that the probability of radiation of one or a finite number of photons with frequency $\omega \to 0$ is equal to zero [4].

As is known, in the usual perturbation theory, this probability is infinite. We hope later to apply this method to the calculation of the operator of the peak part.

In conclusion, I express my deepest gratitude to Academician N. N. Bogoliubov under whose direction the work was completed.

[1] V. A. Fock, Phys. Z. Sowjet Union **12**, 404 (1937)

[2] L. D. Landau, A. A. Abrikosov and I. M. Khalatnikov, Dokl. Akad. Nauk SSSR **95**, 497 (1954)

[3] A. A. Abrikosov, Dissertation, Institute for Physical Problems, Academy of Sciences, USSR, 1955

[4] F. Bloch and A. Nordsieck, Phys. Rev. **52**, 54 (1937)

Translated by R. T. Beyer
287

The Problem of the Asymptote of the Green Function in the Theory of Mesons with Pseudoscalar Coupling

E. S. FRADKIN
P. N. Lebedev Institute of Physics, Academy of Sciences, USSR

(Submitted to JETP editor April 18, 1955)
J. Exper. Theoret. Phys. USSR **29**, 377-379 (September, 1955)

IN investigations [1] using the non-renormalized equations the asymptote of the Green function was found for the case of weak pseudoscalar interaction. In this note the asymptote of the non-renormalized equations for the same problem was found. Moreover, the asymptote found agrees with the renormalized expression obtained in investigation [1].

In contrast to the work of reference 1, the equations for the Green function in our form do not contain any infinities and, when finding the asymptote, it is not necessary to find the small corrections to the Green function (see reference 1), which simplifies the calculation considerably.

It can be shown that, in the first approximation with respect to g^2, the following approximate system of completely renormalized equations results from the system of interlinked renormalized equations (it should be noted that, when $\lim_{p^2 \to \infty} g^2_{\text{prim}} \ln \frac{p^2}{m^2} = \text{const}$, the equations obtained in the same case fully express the asymptote of the exact equations):

$$\Gamma_\sigma(p, p-l, l) = \tau_\sigma \gamma_5 + \frac{g^2}{\pi i}\int [\Gamma_\mu(p, p-k, k) G(p-k) \Gamma_\sigma(p-k, p-k-l, l) \times G(p-k-l)\Gamma_\nu(p-k-l, p-l, -k) - \Gamma_\mu(p^0, p^0-k, k) G(p^0-k)\Gamma_\sigma(p^0-k, p^0-k, 0) \times G(p^0-k)\Gamma_\nu(p^0-k, p^0, -k)] D_{\mu\nu}(k)\, d^4(k); \qquad (1)$$

$$\frac{\partial G^{-1}(p)}{\partial p_\sigma} = \gamma_\sigma - \frac{g^2}{\pi i}\int\Big[\Gamma_\mu(p, p - k, k)\frac{\partial G(p-k}{\partial p_\sigma}\Gamma_\nu(p-k, p, -k) - \Gamma_\mu(p^0, p^0-k, k)\frac{\partial G(p^0-k)}{\partial p_\sigma} \times \Gamma_\nu(p^0-k, p^0, -k)\Big] D_{\mu\nu}(k)\, d^4(k); \quad (2)$$

$$\frac{\partial D^{-1}_{\mu\nu}(k)}{\partial k^2} = \delta_{\mu\nu} + \frac{g^2}{\pi i} T_\rho \frac{1}{2}\int\Big\{\frac{\partial}{\partial k_\sigma}\Big[G(p)\Gamma_\mu(p, p-k, k) \times \frac{\partial G(p-k)}{\partial k_\sigma}\Gamma_\nu(p-k, p, -k)\Big] - \frac{\partial}{\partial k^0_\sigma}\Big[G(p)\Gamma_\mu(p, p-k^0, k^0)\frac{\partial G(p-k^0)}{\partial k^0_\sigma} \times \Gamma_\nu(p-k^0, p, -k^0)\Big]\Big\} d^4p \quad (3)$$

Here g is the renormalized charge, $p^{0\,2} = m^2$, $k^{0\,2} = \mu^2$ are the experimental values of the masses.

The system of equations (1) – (3) should satisfy the following boundary conditions:

$$(p^0 - m)\,G(p^0) = 1, \qquad (k^0 - \mu^2)\,D_{\mu\nu}(k^0) = \delta_{\mu\nu}, \quad (4)$$

τ_μ is the operator of the isotopic spin, T_ρ in Eq. (3) is taken in the spinor, as well as in the isotopic matrices.

We will go over to the new variables $D_{\mu\nu}(k) = \delta_{\mu\nu}D(k)$, $\Gamma_\mu = \tau_\mu\Gamma$; then Eqs. (1) – (3) will go over into the following system of equations:

$$\Gamma(p, p-l, l) = \gamma_5 - \frac{g^2}{\pi i}\int\{\Gamma(p, p-k, k)\,G(p-k)\,\Gamma(p-k, p-k-l, l) \times G(p-k-l)\,\Gamma(p-k-l, p-l, -k) - \Gamma(p^0p^0-k, k)\,G(p^0-k)\,\Gamma(p^0-k, p^0-k, 0) \times G(p^0-k)\,\Gamma(p^0-k, p^0, -k)\}\, D_{\nu\nu}(k)\, d^4k; \quad (5)$$

$$\frac{\partial G^{-1}(p)}{\partial p_\sigma} = \gamma_\sigma - \frac{3g^2}{\pi i}\int\Big[\Gamma(p, p-k, k)\frac{\partial G(p-k)}{\partial p_\sigma}\Gamma(p-k, p, -k) - \Gamma(p^0, p^0-k, k)\frac{\partial G(p^0-k)}{\partial p^0_\sigma} \times \Gamma(p^0-k, p^0, -k)\Big] D(k)\, d^4k; \quad (6)$$

$$\frac{\partial G^{-1}(k)}{\partial k^2} = 1 + \frac{g^2}{\pi i} \times \frac{1}{2}\mathrm{Sp}\int\Big\{\frac{\partial}{\partial k_\sigma}\Big[G(p)\Gamma(p, p-k, k)\frac{\partial G(p-k)}{\partial k_\sigma} \times \Gamma(p-k, p, -k)\Big] - \frac{\partial}{\partial k^0_\sigma}\Big[G(p)\Gamma_\nu(p, p-k^0, k^0)\frac{\partial G(p-k^0)}{\partial k^0_\sigma} \times \Gamma(p-k^0, p, -k^0)\Big]\Big\} d^4p. \quad (7)$$

Following reference 1, we will look for an asymptote for $G(p)$, $D(p)$ and Γ at high momenta in the form

$$G(p) = \beta(p^2)/\hat{p},\ D(p) = d(p^2)/p^2, \qquad \Gamma = \gamma_5\alpha(f^2), \quad (8)$$

where f is the largest vector on which Γ is dependent. As a result of calculations we obtain logarithmically from Eqs. (5) – (7) the following equations:

$$\alpha(\xi) = 1 + \frac{g^2}{4\pi}\int_\xi^0 d(z)\,\alpha^3(z)\,\beta^2(z)\,dz,$$
$$\frac{1}{\beta(\xi)} = 1 - \frac{3g^2}{8\pi}\int_\xi^0 \alpha^2(z)\,\beta(z)\,d(z)\,dz,$$
$$\frac{1}{d(\xi)} = 1 + \frac{g^2}{\pi}\int_\xi^0 \alpha^2(z)\,\beta^2(z)\,dz,$$
$$\xi = \ln(-p^2/m^2). \quad (9)$$

The system of equations (9) is equivalent to the following system:

$$\frac{1}{\beta}\frac{d\beta}{d\xi} = \frac{3g^2}{8\pi}\alpha^2(\xi)\beta^2(\xi)d(\xi), \qquad (10)$$

$$\frac{1}{\alpha}\frac{d\alpha}{d\xi} = \frac{g^2}{4\pi}\alpha^2(\xi)\beta^2(\xi)d(\xi),$$

$$\frac{1}{d}\frac{dd(\xi)}{d\xi} = -\frac{g^2}{\pi}\alpha^2(\xi)\beta^2(\xi)d(\xi).$$

The boundary conditions for β, α, d are equal to logarithmic accuracy, namely $\alpha(0) = \beta(0) = d(0)=1$ and it follows from Eq. (10) that:

$$\beta(\xi) = \alpha^{-3/4}(\xi), \qquad (11)$$
$$d(\xi) = \alpha^{-4}(\xi),$$
$$\alpha(\xi) = \left(1 - \frac{5g^2}{4\pi}\xi\right)^{1/5}.$$

With the aid of Eq. (11) it is easy to find the relationship in this approximation between the primed charge g_{prim} and the renormalized charge. Actually, it is known that

$$g^2_{prim} = \lim_{L\to\infty}(g^2\beta^2(L)\alpha^2(L)d(L)) \qquad (12)$$
$$= \lim_{L\to\infty}\left[g^2\Big/\left\{1 - \frac{5g^2}{4\pi}\ln\left(-\frac{L^2}{m^2}\right)\right\}\right]$$

or

$$g^2 = \lim_{L\to\infty}\left[g^2_{prim}\Big/\left\{1 + \frac{5g^2_{prim}}{4\pi}\ln\left(-\frac{L^2}{m^2}\right)\right\}\right]. \qquad (13)$$

It is evident from Eqs. (12) and (13) that, at least in our approximation, no matter what kind the primed charge g_{prim} is, the experimental charge is equal to zero. This explains the fact that the solution of Eq. (11) at a finite g^2 changes sign at high momenta; moreover, a fictitious pole appears in $d(\xi)$, although, according to the formal general properties of the theory, $d(\xi)$ cannot become negative at large ξ.

One can easily become convinced that, if we substitute for g^2 its value which follows from theory in this approximation, then $d(\xi)$, as one would expect, does not change sign; however, the primed charge at $L\to\infty$ is completely shielded, and g^2 becomes equal to zero. The resultant difficulty, inherent in contemporary theories with point interaction, will be discussed in more detail in a separate paper.

[1] A. A. Abrikosov, A. D. Galanin and I. M. Khalatnikov, Dokl. Akad. Nauk SSSR **97**, 793 (1954)

Translated by E. Rabkin
210

The Interaction of Extraordinary and Ordinary Waves in the Ionosphere and the Effect of Multiplication of Reflected Signals

N. G. Denisov
Gor'kii State University

(Submitted to JETP editor December 9, 1955)
J. Exper. Theoret. Phys. USSR 29, 380-381
(September, 1955)

It is known that the electromagnetic field of a wave traveling in an inhomogeneous magnetoactive medium (the ionosphere), generally speaking, cannot be represented by the superposition of independent extraordinary and ordinary waves. A consideration of the inhomogeneity of the medium leads to the conclusion that during the propagation of waves of one type in the medium, waves of another type appear. Strictly speaking, this interaction exists over the entire extent of the inhomogeneous medium; however, under ionospheric conditions (a slowly changing medium) the observable interaction appears only in limited regions, outside of which it is exceedingly slight. It is essential to speak of a division of the field into ordinary and extraordinary waves only under conditions of slight interaction. As a result of this it is possible to describe these waves in terms of geometrical optics; the interaction itself defines the very special nature of the field in regions of slight interaction separated by a region of considerable interaction.

With normal incidence of an electromagnetic wave upon a plane, laminated, ionized medium located in an external magnetic field, the strongest interaction between extraordinary and ordinary waves is observed during quasi-longitudinal propagation, when the angle between the direction of propagation and the direction of the external field is small. This interaction, which in the ionosphere produces the so-called multiplication of signals effect, can be explained in the following manner. The ordinary wave falling upon an inhomogeneous layer reaches the region where the index of refraction of the ordinary wave $n_1(z)$ and that of the extraordinary wave $n_2(z)$ are very close in value. In this region intense interaction of the two types of waves takes place; as a result of this interaction, an ordinary wave partly penetrates the region of imaginary values of $n_1(z)$ as an extraordinary wave; here the index of refraction of the latter $n_2(z)$ takes on real values and it is partly reflected as an ordinary wave. A wave of the second type passing through the region of interaction is reflected from a superincumbent region of

zero values of the function $n_2(z)$ and on again passing through the region of interaction returns to the receiving point in the form of ordinary wave.

A calculation of this interaction in a nonabsorbing medium was first conducted by Ginzburg for two extreme cases: the first, when an ordinary wave passes almost entirely through the region of interaction (its coefficient of reflection R_1 is small); and the second, when $|R_1|$ is near unity and the coefficient of passage of the extraordinary wave D_2 is small (see reference 1, §79). The influence of absorption on the penetration effect is discussed in detail in the work of Rydbeck[2].

Application of the method of solution proposed in reference 3, which is devoted to the question of inelastic collisions between atoms, permits us to solve this problem fully to some approximation. The method indicated makes it possible to find an asymptotic representation of the particular solution which describes the real process of propagation of the waves in the medium at relatively great distances above and below the region of interaction. It then turns out that the ordinary wave falling upon a layer in the region of interaction produces a reflected wave of the very same type having a coefficient of reflection

$$|R_1| = 1 - e^{-2\delta_0}, \tag{1}$$

and its penetration of the region where $n_2^2 > 0$ characterized by the coefficient

$$|D_2| = e^{-\delta_0}. \tag{2}$$

In formulas (1), (2) the real value of δ_0 is defined by the integral

$$\delta_0 = -i\frac{\omega}{c}\oint \frac{n_2(z) - n_1(z)}{4}\,dz, \tag{3}$$

where the integral is taken around a closed contour encircling two particular points of the integrand at which $n_2 = n_1$; it is assumed that the ordinary wave decreases in the direction of positive z.

It should be noted that if the path of integration in Eq. (3) is taken along the line connecting the points where $n_2 = n_1$, Eq. (2) will give the expression for the coefficient of penetration obtained in reference 1 by an entirely different method, the applicability of which is limited to the case of small values of D_2 ($\delta_0 \gg 1$).

A study of Eqs. (2) and (3) shows that they are applicable also in another limiting case: where $|D_2| \approx 1$ and $|R_1|$ is small. With strong penetration ($\delta_0 \ll 1$) Eqs. (2) and (3) give

$$|R_1| \approx 2\delta_0;\ |D_2| \approx 1 - \delta_0, \tag{4}$$

and a calculation of the integral (3) under these conditions shows that these approximations of the coefficients of (4) fully coincide with the corresponding formulas obtained in reference 1 by a different method, in which the assumption of a small value for R_1 is used from the very beginning.

In our solution, moreover, we were able to compute the extraordinary wave arising as a result of the interaction. This wave is propagated in the direction of the pole of the function $n_2^2(z)$. The coefficient of reflection of this wave turns to be equal to

$$|R_2| = e^{-\delta_0}\sqrt{1 - e^{-2\delta_0}}. \tag{5}$$

As is easily verified, the computation of this coefficient reduced to the satisfying of the relation

$$|R_1|^2 + |R_2|^2 + |D_2|^2 = 1.$$

In this manner the additonal absorption of the electromagnetic wave mentioned in reference 1 is connected with the appearance of the extraordinary wave which is then propagated in the direction of the sharp increase in its index of refraction and completely absorbed by the medium.

The phenomenon of complete absorption of this wave becomes more graphic if we consider the thermal movement of electrons. In reference 4, treating the kinetic energy of plasmic waves in an homogeneous plasma located in a magnetic field, it is shown that under these conditions the pole of the function $n_2^2(z)$ approaches infinity, although a sharp increase of the function itself is also maintained. Moreover, it turns out that in a consideration of the thermal movement of electrons the functions $n_1^2(z)$ and $n_2^2(z)$ are only negligibly distorted in the region of interaction. Consequently, the solution obtained without consideration of the thermal movement of electrons can be immediately extended to the more interesting case in which the possibility of the emergence of plasmic waves during interaction is considered. In this connection the extraordinary wave moving in the direction of the larger values of the function $n_2^2(z)$ acts as a slowly moving plasmic wave, the energy of which in a finite medium is expended in heating the plasma.

Finally, we note that, on the strength of the interaction, the reverse transformation of plasmic waves into electromagnetic waves, is also possible; this leads to the possibility of an emission of plasmic waves from an inhomogeneous magnetoactive medium in the form of electromagnetic radiation.

In conclusion I express my thanks to V. L. Ginzburg for suggesting the problem and for his assitance in the work.

[1] Ia. L. Al'pert, V. L. Ginzburg and E. L. Feinberg, *Propagation of Radio Waves*, Moscow, 1953

[2] O. Rydbeck, J. Appl. Phys. **21**, 1205 (1950)

[3] E. C. Stückelberg, Helv. Phys. Acta **5**, 369 (1932)

[4] B. N. Gershman, *Memorial Volume for A. A. Andronov*, 1955

Translated by G. F. Schultz
211

On Particle Energy Distribution at Multiple Formation

N. M. Gerasimova and D. S. Chernavskii
The P. N. Lebedev Institute of Physics, Academy of Sciences, USSR

(Submitted to JETP editor May 12, 1955)
J. Exper. Theoret. Phys. USSR **29**, 372-374
(September, 1955)

IN Landau's work[1] there was developed a hydrodynamic theory of the formation of particles resulting from the collision of high energy nucleons. As is known, the resolution of this hydrodynamic problem concerning energy spread into evacuated space consists of two parts: wave motion and a nontrivial solution[2].

As regards the problem of multiple formation, the main role in the angular distribution of the particles is played by the nontrivial solution region, since it is here that the principal portion of the entropy of the system lies. The approximate solution of the problem of scattering, given by Landau, represented an asymptotic expression of the nontrivial solution of the scattering section remote from the boundary region separating it from the moving wave. In Landau's solution the latter was completely ignored. Accordingly, the question arises as to how far the disregard of the wave motion is justified when computing particle angular and energy distribution. It is to the examination of this problem that the present letter is devoted.

For the entropy S_p and energy E_p of the wave we have the expression:

$$S_p = nT_0^3 V_0 \int_{x_1/l}^{ct/l} s_p u_p d\left(\frac{x}{l}\right), \tag{1a}$$

$$E = mT_0^4 V_0 \int_{x_1/l}^{ct/l} {}^4/_3 \varepsilon_p u_p^2 d\left(\frac{x}{l}\right). \tag{1b}$$

Here l is the longitudinal extent of the system at the start of the scattering, $mT_0^4 4/3\, \epsilon_p u_p^2$ and $nT_0^3 s_p u_p$ are the densities of the energy and entropy of the wave, T_0 and V_0 are the initial temperature and volume of the system, n and m are constants. Integration is effected over the entire region occupied at the given moment by the moving wave, that is to say, from the boundary line it shares in common with the nontrivial solution section x_1 to the leading edge of the wave $x = ct$.

It should be noted that the coefficients before the integrals in (1a) and (1b) represent respectively the complete entropy and energy of the system. Therefore, the portions of the entropy α and the energy β contained in the moving wave will be equal to

$$\alpha = \frac{S_p}{S} = \int_{x_1/l}^{ct/l} s_p u_p d\left(\frac{x}{l}\right), \tag{2a}$$

$$\beta = \frac{E_p}{E} = {}^4/_3 \int_{x_1/l}^{ct/l} \varepsilon_p u_p^2 d\left(\frac{x}{l}\right), \tag{2b}$$

where u_p is a component of the four-velocity of the element.

Taking into consideration that $u_p \gg 1$ and making use of the Riemannian solution for a simple wave function, we can express ϵ_p, s_p and u_p as follows

$$\varepsilon_p = \left[\frac{(ct-x)(c-c_0)}{(ct+x)(c+c_0)}\right]^{2c_0/c}, \tag{3a}$$

$$s_p = {}^4/_3 \left[\frac{ct-x}{ct+x}\,\frac{c-c_0}{c+c_0}\right]^{c/2c_0}, \tag{3b}$$

$$u_p = {}^1/_2 \left[\frac{ct+x}{ct-x}\,\frac{c+c_0}{c-c_0}\right]^{1/2}, \tag{3c}$$

where c is the velocity of light and $c_0 = c/\sqrt{3}$ the velocity of sound. Substituting (3a), (3b) and (3c) in (2a) and (2b) and introducing a new variable $z = (ct - x)/l$, we obtain for α and β the following evident expressions:

$$\alpha = {}^1/_2 \left(\frac{c-c_0}{c+c_0}\right)^{1/2[(c/c_0)-1]} \times \int_0^{z_1} \left(\frac{z}{(2ct/l)\,z}\right)^{1/2[(c/c_0)-1]} dz, \tag{4a}$$

$$\beta = {}^1/_3 \left(\frac{c - c_0}{c + c_0}\right)^{(2c_0/c)-1} \cdot \tag{4b}$$

$$\times \int_0^{z_1} \left(\frac{z}{(2\,ct/l)\,z}\right)^{(2c_0/c)-1} dz.$$

The magnitude of z_1 is determined from the condition of continuity existing at the boundary line between the nontrivial solution section and the moving wave. If for the nontrivial solution section we use Khalatnikov's method[3], we shall easily obtain an equation for z_1 as follows:

$$z_1 = \left(\frac{2ct}{l} - z_1\right)^{(2c_0-c)/(2c_0+c)} \times \left(\frac{c + c_0}{c_0}\right)\left(\frac{c - c_0}{c_0}\right)^{(2c_0-c)/(2c_0+c)} \tag{5}$$

For t we naturally use the critical time t_k, i.e., the time element corresponding to the beginning of the free scattering, when the energy flux density and the temperature of the moving wave (or to be more exact, at the boundary line separating the moving wave from the non-trivial solution section) diminish to such an extent that further interaction of the particles with each other can be disregarded. As to the magnitude of the critical time element t_k or more exactly, of $2ct_k/l$, it can be said beforehand that it is much larger than unity, while the magnitude of z_1 is of the order of unity and $z_1 \ll 2ct_k/l$.

Making use of this fact and applying formulas (3a) and (3b), we can evaluate the magnitude of $2ct_k/l$ by expressing it in terms of the critical values for energy flux density and temperature; namely,

$$\frac{2\,ct_\kappa}{l} = \frac{c - c_0}{c_0}\,\varepsilon_p^{-(2c_0+c)/4c_0}. \tag{6}$$

But

$$\varepsilon_p = (T/T_0)^4,$$

where T is the temperature of the medium itself at the moment when scattering begins, which temperature it is natural to assume to be equal to uc^2, and T_0 is the initial temperature associated with the full energy of the laboratory system

$$\frac{2\,ct_\kappa}{l} = \left(\frac{c - c_0}{c}\right)\left(\frac{E_0}{\mu c^2}\right)^{(2c_0+c)/4c_0}. \tag{7}$$

Considering that

$$z \ll 2\,ct_\kappa/l,$$

we find that α and β can be expressed as follows:

$$\alpha = {}^4/_3 \left(\frac{c - c_0}{c_0}\right)^{c_0/(2c_0+c)} \times \left(\frac{2\,ct_\kappa}{l}\right)^{-c_0/(2\,c_0+c)} = {}^4/_3 \left(\frac{E_0}{\mu c^2}\right)^{-1/4}, \tag{8a}$$

$$\beta = \frac{c}{6\,c_0}\left(\frac{c + c_0}{c_0}\right)\left(\frac{c - c_0}{c_0}\right)^{(2c_0-c)/(2c_0+c)} \times \left(\frac{2\,ct_\kappa}{l}\right)^{-(2c_0-c)/(2c_0+c)} = \frac{c}{6c_0}\left(\frac{c + c_0}{c_0}\right)\left(\frac{E_0}{\mu c^2}\right)^{-(2c_0-c)/(4c_0+c)}. \tag{8b}$$

Substituting the numerical values in formuals (8a) and (8b), we find that when the energy of the primary nucleon is

$$E_0 = 10^{12}\ \text{eV}$$

the moving wave carries away 14% of the entire entropy and 44% of the energy of the system, and that when the energy is $E_0 = 10^{13}$ ev the wave carries away 0.45% of the entropy and 17% of the energy. The absolute number of particles carried away by the moving wave, at the aforementioned energies, appears to be unchanged, and of the order of unity.

These estimations show that the moving wave carries away a comparatively small portion of the entropy and a small number of particles, but may carry a substantial portion of the energy of the entire system. In any case, it is in the moving wave that the most energetic particle is to be found. It should be noted that the magnitude of the energy of the moving wave is easily affected by whatever assumption is made as to the nature of the particles it contains (all of the results obtained in the preceding refer to the case where the system contains only π-mesons). If we take into account the possibility that along with π-mesons the moving wave may contain also a nucleon[4], the portion of energy that is carried by the wave amounts to 60-70%.

The results obtained indicate that proper consideration of the moving wave substantially influences the estimate of energy distribution at multiple particle formation, when the energy of the mutually colliding particles is $\sim 10^{12} - 10^{13}$ ev.

In conclusion, we wish to express our deep gratitude to S. Z. Belen kii for his valuable advice and suggestions.

[1] L. D. Landau, Izv. Akad. Nauk SSSR, Ser. Fiz. 17, 1 (1953)

[2] L. D. Landau and E. M. Lifshitz, *The Mechanics of Continuous Media*, GITTL 1953, p 434

[3] I. M. Khalatnikov, J. Exper. Theoret. Phys. USSR 27, 529 (1954)

[4] C. Z. Belen'kii, Dokl. Akad. Nauk SSSR 99, 523 (1954); J. Exper. Theoret. Phys. USSR 28, 111 (1955)

Translated by L. Rich
206

Investigation of the Field of Partial Pressures in a Diffusing Condensing Chamber

V. K. Liapidevskii
Moscow Engineering-Physics Institute

(Submitted to JETP editor November 1, 1954)
J. Exper. Theoret. Phys. USSR 29, 263-264
(August, 1955)

THE distribution of supersaturations inside a diffusion chamber, and consequently the height and quality of the sensitive layer, depend on the temperature field and on the partial-pressure field. The temperature field inside a diffusion chamber was investigated in references 1 and 2. This communication describes a procedure and measurement results for the partial-pressure field.

A special instrument, namely an expansion diffusing chamber, was constructed to investigate the partial pressure field. The chamber is a glass-walled crylindrical container. The bottom of the chamber consists of two glass disks screwed together, and is cooled by liquid nitrogen, flowing through a spiral groove cut in the upper disk. The flow of nitrogen, and consequently the temperature of the bottom, are regulated by changing the pressure in a Dewar flask with a valve. The cover of the chamber is a brass plate with holes 7 mm in diameter distributed uniformly over the entire area. The brass plate is covered on the top with a rubber diaphragm which separates the working volume of the diffusion chamber from the volumes that connect with the atmosphere and with the vacuum system. The expansion is carried out in a container located above the working volume. A mercury manometer records the pressure in this container before the expansion and the common pressure in the system after the expansion. The degree of expansion is thus determined from the ratio of the pressures. The vapor source is the surface of ethyl alcohol filling a trough that is fastened to the upper cover. The diffusion chamber is filled with air at atmospheric pressure.

Generally speaking, the vapor partial pressure and temperature vary with the height within the volume of the diffusion chamber. Consequently, the cloud produced by the expansion does not form throughout the chamber, but only in those regions where the partial pressure exceeds a certain value. Knowing the temperature distribution and the degree of expansion, it is possible to determine the partial pressure of the vapor at the cross section where the boundary of a dense cloud produced by condensation on neutral or charged centers is located. By varying the degree of expansion, it is thus possible to determine the partial pressure field over the entire volume of the chamber.

The temperature inside the chamber is measured by a horizontally placed thermocouple, the height of which can be changed by means of a permanent magnet. The partial-pressure distribution obtained by the above method is shown in Fig. 1 (with the temperature distribution in the chamber being approximately as represented by curve 1 of Fig. 2).

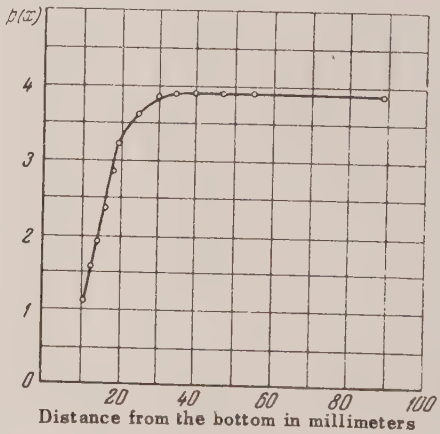

FIG. 1 Partial-pressure distribution in chamber. Height of sensitive layer is 15 mm.

The partial pressure is apparently constant over a considerable volume of the chamber, apparently because of the thorough mixing of the gas and the vapor. The fact that the temperature is constant in any horizontal cross section inside the chamber also indicates that the gas and vapor are thoroughly mixed.

To investigate the effect of the condensation on the partial pressure distribution, the chamber was irradiated inside with a gamma-ray source in such a way that, unlike in the preceding case, the expansion caused condensation on charged, rather than

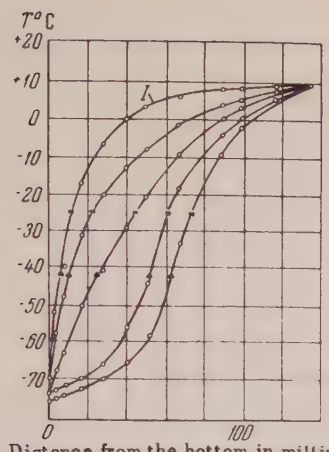

FIG. 2. Temperature distribution in chamber. Asterisks and triangles denote the temperatures of the upper boundary of the sensitive layer produced by a small and large number of condensation centers, respectively.

neutral, centers. Measurements have shown that the condensation on charged centers does not significantly affect the partial pressure distribution above the sensitive layer.

It was shown earlier[2] that the height of the sensitive layer changes with the temperature distribution inside the chamber. For any temperature distribution, the upper boundary of the sensitive layer can be established as being the section at which the temperature $T(x_0)$ has a value corresponding to the saturated vapor pressure $p_s(x_0) = p(x_0)/S_1$ where $p_s(x_0)$ is the pressure of the saturated vapor at a temperature $T(x_0)$, $p(x_0)$ is the partial pressure of the vapor at the upper boundary of the sensitive layer, and S_1 is the superstauration at which condensation on the ions begins. As was mentioned earlier, measurements performed by the expansion method show that the pressure $p(x_0)$ is constant over a considerable volume of the chamber. Therefore, if we assume that a change in the temperature distribution does not affect substantially the partial pressure of the vapor above the sensitive layer, the upper boundary of the sensitive layer (where the supersaturation equals S_1) should have the same temperature regardless of the temperature distributions. This deduction is easily verified experimentally. Figure 2 shows five different temperature distributions. The temperature at which condensation on the ions begins is marked with an asterisk on each curve. It is apparent that the upper boundary of the sensitive layer actually has an approximately constant temperature. Consequently, the assumption that in the region above the sensitive layer the partial pressure of the vapor does not change significantly with the temperature distribution is in agreement with the experimental data.

If the number of condensation centers inside the chamber increases (for example, when the chamber is irradiated by the gamma-ray source), the height of the sensitive layer decreases. The triangle on each temperature-distribution curve of Figure 2 designates the temperature of the upper boundary of the sensitive layer at which the ion concentration is thirteen times the initial concentration. It can be seen that the upper boundary of the sensitive layer remains at the same temperature as before for various temperature distributions. Decreasing the surface area of the evaporating liquid affects the variation in height of the sensitive layer in the same manner as increasing the ion concentration. The data given here shows that changing the condensation conditions over a wide range hardly affects the character of the partial pressure distribution above the sensitive layer.

In conclusion, I express my gratitude to M. S. Kozodaev and Professor M. F. Shirokov for interest in the work and for valuable comments.

[1] H. L. Morrison and G. I. Plain, Rev. Sci. Instr. **23**, 607 (1952)

[2] V. K. Lapidevskii and Iu. A. Shcherbakov, J. Exper. Theoret. Phys. USSR **27**, 103 (1954)

Translated by J. G. Adashko
190

The Problem of the Generalization of the Statistical Theory of the Atom

L. P. RAPOPORT
Voronezh State University

(Submitted to JETP editor March 1, 1955)
J. Exper. Theoret. Phys. USSR **29**, 376-377
(September, 1955)

THE known non-relativistic Hellman equations, generalizing the statistical theory of the atom for the case of electron groupings by the orbital numbers[1], can be generalized by incorporating relativistic and spin-orbital corrections for energy. In connection with the attempts made to use statistical methods for the calculation of the density of distribution of nucleons in nuclei[2-4], the inclusion into these calculations of a term

which takes into account the spin-orbital interaction, and also the possibility of calculating the density of particles with a given orbital momentum represents particular interest.

We will consider the Dirac equation for the radial G and F functions in a centrally-symmetrical field with the potential V

$$\left(\frac{d}{dr}-\frac{1-k}{r}\right)G=\frac{1}{\hbar c}(E+eV+E_0)F,$$
$$\left(\frac{d}{dr}+\frac{1+k}{r}\right)F=\frac{1}{\hbar c}(E_0-E-eV)G, \qquad (1)$$

where $k = l + 1$ for $j = l + 1/2$; $k = -l$ for $j = l - 1/2$; $E_0 = mc^2$. Introducing new functions $g = rG$ and $f = rF$ and eliminating the function f from equations (1), for the function g we obtain

$$\frac{d^2g}{dr^2}-\frac{k(k-1)}{r^2}g=\frac{E_0^2-(E+eV)^2}{\hbar^2c^2}g + \frac{e}{E_0+E+eV}\frac{dV}{dr}\frac{dg}{dr} - \frac{e}{E_0+E+eV}\frac{k}{r}\frac{dV}{dr}g. \qquad (2)$$

A comparison with the non-relativistic Schrödinger equation and an evaluation of the terms located on the right-hand side of Eq. (2), shows that the second term is much smaller than the remaining terms, and henceforward we will omit it.

We will now divide the atom into spherical layers of thickness s and we will consider s so small that in the layer under consideration V, $1/r^2$, $1/r$ remain constant. Then for the electron in this spherical layer we have

$$g_n = A\sin\left(n\frac{\pi r}{s}-n\frac{\pi r_k}{s}\right), \qquad (3)$$

where r_k is the radius of the layer being considered, and $n = 1,2,3,...$

Substituting Eq. (3) in Eq. (2) and solving with respect to E, we obtain for the energy of the electron in the spherical layer in the state n:

$$E_n = E_0\left\{1+\left(\frac{\hbar}{mc}\right)^2 \times\left(\pi^2\frac{n^2}{s^2}+\frac{l(l+1)}{r^2}-\frac{e}{2E_0}\frac{k}{r}\frac{dV}{dr}\right)\right\}^{1/2}-eV, \qquad (4)$$

where the substitution $k(k-1) = l(l+1)$ is made and it is assumed that $E_0 + E + eV \approx 2E_0$.

The first two terms in the round brackets of Eq. (4) represent the kinetic energy, and the third term the spin-orbital energy. The sum of these terms is considerably smaller than the rest energy of the electron E_0. We will now consider that at any definite l each of the states with $n = 1, 2, 3,...$ when the spin is taken into account has $2(2l + 1)$ - multiple degeneration and that all the possible states are occupied. Then for the total (kinetic plus spin-orbital) energy W_k we obtain:

$$4\pi r^2 s W_k \approx \frac{\hbar^2}{2m}\sum_l\left\{2(2l+1)\frac{\pi^2}{s^2}\sum_1^n n^2 + \frac{n2(2l+1)l(l+1)}{r^2}\right\} - \sum_l\frac{en(2l+1)}{4}\lambda_k^2\frac{1}{r}\frac{dV}{dr} + (\text{relativistic corrections for the kinetic energy}) \qquad (5)$$

where $\lambda_k = \hbar/mc$.

In the statistical case, for large n, we have $\sum_1^n n^2 \approx \frac{n^3}{3}$; therefore, dividing Eq. (5) by $4\pi r^2 s$ and introducing the density of the electrons with a given l, $\rho_l = [2(2l+1)/4\pi r^2]\,(n/s)$, we obtain for the total energy E:

$$E=\sum_l\int\left\{\frac{2\pi^2\hbar^2r^4}{3m(2l+1)^2}\rho_l^3+\frac{\hbar^2\cdot l(l+1)}{2m}\frac{\rho_l}{r^2} - \frac{1}{8}\lambda_k^2\frac{e}{r}\frac{dV}{dr}\rho_l + (\text{relativistic corrections}) - eV\rho_l\right\}div. \qquad (6)$$

Varying Eq. (6) with respect to ρ_l with the additional condition $\int\rho_l dv = N_l$, where N_l is the total number of electrons in the atom with a given l, and neglecting the relativistic corrections for the kinetic energy, we obtain the expression for ρ_l, which, when substituted into the Poisson equation $\nabla^2V = 4\pi e\Sigma\rho_l$, yields the Thomas-Fermi equation for the potential V:

$$\frac{d^2(rV)}{dr^2}=\frac{\sigma}{r}\sum_l(2l+1)\left\{e(V-V_l)+\frac{1}{8}\lambda_k^2\frac{e}{r}\frac{dV}{dr}-\frac{\hbar^2}{2m}\frac{l(l+1)}{r^2}\right\}^{1/2}, \qquad (7)$$

where $\sigma = 2e\sqrt{2}/\pi\hbar$, V_l is the Lagrange multiplier. Equation (7) differs from the Hellman equation by an additional term which takes into account the spin-orbital interaction. The relativistic corrections for the kinetic energy were disregarded for simplicity.

It becomes possible to use the equation obtained for the calculation of the density of

nucleons in the nucleus, where the spin-orbital term is particularly significant.

[1] H. Hellman, Acta Phys.-Chim. URSS **4**, 225 (1936)

[2] D. Ivanenko and V. Rodichev, Dokl. Akad. Nauk SSSR **70**, 605 (1950)

[3] P. Gombash, Uspekhi Fiz. Nauk **49**, 385 (1953)

[4] L. Rapoport and V. Filimonov, J. Exper. Theoret. Phys. USSR **27**, 243 (1954)

Translated by E. Rabkin
209

Total Cross Sections of Nuclei of Certain Elements for Neutrons with Energies of 590 mev

V. P. Dzhelepov, V. I. Satarov and B. M. Golovin
Institute for Nuclear Problems, Academy of Sciences, USSR

(Submitted to JETP editor May 30, 1955)
J. Exper. Theoret. Phys. USSR **29**, 369-371 (September, 1955)

USING the synchrocyclotron of the Institute of Nuclear Problems we performed experiments for the purpose of determining the total cross section of protons, deuterons and more complex nuclei for neutrons with average effective energies of 590 mev. The neutrons were obtained as a result of "charge exchange" in beryllium of protons accelerated to energies of 680 mev. The above cross sections were measured on the basis of the loss of neutrons from the beam.

The general experimental scheme is shown in Fig. 1. The absorbers of materials under investigation were placed immediately in front of the steel collimator (diameter of the aperture: 3cm) which was placed within the protective wall. The neutrons, having traversed the absorber and the collimator were detected by the telescope T_1, composed of three scintillation counters (with tolane crystals) which registered the recoil protons emitted at an angle of 20 degrees from a polyethylene scatterer placed in the beam. The experiments were performed under conditions of good geometry. The neutrons scattered in the sample at an angle greater than 15 minutes could not strike the scatterer and consequently were not detected by the telescope. The intensity of the neutron beam was continuously controlled by means of a similar telescope T_2. The resolving time of coincident events of the telescopes was 6×10^{-8} sec.

The energy threshold of the detector for neutrons was 470 mev, determined by the thickness of tungsten filters placed between the second and third counters. The neutron energy distribution in the beam was determined in our laboratory by Fliagin[1]. The results of these measurements are shown in Fig. 2. With the energy threshold of the detector set to the above indicated value, the average effective energy of the neutrons for which we determined the cross sections, $E^{\text{eff}}_{\text{n, average}} = 590$ mev. The cross sections were determined on the basis of the formula:

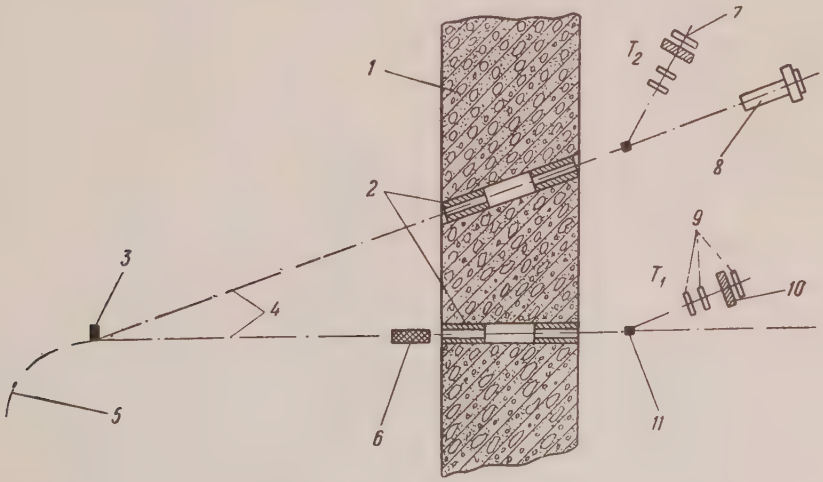

FIG. 1. Experimental Arrangement. *1* – Concrete shield; *2* – Collimators; *3* – Target (Be); *4* – Neutrons; *5* – Protons ($E_p = 580$ mev); *6* – Sample; *7* – Telescope; *8* – Bi- Chamber; *9* – Detecting telescope; *10* – Filter; *11* – Scatterer

$$\sigma_t = \frac{1}{nx} \ln \frac{N_0}{N_n},$$

where: N_0 and N_n are relative neutron intensities, corrected for the background and measured in the presence of the sample in the beam, and without it. n = number of nuclei per cubic centimeter of sample material, and x = thickness of the sample in centimeters.

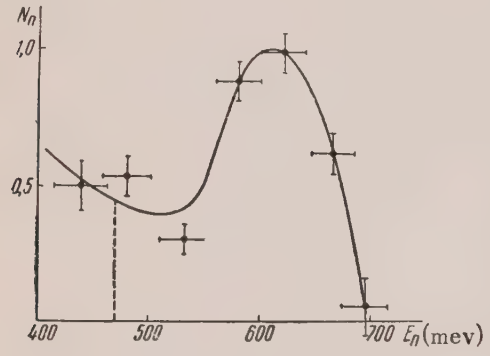

FIG. 2. Neutrons Energy Spectrum

The results of control experiments, performed with Al and Cu absorbers of various thicknesses, showed that the semi-logarithmic plot of the decrease of the neutron beam is, indeed, linear with respect to the absorber thickness.

The total cross section for neutron scattering in hydrogen was determined on the basis of the difference of the cross sections of carefully purified polyethylene and graphite. The cross section of oxygen was determined on the basis of data obtained for total cross sections for neutron interactions with water and hydrogen; the cross section of deuterium was determined on the basis of the difference of the cross sections of heavy water (D_2O) and oxygen.

The results of the measurements are shown in the following Table (third column). The limits of accuracy of the magnitudes of the cross sections, indicated in the Table, represent the average quadratic errors, determined by the differences of the results of a large number (30-40) of separate measurements of cross sections, from the arithmetical average .

The analysis of the data obtained and their comparison with the results of measurements performed at lower neutron energies permits the following conclusions:

1. The total cross section for the interaction of neutrons with protons, practically does not change in the neutron energy interval from 270 to 590 mev. The magnitude of this cross section obtained at 590 mev, and also the fact, that according to references 2 and 3 total cross sections for the production of neutral and charged π-mesons in $(n-p)$ collisions at that energy represent $\sim 6 \times 10^{-27}$cm^2 and $(3-4) \times 10^{-27}$cm^2 respectively, permit the conclusion that the total cross section of the elastic $(n-p)$ scattering, $\sigma_t^{elast}(n-p)$, at this energy, equals $\sim$ (26-28) $\times 10^{-27}$cm^2. Considering that at 270 mev, $\sigma_t^{elast} \times (n-p)$ is 35×10^{-27}cm^2 [4], then the observed

Substance	Geometrical cross section* of the nucleus πR^2 in 10^{-27} cm^2	σ_t in 10^{-27} cm^2 E_n=590 mev	Transparence of the nucleus $\eta = 1 - \sigma_t / 2\pi R^2$
H	—	36±2	—
D	—	72±2,5	—
D—H	—	36±2	—
Be	255	261±4	0.49
C	310	319±2	0.48
O	375	407±5	0.46
Al	515	631±9	0.39
Cu	945	1250±40	0.34
Sn	1430	1980±40	0.31
W	1900	2780±60	0.27
Pb	2060	2920±70	0.29
U	2260	3290±70	0.27

* The geometrical cross sections of the nuclei are determined on the basis of nuclear radii $R = 1.37 \times A^{1/3} \times 10^{-13}$cm, determined from known data on total nuclear cross sections for neutrons with energies of 15-20 mev when the nuclei can be assumed to be non-transparent.

decrease of this cross section is about 20% when the energy of the neutrons is raised from 270 to 590 mev. Since the total cross section of the elastic ($n - p$) scattering represents the sum of interactions of nucleons in states with isotopic spins $T = 0$ and $T = 1$, and since, on the basis of available data [5,6], the cross section for elastic ($p - p$) scattering (cross section of interaction in state with $T = 0$) remains constant in the indicated energy range, then the observed decrease of $\sigma_t^{elast}(n - p)$ is determined by the decrease with energy of the cross section of interaction of nucleons in a state of isotopic spin T equal to zero. This deduction, among others, indicating the difference in nucleon interaction in states with $T = 0$ and $T = 1$, was made by us previously[7], where the problem of ($n - p$) interactions at high energies was studied in more detail.

2. The cross section of ($n - p$) interaction when the energy was raised from 270 mev to 590 mev, increased by about 25%. The difference of total cross sections of (n - d) and ($n - p$) interactions for this energy interval increased by more than 60%. A comparison showed that within experimental errors the difference of cross sections $\sigma_t(n - d) - \sigma_t(n - p)$ found at $E_n = 590$ mev coincides in magnitude with the cross section for ($p - p$) interaction determined in reference 8 for protons with the same energy. The latter fact, in the light of conditions of charge symmetry of nuclear forces, the existence of which is confirmed for high energy of nucleons[9], shows that interference effects at 590 mev introduce a small contribution to the cross section of ($n - d$) interaction. In such case the observed increase of this cross section in the 270-590 mev energy interval is explained by the increase of the cross section of the interaction of neutrons with neutrons, depending as in the case of two protons interaction on the increase of the probability of inelastic ($n - n$) resonances.

3. The total cross sections of complex nuclei when the energy is varied from the interval 200-400 mev, where they are practically constant, to 590 mev vary differently, depending on the atomic weight.

Thus, the cross sections of light nuclei, such as Be, C, O increase by 10-15%. The cross sections of nuclei of heavy elements remain unchanged within experimental errors. The transparency of nuclei of elements of low A is ~ 0.5 (see Table); for elements with high A it is equal to ~ 0.3.

The observed increase of the total cross sections of light nuclei when the neutron energy is raised from 400 to 590 mev is explainable by the growth of cross sections of elementary nucleon-nucleon interactions [particularly the cross section for ($n - n$) interactions] in the energy range under consideration. The cause of the invariability, for these energies, of the total nuclear cross sections of elements with high A, is at present unclear. The quantitative analysis (for example on the basis of the optical model of the nucleus) of such behavior of these cross sections, could be considerably helped by data on the energy dependance of total cross sections for inelastic and diffraction scattering of neutrons by nuclei in the energy range under study.

[1] V. B. Fliagin, Report Inst. Nuclear Problems, Acad. Sci., USSR, 1954

[2] V. P. Dzhelepov, V. B. Fliagin and K. O. Oganesian, Report Inst. Nuclear Problems, Acad. Sci., USSR, 1954

[3] I. M. Kazarinov and I. N. Simonov, Report Inst. Nuclear Problems, Acad. Sci., USSR, 1954

[4] E. Kelly, C. Leith, E. Segre and C. Wiegand, Phys. Rev. 79, 96 (1950)

[5] O. Chamberlain, E. Segre and C. Weigand, Phys. Rev. 83, 923 (1951)

[6] M. G. Meshcheriakov, N. P. Bogachev, B. C. Neganov and E. V. Piskarev, Dokl. Akad. Nauk SSSR 99, 955 (1954); N. P. Bogachov and I. K. Vzorov, Dokl. Akad. Nauk SSSR 99, 931 (1954)

[7] V. P. Dzhelepov, I. M. Kazarinov, B. M. Golovin, V. B. Fliagin and V. I. Satarov, Izv. Akad. Nauk SSSR, Ser. Fiz. 19, 5 (1955)

[8] A. Shaprio, C. Leavitt and F. Cheu, Bull. Am. Phys. Soc. 29, 4, 75 (1954)

[9] V. P. Dzhelepov, B. M. Golovin and V. I. Satarov, Dokl. Akad. Nauk SSSR 99, 943 (1954)

Translated by M. Ter-Pogossian
205

Neutron Spectrometry Based on the Measurement of the Decelerating Time of Neutrons

L. E. Lazareva, E. L. Feinberg and F. L. Shapiro
The P. N. Lebedev Institute of Physics, Academy of Sciences, USSR

(Submitted to JETP editor July 6, 1955)
J. Exper. Theoret. Phys. USSR 29, 381-383 (September, 1955)

THE process of the deceleration of neutrons in a medium possesses a property which permits us to develop a new method of neutron spectrometry. This property is the gradual monochromatization of neutrons resulting, essentially, from the fact that, of the neutrons introduced into the medium, the fastest neutrons collide relatively more frequently with the nuclei of the decelerator. If the mass of the nuclei of the decelerator M (the mass of the

neutron is taken as unity) is large, $M \gg 1$, then the deceleration times are large enough to be measured easily. Such a change in the neutron spectrum $n(v,t)$ with respect to time t (v is the velocity) follows also from the so-called acceleration theory*. Since

$$\frac{\partial q}{\partial t} = -\frac{v}{\lambda_c} q + \frac{\xi v^2}{2\lambda_s} \frac{\partial q}{\partial v}, \qquad q = \frac{\xi v^2}{2\lambda_s} n, \quad \xi \approx \frac{2}{M+1}, \tag{1}$$

where λ_c and λ_s are the path lengths of capture and of scattering; then after substituting the variables

$$\omega = \int_{v_2}^{v} \frac{\lambda_s dv}{v^2 \xi}, \qquad q = e^{-\Omega(\omega)} \chi, \tag{2}$$

$$\Omega = -\int_{v}^{v_1} \frac{\lambda_s}{\lambda_c} \frac{2dv}{\xi v}$$

we arrive at an equation for χ (apparently, ω has the meaning of characteristic deceleration time):

$$\frac{\partial \chi}{\partial t} + \frac{\partial \chi}{\partial \omega} = 0. \tag{3}$$

The solution of this equation $\chi = \chi\ (t - \omega)$, that is,

$$n(v, t) = \frac{2\lambda_s}{\xi v^2} \times \exp\left\{-\int_{v}^{v_1} \frac{2\lambda_s}{\lambda_c} \frac{dv}{\xi v}\right\} \chi\left(t - \int_{v_2}^{v} \frac{2\lambda_s dv}{\xi v^2}\right), \tag{4}$$

where v_1 and v_2 are constants. Here it is easy to satisfy the initial condition and to obtain a solution for the general case. Let the neutron spectrum at the initial instant of time be given by the function $n(v,0) = F\left(\frac{v - v_0}{\Delta_0}\right)$, where v_0 is some characteristic velocity, Δ_0 is the initial width of the spectrum. In practice, even when the source yields monochromatic neutrons with an energy of the order of 1 mev, however, even after the first inelastic collision we obtain $\Delta_0 \sim v_0$.

Let, further, λ_s be independent of v; then the "deceleration time" up to a velocity $v \ll v_2$ will be equal to $\omega = 2\lambda_s / \xi v$ and

$$n(v, t) = \left(1 - \frac{\xi v t}{2\lambda_s}\right)^{-2} \times \exp\left\{\int_{v_t}^{v} \frac{\lambda_c}{\lambda_s} \frac{dv}{v}\right\} F\left(\frac{v_t - v_0}{\Delta_0}\right), \tag{5}$$

$$v_t = v \Big/ \left(1 - \frac{\xi v t}{2\lambda_s}\right).$$

The center of the distribution at the instant t is displaced to the point where the argument F is equal to zero, $v = v_c = v_0 \Big/ \left(1 + \frac{\xi v_0 t}{2\lambda_s}\right) \approx \frac{2\lambda_s}{\xi t}$. The distribution acquires a width determinable from the the value v, for which the argument F is equal to ~ 1, which is much smaller than the initial value:

$$\Delta_1 \sim \Delta_0 (v_c / v_0)^2. \tag{6}$$

This result follows at once also from the relationship of the deceleration time with the initial neutron velocity v_0 and the velocity v, which is expressed by the ratio:

$$\omega = \frac{2\lambda_s}{\xi} \left(\frac{1}{v} - \frac{1}{v_0}\right). \tag{7}$$

Differentiating, we have:

$$\frac{\delta v}{v^2} = \frac{\delta v_0}{v_0^2}, \quad \overline{\delta v} = \overline{\delta v_0}\ \frac{v^2}{v_0^2} \ll \overline{\delta v_0}. \tag{8}$$

Thus there occurs a narrowing of the neutron spectrum (monochromatization).

However, the substitution of the integral kinetic equation by a differential equation holds only when $\xi v\ (\partial q / \partial v) \ll q$, that is, the spectrum is quite diffused. One can easily become convinced that even for an initially diffused spectrum the inequality may finally be disturbed. This does occur, as can be easily verified (by considering $\xi v_c t / 2\lambda_s \sim 1$, $\Delta_0 \sim v_0$), when the deceleration approaches the stage $v_c \sim \xi v_0$. In lead at an initial energy of the order of 1 mev a similar deceleration corresponds to $\sim 10^3 - 10^4$ ev. At a further deceleration, when the condition λ_s = const is retained, no broadening can occur (since, if it would occur, the evaluations given above would enter into action, from which it becomes evident that a narrowing of the spectrum would occur again). However, there will also not occur any narrowing of the spectrum: in accordance with the determination of the moments of distribution[1], the dispersion, as it follows from exact theory, becomes equal to

$$\sqrt{\overline{\delta v^2} / v^2} = 3 / 2M = {}^3/_4 \xi, \tag{9}$$

that is, at $v_c < \xi v_0$ it will remain constant (until such time when the thermal movement of the atoms

of the medium begins to produce an effect). A more complete theory of the deceleration of neutrons in heavy media was developed by Kazarnovskii[2].

Thus, by carrying out measurements with neutrons at given instants of time after their introduction into the decelerator, it is possible, if we know their energy from Eq. (7), to use this process for the spectral investigation of neutron reactions; moreover, lead which is available in fairly pure form is a very adequate decelerator in this case.

With regard to the possibilities of this method, one may advance the following considerations (these were given in the report by F. L. Shapiro at the Seminar of the Academy of Sciences of the USSR in 1950). At an equal intensity of the source, the neutron current of a given energy inside of a fairly large mass of lead exceeds considerably the current attainable in neutron spectrometers on the principle of time of flight, in which the detector is located at a distance of several meters from the source. In fact, the neutron current in lead in the vicinity of the source is equal to

$$nv = \Phi_1 \approx \frac{Q}{(4\pi\tau_{\mathrm{Pb}})^{3/2}} \frac{4\lambda_{s\,\mathrm{Pb}}}{\xi v^2}. \qquad (10)$$

For the current at a distance R from the source of the fast neutrons surrounded by paraffin, (an arrangement generally used in the time-of-flight method), we have:

$$\Phi_2 < \frac{Q}{(4\pi\tau_n)^2} \frac{2\lambda_{sn}}{v^2} \frac{S}{4\pi R^2}, \qquad (11)$$

where S is the area of the paraffin decelerator. Assuming that $\tau_{\mathrm{Pb}} = 4 \times 10^3\,\mathrm{cm}^2$, $\tau_{\mathrm{paraf}} = 60\,\mathrm{cm}^2$, $\lambda_{s\mathrm{Pb}} = 3\,\mathrm{cm}$, $\lambda_{s\,\mathrm{paraf}} = 0.8\,\mathrm{cm}$, $S = 200\ \mathrm{cm}^2$ and $R = 3\mathrm{m}$, we find:

$$\Phi_1/\Phi_2 > 2 \cdot 10^3.$$

A more detailed evaluation, taking into account the leakage of neutrons during deceleration in a finite volume, shows that, by using a mass of lead of several ten-folds of tons, a gain in the neutron current can be attained of the order of 3 – 4 as compared with the time-of-flight method. This evaluation was also substantiated experimentally by measuring the densities of neutrons generated by an Ra-Be source inside a lead cube having dimensions of ~1 m^3, and in air at a distance of ~1 m from the same source surrounded by paraffin.

The high "luminosity" of the method of decelerating time makes it possible to carry out experiments on the spectrometry of slow neutrons, even if we possess only a comparatively simple and accessible source such as the reaction $D + T$ in an ionic accelerating tube of several hundred kilovolts.

The second advantage of this method of spectrometry by the decelerating time is the simple possibility of measuring the cross sections of the absorption, which is particularly important in the cases when the absorption is small as compared with the scattering. On the one hand, the passage of a thin sample, surrounding the neutron detector, placed in the mass of lead, is dependent only on the cross section of the neutron absorption in the sample. On the other hand, the small γ - background inside a large mass of lead permits us to measure simply the cross section of capture from the intensity of the captured γ - rays.

A disadvantage of the method proposed is the limited resolving capacity (~ 30% by energy) determinable by the dispersion (8). It may be assumed, however, that owing to the advantages mentioned above the method of the time deceleration, irrespective of its small resolving capacity, will prove to be a useful addition to the other known methods of neutron spectroscopy. The practical realization of this method[2] justified the above considerations.

In conclusion, the authors wish to thank I. M. Frank for valuable discussion.

---

* Presented by E. L. Feinberg at a Seminar at the Academy of Sciences, USSR, 1944.

[1] R. E. Marshak, Rev. Mod. Phys. 19, 185 (1947)

[2] A. A. Bergman, A. I. Isakov, I. D. Murin, F. L. Shapiro, I. V. Shtranikh and M. V. Kazarnovskii, Report Given by the USSR at the International Conference on the Peaceful Uses of Atomic Energy in Geneva, 1955

Translated by E. Rabkin
212

Diffusion Coefficient of Particles in a Magnetized Interstellar Medium

A. A. Logunov and Ia. P. Terletskii
Moscow State University

(Submitted to JETP editor May 25, 1955)
J. Exper. Theoret. Phys. USSR 29, 701-702
(February, 1955)

THE diffusion of charged particles in a magnetized interstellar medium is very important for the explanation of the properties of the primary cosmic radiation[1]. The mechanism of passage of charged particles through a magnetized interstellar medium is similar to the process of diffusion of particles in gases. It follows from the mechanism

of increase of magnetic field in interstellar medium that the interstellar magnetic field will be sufficiently homogeneous in regions of dimensions of the pulsation L_k, which have a kinetic energy density equal to the magnetic energy density of the medium[2-4]. Charged particles moving in an interstellar magnetic field will go from one homogeneous region to another. Because of the turbulent character of the magnetic field, it can be assumed that the directions of the homogeneous regions of the magnetic field are distributed randomly.

We want to examine the dependence of the diffusion coefficient on the particle energy. If the energy is such that the mean radius of curvature of the particle trajectory is much smaller than L_k, then, due to the chaotic structure of the magnetic field, the particle will be moving randomly. For the mean free path we can take the mean dimension of the homogeneous regions of the magnetic field. In this energy interval, we can therefore consider the diffusion coefficient as being constant and equal to

$$D \approx cL_k. \tag{1}$$

Consider now the case when the particle energy is such that the mean radius of curvature of the trajectory of the particle in the magnetic field is much larger than the dimension of the homogeneous regions of the magnetic field. The scattering will be mostly in the forward direction, and we have first to evaluate the transport mean free path of the particle in the interstellar magnetized medium. It is known[5,6] that the transport mean free path is the mean distance travelled by the particle after it has passed through an infinite number of randomly distributed homogeneous regions of the magnetic field:

$$l = L_k(1 + \overline{\cos\theta_k} + \overline{\cos\theta_k^2} + \ldots) = L_k/(1 - \overline{\cos\theta_k}), \tag{2}$$

where θ_k is the scattering angle due to one homogeneous region of the magnetic field.

The radius of curvature of the trajectory of a particle with momentum P in a magnetic field H is equal to

$$R_k = cp/eH\sin\theta, \tag{3}$$

where θ is the angle between the momentum and the magnetic field. The mean dimension of a homogeneous region of the magnetic field is L_k; hence,

$$\overline{\theta_k^2} \simeq \frac{L_k^2 e^2 H^2 \overline{\sin^2\theta}}{c^2 p^2}, \tag{4}$$

and

$$l = \frac{L_k}{1 - \overline{\cos\theta_k}} \simeq \frac{2L_k}{\overline{\theta_k^2}} = \frac{2c^2p^2}{L_k e^2 H^2 \overline{\sin^2\theta}}; \tag{5}$$

but for extreme relativistic energies $p \sim E/c$, and

$$l \simeq E^2/L_k e^2 H^2, \tag{6}$$

therefore, for high energies the diffusion coefficient will be:

$$D \approx cE^2/L_k e^2 H^2. \tag{7}$$

If one assumes that the dependence of the diffusion coefficient on the energy is monotonic, it is easy to determine the dependence for intermediate energies. It is clear that for some energy interval in the intermediate region, this dependence may be considered as linear. This is to some extent a complementary argument for our assumption of linear dependence for the diffusion coefficient.

[1] Ia. P. Terletskii, Works of the third meeting on cosmogony (Published by Acad. of Sciences, USSR, 1954)

[2] A. Schlüter and L. Biermann, Z. Naturforsch 5, 5 (1950)

[3] G. K. Batchelor, Proc. Roy. Soc. (London) **201**, 405 (1950)

[4] A. A. Logunov and Ia. P. Terletskii, Izv. Akad. Nauk SSSR, Ser. Fiz. 17(No. 1) (1950)

[5] E. Fermi, *Nuclear Physics*, 1951

[6] *Scientific and Technical Foundations of Nuclear Energetics*, edited by Clark Goodman

Translated by E. S. Troubetzkoy
259

Determination of the Dielectric Constant of Superconductors

M. IA. AZBEL'

(Submitted to JETP editor July 15, 1955)
J. Exper. Theoret. Phys. USSR 29, 705-707
(November, 1955)

ABRIKOSOV[1] has obtained formulas for the determination of the dielectric constant of superconductors, taking into account its abnormally large value (see, for example, Ginzburg[2]). However, the question of the existence of an anomalously large polarizability in superconductors has not yet received final settlement, since the corresponding calculations, carried out on the results of the measurements by Galkin[3] at a frequency of $\omega = 2.8 \times 10^{11}$ sec^{-1}, have not indi-

cated any change in the sign of the dielectric constant $\epsilon = \epsilon_0 - (c^2/\omega^2\delta_0^2)$ (δ_0 is the penetration depth of the static magnetic field in the superconductor). Galkin and Kaganov[4] have attributed this to the weak dependence of δ_0 on the frequency.

It is shown in the present work that the results of Galkin's experiments[3] can be understood if we take into account the anisotropy of superconductors. As is seen below, consideration of the anisotropy makes an essential change in the expression for the surface impedance of superconductors.

In this investigation we consider the surface impedance of the superconducting metal for an arbitrary dispersion law for the normal electrons $\epsilon = \epsilon(\mathbf{p})$ (ϵ and p are their energy and quasimomentum). The complete set of equations in this case has the form

$$E_\alpha''(z) + \frac{\omega^2\varepsilon_{\alpha k}}{c^2}E_k = \frac{4\pi i\omega}{c^2}j_\alpha \quad (\alpha = x, y); \tag{1}$$

$$(\varepsilon_{\alpha k}E_k = \varepsilon_{\alpha x}E_x + \varepsilon_{\alpha y}E_y + \varepsilon_{\alpha z}E_z); \tag{2}$$

$$j_z = \frac{\omega}{4\pi i}D_z;$$

$$\mathbf{j}e^{i\omega t} = \frac{2e}{(2\pi\hbar)^3}\int \mathbf{v} f\, dp_x dp_y dp_z; \tag{3}$$

$$\frac{\partial f}{\partial t} + \frac{\partial f}{\partial z}v_z + \frac{\partial f}{\partial \mathbf{p}}e\mathbf{E}e^{i\omega t} + \frac{f-\bar{f}}{\tau} = 0; \tag{4}$$

$$\varepsilon_{ik} = \varepsilon_{ik}^0 - \frac{c^2}{\omega^2}(\delta^{-2})_{ik} = \varepsilon_{ik}^0 - \frac{(\omega_0^2)_{ik}}{\omega^2}; \tag{5}$$

$$\bar{f} = \int\limits_{\varepsilon(\mathbf{p})=\varepsilon} f\frac{dS}{v} \Big/ \int\limits_{\varepsilon(\mathbf{p})=\varepsilon}\frac{dS}{v}; \tag{6}$$

$$f\Big|_{\substack{z=0\\ v_z>0}} = (1-q)f_0 + qf\Big|_{\substack{z=0\\ -v_z}} \tag{7}$$

Here ϵ_{ik} is the dielectric constant tensor, δ_{ik} the tensor of the penetration depth of a static magnetic field in a superconductor, τ the relaxation time of the normal electrons at a given temperature, $\mathbf{v}$ the velocity of the electron, ω the frequency of the electromagnetic field, ϵ_0 is the limiting energy, f the distribution function of the electrons, $\mathbf{E}$ the variable electric field intensity, $\mathbf{j}$ is the current density, q the reflection coefficient of the electrons from the surface; the axis Oz coincides with the inwardly drawn normal to the surface of the metal.

We linearize the kinetic equation (4) by setting

$$f = f_0 - e\tau^*\frac{\partial f_0}{\partial\varepsilon}e^{i\omega t}\psi; \quad \tau^* = \frac{\tau}{1+i\omega t};$$

[$f_0(\epsilon)$ is the equilibrium Fermi distribution function]. Taking into account that $D_i = \epsilon_{ik}^0 E_k$ and

$$\int\psi dS = \frac{(2\pi\hbar)^3}{2e^2\tau^*}\rho' = \pi^2\hbar^3\varepsilon_{zk}^0 E_k'(z) \Big/ e^2\tau\int\limits_{\varepsilon(\mathbf{p})=\varepsilon_0}\frac{dS}{v},$$

we get from Eqs. (1)-(7):

$$(1-\delta_{i3})E_i''(z) + \frac{\omega^2\varepsilon_{ik}}{c^2}E_k(z) \tag{8}$$

$$= \frac{3i}{l\delta^2}\left\{\int\limits_{-\infty}^{\infty}K_{ik}(z-\mu)E_k(\mu)\,d\mu + \int\limits_{-\infty}^{\infty}Q_{ik}(z-\mu)E_k'(\mu)\,d\mu\right.$$

$$-[1-(-1)^{\delta_{k3}}q]\int\limits_0^{\infty}P_{ik}(|z|+\mu)E_k(\mu)\,d\mu\cdot$$

$$\left.+(1+q)\int\limits_0^{\infty}R_{ik}(|z|+\mu)E_k'(\mu)\,d\mu\right\};$$

$$\delta_{ik} = \begin{cases}1 & (i=k)\\ 0 & (i\neq k),\end{cases}$$

where

$$K_{ik}(\omega) = \frac{4}{S}\int\limits_{n_z\geqslant 0}\frac{n_i n_k}{n_z}\exp\left\{-\frac{|\omega|}{e^* n_z}\right\}dS;$$

$$Q_{ik}(\omega) = \operatorname{sign}\omega\,\frac{4}{S}\int\limits_{n_z\geqslant 0}\frac{n_i a_k}{n_z}\exp\left\{-\frac{|\omega|}{e^* n_z}\right\}dS;$$

$$P_{ik}(\omega) = \frac{4}{S}\int\limits_{n_z\geqslant 0}\frac{n_i n_k}{n_z}\exp\left\{-\frac{\omega}{e^* n_z}\right\}dS;$$

$$R_{ik}(\omega) = \frac{4}{S}\int\limits_{n_z\geqslant 0}\frac{n_i a_k}{n_z}\exp\left\{-\frac{\omega}{e^* n_z}\right\}dS;$$

$$\overline{l\delta^2} = 3(2\pi\hbar)^3 c^2/4\pi\omega e^2 S;$$

$$a_k = \pi^2\hbar^3\epsilon_{zk}^0/e^2 l\int\frac{dS}{v}; \quad l = v\tau.$$

In Eq. (8) the field function remains even in the region outside the metal: $\mathbf{E}(-z) = \mathbf{E}(z)$.

Transferring from the equations for the function $\mathbf{E}_i(z)$ to the equations for its Fourier transform, we find that in the zeroth approximation, for $\delta/|l^*| \ll 1$, Eq. (8) can be written in the form:

$$E_\alpha''(z) + (\omega^2\epsilon_{\alpha\beta}^{\text{eff}}/c^2)E_\beta(z) = (3i/l\delta^2) \tag{9}$$

$$\times\int\limits_{-\infty}^{\infty}K_{\alpha\beta}(z-\mu)E_\beta(\mu)\,d\mu\ (\alpha,\beta = x, y),$$

where

$$\epsilon^{\text{eff}}_{\alpha\beta} = \epsilon_{\alpha\beta} + \frac{1}{2} i S_\alpha \frac{\omega^{02}_{z\beta}}{\omega^2} \frac{1 - (\omega^{02}_{zz}/\omega^{02}_{z\beta})(\epsilon^0_{z\beta}/\epsilon^0_{zz})}{\omega\tau(\epsilon_{zz}/\epsilon^0_{zz}) + 4i}; \quad (10)$$

$$S_\alpha = \frac{8}{\overline{v}} \int \frac{1}{\frac{dS}{v}} \int_0^{2\pi} N_\alpha d\varphi \int_0^{\pi/2} tg\,\theta \left\{ \frac{\overline{v}}{v(\varphi, \theta)} - \overline{v}\left(\varphi, \frac{\pi}{2}\right) \right\} d\theta; \quad \overline{v} = \frac{1}{S}\int v\, dS;$$

$$\mathbf{v} = (v \sin\theta\cos\varphi,\ v\sin\theta\sin\varphi,\ v\cos\theta);$$

$$N_\alpha = \begin{cases} \cos\varphi & (\alpha = x) \\ \sin\varphi & (\alpha = y). \end{cases} \quad (11)$$

The integration in Eq. (11) is carried out over the Fermi surface $\epsilon(\mathbf{p}) = \epsilon_0$.

In the simplest case of perfect reflection ($q = 1$) of the electrons from the metal surface the tensor of surface impedance is

$$Z_{\alpha\beta} = -\frac{4\pi i\omega}{c^2} \frac{\partial E_\alpha(0)}{\partial E_\beta(0)} \frac{8i\omega}{c^2} \overline{(l\delta^2)}^{4/3} \times \int_0^\infty \frac{t\,dt}{t^3\delta_{\alpha\beta} + 3ik_{\alpha\beta} - (\omega^2\epsilon^{\text{eff}}_{\beta\alpha}/c^2)\overline{(l\delta^2)}^{2/3}}; \quad (12)$$

$$k_{\alpha\beta} = \frac{8\pi}{S} \int_0^\pi \frac{M_\alpha N_\beta d\varphi}{K\left(\varphi, \frac{\pi}{2}\right)}$$

[$K(\phi, \theta)$ is the Gaussian curve of the Fermi surface].

It is seen from Eq. (10) that the effective dielectric constant is a complex quantity. Hence, it is not sufficient to know X and R for the measurement of ϵ^0 and the determination of the sign of ϵ. We note that the direction of the principal axes of the surface impedance tensor $z_{\alpha\beta}$ depends on the frequency.

These results [Eqs. (10)-(12)] apply not only to single crystals but also to polycrystals with sufficiently large crystal dimensions.

In conclusion, I consider it my pleasant duty to express my thanks to I. M. Lifshitz for his discussions of the results of the research.

[1] A. A. Abrikosov, Dokl. Akad. Nauk SSSR **86**, 43 (1952)

[2] V. L. Ginzburg, Uspekhi Fiz. Nauk **42**, 169, 333 (1950)

[3] A. A. Galkin, Dokl. Akad. Nauk SSSR, No. 6 (1952)

[4] A. A. Galkin and M. I. Kaganov, J. Exper. Theoret. Phys. USSR 25, 761 (1953)

Translated by R. T. Beyer
262

The Role of Spin in the Study of the Radiating Electron

A. N. MATVEEV
Moscow State University

(Submitted to JETP editor January 24, 1955)
J. Exper. Theoret. Phys. USSR 29, 700-701
(February, 1955)

IN his recently published paper, Nelipa[1] claims that the ratio of the magnitude of the integrated radiation of the electron to the magnitude of the integrated radiation of a spinless particle is equal to $1 + (mc^2/E)^2$. Our calculations[2], which take into account quantum corrections of all orders, show that this is not so.

We obtained the following formulas, which may be applied to the radiation of all the spectrum, for arbitrary energies of the electron or of a spinless particle.

$$dW^{(1/2)} = \frac{ce^2}{\pi V\overline{3}}\left(\frac{mc}{h}\right)^2 \times \xi d\xi \left[\int_{\frac{\xi}{1-\xi}\frac{1}{\zeta}}^\infty K_{1/3}(x)\,dx + \frac{\xi^2}{1-\xi} K_{1/3}\left(\frac{\xi}{1-\xi}\frac{1}{\zeta}\right)\right]; \quad (1a)$$

$$dW^{(0)} = \frac{ce^2}{\pi V\overline{3}}\left(\frac{mc}{h}\right)^2 \xi d\xi \int_{\frac{\xi}{1-\xi}\frac{1}{\zeta}}^\infty K_{1/3}(x)\,dx;$$

$$\xi = \frac{h\omega}{E},\ \zeta = \frac{3}{2}\frac{h}{R_0 c}\left(\frac{E}{mc^2}\right)^2. \quad (1b)$$

For $h = 0$ these formulas give the classical formula for the differential spectrum:

$$dW = \frac{3V\overline{3}}{4\pi}\frac{ce^2}{R^2}\left(\frac{E}{mc^2}\right)^4 y\,dy \int_y^\infty K_{1/3}(x)\,dx, \quad (2)$$

$$y = \frac{\omega}{\omega_c},\ \omega_c = \frac{3}{2}\frac{c}{R}\left(\frac{E}{mc^2}\right)^3,$$

obtained by Ivanenko and Sokolov[3], and later by Schwinger[4]. If one considers only quantities of first order in h (first quantum correction), one obtains the quantum-theoretical formulas for the differential spectrum obtained by Sokolov and Ternov[5] and Schwinger[6] which are exact to the first order in h.

Formulas for total radiation energy, which are exact for arbitrary energies of the radiating particles, have the following form (see also reference 7):

$$W^{(1/2,\,0)} = W_{cl}\,\varphi^{(1/2,\,0)}(\zeta); \tag{3}$$

$$\varphi^{(1/2)}(\zeta) = \frac{3\sqrt{3}}{8}\pi\left\{\frac{\partial}{\partial\zeta}\frac{\Phi_{2/3}\left(\frac{i}{\zeta}\right)}{\zeta^2} - \frac{\zeta^2}{3}\frac{\partial^3}{\partial\zeta^3}\frac{\Phi_{2/3}\left(\frac{i}{\zeta}\right)}{\zeta} - \frac{\sqrt{3}}{2\pi}\frac{1}{\zeta^2}\right\}, \tag{3a}$$

$$\varphi^{(0)}(\zeta) = \frac{3\sqrt{3}}{8}\pi\left\{\frac{\partial}{\partial\zeta}\frac{\Phi_{2/3}\left(\frac{i}{\zeta}\right)}{\zeta^2} - \frac{\sqrt{3}}{2\pi}\frac{1}{\zeta^4}\right\};$$

$$\Phi_\nu(z) = i^{-\nu}[J_\nu(z) - \mathbf{J}_\nu(z)] + i^{\nu}[J_{-\nu}(z) - \mathbf{J}_{-\nu}(z)], \tag{3b}$$

where J_ν is the Bessel function and $\mathbf{J}_\nu$ the Anger's function.

For relatively small energies ($\zeta \ll 1$) of the radiating particles, we obtain from the above formulas:

$$\frac{W^{(1/2)}}{W^{(0)}} \approx 1 + \frac{8}{3}\zeta^2 - \frac{275\sqrt{3}}{18}\zeta^3 + \ldots,$$

which shows that the spin is involved only in quantities ζ^2, i.e., in quantities of second order in h. This is why Schwinger's spinless calculation[4], correct to the first order in h, gives the same result as the first quantum correction for particles with spin made by Sokolov, Klepikov and Ternov[7]. Nelipa's evaluation cannot be correct because it does not depend on h.

For extreme relativistic energies ($\zeta \gg 1$) the radiation of a spinless particle differs essentially from that of an electron. This may be seen on the graph, where the spectra of the electron (solid line) and of a spinless particle (dashes-crosses) have been plotted. For comparison under the same circumstances, the spectrum given by classical theory has also been plotted (dotted line). The limit of the spectrum in the high frequency region is given by the energy-momentum conservation law ($\omega_{max} \approx E/h$).

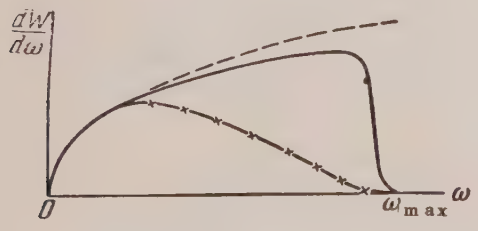

The particularities of the spectra are obvious and do not need further explanations. As it was noted by Sokolov, the main difference between radiation spectra of an electron and a spinless particle is related to the appearance of the electronic magnetic moment which takes place for high energies ($\zeta \gg 1$). This question will be considered in more detail elsewhere.

[1] N. F. Nelipa, J. Exper. Theoret. Phys. USSR **27**, 427 (1954)

[2] A. N. Matveev, Thesis, Moscow State University, 1954

[3] D. Ivanenko and A. Sokolov, Dokl. Akad. Nauk SSSR **59**, 1551 (1948)

[4] J. Schwinger, Phys. Rev. **75**, 1912 (1949)

[5] A. A. Sokolov and I. M. Ternov, J. Exper. Theoret. Phys. USSR **25**, 698 (1953)

[6] J. Schwinger, Proc. Nat. Acad. Sci. **40**, 132 (1954)

[7] A. A. Sokolov, N. P. Klepikov and I. M. Ternov, J. Exper. Theoret. Phys. USSR **24**, 249 (1953)

Translated by E. S. Troubetzkoy
258

Investigation of the Structure of Extensive Air Showers at Sea Level

A. T. Abrosimov, A. A. Bedniakov, V. I. Zatsepin, Iu. A. Nechin, V. I. Solov'eva, G. B. Khristiansen and P. S. Chikin

(Submitted to JETP editor May 3, 1955)
J. Exper. Theoret. Phys. USSR **29**, 693-696 (November, 1955)

In reference 1 a qualitative indication was found that the spatial distribution of the electron component of extensive air showers at sea level is essentially different from that expected from the point of view of the electron-photon picture of the development of showers in the atmosphere. In the summer of 1953 we carried out in Moscow a detailed investigation of the spatial distribution of different components of extensive air showers at small distances from the axis of the shower by the method of correlated hodoscopes*. We report below preliminary results.

To study the spatial distribution of electrons of the shower, density indicators were used, consisting of groups of 24 counters of identical areas, each of which was contained in a hodoscopic cell of a neon hodoscope[2]. In the apparatus were used counters of three different areas: 24, 100 and 330 cm^2, which made it possible to study the

showers in a wide range of particle densities. Forty-seven density indicators were distributed uniformly in a circle of radius 7 m, and 9 indicators were at distances 15, 20 and 30 m from the center of the arrangement (Fig. 1). All density indicators were placed under a thin veneer roof (2.5 gm/cm^2).

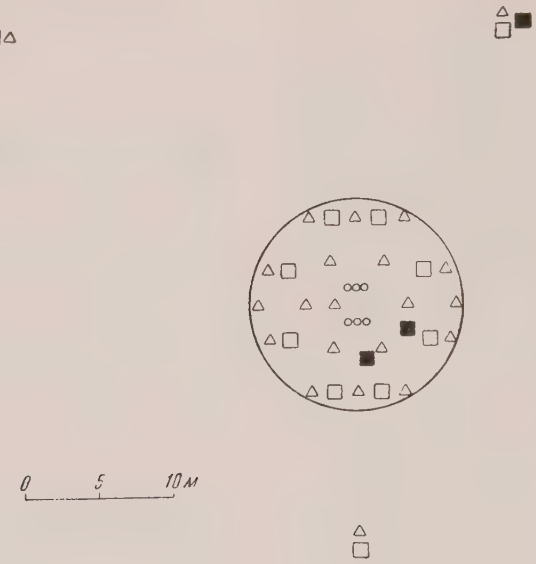

FIG. 1. Arrangement of apparatus. Key: □ - 24 counters of area 330 cm^2 each, △ - 24 counters of area 100 cm^2 and 24 counters of area 24 cm^2 each, ■ - detector of penetrating particles, O - group of counters 4×330 cm^2, inserted in coincidence. Six of such groups constitute an independent indicator of density.

For the study of nuclearly interacting particles, detectors of penetrating particles were used. These consisted of three trays of counters, shielded from all sides by lead and iron (Fig. 2). In the arrangement there were four such detectors, placed at various intervals from the center of the apparatus (Fig. 1). The apparatus was triggered by the coincidence of six groups of counters, placed in the center of the apparatus (Fig. 1) and belonging at the same time to one of the density indicators. The area of a single group of counters was 4×330 cm^2.

When the axis of the shower fell in the central part of the apparatus, the totality of data of all density indicators gave the distribution of flux density of shower particles near the axis of the shower. In this case, assuming that the showers have axial symmetry, it was possible to define the position of the axis of the shower. The position of the axis was defined to an accuracy of 1 m; this accuracy was determined by the basic intervals between density indicators (~ 3 m), the sharpness of increase of density of current of particles towards the axis of the shower, and the accuracy with which each indicator registered the density of shower particles ($\sim 30\%$).

For each shower with axis in the central part of the apparatus, it was possible to construct the function of spatial distribution. The density indicators gave the magnitude of the flux density of shower particles at different distances r from the axis of the shower. The density of particles ρ at the position of an indicator was defined by the formula

$$\rho\sigma = \ln \frac{n}{n-m}, \qquad (1)$$

where n is the total number of counters in the indicator, m is the number of discharged counters, σ is the area of each counter.

Insofar as the accuracy of definition of the

curve of spatial distribution of individual showers is low, we carried out an averaging with respect to the number of particles of curves of spatial distribution for showers lying in a sufficiently narrow interval. We defined the total number of particles in the shower N using the spatial distribution experimentally obtained at distances of 2 to 20 m and beyond this, making a smooth transition to the distribution $1/r^{2.6}$ justified according to reference 3 for large distances, beginning at 70 m from the axis of the shower.

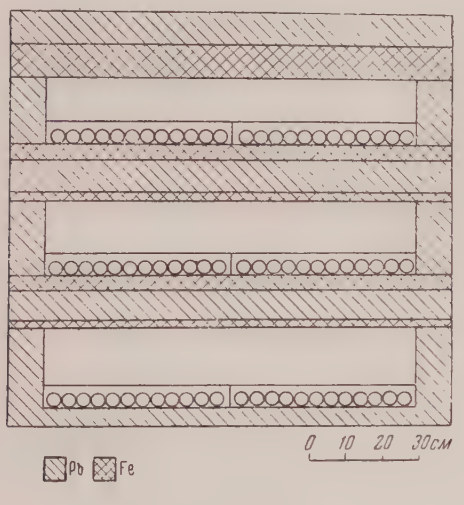

FIG. 2. Section of the detector of penetrating particles. The shielding of the particles from the ends is the same as from the sides.

Because of the inclusion of all counters of the detector in the hodoscope it was possible to distinguish whether the particle incident on the detector was nuclearly interacting. In order to do this, we used the property of a nuclearly interacting particle, i.e., it has a high probability of creating an electron-nuclear shower in going through dense material. The presence of electron-nuclear showers was observed by the coincidence of a large number (≥ 3) of counters in the second and third rows of the detector. The data obtained in this way were analyzed statistically. The mean density of the flux of nuclearly interacting particles $\rho_{(n.i.)}$ was defined by the formula

$$\rho_{n.i.}\ \Sigma = \frac{\ln [k/(k-l)]}{1-\exp(-\mu d)}, \qquad (2)$$

where k is the number of showers with a number of particles in the interval N, $N + \Delta N$ and with axes in the interval r, $r + \Delta r$ from the center of the detector, in which case in l out of k showers, the detector of area Σ registers the presence of nuclearly interacting particles; $1/\mu$ g/cm^2 is the interaction length of nuclearly interacting particles, calculated on the assumption that the effective cross section for production of electron-nuclear showers is geometrical; d g/cm^2 is the thickness of material in which the nuclearly interacting particle gives rise to electron-nuclear showers.

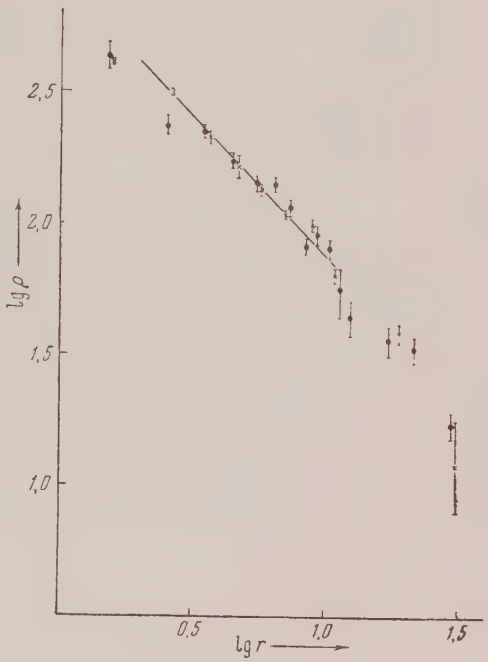

FIG. 3. Spatial distribution of charged particles in extensive air showers with number of particles: ×-$\bar{N} = 4 \times 10^4$, ●-$\bar{N} = 4 \times 10^5$. Solid curve-spatial distribution obtained in a mountainous region (Pamir[4]), (at 3860 m above sea level).

In Fig. 3 are given the spatial distributions of densities of electron current from two groups of showers, differing from each other in number of particles N by an average factor of 10. The spatial distribution for one group of showers was obtained by averaging over 50 showers with numbers of particles lying in the interval $2 \times 10^5 - 10 \times 10^5$ ($\bar{N} = 4 \times 10^5$); the spatial distribution for the other group of showers was obtained by averaging over 50 showers with particle numbers in the interval $2 \times 10^4 - 6 \times 10^4$ ($\bar{N} = 4 \times 10^4$). At distances from 2 to 10 m the spatial distribution** obtained can be approximated by the function $1/r^n$, where $n = 0.93 \pm 0.08$ for showers with $\bar{N} = 4 \times 10^5$ and $n = 1.0 \pm 0.05$ for showers with $\bar{N} = 4 \times 10^4$.

The spatial distribution of nuclearly interacting particles is given in Fig. 4. The data refer to

showers with numbers of particles in the interval $1.5 \times 10^4 - 4 \times 10^5$ ($\overline{N} = 8 \times 10^4$). The curve goes as $1/r^n$, where $n = 1.1 \pm 0.2$.

A very important conclusion from the results obtained is the presence in showers observed at sea level of a sharply defined core. In fact, right up to the axis of the shower, at least to 2 m, in showers of various energies, a sharp rise was observed in the density of the electron and nuclearly interacting component, varying approximately as $1/r$. We note that the spatial distribution $1/r$ along the axis is characteristic of the electron-photon cascade showers near the maximum of their development. It is essential that the sharpness of the core of the shower depends not only on the total energy of the shower, but also on the stage of development in the atmosphere. This conclusion follows from comparison of our data with corresponding data of references 4 and 5, relating to a mountainous region. The comparison is made on Figs. 3 and 4, where account is taken of the difference in density of air at sea level and in the mountainous region. The experimental data obtained indicate the identity of structure of the central region of extensive showers at two different stages of their development.

Consequently, a process should exist which leads to a continual renovation of this region of the shower. In the lower layers of the atmosphere this process is the continual transfer of energy from nuclearly interacting particles of high energy, concentrated in the core of the shower, to the flux of electrons and nuclearly interacting particles, studied by us, of the central part. We note that the spatial distribution is $1/r$.

In conclusion, the authors express their deep appreciation to G. T. Zatsepin for valuable advice and discussion of results and to N. A. Dobrotin for a great deal of help and a constant interest in this work.

The authors express also their thanks to G. V. Bogoslovskii, B. V. Subbotin and M. S. Tuliankina, who took part in the carrying out of measurements.

FIG. 4. Spatial distribution of nuclearly interacting particles: ●-results of the present work, ×-results obtained in a mountainous region (Pamir[5]), (at 3860 m above sea level).

* The method of correlated hodoscopes is based on the measurement of the density of the shower by a hodoscopic system of counters simultaneously at several places of the plane on which the shower impinges.

** A detailed analysis shows that the inaccuracy in the definition of the position of the axis distorts the form of the spatial distribution function at distances less than 2 m from the axis.

[1] L. Kh. Eidus, Dokl. Akad. Nauk SSSR **81**, 1035 (1951)

[2] L. N. Korablev, Dokl. Akad. Nauk SSSR **62**, 215 (1948)

[3] L. Kh. Eidus, N. M. Blinova et al, Dokl. Akad. Nauk SSSR **80**, 577 (1951)

[4] Iu. N. Vavilov, S. I. Nikol'skii and E. I. Tukish, Dokl. Akad. Nauk SSSR **93**, 233 (1953)

[5] Iu. N. Vavilov, S. I. Nikol'skii and V. P. Sarantsev, J. Exper. Theoret. Phys. USSR **28**, 505 (1955); Soviet Phys. **1**, 399 (1955)

Translated by G. E. Brown
255

Concerning some General Relations of Quantum Electrodynamics

E. S. FRADKIN
P. N. Lebedev Institute of Physics, Academy of Sciences, USSR

(Submitted to JETP editor March 9, 1955)
J. Exper. Theoret. Phys. USSR 29, 258-261 (August, 1955)

IN this letter, the derivations of several general relationships connected with the qauge invariance of quantum electrodynamics are presented.

1. In quantum electrodynamics, the following relation holds in the presence of the photon field G:

$$G^{-1}(p, p'+s) - G^{-1}(p-s, p') = -S_\mu \frac{\delta G^{-1}(pp')}{\delta e A_\mu(s)} \quad (1)$$
$$= S_\mu \Gamma_\mu (pp's).$$

In fact, according to reference 1, Eqs. (7)-(12), we have,

$$G^{-1}(p, p'+k) - G^{-1}(p-k, p') = \hat{k}\delta(p-p'-k) \quad (2)$$
$$-\frac{e^2}{(2\pi)^4 i}\int \gamma_\mu \{G(p+s, s_1)\Gamma_\nu(s_1, p'+k, s_2) - G(p-k+s, s_1)\Gamma_\nu(s_1 p' s_2)\} \times D_{\nu\mu}(s_2 s)\, d^4s d^4 s_1 d^4 s_2.$$

In addition, it can be stated that:

$$k_\mu \Gamma_\mu(pp'k) = \hat{k}\delta(p-p'-k) + \frac{e^2}{(2\pi)^4 i}\int \gamma_\rho \left[\left\{G(p+s, s_3) k_\mu \Gamma_\mu(s_1 s_4 k) G(s_2 s_1) \times \Gamma_\nu(s_1 p' s_2) d^4 s_3 d^4 s_4 + G(p+s, s_1) \times k_\mu\left(-\frac{\delta^2 G^{-1}(s_1 p')}{\delta e A_\mu(k)\delta e A_\nu(s)}\right)\right\} D_{\nu\rho}(s_2 s) + G(p+s, s_1) \times \Gamma_\nu(s_1 p' s_2) k_\mu \frac{\delta D_{\nu\rho}(s_2 s)}{\delta e A_\mu(k)}\right] d^4 s_1 d d^4 s_2 d^4 s. \quad (3)$$

Making use of Eq. (1) and its functional derivative with respect to A, and taking into account the fact that in Eq. (3) the last term is equal to zero, because of the transverse nature of the polarization operator [see Eq. (5) below], we have

$$k_\mu \Gamma_\mu(pp'k) = \hat{k}\delta(p-p'-k) \quad (4)$$
$$-\frac{e^2}{(2\pi)^4 i}\int \gamma_\nu \{G(p+s, s_1)\Gamma_\nu(s, p'+k, s_2) - G(p-k+s, s_1)\Gamma_\nu(sp's_2)\} D_{\nu\mu}(s_2 s)\, d^4 s d^4 s_1 d^4 s_2.$$

It can be seen from Eqs. (2) and (4) that Eq. (1) can be regarded as one of the consequences of the exact system of equations for Green's function. Equation (1) permits us to conclude that the polarization operator is transverse in nature, and consequently the rest mass of the photon is zero. Indeed, referring to the expression for the polarization operator given in reference 1 [Eq. (11)], and making use of Eq. (1), we obtain

$$k_\nu P_{\mu\nu}(p, k) = \frac{e^2}{(2\pi)^4 i}\,\mathrm{Sp}\left\{\int \gamma_\mu G(p+s, s_1) \times [G^{-1}(s_1, s_2 - k) - G^{-1}(s_1 + k, s_2)]\, G(s_2 s)\, d^4 s_2 d^4 s_1 d^4 s\right\} = 0. \quad (5)$$

Relation (1) is equivalent to the infinite series expansion of the relation for $J = 0$. The terms of the expansion can be obtained from Eq. (1) by means of successive differentiation with respect to $A_{\nu_n}(S_n)$, or (see the work of Green[2])

$$G^{-1}(p) - G^{-1}(p-s) = s_u \Gamma_\mu(p, p-s, s); \quad (6)$$
$$\Gamma^{(n)}_{\nu_1 \ldots \nu_n}(p-k, p-k-\sum_{m=1}^{n} s_m, s_1 \ldots s_n) - \Gamma^{(n)}_{\nu_1 \ldots \nu_n}\left(p, p-\sum_{m=1}^{n} s_m, s_1 \ldots s_n\right)$$
$$= k_\mu \Gamma^{(n+1)}_{\mu\nu_1 \ldots \nu_n}\left(p, p-k-\sum_{m=1}^{n} s_m, k, s_1 \ldots s_n\right),$$
$$\partial G^{-1}(p)/\partial p_\mu = \Gamma_\mu(p, p, 0),$$
$$-\frac{\partial^2 G^{-1}(p)}{\partial p_\mu \partial p_\nu} = \left.\frac{\partial \Gamma_\mu(p, p-s, s)}{\partial s_\nu}\right|_{s=0} + \left.\frac{\partial \Gamma_\nu(p, p-s, s)}{\partial s_\mu}\right|_{s=0},$$

where

$$\Gamma^{(n)}_{\nu_1 \ldots \nu_n}\left(p, p-\sum_{m=1}^{n} s_m, s_1 \ldots s_n\right) = \left(\prod_{m=1}^{n} \frac{\delta}{\delta e A_{\nu_m}(s_m)}\right)\left(-G^{-1}(p, p')\right)\Big|_{J=0}$$

2. Relations (1) and (6) simplify to a considerable degree the calculations concerned with the longitudinal component of the electromagnetic field. Indeed, Green's function of the photons can be represented as follows:

$$D_{\mu\nu}(k) = \frac{k^2\delta_{\mu\nu} - k_\mu k_\nu}{k^4} d(k^2) + \frac{k_\mu k_\nu}{k^4} d_l(k^2). \quad (7)$$

Substituting Eq. (7) into the mass operator of the electron, we obtain the following expression for Green's function of the electron for $J = 0$:

$$\{\hat{p} - m - \sum_t (p)\} G(p) = 1 + \sum_l (p) G(p); \quad (8)$$

$$\sum_t (p) = \frac{e^2}{(2\pi)^4 i} \int \gamma_\mu G(p+s) \Gamma_\nu (p+s, p, s) \times \frac{s^2 \delta_{\mu\nu} - s_\mu s_\nu}{s^4} d(s^2) d^4 s,$$

$$\sum_l (p) \quad (9)$$

$$= \frac{e^2}{(2\pi)^4 i} \int \gamma_\mu G(p+s) \Gamma_\nu (p+s, p_1, s) \frac{s_\mu s_\nu}{s^4} d_l(s^2) d^4 s.$$

Taking into account Eq. (6), we have,

$$\sum_l (p) G(p) = -\frac{e^2}{(2\pi)^4 i} \int \gamma_\mu G(p+s) \frac{s_u}{s^4} d^4 s. \quad (10)$$

It is known[3] that if the diagram with intersecting photon lines is not taken into consideration, the term Σ_t will not contain any infinities, and consequently, the limiting value of the approximation obtained in this manner will be determined by the longitudinal field component. In this case, it is not necessary to consider the non-linear equations given by Landau[3]; rather, it is sufficient to solve the linear equation

$$(\hat{p} - m) G(p) = 1 - \frac{e^2}{(2\pi)^4 i} \int G(p+s) \frac{\hat{s}}{s^4} d_l(s) d^4 s. \quad (11)$$

Following Landau, let us find the limiting value of $G(p)$ for large values of p^2 in the form $G(p) = \beta(p)/\hat{p}$; then, (11) can be written as:

$$\beta(r) = 1 - \frac{e^2}{16\pi^2} \int_\xi^\eta \beta(z) d_l(z) dz, \quad (12)$$

where $\xi = \ln(-p^2/m^2)$, $\eta = \ln(-L^2/m^2)$, L is the upper cut-off momentum, which must be allowed to go to infinity in the limiting case. Eq. (12) yields the solution which was obtained in reference 3,

$$\beta(\xi) = \exp\left\{-\frac{e^2}{16\pi^2} \int_\xi^\eta d_l(z) dz\right\}. \quad (13)$$

Furthermore, it follows from Eq. (6) that if one of the momenta of the Γ_μ-function is considerably larger than the other, and larger than m^2, the limiting value of Γ_μ is given by:

$$\Gamma_\mu(p, s) \approx \gamma_\mu \beta^{-1}(\xi), \quad (14)$$

with logarithmic accuracy*; here, ξ represents the larger momentum.

Keeping in mind that the polarization operator is independent of the longitudinal component of the electromagnetic field (proof presented below), it is easy to see that in order to obtain the limiting value of Green's function of the photons in our approximation, it is sufficient to calculate the polarization operator by methods of the perturbation theory and substitute it into the equation of Green's function of the photons. Simple calculations yield:

$$d(k) = \left[1 + \frac{e^2}{12\pi^2} \ln \frac{L^2}{k^2}\right]^{-1}. \quad (15)$$

In this manner we can find all the limiting values found in reference 3.

3. Making use of references 4 and 5, it is easy to obtain an explicit expression for the changes in the S-matrix caused by the introduction of an interaction of the type $j_\mu \partial\phi/\partial x_\mu$, where j_μ is the electronic current. In particular, letting

$$A_\mu = A_\mu^t + A_\mu^l = A_\mu^t + \frac{\partial \varphi}{\partial x_\mu}$$

(ϕ is some real function), we can transform exactly the longitudinal component of the interaction.

The expectation value of the S-matrix for the vacuum-vacuum states acquires then the following form, in notation of reference 5:

$$\frac{\langle S \rangle_0}{c} = \exp\left\{ie \int \int_0^1 d\lambda \, \mathrm{Sp}\, \gamma_\mu G\left(xx\lambda \frac{\delta}{\delta j^t}\right) \frac{\delta}{\delta j^t} d^4 x\right.$$

$$+ \sum_{k=0}^{\infty} \frac{i^n}{k!} \int dx_1 \, dx_1' \, dx_2 \, dx_2' \ldots dx_k' dx_k \bar{\eta}(x_2)$$

$$\times G\left(x_2 x_1' \frac{\delta}{\delta j^t}\right) \eta(x_1') \ldots) + \bar{\eta}(x_k) G\left(x_k x_k' \frac{\delta}{\delta j^t}\right) \eta(x_k')$$

$$\times \exp\left(\frac{ie}{2} \left\{ \sum_{(n,m)\, m+n=1}^{k} (e) [\Delta_l(x_m - x_n) \right.\right.$$

$$+ \Delta_l(x_m' - x_n') - 2\Delta_l(x_m - x_n')$$

$$\left.\left. - 2 \sum_{m=1}^{k} \int \left[\frac{\partial \Delta_l(x_m - z)}{\partial z_\mu} - \frac{\partial \Delta_l(x_m' - z)}{\partial z_\mu}\right]\right) j_\mu^l(z) d^4 z \right\}$$

$$\times \exp\left\{i \int \left[j_\mu^t(x) \frac{D_{\mu\nu}^t(x-y)}{2} j_\nu^t(y) \right.\right. \quad (16)$$

$$\left.\left. + j_\mu^l(x) D_{\mu\nu}^l(x-y) j_\mu^l(y) \right] d^4 x d^4 y \right\},$$

where

$$\Delta_l(xx') = -i\langle\varphi(x)\varphi(x')\rangle_t,$$

$$D^t_{\mu\nu}(x-y) = \frac{1}{(2\pi)^4}\int \frac{k^2\delta_{\mu\nu} - k_\mu k_\nu}{k^4} e^{ik(x-y)}d^4k;\ D^l_{\mu\nu}$$

$$= \frac{1}{(2\pi)^4}\int \frac{k_\mu k_\nu}{k^2}\Delta_l(k^2)\, e^{ik(x-y)}d^4k,$$

$\Delta_l(k^2)$ is any positive function of k^2 and $j_\mu = j^t_\mu + j^l_\mu$ are the external sources of the transverse and the longitudinal components of the interaction with the photons (the interaction with an external field being given by $j_\mu A_\mu = j^t_\mu A^t_\mu + j^l_\mu A^l_\mu$).

The use of functional differentiation with respect to the sources of the photon or the electron fields reveals an obvious dependence of Green's functions on the longitudinal component of the field. In particular, from Eq. (16) we obtain the following relations:

$$G(x, y)$$

$$= G(x, y)_0 \exp\{-ie^2(\Delta_l(0) - \Delta_l(x-y))\},$$

$$\frac{\delta G(x, y)}{\delta j_\mu(z)}$$

$$= \frac{\delta G(x, y)}{\delta j^t_\mu(z)} + \frac{\delta G(x, y)}{\delta j^l_\mu(z)} = \left(\frac{\delta G(x, y)}{\delta j^t_\mu(z)}\right)_0$$

$$\times \exp\{-ie^2[\Delta_l(0) - \Delta_l(x-y)]\} + ieG(x, y)_0$$

$$\times\left[\frac{\partial\Delta_l(x-z)}{\partial z_\mu} + \frac{\partial\Delta_l(y-z)}{\partial z_\mu}\right]$$

where the index 0 denotes that the given quantity represents the unperturbed solution, where the longitudinal component of the interaction is totally absent.

Since the quantity $\delta G(x, x)/\delta j_\mu(z)$ is not dependent on the longitudinal component of the field, according to Eq. (18), the polarization operator is also independent of the longitudinal component. It follows from Eq. (17) that no gauge transformation is capable of removing the infinities which are caused by the transverse component of the interaction, and, therefore, in general, the most convenient choice of a gauge transformation is $\Delta_l = 0$ (see also reference 3).

* *Translator's note:* The expression "logarithmic accuracy" denotes the following:

$$P/\xi \geq \log\xi,\ P \ll \xi.$$

[1] E. S. Fradkin, J. Exper. Theoret. Phys. USSR 26, 752 (1954)

[2] H. S. Green, Phys. Rev. 95, 548 (1954)

[3] L. D. Landau et al, Dokl. Akad. Nauk SSSR 95, 773 (1954)

[4] E. S. Fradkin, Dokl. Akad. Nauk SSSR 98, 47 (1954)

[5] E. S. Fradkin, Dokl. Akad. Nauk SSSR 100, 897 (1955)

Translated by G. Makhov
188

Note on Subsequent Transitions in Meson-Atoms

M. I. Podgoretskii
P. N. Lebedev Institute of Physics, Academy of Sciences, USSR

(Submitted to JETP editor January 20, 1955)
J. Exper. Theoret. Phys. USSR 29, 374-375 (September, 1955)

MUCH experimental work has been done on the study of γ-quanta which are emitted during various transitions in meson atoms, and great precision has been achieved in measuring the energies of these γ-quanta. Of the various transitions which have been studied some are subsequent, for instance $3d \rightarrow 2p$ and $2p \rightarrow 1s$. However, in practice, the possible connection between the transitions has not been experimentally investigated. During the subsequent radiative transitions in meson atoms noticeable angular correlation between the directions of emission of the γ-quanta should be observed in many cases. According to the general laws for subsequent transitions (see reference 1, Ch. VII) the angular correlation is determined only by the knowledge of the total momenta of the initial, final and intermediate states. Since the orbital momenta of the levels of the meson atoms are well-known, in the given case the correlation is determined only by the magnitude of the meson spin. Thus there exists a possibility of the direct determination of the meson spin by measuring the angular correlation. In principle, this applies to the negative mesons of arbitrary type, and in particular, to the heavy mesons.

As an illustration let us consider μ mesons. By

the way, we should note that the commonly assumed opinion that the meson has spin equal to ½ is based not on very dependable, but only on indirect evidence; in reference to the choice between the values ½ and 3/2 for the spin, a choice cannot be made at the present time.

The levels of the meson atoms are degenerate in orbital momentum and this makes the identification of the transitions difficult. However, the effect of the finite size of the nucleus leads to the removal of the degeneracy for large Z. For instance, for the meson atom formed in the nucleus of lead the $2s$ level is approximately 1 mev above the $2p$ level [2]. Consider now the μ meson which got to the $2s$ level during the formation of the meson atom and by subsequent transitions; it goes over into the ground state of the meson atom by the way of the subsequent radiative transitions $2s \rightarrow 2p \rightarrow 1s$. If the spin of the meson is ½ or 3/2, then the angles between the γ-quanta are distributed almost isotropically, i.e., $W(\theta) \sim \sin\theta$. On the other hand, if the spin is zero, $W(\theta) \sim (1 + \cos^2\theta)\sin\theta$. In an analogous way, we can observe the difference between spins of ½ and 3/2. In particular, for the transition $3p \rightarrow 2s \rightarrow 2p$ the angular distribution is exactly isotropic if the spin is ½ and non-isotropic if the spin is 3/2.

During the cascade emission of γ-quanta by nuclei, the angular correlation can in some cases be strongly supressed because of the interaction of the magnetic moment of the nucleus with the magnetic field caused by the electron shell. The estimates given in reference 1 show that this phenomenon does not appear if the lifetime of the intermediate state $t \leq 3 \times 10^{-11}$ sec. Approximately the same estimates are valid in the case under consideration, the only difference being that the role of the magnetic moment of the nucleus is replaced by the magnetic moment of the meson atom. The lifetimes of meson-atom transitions are very small. For instance, for lead the lifetime of the μ meson in $2s$ state is $\sim 10^{-17}$ sec, and for $Z = 25$, $t \sim 2 \times 10^{-13}$ sec[2]. Therefore, as a rule, we can neglect the effect of the electron orbits.

For meson atoms an additional question can arise concerning the interaction of the magnetic moments of the meson atom and the nucelus. We will not consider this question here in detail, but note that in practice it is always possible to study the meson atoms formed in nuclei with zero momentum, where the above interaction is absent. Another complication arises if the mesons experience very large nuclear capture (for instance π-mesons). In this case we must exclude from consideration levels for which the probability of nuclear capture is much greater than the probability of the radiative transition. For not too large Z the above applies only for levels with zero orbital momentum.

The author is thankful to I. S. Shapiro for participating in the discussion.

[1] L. W. Groschev and I. S. Shapiro, *Spectroscopy of Atomic Nuclei*, GITTL, Moscow, 1952

[2] J. A. Wheeler, Rev. Mod. Phys. 21, 133 (1949)

Translated by M. Polonsky
207

Rotation of the Plane of Polarization in a Longitudinal Magnetic Field at a Wavelength of 3 cm

D. I. MASH
P. N. Lebedev Institute of Physics
Academy of Sciences of the USSR
(Submitted to JETP editor May 6, 1955)
J. Exper. Theoret. Phys. USSR 29, 390-392
(September, 1955)

WITH the development of radio direction finding and the appearance of ferromagnetic dielectrics [1], the rotation of the plane of polarization in a magnetic field (Faraday effect) has become of great practical importance and has found extensive application in UHF techniques.

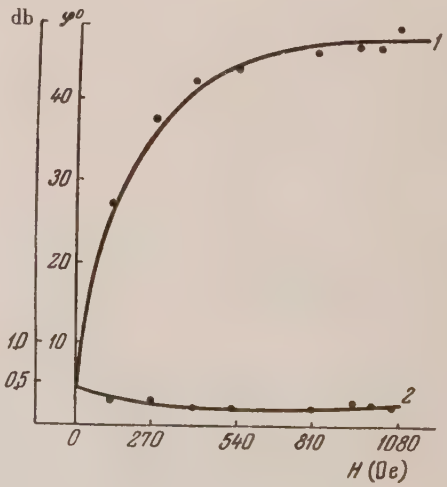

FIG. 1. Dependence of (*1*) angle of rotation of the plane of polarization φ in degrees, (*2*) losses, in decibels, on the magnetic field intensity for a sample of NZ-500 45 mm long.

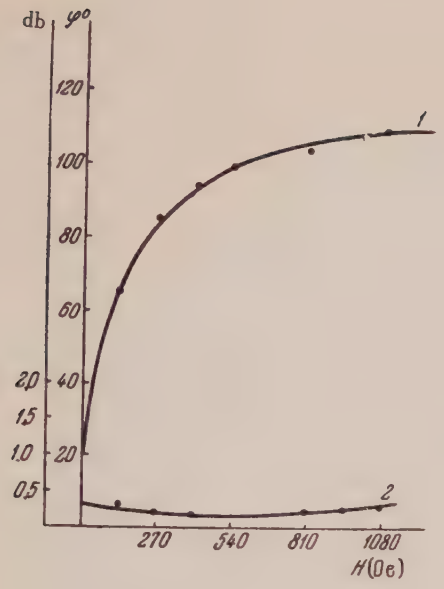

FIG. 2. Dependence of (*1*) angle of rotation of the plane of polarization φ in degrees, (*2*) losses, in decibels, on the magnetic field intensity for a sample of NZ-500 77 mm long.

The Faraday effect has been utilized in the design of microwave switches, one-way transmission systems, electrically controlled attenuators, devices for the measurement of weak magnetic fields, for obtaining circular polarization, for high-frequency modulation, for beacon rotation in radio direction finding, for automatic control of high-frequency signals, etc.

The application of the Faraday effect to wavelengths of the order of a few centimeters is limited by high-frequency losses introduced by ferromagnetic semiconductors – ferrites, which are used as the rotating medium. It has therefore been important to investigate commercial ferrites as to the possibility of their application and practical utilization of magnetic rotation of the plane of polarization in the centimeter-wave region.

We investigated the "oxyfers" (RCh-10, RCh-15, RCh-50) and the Ni-Zn ferrites (NZ-100, NZ-250, NZ-500, NZ-L, NZ-L_2, NZ-31, NZ-38, NZ-40, NZ-41, NZ-43 and NZ-45) in the form of thin discs completely filling the wave guide and in the form of thin cylinders placed along the axis of a cylindrical wave guide. The measurements were carried out by a wave with $\lambda = 3$ cm, using a method similar to that described in reference 2. The ferrites NZ-500, NZ-250 and NZ-L showed relatively small losses. Best results were obtained with the ferrite NZ-500 in powder form, annealed at 1000° C. The pulverized ferrite filled a polystyrene or a quartz tube having external and internal diameters 7.0 and 5.7 mm, respectively.

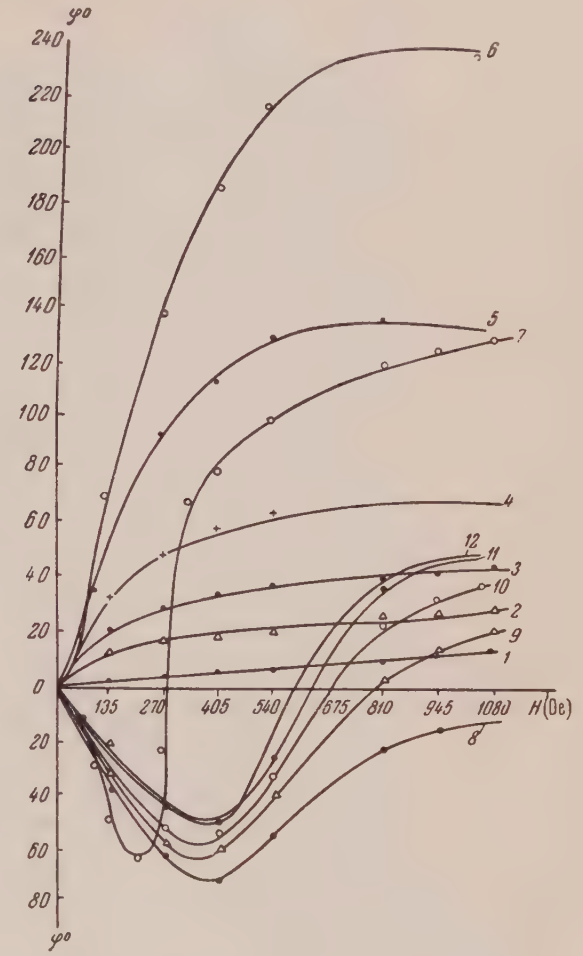

FIG. 3. Dependence of φ on *H* for the NZ-100 ferrite rods of diameters: 1-3 mm, 2-4 mm, 3-5 mm, 4-6 mm, 5-7 mm, 6-8 mm, 7-9 mm, 8-10 mm, 9-11 mm, 10-12 mm, 11-13 mm, 12-14 mm.

Figure 1 shows the dependence of the angle φ of rotation of the plane of polarization (in degrees), and of the losses (in decibels), on the intensity of the external longitudinal field *H* for the NZ-500 ferrite sample, in powder form, filling a quartz tube of 45 mm length. Figure 2 shows the same relation for a sample of powder form ferrite NZ-500 in a quartz tube 77 mm long. The first sample was prepared for use in a one-way transmission system. The desired angle of rotation of 45 degrees was attained at a relatively weak magnetic field of 540 oersteds, where saturation was reached. The second sample was prepared for the construction of a high-frequency switch. The desired angle of

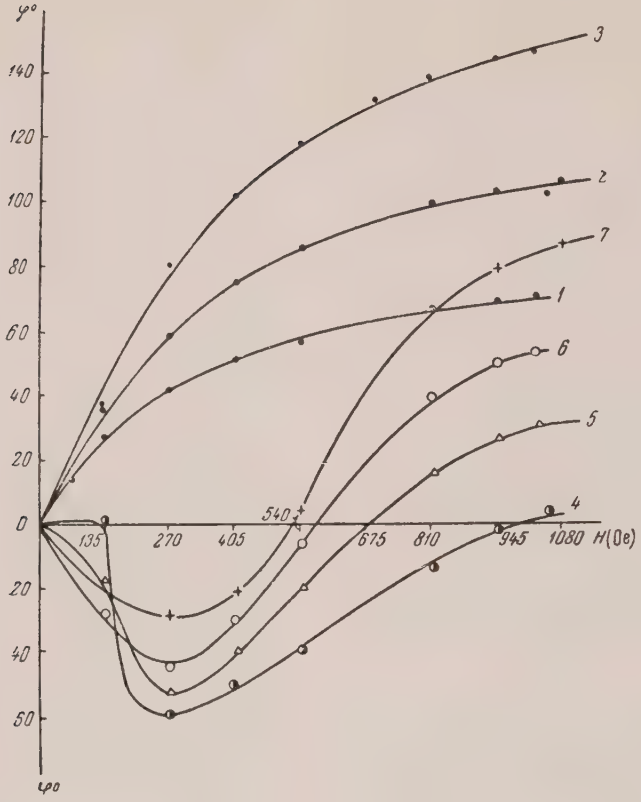

FIG. 4. Dependence of φ on H for the NZ-40 ferrite rods of diameters: 1-7 mm, 2-8 mm, 3-9 mm, 4-10 mm, 5-11 mm; 6-12 mm, 7-13 mm.

rotation of the plane of polarization of 90 degrees was attained with the external field of 400 oersteds. In both cases the wave at the output remains linearly polarized, and the high-frequency losses do not exceed 0.5 db. The latter fact demonstrates that the high-frequency losses, being quite small (0.5 db) are not caused by absorption in the ferrite but by reflection off the sample, since in this experiment the sample did not specially fit the wave guide. The ferrite NZ-500, not showing losses at the wavelength of 3 cm, may therefore be used successfully in UHF applications.

In connection with the fact that waves of higher modes may become excited in ferrite rods of large diameter, it was very important to investigate how the rotation of the plane of polarization (dependence of φ on H) changes with the diameter of the ferrite rods. The dependence of φ on H for rods of various diameters was investigated with a NZ-100 ferrite sample 41.3 mm long (Fig. 3) and a NZ-40 ferrite sample 36.5 mm long (Fig. 4). From Figs. 3 and 4 it may be seen that the normal dependence of φ on H is obtained for relatively thin ferrite rods of 3 to 8 mm in diameter (waveguide diameter 21.8 mm). The ferrite rods of larger diameter, in which waves of higher modes are excited, show an anomalous dependence of φ on H, a fact which should be taken into account when ferrite rods are used.

[1] I. G. Dorfman, Izv. Akad. Nauk SSSR, Ser. Fiz. 16, 412 (1952)

[2] C. L. Hogan, Bell System Tech. J. 31, 1 (1952)

Translated by S. H. Kasha
218

[+] Deceased

DOKLADY AKADEMII NAUK SSSR VOLUME 105, NO. 2 NOVEMBER 11, 1955

DOKLADY AKADEMII NAUK SSSR VOLUME 105, NO. 3 NOVEMBER 21, 1955

DOKLADY AKADEMII NAUK SSSR VOLUME 105, NO. 4 DECEMBER 1, 1955

DOKLADY AKADEMII NAUK SSSR VOLUME 105, NO. 5 DECEMBER 11, 1955

DOKLADY AKADEMII NAUK SSSR VOLUME 105, NO. 6 DECEMBER 21, 1955

JOURNAL OF TECHNICAL PHYSICS, USSR VOLUME 25, NO. 11 1955

JOURNAL OF TECHNICAL PHYSICS, USSR VOLUME 25, NO. 12, 1955

JOURNAL OF TECHNICAL PHYSICS, USSR VOLUME 25, NO. 13 1955

CONTENTS

(*Contents continued on inside back cover*)